City Research Online

City St George's, University of London

Citation: Reading, A. R. (1977). The formation of odorous compounds during the combustion of diesel fuel. (Unpublished Doctoral thesis, The City University)

This is the accepted version of the paper.

This version of the publication may differ from the final published version. To cite this item please consult the publisher's version.

Permanent repository link: https://openaccess.city.ac.uk/id/eprint/37838/

Copyright and Reuse: Copyright and Moral Rights remain with the author(s) and/or copyright holders. Copies of full items can be used for personal research or study, educational, or not-for-profit purposes without prior permission or charge, unless otherwise indicated, provided that the authors, title and full bibliographic details are credited, a hyperlink and/or URL is given for the original metadata page and the content is not changed in any way. For full details of reuse please refer to City Research Online policy.

City Research Online: http://openaccess.city.ac.uk/ publications@citystgeorges.ac.uk

470

A THESIS

entitled

THE FORMATION OF ODOROUS COMPOUNDS DURING THE COMBUSTION OF DIESEL FUEL

by

ANDREW ROBERT READING

Submitted for the

Degree of Doctor of Philosophy

of The City University

1977

ABSTRACT

One of the most frequently encountered problems in the general area of pollution is that of diesel exhaust odour, particularly in cities, where the use of diesel-powered buses and lorries provide the inhabitants with much cause for complaint. Despite this, the diesel engine has much to offer in terms of reliability and economy. Thus, if the widespread use of diesel engines is to be extended to include light transport vehicles, such as passenger cars, then the diesel exhaust odour problem must be considerably reduced. In order to contribute to this objective, the present work has attempted to establish the mechanism by which odorants are formed during the combustion process and to elucidate the conditions which influence the processes of formation.

Section 1 describes briefly general aspects of hydrocarbon oxidation, the mechanism of which has been deduced largely from laboratory studies using static vacuum and flow systems. The observations emanating from these studies are relevant to the combustion of diesel fuel in an engine. Thus the four stages of combustion which have been defined are described with particular reference to the ignition delay period during which many of the odorants are formed. In order to provide background information relating to 'odour-science', the various aspects of odorant perception and their measurement are described. Finally, a description is given of the two main diesel exhaust odour research programmes, one of which resulted in the development of an objective odour assessment method.

An account of the apparatus and techniques used during the course of this work is given in Section 2. Objective methods of odour assessment using electronic analogues of the olfactory sensory process were briefly investigated and the problems of temperature and water vapour associated with the use of such devices for the measurement of diesel exhaust odour were considered. The main experimental programme concerned the controlled

oxidation of diesel and pure hydrocarbon fuels in a stainless—steel reactor incorporated into a static vacuum system. Investigation of the combustion phenomena taking place during diesel fuel oxidation under various conditions of stoichiometry, pressure and temperature revealed that the kinetic behaviour of this fuel was very similar to that observed for a high molecular weight, straight-chain alkane fuel. For comparison, oxidation experiments using hexadecane, 1-decene and butylbenzene were performed under cool-flame and hot-ignition conditions. Analysis of the reaction products was carried out at various stages during the reaction using liquid- and gas-chromatography.

The results obtained during the course of this work are presented in Section 3. The complex nature of diesel fuel was revealed by the gas-chromatographic analyses performed, the chromatograms obtained serving to 'finger print' the fuel used. Kinetic data for the oxidation of various fuels are presented, followed by the qualitative and semi-quantitative results derived from the gas- and liquid-chromatographic analyses of the oxidation products. The liquid-chromatographic data are most important, since the results provide a quantitative measurement of odour intensity. The gas-chromatographic analyses were used to assess the efficiency of the 'odour-trapping' procedure and to monitor any composition changes which occured during the oxidation process. Identification of the individual products formed was precluded by the complexity of the chromatograms and the practical limitations of the system.

In Section 4, the analytical and kinetic results are rationalised on the basis of a chain-thermal oxidation mechanism which is well established for many hydrocarbon-oxidant systems. A description is given of the complex interactions between the oxidation processes involving the various types of chemical compound present in diesel fuel, represented by pure alkanes, alkenes and aromatic compounds. The kinetic data recorded, indicated that

fuel combustion is initiated in the aliphatic fraction of the fuel, while the analyical results showed that for all of the fuels tested, odorants were formed in the highest concentration under cool-flame conditions. The wide range of products formed is explained in terms of a mechanism involving alkylperoxy radical isomerisation and decomposition.Aromatic molecules present in the fuel have a high resistance to oxidation and therefore contribute extensively to the partially oxidised aromatic fraction of the exhaust. However, it has been shown that aromatic molecules can be formed from straight - chain aliphatic molecules, eg. hexadecane, provided that the carbon chains are fairly long. During hot ignition, the odorants produced during the first-stage reactions are almost completely destroyed. The heterogeneous distribution of the fuel-oxidant mixture in a diesel results in stoichiometries existing in some regions of the combustion chamber which are too lean or too rich to support combustion, while other regions act as cool-flame quench zones. The formation of partial oxidation products, and therefore odorants, in these regions is expected to be very high. The results obtained have been incorporated into a model of diesel fuel spray combustion, which affords a qualitative description of the odorant formation process.

ACKNOWLEDGEMENTS

I would like to acknowledge the advice and assistance given to me by my supervisors, Dr. R.T. Pollard and Professor C.F.Cullis.

I would also like to express my gratitude to my colleagues of the [redacted] for the interest and companionship they have shown during my period of research at The City University.

Finally, I wish to thank my wife, [redacted], for the invaluable encouragement and assistance she has given which has made this Thesis possible.

C O N T E N T S

SECTION 1

INTRODUCTION

SECTION 1

1.1 A Challenge to the Gasoline Engine

The two principal power plants used today for the propulsion of road transport vehicles are the gasoline engine and the diesel engine. Until recently the gasoline engine had a monopoly over light - to - medium power range duties while the diesel engine was unsurpassed for heavy - duty operation, since it had been perfected to produce dependable power with minimum maintenance and fuel consumption.

In these economically stringent times, diesel engine manufacturers are seriously considering the prospect of diesel powered passenger cars, since the diesel engine has much to offer in terms of low specific fuel consumption.This advantage is however, considerably reduced when one considers that the diesel engine is 20 to 30 years behind the gasoline engine, in terms of power - to - weight ratio, noise, vibration and cold starting.[1] If it is assumed that these disadvantages could be overcome given the incentive, there still remains the problem of exhaust emission. Compared with the gasoline engine, the diesel engine offers low emission of carbon monoxide and low emission of polycyclic aromatic hydrocarbons. The unburnt hydrocarbons, nitrogen oxides, odour and soot are however, not so attractive. Legislation restricts the levels of emitted carbon monoxide, hydrocarbons, nitrogen oxides and soot and this has given engine designers the incentive to reduce these emissions quite considerably. This is not the case with exhaust odour which has eluded legislation, partly bacause of the inherent difficulties of odour measurement. Research carried out over the past ten years has removed some of the mystery surrounding diesel exhaust odour. The major odorants have been identified and a prototype for their measurement has been produced.

It is only too evident that the majority of the public consider diesel exhaust odour to be highly unacceptable. It is also obvious that

this problem must be alleviated before the diesel engine can compete with the gasoline engine for the light duty sector of the market. Now that the instrumentation for odour assessment is available, research into the emission of odorants can be performed with greater efficiency and rapidity. An understanding of the mechanism by which odorants are formed during the combustion cycle may suggest engine design modifications for the reduction of odour emission with obvious advantages to all concerned.

1.2 Ecological Aspects of Diesel Engine Operation

The diesel engine has two detrimental effects on the environment, i.e. it causes the generation of noise and it is responsible for the emission of pollutants. The first effect receives much attention from the design engineer and is not directly related to the subject of the present study; it will not therefore be discussed any further. The pollution aspect has two facets. The first is the adverse physiological effects suffered by animal and plant life from exposure to diesel engine exhaust, and the second is the effects associated with odour emission, i.e. the derating of the aesthetic quality of the environment and the physiological and psychological stress which this can cause.[2]

Larsen[3], has defined twelve steps in the approach to the problem of obtaining clean air and it will be useful if these are reviewed within the context of diesel engine operation. The suggested steps are:-

(1) To determine the effects of the concentrations and exposure duration of various pollutants on people, animals, plants and property.

(2) To decide which effects should be prevented.

(3) To select ambient air quality standards which will prevent these effects.

(4) To measure and evaluate ambient air pollution concentrations.

(5) To calculate the overall source reductions needed to achieve

selected ambient air quality standards.

(6) To measure or estimate emissions from each source type in an area.

(7) To decide how much each source type could be permitted to emit and still achieve the ambient air standards required.

(8) To select or develop means for achieving the necessary reduction in emissions.

(9) To decide the date after which each source type should be controlled.

(10) To set emission standards.

(11) To enforce emission standards.

(12) To continue monitoring sources of emission and the ambient atmosphere in order to ensure that adequate air quality is being obtained.

Steps 1 to 12 have been applied to specific diesel exhaust components i.e. smoke, NO_x , CO and total hydrocarbons (HC). The motivating influences which have contributed to this achievement are, (a) the public awareness of the problem, which is in part related to the degree of undesirability of the noxious emissions, and (b) the ease with which each specific exhaust component can be measured and controlled.

When compared to the pollutants already featured in the legislation, odour has a particularly elusive character. Its cause, measurement and control have presented problems of such complexity that legislation is at the present impossible, despite the intensive investigations which have been carried out during the last twelve years.

A quotation from a report[4] of the U.S. House of Representatives, illustrates the underlying philosophy of pollution and public awareness, 'The quality of the environment is not a human health issue per se. It is more a matter of unacceptability, at face value, of offensive odours,

discoloured water, low visibility, eg. irritation, littered landscapes and soiling'. Two points that are worth noting are, first that the quality of the environment is a highly subjective matter, and second, that public objection about the more insidious and less overt characteristics of pollution is less likely, although these characteristics may be potentially more harmful.

The toxicity and carcinogenicity of some of the components of diesel engine exhaust have been the subject of investigations over a much longer period of time than that devoted to odour research. A literature review[5] undertaken as part of this study, showed that interest in the carcinogenic potential of engine exhausts was being expressed in the early 1950's. Since the publication of these early reports, the analytical techniques employed and the methods used to test the physiological activity of the potentially harmful pollutants have undergone extensive improvement. These developments have encouraged investigations into the effects of exhaust components emitted in much lower quantities than those under legislative control. It has been stated[6] that over 2000 partial oxidation products are present in diesel exhaust. Although some of these components may be physiologically harmful in high concentrations, they are emitted in such small quantities that they are considered harmless, except possibly in confined spaces. Other species identified in the exhaust are however, suspected of presenting a serious health hazard even in very low concentrations. The carcinogenic polycyclic aromatic hydrocarbons and their nitrogen containing heterocyclic analogues, the aza-arenes, are two classes of compounds which warrent further investigation in this context. Examples of polycyclic aromatic hydrocarbons documented[7] as being components of of diesel engine exhaust, are shown in Figure 1.1 . Perhaps the most notorious of these is benz(a)pyrene, (BaP) which, for historical reasons, is perhaps the most well known carcinogen. The potentially carcinogenic properties

Figure 1·1

Examples of P.C.A.H. Identified in Diesel Exhaust

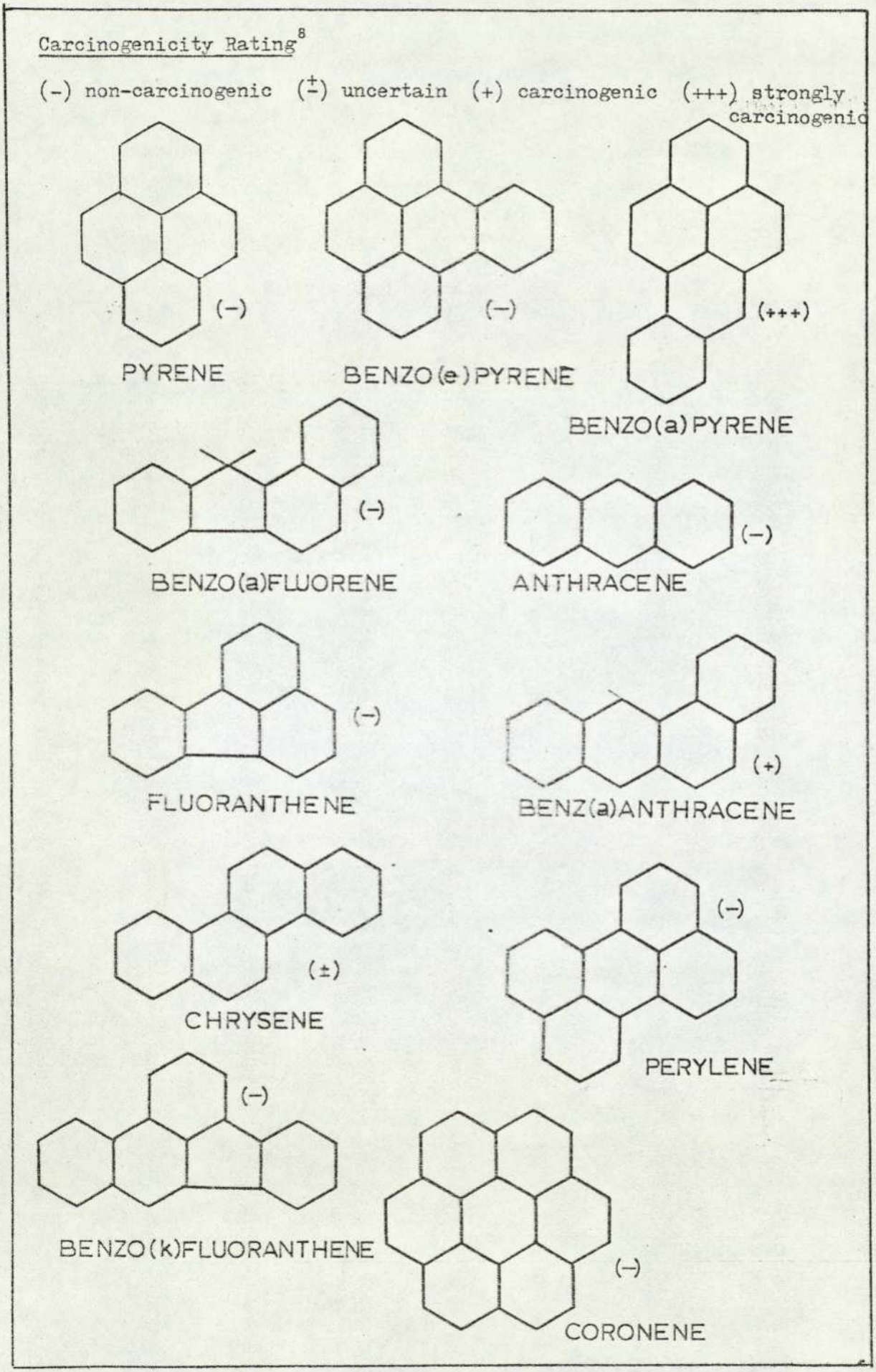

exhibited by BaP and other carcinogens can be enhanced by the presence of other chemical compounds which may act as irritants, co- or anti-carcinogens or transport media. Many compounds emitted by diesel engines have these other characteristics and their combined effect has been discussed in some detail in the aforementioned literature review.

The following conclusions summarise the present state of knowledge concerning the carcinogenic potential of diesel and gasoline exhaust.

(1) A wide range of polycyclic aromatic hydrocarbons has been identified in the exhausts of both the gasoline[9-11] and the diesel[8,10,12-14] engine. A small number of these are known to be carcinogenic.

(2) The aliphatic fraction of the exhaust, normally ignored in carcinogenicity tests, since it does not contain p.c.a.h, has also been demonstrated to be carcinogenic[15], possibly due to the presence of epoxides.

(3) Under normal, efficient combustion conditions, the diesel engine is known to produce less p.c.a.h. than the gasoline engine.

(4) Under inefficient combustion conditions, ie: overfuelling, the levels of emitted p.c.a.h. from the diesel engine were observed to increase dramatically to levels far higher than those produced by the gasoline engine. Under these conditions, the associated production of soot and other pollutants including unburnt fuel aerosols combine to produce a chemical environment which has greatly enhanced carcinogenic potential.

(5) The emission of p.c.a.h. by gasoline engines appeared to be strongly dependent on the composition of the fuel and lubricating oil, although a more recent publication[16] suggests that the effect on the ambient p.c.a.h. levels, of increasing the aromatic content of the fuel and oil, is negligible. The fuel and lubricating oil compositions have little effect on the emission of p.c.a.h. by diesel engines.

(6) For both types of engine, the operating conditions such as speed, load, F/A rates and temperature all had a substantial effect on

the emission of p.c.a.h. However, transient operating modes, particularly acceleration, were shown to produce the highest levels.

(7) Epidemiological studies[17] into the possible relationship between mortality rates and occupational exposures to higher than normal concentrations of diesel and gasoline exhaust have shown that no excess deaths from lung cancer occurred among motor mechanics, garage hands; drivers of cars lorries or buses, bus and tram conductors; drivers of horse-drawn vehicles, road men, council labourers, dustmen. Investigation more specific to diesel engine operation[18-20] produced similar findings.

It is evident, from the foregoing discussion, that much can be done to reduce the emission of certain pollutants from the diesel engine by careful design, operation and maintenance. The diesel exhaust odour problem is not so easily eliminated, owing to the lack of reliable instrumentation for the assessment of the effects of engine design and operation on the emission of odorants. Recent advances in the field of diesel odour have led to the identification of the major odour components and to the development of an instrumental technique for odour assessment based on this knowledge. A full appraisal of both the theoretical and practical aspects of the odour assessment technique will undoubtedly precede any move to use it as the basis for legislation.

1.3 The Combustion of Hydrocarbon Fuels

Although much of the information concerning the oxidation of hydrocarbons has been obtained from studies carried out in static vacuum systems using low molecular weight fuels, ($CN \leq 10$), at sub-atmospheric pressures, the results thus obtained are nevertheless directly applicable to the mechanisms operating at much higher pressures within the chambers of internal combustion engines.[21] A brief review of theories of hydrocarbon oxidation is therefore given below.

The gas phase oxidation of a straight chain hydrocarbon with a carbon number > 4, represented by the general formula C_nH_{2n+2}, is classed as a degenerately branched chain reaction, the theory of which has been developed in full by Semenov.[22]

1.3.1 Initiation

Initiation of the process at temperatures within the cool flame regime, (250-400°C), involves attack of the fuel by molecular oxygen to produce an alkyl radical and a hydroperoxy radical.[23,24]

$$C_nH_{2n+2} + O_2 \longrightarrow \dot{C}_nH_{2n+1} + H\dot{O}_2 \qquad (1)$$

This reaction predominates over pyrolysis, since the latter reaction has a very high activation energy which precludes its occurrence below 400°C. It is still not certain whether reaction (1) occurs homogeneously[25] or heterogeneously;[26,27] but it is accepted that the process has a moderately high activation energy ie: 40-55 kcal $mole^{-1}$. Owing to the high endothermicity, the reaction is slow and selective, the point of oxygen attack in the fuel molecule being determined by the C-H bond strength; tertiary C-H bonds are the most readily attacked and primary C-H bonds the least readily attacked. At high temperatures small differences in bond strengths are less important. Once the primary chain cycle has been initiated, the major fuel-removing reactions will be those involving attack by atoms or radicals such as $\dot{O}H$, $H\dot{O}_2$, $\dot{C}_nH_{2n+1}OO$, $\dot{H}$ and $\dot{C}H_3$.

eg. $\dot{OH} + C_nH_{2n+2} \longrightarrow H_2O + \dot{C}_nH_{2n+1}$ (2)

$H\dot{O}_2 + C_nH_{2n+2} \longrightarrow H_2O_2 + \dot{C}_nH_{2n+1}$ (3)

Reaction (3) would account for the hydrogen peroxide recovered under certain conditions, although the yield may be low owing to the heterogeneous decomposition of this compound to oxygen and water.

At temperatures of about 400°C, initiation still occurs primarily via an abstraction mechanism(reaction 1). However, as the temperature increases further, pyrolysis becomes more important, particularly under oxygen-deficient conditions.

$C_nH_{2n+2} \longrightarrow \dot{C}_{n-1}H_{2n-1} + \dot{C}H_3$ (4)

1.3.2 Propagation

Two possible steps are available for propagation of chains, both reactions involving the attack of molecular oxygen on the alkyl radical formed by reaction (1)

$\dot{C}_nH_{2n+1} + O_2 \rightleftharpoons C_nH_{2n+1}\dot{O}O$ (5)

$\dot{C}_nH_{2n+1} + O_2 \longrightarrow C_nH_{2n} + H\dot{O}_2$ (6)

Reaction (5) is indicated as a reversible reaction in which the equilibrium at temperatures below 300°C lies well over to the right. The activation energy for this process is effectively zero.[23] At higher temperatures the reverse reaction becomes slightly more effective, setting up a competition for oxygen between reactions (5) and (6). The relative importance of these two reactions has led to two theories[28] regarding chain propagation at low temperatures. Reaction (5) which leads to the formation of an alkylperoxy radical forms the basis of one mechanism,[29-33] while reaction (6) which produces the conjugate alkene forms the basis for the other.[34] Of these two mechanisms the alkylperoxy radical isomerisation scheme is favoured on the basis of experimental consideration,[31,33,35-37] especially for the low

temperature oxidation of fuels with more than four carbon atoms.

The elegance of the alkylperoxy radical isomerisation scheme lies in its ability to account for the diversity and complexity of the products formed. The alkylperoxy radical produced via reaction (2) can undergo homogeneous intramolecular rearrangement to form the hydroperoxy-alkyl radical, the decomposition of which leads to the formation of a hydroxyl radical and stable products, including O-heterocycles, carbonyl compounds and alcohols with rearranged carbon skeletons:

$$C_nH_{2n+1}\dot{O}O \longrightarrow \dot{C}_nH_{2n}OOH \qquad (7)$$

$$\dot{C}_nH_{2n+1}OOH \longrightarrow P + \dot{O}H \qquad (8)$$

The chain cycle is then completed by the unselective attack of the highly reactive hydroxyl radical on the fuel.

$$C_nH_{2n+2} + \dot{O}H \longrightarrow \dot{C}_nH_{2n+1} + H_2O \qquad (9)$$

1.3.3 Branching

The observation of certain thermo-kinetic phenomena, such as cool-flames and the negative temperature coefficient, implies the existence of a degenerately branched chain reaction in the propagation sequence. The long ignition delays, induction periods and the slow acceleration of the reaction is reconciled with the formation of a relatively stable intermediate product which has a lifetime of several seconds. This intermediate can then go on to form stable final products or decompose in a branching reaction to form two or more reactive chain centres.

Aldehydes,[38] peroxides[38,39] and peracids[40] are examples of intermediates which act as branching agents in many hydrocarbon oxidation systems. The branching agent gradually accummulates during the course of the reaction until a critical concentration is reached. When this concentration is exceeded, an autocatalytic and exponential increase of the reaction rate occurs during which the branching agent is rapidly consumed. The fall in

concentration of the branching agent results in a decrease in the rate of reaction. The mechanism therefore exhibits self-limiting properties which, if the prevailing conditions are such as to preclude ignition, results in the passage of a cool-flame. If, however, the rate of reaction is such that the rate of heat production exceeds the rate of heat dissipation through diffusional processes, then the reaction rate undergoes chain thermal acceleration, culminating in hot ignition.

In the low temperature region where the oxidation is quite selective, Fish[30,41] suggests that degenerate branching results from the alkylmonohydroperoxide produced by a linear chain involving intermolecular abstraction of hydrogen by the alkylperoxy radical as shown below:-

$$C_nH_{2n+1}\dot{O}O \xrightarrow{C_nH_{2n+2}} \dot{C}_nH_{2n}OOH \longrightarrow R\dot{O} + \dot{O}H \qquad (10)$$

$$\uparrow \quad O_2 \qquad + \qquad C_nH_{2n+1}$$

At high temperatures reaction (6) predominates, leading to a high stationary concentration of the conjugate alkene.

$$\dot{C}_nH_{2n+1} + O_2 \longrightarrow C_nH_{2n} + H\dot{O}_2 \qquad (6)$$

The primary chain cycle is then completed by the reaction:-

$$C_nH_{2n+2} + H\dot{O}_2 \longrightarrow \dot{C}_nH_{2n+1} + H_2O_2 \qquad (3)$$

At these elevated temperatures, the hydrogen peroxide decomposes homogeneously to form $\dot{O}H$ radicals in a branching step.

$$H_2O_2 + M \longrightarrow 2\dot{O}H + M \qquad (11)$$

The $\dot{O}H$ radical formed can then participate in a further propagation step.

$$C_nH_{2n+2} + \dot{O}H \longrightarrow \dot{C}_nH_{2n+1} + H_2O \qquad (2)$$

Pyrolysis will also be occurring to an appreciable extent leading to the destruction of the alkyl radicals formed in reaction (2).

1.3.4 Termination

Under cool-flame conditions, chain termination occurs through homogeneous recombination and disproportionation of radicals or possibly as a result of their destruction at the walls. Wall termination is likely to predominate at low initial pressures and low radical concentrations. A reflection of the role played by wall termination is afforded in the dependence of the induction period on surface conditions.[42] Radical stability also determines the extent to which wall reactions are involved in the termination stages. Alkylhydroperoxide radicals are fairly stable and therefore heterogeneous termination will be a common fate.

$$C_nH_{2n+1}\dot{O}O \longrightarrow \text{wall} \qquad (12)$$

$$\dot{C}_nH_{2n+1}OOH \longrightarrow \text{wall} \qquad (13)$$

$$H\dot{O}_2 \longrightarrow \text{wall} \qquad (14)$$

At higher fuel conversions, radical concentrations are larger and homogeneous termination becomes more important.

$$2\dot{C}_nH_{2n+1} + M \longrightarrow C_{2n}H_{4n+2} + M \qquad (15)$$

$$2C_nH_{2n+1}\dot{O}O \longrightarrow C_nH_{2n+1}OOC_nH_{2n+1} + O_2 \qquad (16)$$

$$C_nH_{2n+1}\dot{O}O + H\dot{O}_2 \longrightarrow C_nH_{2n+1}OOH + O_2 \qquad (17)$$

$$H\dot{O}_2 + H\dot{O}_2 \longrightarrow H_2O_2 + O_2 \qquad (18)$$

Except for methyl and ethyl radicals, which have a small number of degrees of freedom, the third-body requirement for energy dissipation is unnecessary.

At low temperatures, reaction (18) can be considered as a termination step since the hydrogen peroxide formed is reasonably stable, reaction (11) occurring only infrequently.

At high temperatures various heterogeneous[43,44] steps have been postulated,

$$\dot{O}H \longrightarrow \text{wall} \qquad (19)$$

$$\dot{H}O_2 \longrightarrow \text{wall} \qquad (20)$$

$$\dot{H} \longrightarrow \text{wall} \qquad (21)$$

and certain homogeneous recombination reactions have also been proposed.

$$\dot{C}H_3 + \dot{C}H_3 + M \longrightarrow C_2H_6 + M \qquad (22)$$

1.4 Diesel Engine Design and Combustion

One very important aspect of diesel engine combustion is the highly heterogeneous nature of the process. Unlike the gasoline engine, in which the fuel and air are homogeneously mixed prior to spark-induced ignition, the diesel engine combustion process is initiated by injecting a suitable liquid fuel into a hot, highly compressed air mass contained in the cylinder. A highly exothermic spontaneous reaction occurs, causing the trapped gases to expand rapidly, forcing the piston down to produce the power stroke of the cycle.

The fuel spray injection process produces a fuel-air distribution pattern which changes as a function of time. The stoichiometry of the fuel air mixture varies from zero to infinity and is dependent on the injection process and the air motion within the combustion chamber. Within the space-temporal co-ordinates of the chamber, fuel-air ratios too-lean and too-rich to burn coexist with those of the correct stoichiometry for autoignition, the nature of the ensuing combustion mechanism showing a strong dependence on the mixing process. Under most engine operating conditions, ignition takes place before all the fuel is injected: it has been found that the ratio of the fuel present in the combustion chamber at the start of combustion, to the total amount of fuel injected, has a marked effect on the resulting combustion process and consequently on the formation of pollutants.

1.4.1 Fuel Injection and Combustion Chamber Design

The achievement of efficient combustion in the diesel engine is dependent on the careful design, manufacture, testing and maintenance of the fuel injection equipment. As an example of the duty required of the fuel pump and injectors of a present day high speed engine ie: an engine developing 40 b.h.p. at 1,500 rpm. the fuel pump measures, accurately, a volume of fuel oil less than $0.25mm^3$. This minute quantity is delivered to

the fuel valve at a pressure greater than 2,000psi to be atomised by injection into the combustion space through nozzle holes ca 0.025mm in diameter. The process is completed within $5x10^{-2}$sec. and is repeated between 12 and 13 times every second.

With regard to the combustion chamber design, two differing configurations predominate. These are the pre-combustion or indirect injection chamber and the open or direct injection chamber. The pre-combustion chamber is the older design of the two and in its conception the fuel is made to seek out the air, whereas in the direct injection chamber the reverse is the case. The pre-combustion chamber is divided into two parts in order to produce an air-blast effect. The larger part is formed by a cavity machined in the crown of the piston and takes the form of a shallow saucer-like depression. The smaller part forms an ante-chamber and contains about one-third of the total compression volume. It is into this latter part that the whole of the fuel is injected. The smaller chamber is connected via throat and orifice to the main chamber, see Figure 1·2 and it is through this orifice that air flows from the main volume on compression. The air is raised above the normal compression temperature due to conductive heat transfer from the orifice and throat surfaces. On ignition, the rapid expansion of the gas drives the fuel out into the main chamber where it is able to complete the combustion process. The fuel-air mixing is therefore mainly due to combustion-generated motion. The mixture which comes from the pre-chamber is composed of partially burned, partially vaporised fuel intermingled with air and this, when dispersed throughout the main combustion chamber, readily absorbs the available oxygen. This type of chamber has proved very effective at promoting combustion at a rate high enough to enable the engine to operate over a wide range of speeds and to function with a variety of fuels. The injector possesses only a single hole and the engine has very good fuel consumption provided the

operating conditions are not varied widely.

The open or direct combustion chamber is formed by a cavity machined centrally in the piston crown, the injector being situated in the head, over the centre of the cylinder. In most engines the injector is provided with several spray holes, four being most generally used. Viewed in plan the holes are equally spaced but, in elevation they are arranged around a cone so that the fuel is directed in a somewhat downward direction. The vertical angle between opposite sprays, known as the cone angle, is fairly wide, ranging from about 130° to 160° according to the requirements of the chamber. The mixing of the fuel and air depends mainly upon the spray atomisation, penetration and air motion. A typical fuel injection arrangement showing the direct combustion chamber is shown in Figure 1·3.

1.4.2 The Combustion Process

Since the diesel engine first assumed its role as one of the primary sources of power, the combustion process occurring in the engine has been the subject of intense investigation resulting in an engine which displays greatly improved efficiency and flexibility. However, despite these advances much of the combustion process is little understood due to its highly complex heterogeneous nature. One fundamental aspect is the ignition delay period, which if understood may provide the answers to combustion related problems such as pollutant formation, mechanical stress, noise and the overall engine efficiency.

Reference to Figure 1·4 will assist in the definition of ignition delay and its occurrence in the sequence of events which constitute the combustion process.[45] Illustrated in the Figure is the pressure profile recorded in the combustion chamber during the compression ignition stroke. Curve 1 shows the smooth pressure-time curve resulting from the adiabatic compression of the gaseous charge in the cylinder without combustion taking

Figure 1·2

The Indirect Combustion Chamber

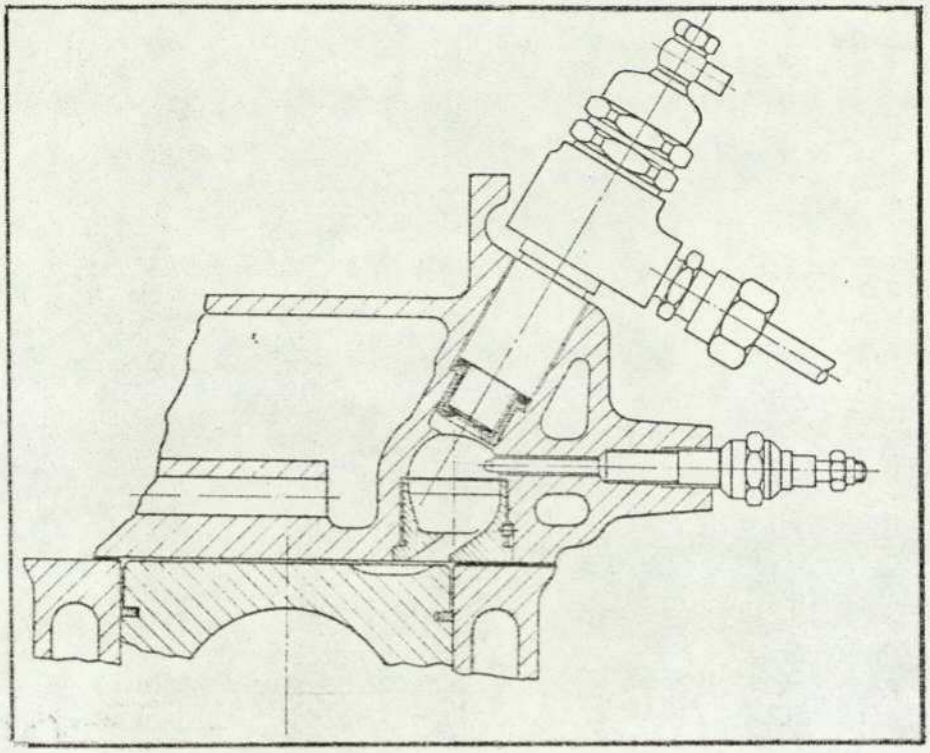

Figure 1·3

The Direct Combustion Chamber

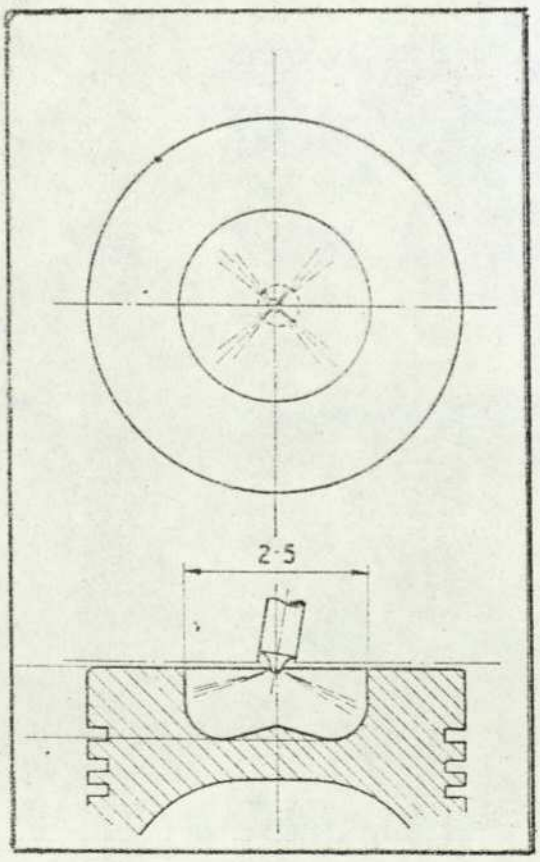

Figure 1·4

Time-Pressure Diagram of Compression and Expansion Strokes in a Diesel Engine

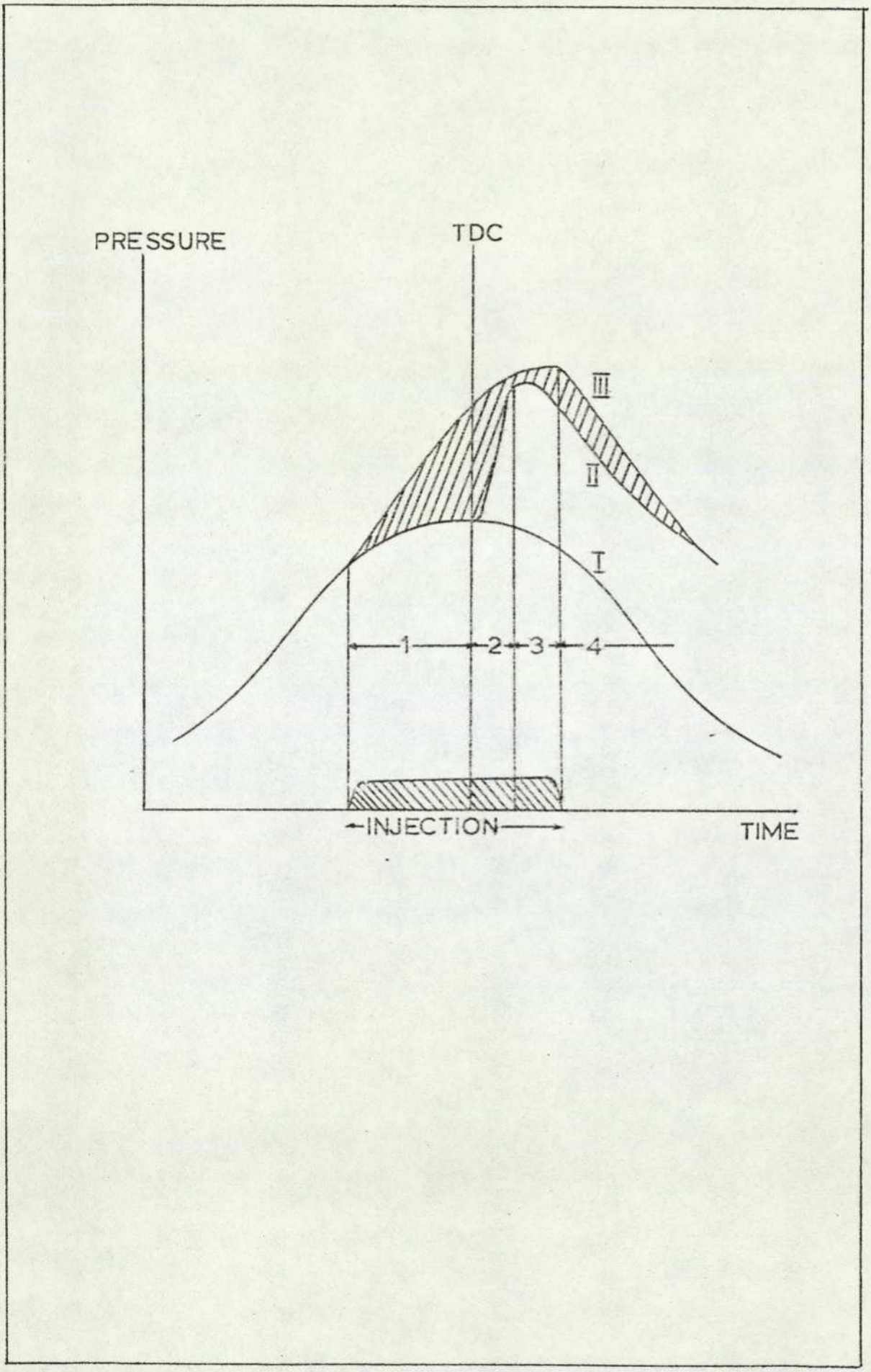

place, e.g. under inert atmosphere conditions. Curve II depicts the ideal combustion of a homogeneous fuel-oxidant mixture commencing immediately on fuel injection, resulting in the formation of carbon dioxide and steam. Curve III illustrates the actual combustion curve, a more complex pressure-time trace resulting from the interaction of physical and chemical phenomena.

To assist in the description of the combustion trace, it is convenient to divide it into four consecutive time periods.[46] Period 1 is the ignition delay period, which commences as depicted with injection of fuel into the cylinder and terminates when the pressure rise caused by combustion results in deviation from the motored pressure-time trace. This period is defined more precisely as the pressure rise delay period and is shorter in duration and more reproducible than the illumination delay[47] period . . This latter period starts simultaneously with injection and continues until chemiluminescent radiation, possibly from the excitation of formaldehyde molecules and high temperature carbon atoms, is observed. The ignition delay period is fundamental in determining the character of the resulting combustion mechanism and a more explicit description of its nature will be given later.

Period 2 is characterised by a rapid pressure rise which results from the exponential acceleration of the reaction rate to an explosive state and the propagation of flame fronts through the boundary layers enveloping the individual fuel sprays. The combustion in this period is essentially the burning of a premixed flame.[48]

Period 3 lasts longer than the previous period and has the characteristics of a diffusion flame[49] . The temperature in the cylinder at this stage of the combustion process is very high and consequently the evaporation and combustion rates are exceedingly large. The rate of fuel injection therefore exhibits limiting control over the rate of the combustion process.

Period 4 consists of the continuation of the combustion process during the last part of the expansion stroke[47] after fuel injection has ceased. Information about the nature of the processes occurring during this period is very limited.

An attempt to describe some of the aspects which contribute to the complexity of the physical and chemical phenomena involved in the aforementioned transitory periods will now follow commencing with period 1, the ignition delay period.

1.4.2.1 The Ignition Delay, Period 1

The injection of the liquid fuel into the combustion chamber in the form of a spray marks the commencement of the ignition delay period. During this period a combination of physical and chemical processes determine the nature of the resulting combustion mechanism starting with autoignition. The physical processes involved may be listed as follows:-

1. Spay disintegration and droplet formation.
2. Heating of the liquid fuel and evaporation.
3. Diffusion of the vapour into the air to form a combustible mixture.

At some stage during these processes the rates of the chemical reactions increase until the combustion becomes completely chemically controlled. The chemical processes involved are:-

1. The decomposition of the heavy molecular weight hydrocarbons into lighter molecules.

2. The preignition reactions between these lower molecular weight hydrocarbons and other fuel components and oxygen.

Much discussion has centred on the relative importance of the physical and chemical processes in determining the length of the ignition delay period. Both processes are initiated on injection and initially physical processes must occur before gas phase oxidation can take place.

However, the two types of process overlap to a large extent and the chemical phenomena very rapidly assume control of the combustion process.

A qualitative description of the ignition delay period begins with disintegration of the fuel jet. Fuel initially enters the combustion chamber as a sheet or ligament ultimately breaking up into a spray of different size droplets with different distribution patterns. The initial pressure of the jet is low and therefore the initial velocity relative to air is low. At this stage, jet disintegration is caused by ever present surface effects producing large slow moving droplets of spherical geometry. As the pressure increases, aerodynamic forces feature more prominently in the turbulence and the droplet size decreases as the velocity increases. In a modern diesel engine, turbulence is high enough to produce jet disintegration at very short distances from the injector nozzle[50]. Figure 1.5 illustrates a cross-sectional view of the spray structure in stagnant air. Particles of air are entrained in the spray at the point of turbulence and consequently the mass-flow in the x direction increases. According to the law of conservation of momentum and due to the frictional drag, the velocity of the droplets in the x direction decreases whilst a concurrent spread in the y direction takes place.

The formation of small diameter droplets is critical in determining the length of the ignition delay[51]. The surface to volume ratio and the heat transfer coefficient both increase as the droplet size decreases thus resulting in an increase in the rate of vaporisation.[47]

The first droplets are relatively large and slow-moving and start at the centre of the spray only to be pushed sideways to the spray periphery by the rush of incoming droplets which are smaller and travelling at higher velocities. The droplets at the axis become less efficiently atomised. At the spray front the droplets meet the highest aerodynamic resistance but the spray penetrates the air because the droplets retarded at the front are continually replaced by new high momentum ones. Accordingly the droplets

Figure 1·5

Cross-Sectional View of Fuel Spray in Stagnant Air

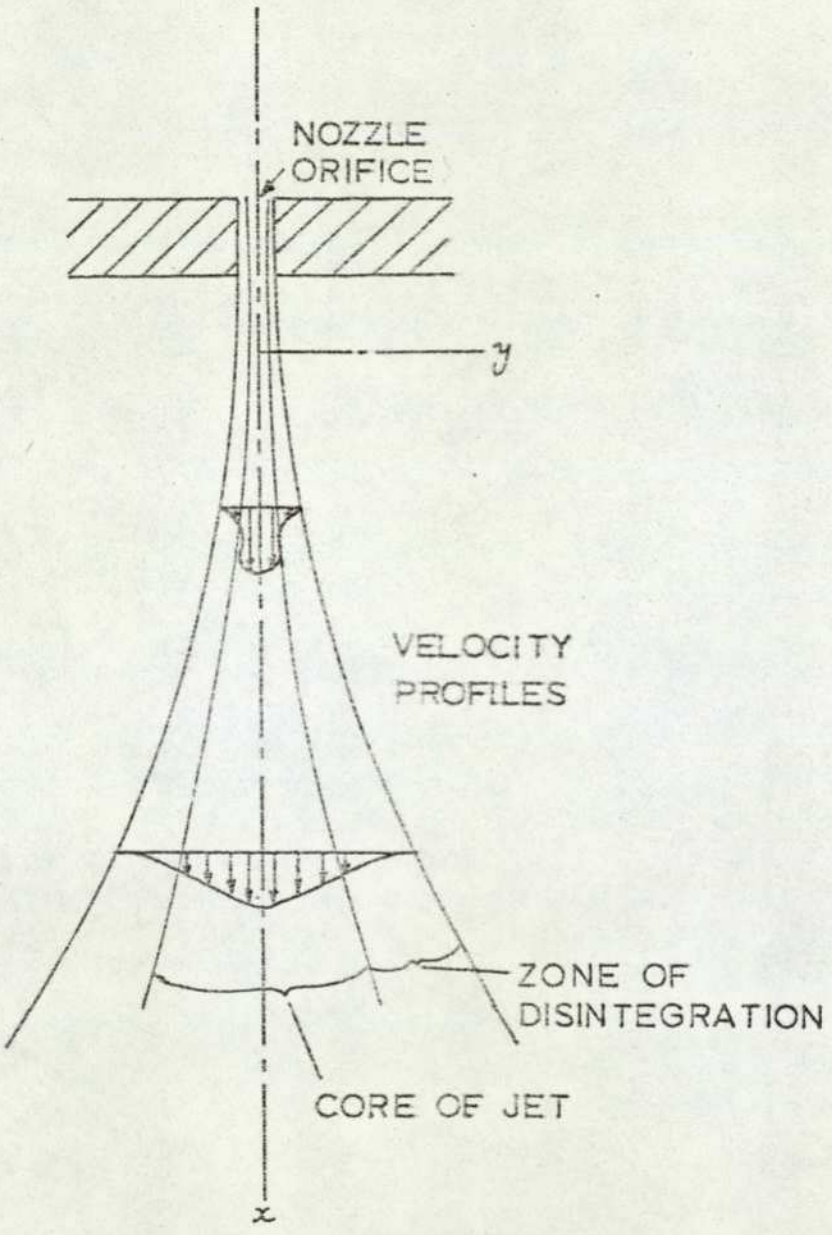

somewhere in the periphery of the spray are the earliest ones in the injection sequence. These evaporate very quickly and mix with the air.

It is interesting to note that all the evidence collected from outside engines i.e. constant volume bomb experiments, suggests that jet disintegration is not an important part of the physical delay period. Chow[52] and Yu[53] indicate, however, that neither injection lag nor jet disintegration are negligible in an engine.

Standard texts are available for the rigorous mathematical treatment of droplet formation and distribution patterns. Qualitatively the droplet breakup continues whenever the Weber number, which is the ratio of inertia body forces to surface tension forces, is exceeded. Hinze[54] suggests that the critical Weber number is 10. Droplet diameter decreases with a reduction in injector nozzle orifice diameter[55,56] and an increase in cylinder pressure.[57]

The complexity of the spray characteristics increases with the extent of droplet vaporisation. The literature contains many attempts to model the vaporisation process, some of the more exacting analogues approaching empirically derived results. The vaporisation process is critical in determining the nature of the ensuing combination mechanism. A complete description of spray formation and droplet vaporisation, for example, would indicate where in the temporal and spatial coordinates of the combustion chamber, autoignition was most probable, and by which particular fuel component or components it was initiated. Greater understanding of pollutant formation and possible methods for their elimination would then be achieved.

A preliminary investigation of the physical and chemical counterparts of the ignition delay may suggest that the fuel vaporisation is the rate-determining process. Constant volume bomb investigations by Hurn[58] have revealed, however, that the pressure drop due to fuel vaporisation begins almost immediately with injection and that the rate of the pressure drop is directly proportional to the estimated rate of fuel injection.

These observations indicate the very fast evaporation rate for the fuel in question. Miller on the other hand has produced high-speed photographic evidence[59] to show that combustion begins long before vaporisation is complete. Further photographic information is provided by Rothrock and Waldron[60] who photographed fuel in the diesel combustion chamber and concluded that there was considerable vaporisation of the injected fuel before combustion and that this vaporisation affected the course of combustion.

Wentzel's approach to the problem involved computation of the time required to vaporise fuels[61], which led to the conclusion that small droplets vaporised within 0.5×10^{-3} seconds. Schmidt[62] recognised Wentzel's calculated results but suggested a formula for ignition delay based on chemical reaction rates alone.

Out of this confusion of evidence the following observations may be made unequivocally:-

1. An increase in inlet air pressure and temperature, in fuel temperature and in water jacket temperature, produces a decrease in ignition delay to varying degrees.

2. Ignition delay decreases with engine speed. Although this has been attributed to turbulence, Small[63], showed that, in a bomb, increased turbulence did not give increased ignition delay. The effect on ignition may be explained in terms of an increase in cylinder temperature with speed.

3. The apparent existence of chemical control is indicated by the data contained in Figure 1·6, which illustrates the ignition delay for three different fuels plotted against air temperature. Inspection of this shows that, at any intake air temperature, gasoline (which has the highest volatility) exhibits the longest ignition delay and yet diesel fuel with much lower volatility has a much shorter ignition delay. Whilst there is no doubt that the rate of physical processes such as evaporation and diffusion increase with fuel volatility, it appears that these factors

Figure 1.6

Ignition Delay vs. Air Temperature for Three Different Fuels

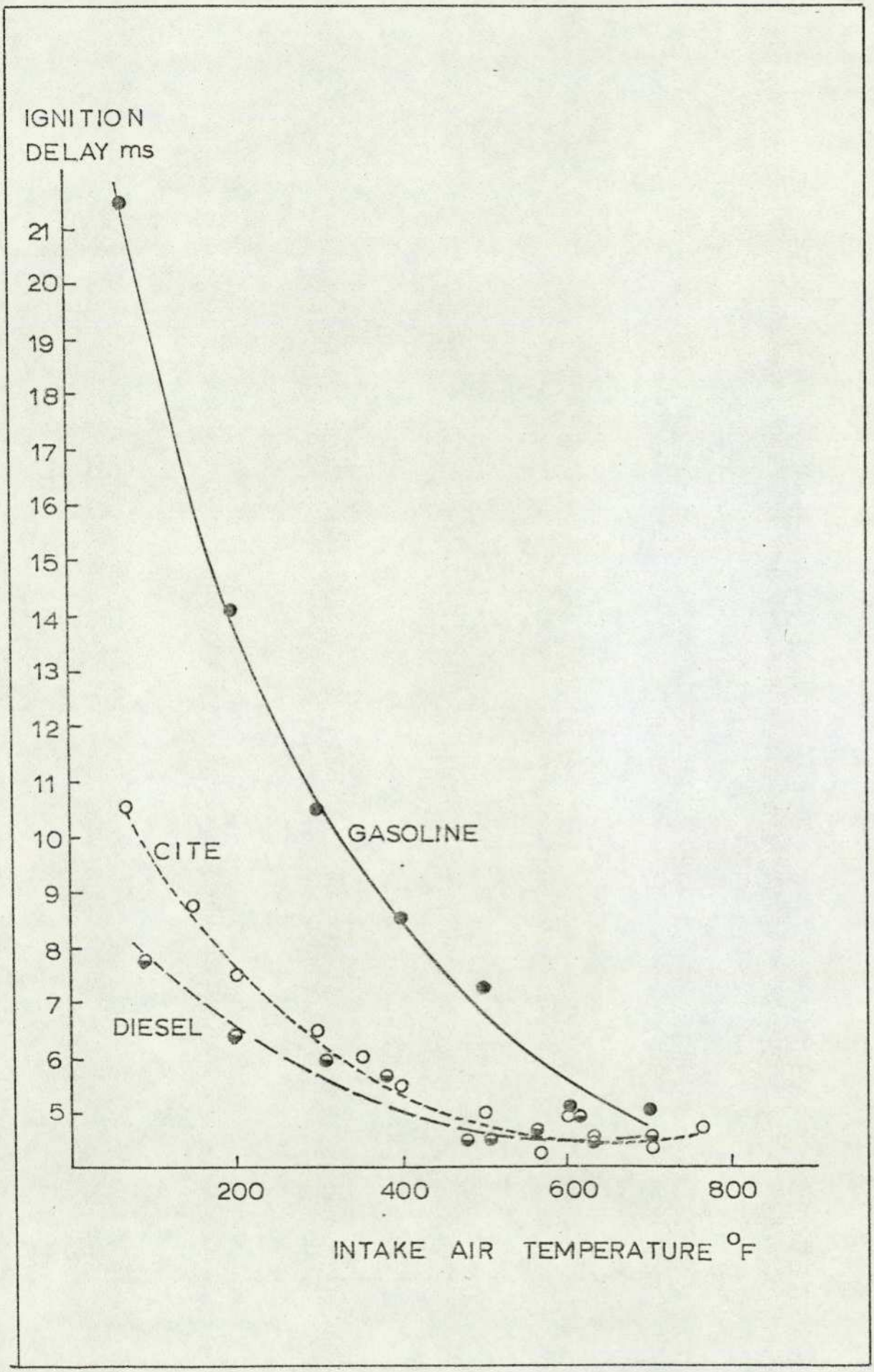

are of secondary importance compared with the chemical nature of the fuel. In addition it has been observed that isooctane and n-heptane have markedly different ignition lags but about the same volatility.

4. Constant volume bomb results would appear to indicate the rate-controlling nature of the chemical processes in that the ignition delay is a function of air temperature and pressure and oxygen concentration[47] all of which affect the rate of chemical reactions. Meanwhile the effects of the amount of fuel injected, the rate of fuel injection, injection needle opening pressure and nozzle size (all of which affect the physical processes) were observed to be small. Other observations made by Stringer et al[64] using a continuous flow apparatus have shown the great influence of temperature and pressure - in that order - on the ignition delay of many fuels. Factors which affect the physical processes such as air velocity, air-fuel ratio and intensity of air turbulence, have a negligible effect on ignition delay.

5. It has been shown that small concentrations of additives affect ignition delay and since the influences of these on the physical processes of spray formation etc. is slight, it is apparent that these compounds act in a chemical manner.

A closer investigation of the vaporisation process would appear to be warranted, since the oxidation of the fuel is initiated in the vapour phase, and the mechanism by which suitable conditions favourable to autoignition are generated ought to be considered.

1.4.2.1.1 Physical Ignition Delay Period 2

One of the most comprehensive definitions of the physical delay period states[65] that it is the time required for the physical changes to occur as the fuel changes from its liquid phase at the injection temperature to the vapour phase at the self-ignition temperature. The mathematical

treatment of this fuel vaporisation process is somewhat complex and fraught with a number of basic assumptions, the validity of which, as the literature shows, is open to much debate. El Wakil et al[51], for example, have formulated two models. The first considers the vaporisation of a single droplet and the second assumes the spray characteristics to be predominant. The single droplet model is based on the empirical heat and mass transfer coefficients of Ranz and Marshall[66] with corrections for high rates of mass transfer. The equations initially developed for steady-state vaporisation conditions were applied in the unsteady state behaviour on the assumption that a quasi-steady theory would be adequate. A critique of the equations and assumptions has been made[67] and the model is reported to work for droplet diameters>200 μm.

The single droplet model is justified in the case of diesel engine operation, since very short jet disintegration distances are involved, However allowance must be made for the three main interactions which occur, viz: reduction of the local air vapour mixture temperature, reduction in mass transfer because of locally high partial vapour pressures of the fuel, and local air motion caused by transfer of momentum from the droplets to the air. El Wakil[51] has made allowances for the first of these assumptions in his second model which is based on the concept of adiabatic saturation.

Henein[65] concludes from his studies that the physical delay period is not the rate-controlling process in the overall ignition delay period. The chemical reactions leading to autoignition are thus believed to be the rate controlling processes, a deduction supported by experimental observations in both engine and constant volume bomb systems.

1.4.2.1.2 Chemical Ignition Delay

The chemical ignition delay is defined as the period of time which elapses between the end of the physical delay and the point of self-ignition. During this period, reactions leading to the self-ignition point occur at an increasing rate as the temperature of the reactants increases. The end of the chemical delay period is often experimentally determined as the point at which the pressure rise deviates from the cylinder pressure time-trace obtained from injection of the fuel into an inert nitrogen atmosphere. At this point the reactions are sufficiently exothermic to invoke the rise in cylinder pressure above the motored pressure-time recording.

It is evident from the discussion of hydrocarbon oxidation in Section 1.3 that the chemical ignition delay encountered in the engine is synonymous with the time required for the critical concentration of the branching agent to accumulate.

The oxidation mechanism can be represented by a simple series of consecutive reactions, governed by first order kinetics with respect to the fuel.

$$[\text{Fuel}] \xrightarrow{k_1} [\text{I}] \xrightarrow{k_2} [\text{Products}]$$

The rate of fuel consumption can be expressed as:

$$-\frac{d[\text{Fuel}]}{dt} = k_1[\text{Fuel}] \qquad (1)$$

and the rate at which the intermediate is formed by:

$$\frac{d[\text{I}]}{dt} = k_1[\text{Fuel}] - k_2[\text{Products}] \qquad (2)$$

The rate of formation of the products can be similarly defined:

$$\frac{d[\text{Products}]}{dt} = k_2[\text{I}] \qquad (3)$$

Now if steady state conditions are assumed where:

$$\frac{d[\text{Fuel}]}{dt} + \frac{d[\text{I}]}{dt} + \frac{d[\text{Products}]}{dt} = 0 \qquad (4)$$

integration of equation (1) gives

$$[\text{Fuel}] = [\text{Fuel}]_o e^{-kt} \tag{5}$$

where $[\text{Fuel}]_o$ = the initial concentration of the fuel.

Substitution of (5) into (2) gives:

$$\frac{d[I]}{dt} = K_1 [\text{Fuel}]_o e^{-k_1 t} - k_2[I] \tag{6}$$

and integration yields:

$$[I] = [\text{Fuel}]_o \frac{k_1}{k_2 - k_1} (e^{-k_1 t} - e^{-k_2 t}) \tag{7}$$

The rate of change in product concentration can be ascertained using the fact that

$$[\text{Product}] = [\text{Fuel}]_o - [\text{Fuel}] - [I] \tag{8}$$

which leads to

$$[\text{Product}] = [\text{Fuel}]_o \left(1 - \frac{k_2 e^{-k_1 t} - k_1 e^{-k_2 t}}{k_2 - k_1}\right) . \tag{9}$$

The variations with time of [Fuel], [I] and [Products] are shown schematically in Figure 1.7. The concentration of the fuel falls exponentially with time according to equation (5). That of the intermediate, I, starts at zero and finishes at zero since I is finally converted to products. The rate of formation of the products is proportional at any time to the concentration of the intermediates. Thus the rate is initially zero, passes through a maximum when [I] is a maximum and gradually falls again to zero.

The above steady-state treatment of the reaction scheme assumes isothermal conditions. An increase in the temperature arising from the exothermicity of the reaction governed by k_2 will increase the overall reaction rate. The effects of temperature and other parameters on the rate of formation of the intermediate will now be studied in more detail.

Figure 1·7

The Variations with Time of [Fuel], [I] and [Products]

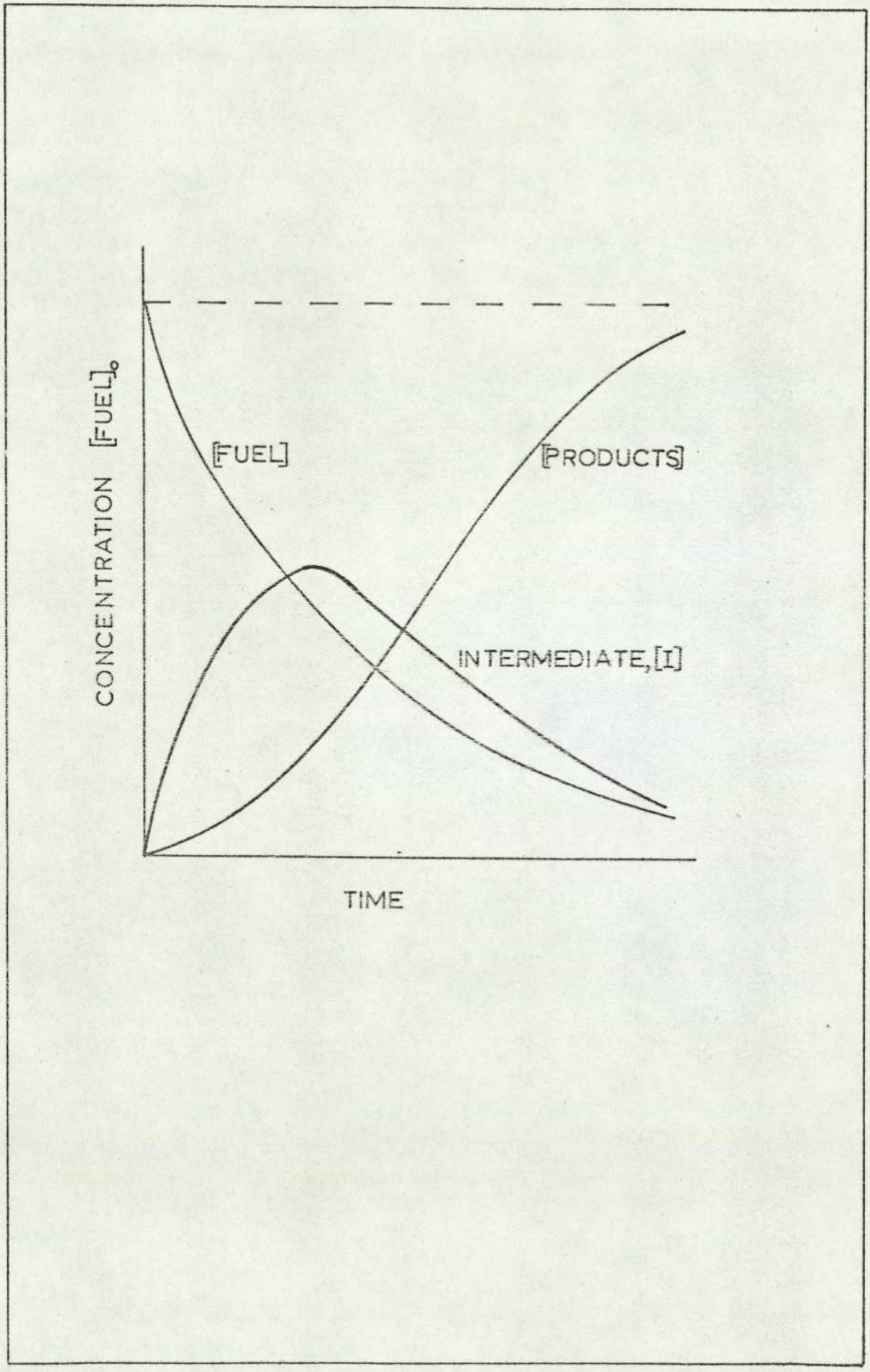

Consider the more definitive scheme,

$$(2)\quad a[\text{Fuel}] + b[O_2] \xrightarrow{k_1} c[I] \xrightarrow{k_2} d[\text{Products}]$$

where a, b, c and d are the number of moles involved in the reaction. In the initial stages of the reaction the rate of accumulation, $\nu_{[I]}$, of the intermediate can be represented by

$$\nu_{[I]} = \frac{d[I]}{dt} = k_1[\text{Fuel}]^a[O_2]^b \qquad (10)$$

since the second stage of the reaction involving the decomposition of I is insignificant until $[I] \longrightarrow [I]$ max.

The rate constant, k_1, is related to the activation energy of the process and the temperature by the Arrhenius equation, ie:

$$k_1 = Ae^{-Ea/RT} \qquad (11)$$

where A is the pre exponential factor, Ea is the activation energy, R is the universal gas constant and T is the absolute temperature.

Substituting (11) in (10) gives,

$$\nu_{[I]} = \frac{d[I]}{dt} = Ae^{-Ea/RT}[\text{Fuel}]^a[O_2]^b \qquad (12)$$

and since the chemical ignition delay, ψc, is inversely proportional to the rate of reaction, ie:

$$\nu_{[I]} \propto 1/\psi_c \qquad (13)$$

equation (12) becomes,

$$\frac{1}{\psi c} = A_1 e^{-Ea/RT}[\text{Fuel}]^a[O_2]^b \qquad (14)$$

where A_1 contains a constant of proportionality.

Since the ignition of hydrocarbon - air mixtures occurs between narrow limits of the F/A ratio, it can be assumed that the ratio of the fuel to oxygen concentration is constant and that equation (14) can be reduced to:-

$$\frac{1}{\psi c} = A_2 e^{-Ea/RT} \qquad (15)$$

where A_2 contains a parameter related to the fuel concentration.

The critical concentration of the intermediate compound, [I], which

is needed to start the reaction and cause a detectable pressure increase may be considered constant and to depend upon the total mass and heat capacity of the charge in the combustion chamber. The ignition delay, I.D. in a diesel engine can therefore be expressed as follows:-

$$I.D. = A^1 e^{Ea/RT} \qquad (16)$$

where A^1 is a constant which depends on the design of the combustion system.

The activation energy,Ea, sometimes called the global activation energy, increases in magnitude as the cetane number of the fuel decreases. The ignition delay is therefore expected to increase as the cetane number increases, as Figure 1·8 shows. The cetane number of a fuel has only qualitative significance and simply serves to place fuels in order of ease of ignition. The cetane number increases almost linearly with the number of carbon atoms in the main backbone , while addition of side chains decreases the cetane number. It will be noticed that these trends are a reversal of those obtained in relation to the octane number, ie: fuels with high cetane numbers eg: high molecular weight alkanes have low octane numbers and fuels with low cetane numbers eg: aromatic fuels have high octane numbers, Table 1·1

A review of ignition delay formulae[47] derived empirically from experiments performed in engines, flow systems and volume bombs, indicates that the inclusion of a pressure term in equation (16) improves the general applicability of the relationship, ie:

$$I.D. = \frac{A^1 e^{E/RT}}{p^n} \qquad (17)$$

where p is the absolute pressure raised to an exponent n. Inspection of this formula indicates that an increase in either the pressure or temperature results in a decrease of the ignition delay. Moreover, I.D. is more sensitive to temperature changes than to pressure changes.

Figure 1.8

The Variation of Ignition Delay with Cetane Number

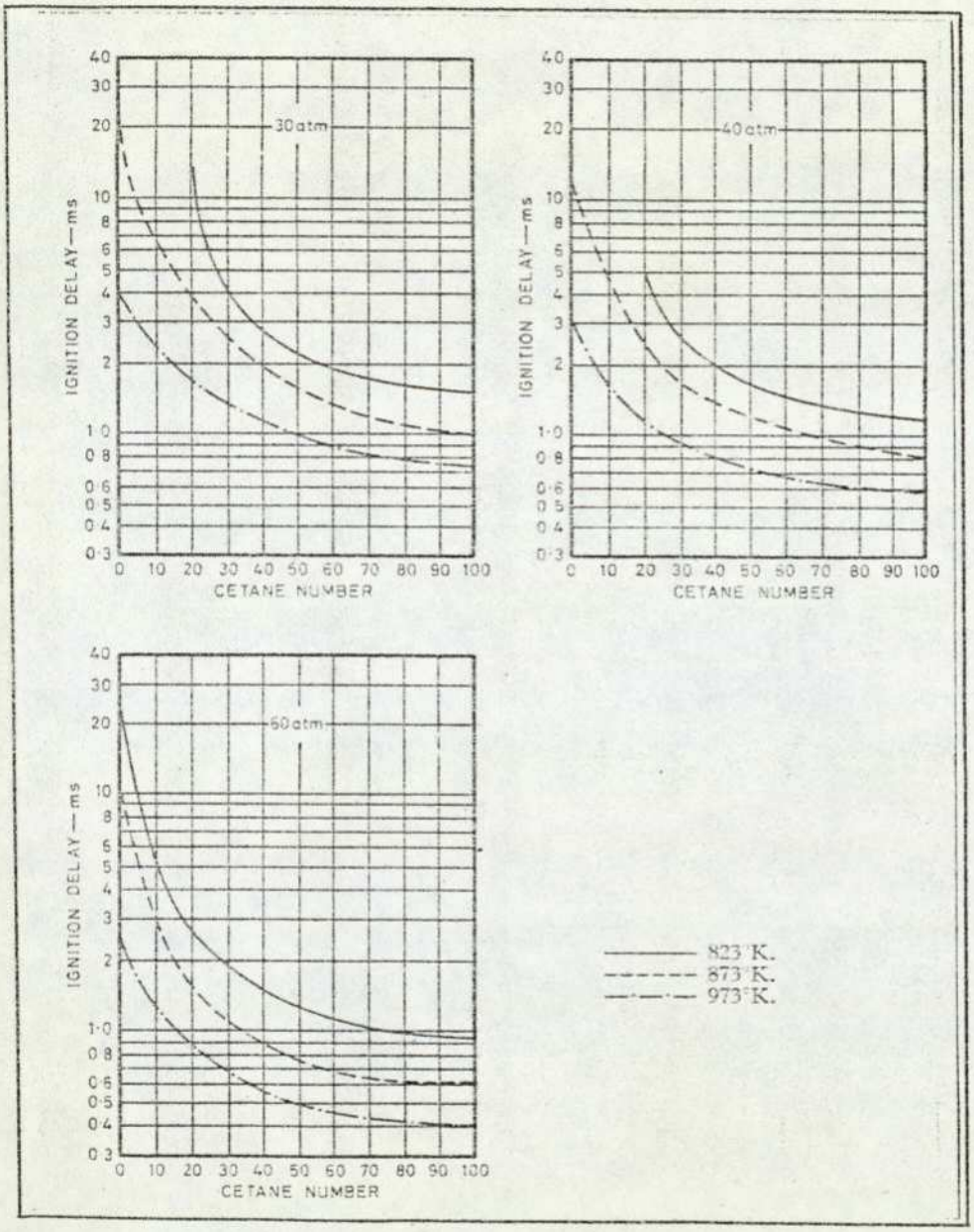

Table 1·1

Cetane and Octane Numbers of Various Hydrocarbon Fuels

Fuel	Cetane No.	Octane No.	
		Research	Motor
n-heptane	56·3	0	0
n-octane	63·8		
n-decane	76·9		
n-dodecane	87·6		
n-tetradecane	96·1		
n-hexadecane	100·0		
Octadecane	102·6		
1-octene	40·5	28·7	34·7
1-decene	60·2		
1-dodecene	71·3		
1-tetradecene	82·7		
1-hexadecene	84·2		
1-octadecene	90·0		
Methylcyclohexane	20·0	74·8	71·1
Dicyclohexane	47·4		
Decalin	42·1		
Isooctane			100
Benzene			140
Cyclohexane			77
n-Pentane			62

1.4.2.2 Premixed Burning. Period 2

The second stage of the combustion process is characterised by a rapid increase in the cylinder temperature and pressure, as those regions of the combustion chamber containing fuel and air of the correct stoichiometry undergo spontaneous ignition. The rapid rise in temperature resulting from this highly exothermic process serves to increase the rate of vaporisation and diffusion, thus extending the ignition region.

Henein[68] has formulated a very useful phenomenological model, which places the chemical and physical mechanisms involved in the combustion process in the spatial and temporal coordinates of the combustion chamber. This model has been formulated on the basis of photographs showing flame development and other observations produced by many independent workers. A brief description of the model will now follow.

1.4.2.2.1 Henein's Phenomenological Combustion Model

Photographs produced by Scott[69] showing the spray configuration in a direct - injection engine at the start of combustion enabled Henein to represent schematically[68] the shape of the spray as shown in Figure 1.9 The average distance between the fuel droplets is expected to change with their location in the spray, and is greatest near the edge downstream from the centre-line of the spray where the smaller droplets are concentrated. The average local fuel-air ratio,and consequently the combustion mechanisms, are therfore expected to vary from one location to another. The distribution pattern of the F/A ratio for fuel in both the liquid phase and the vapour phase, is shown in Figure 1.9 . This distribution varies with the radial distance from the injector nozzle hole. However, at the downstream edge of the spray and for all distances, the F/A ratio always approaches zero and increases as the centre of the spray core is approached. Henein assumes,[68]

Figure 1·9

Schematic Diagram for a Fuel Spray Injected in Swirling Air

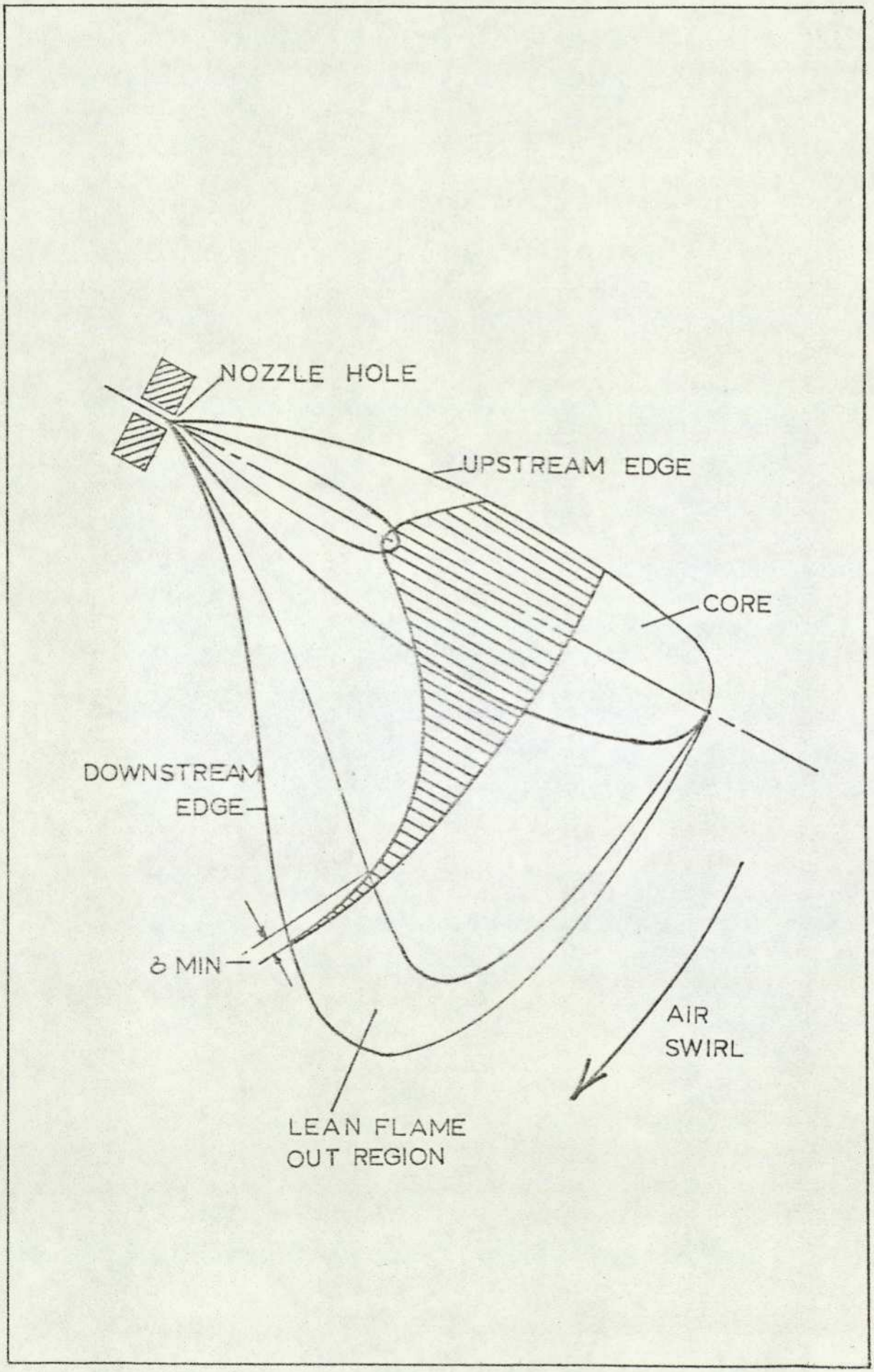

with justification, that most of the droplets carried away from the core will be completely evaporated before the start of combustion. Ignition therefore occurs, in the premixed fuel and air near the downstream edge of the spray. This statement is supported not only by the adiabatic saturation model of El Wakil,[51] but also by photographs of the actual combustion process.

Figure 1-10 shows the regions into which Henein subdivided the spray. The Lean Frame Region (LFR) contains F/A ratios which range from infinity near the spay core centre to a value which approaches zero near the spray edge. At some points near the extremities of the spray, the F/A ratio will be of the correct stoichiometry for autoignition and ignition nuclei will develop. Photographic evidence[69-71] verifies that the ignition process does commence in the spray envelope near the downstream edge of the spray. Flame fronts propagate from these ignition centres and combustion spreads through the spray envelope. Henein and Bolt[72] suggest that an alternative two-stage ignition process may occur in the microvolume regions under consideration.

The LFR has a low mass-averaged F/A ratio[70] which leads to complete combustion of the fuel. From the pollutant formation aspect, the LFR is relatively free of HC formation but NOx may be formed in high local concentrations. Under very light loads, the temperatures may not be high enough to produce NOx concentrations during this early stage of the combustion process.

The spray region enveloping the LFR consists of F/A ratios below the lean ignition limit, and is termed the Lean Flame Out Region, LFOR. Here the main reactions are fuel decomposition and partial oxidation. The thermal decomposition products consist of low molecular weight hydrocarbons, while aldehydes typify the oxygenated products formed. It is believed that this region is one of the main contributors to the emission of HC and of some of the odorous constituents in the exhaust.

The extent of the LFOR determines its contribution to the total

Figure 1·10

Henein's Phenomenological Model - Mechanisms of Combustion of a Fuel Spray Injected in Swirling Air

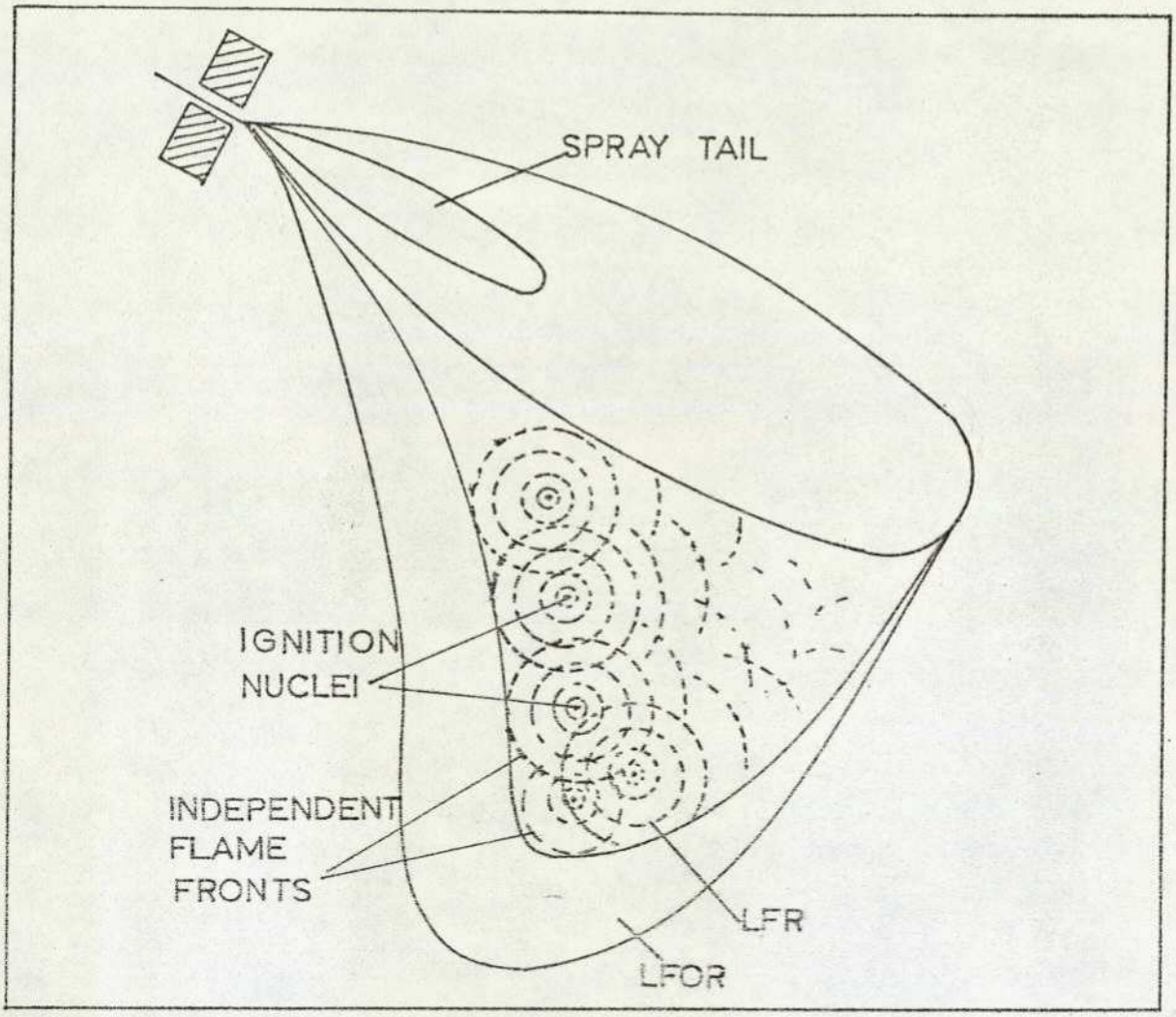

Figure 1·11

Schematic Diagram of Diffusion Flame Surrounding a Fuel Droplet

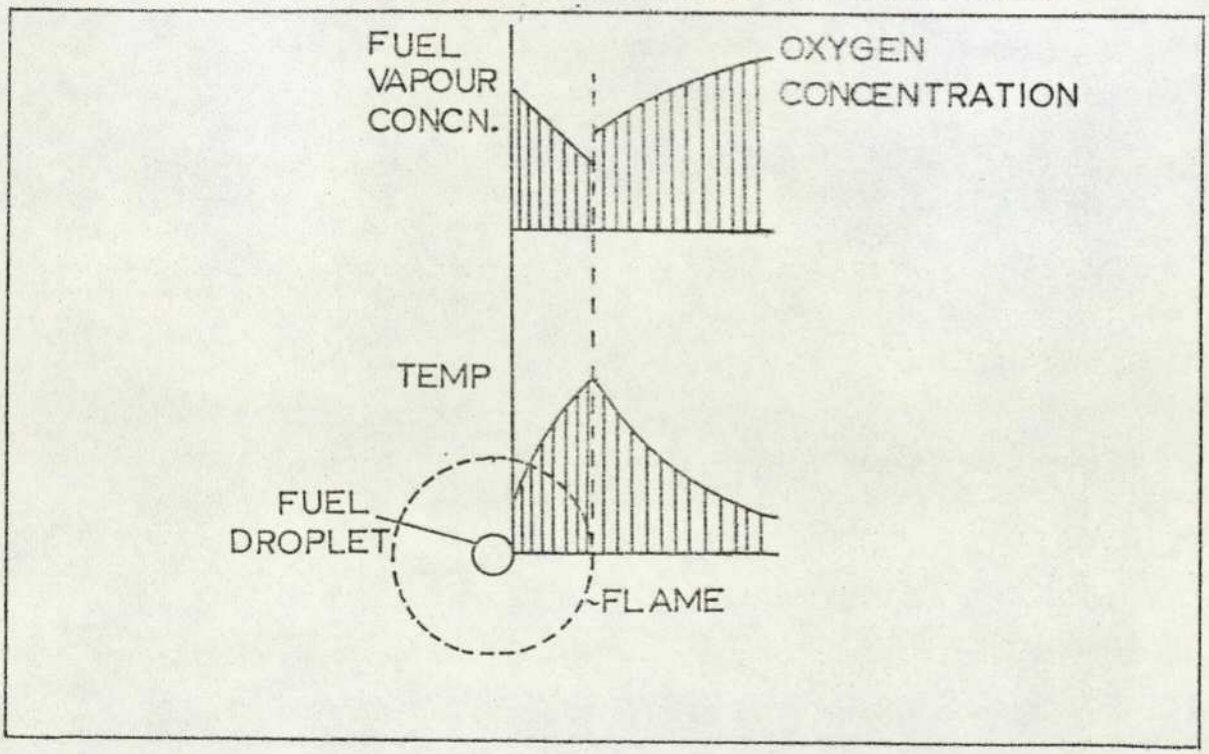

output of pollutants. It is important, therefore, to consider those factors which are likely to affect the size of the LFOR. High temperatures and pressures promote combustion of leaner mixtures and thus the LFOR is reduced. The cylinder temperature and pressure are related to the overall F/A ratio turbocharging and coolant temperature. In addition to these factors, the air swirl and the chemical composition of the fuel also affect the extent of the LFOR, thus illustrating the complexity of interdependent relationships which determine how much fuel is subjected to combustion at the lean flame limit.

At the borders between the LFOR and the LFR, Henein[68] suggests that hydrocarbon fuel molecules react to form carbon monoxide, hydrogen and steam together with the species $\dot{O}$,$\dot{H}$ and $\dot{O}H$. Fristrom and Westernberg[73] suggest that a paraffin fuel molecule undergoes the reactions,

$$C_nH_{2n+2} + \dot{O}H \longrightarrow \dot{C}_nH_{2n+1} + H_2O \qquad (1)$$

$$\dot{C}_nH_{2n+1} \longrightarrow C_{n-1}H_{2n-2} + \dot{C}H_3 \qquad (2)$$

$$C_{n-1}H_{2n-2} + O \longrightarrow \text{Oxygenated Products} \qquad (3)$$

Flame quenching in the LFOR is suggested as the mechanism by which oxygenated hydrocarbons, carbon monoxide and other intermediate compounds are formed. These reactions are discussed in more detail in Chapter 4

1.4.2.3 Diffusion-Controlled Burning, Period 3

Following ignition and combustion in the LFR, the flame propagates toward the spray core. Here the fuel drops are larger but the increase in local air temperature due to the exothermicity of the ignition process increases the rate of vaporisation and diffusion. Some of the smaller droplets will completely vaporise before being burnt within the rich ignition limit, while the larger droplets may be surrounded by a diffusion-type flame as shown in Figure 1·11. Landen[74] has obtained very convincing photographic evidence of the vapour surrounding individual droplets of fuel

undergoing diffusion burning, while Henein[47] states that many other[75] investigators have not observed such phenomena.

As the temperature of the combustion volume increases, the rate of the chemical reactions become so large in comparison with the rate of fuel injection that the latter process becomes the rate-determining step.

Pollutant formation during the diffusion burning of the spray core and the spray tail is very high, especially at high loads. Unburnt hydrocarbons, carbon monoxide, oxygenated compounds and carbon - which imparts luminosity to the flame - are all readily produced, together with NO_x, since the temperatures are very high.

The spray tail consists of the last fraction of fuel injected. The pressure differential across the injector nozzle is quite low at this stage, and therfore spray penetration and atomisation are low. Under high load conditions, insufficient oxygen for complete combustion reaches the spray tail. Due to the high temperatures, the fuel undergoes rapid evaporation and thermal decomposition. Partial oxidation of the pyrolysis products leads to many oxygenated products and carbon monoxide. The spray tail and fuel originating from secondary injection are now accepted as the major sources of carbon particles, (smoke) carbon monoxide and unburnt hydrocarbons.

Some of the fuel injected impinges on the combustion chamber wall. This situation arises particularly with small, high speed direct injection engines because of the shorter spray path and the limited number sprays. Combustion of this part of the fuel depends upon the rate of evaporation and mixing of fuel and oxygen. If the gas near to the liquid film surface has a low oxygen concentration, or the mixing is not efficient, evaporation will occur without complete combustion. Under these conditions, the fuel vapour will be pyrolysed and form unburnt hydrocarbons, partial oxidation products and carbon particles.

The Henein[68] model describes the progression of combustion in each

region of the spray. Figure1·12 summarises this progression and relates it to the cylinder pressure and mass average temperature at the start of combustion in each region. The formation of pollutants from each region, excluding wall impingement is shown schematically in Figure 1·13

Figure 1•12

Progression of Spray Combustion, Cylinder Pressure and Mass Average Temperature

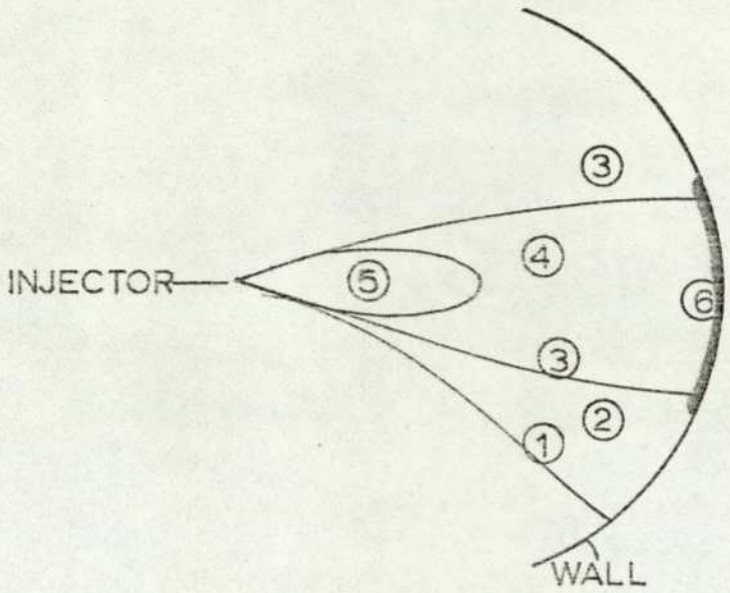

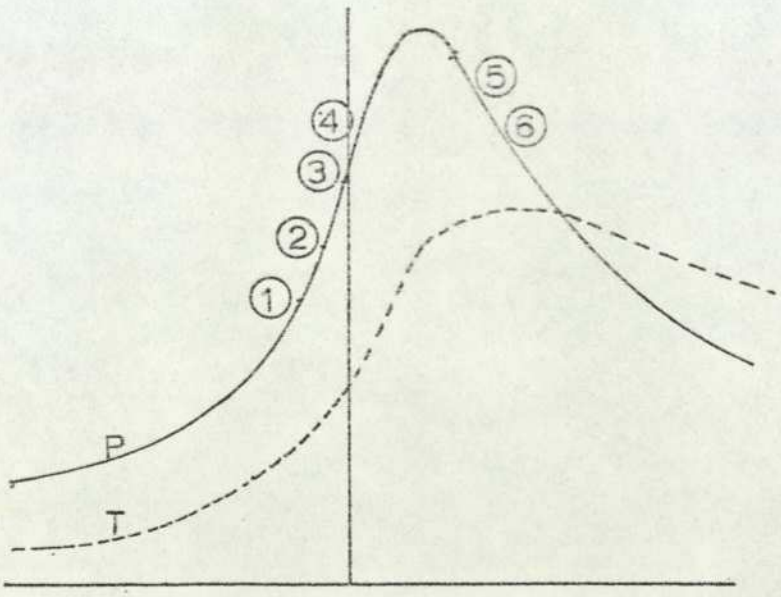

Figure 1·13

Emission Formation in a Fuel Spray Injected in Swirling Air

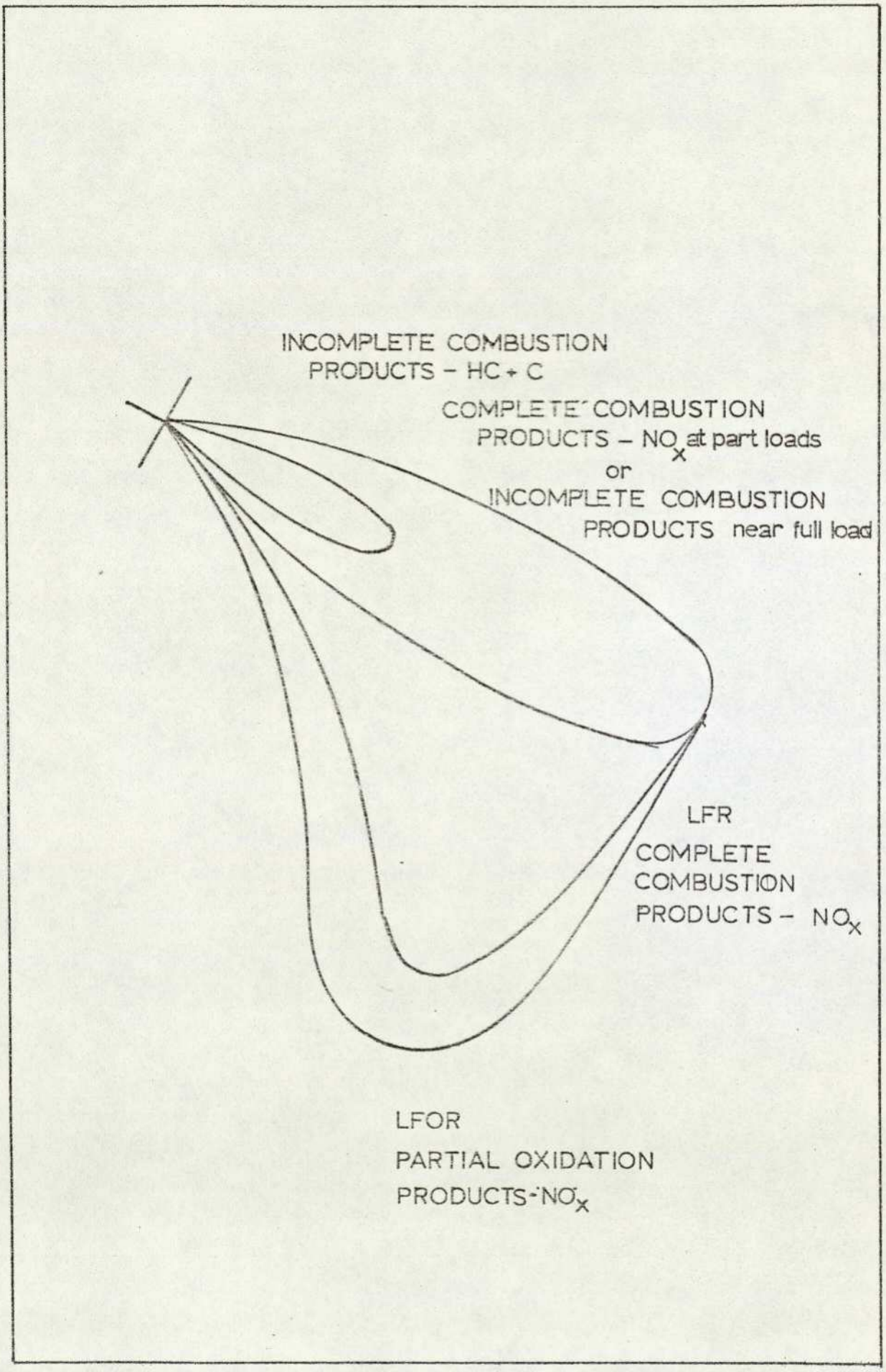

1.5 Aspects Of Odour Assessment

Rounds and Pearsall[76] suggest that four independent factors are integrated when an individual perceives an odorant, ie: (a) the odour quality (pungent, sweet etc.), (b) the odour intensity (strong, faint etc.), (c) the irritation quality (whether the nose, throat and/or eyes are affected), and (d) the irritation intensity (whether acute, slight etc.). Dravnieks,[77] on the other hand, proposes four 'odour dimensions' ie: intensity, detectability, acceptability and quality. The complexity of the perception mechanism is appreciated, when it is realised that odour sensation can differ in psychophysical (sensory) intensity, which is not synonymous with concentration difference. Odours can differ in acceptability or hedonic attribute (pleasantness versus unpleasantness) and in quality or character. Quality is understood in terms of the degree of similarity to various other odours. However, it is claimed that the most significant factor involved in odour comparison is the hedonic difference between the two odours.[78-79] Odours are frequently evaluated by human panels in pursuit of a variety of objectives; the panel selection methods and training vary accordingly. Selected, sensitive, consistent panallists, trained to optimise their sense of smell, are essential to product quality work but in pollution work have limited value.[77] Instead panels are selected to reflect a broad range of population sensitivities and thus provide more useful data relevant to the variety of human response patterns with which pollutant work is concerned. The training of such panellists must be performed with much care since unintentional manipulation by leading questions, biased scales, predictable odour presentation sequences etc; result in a high degree of consistency but reduce the significance of the results.

The following list of points will serve to illustrate some of the difficulties which can arise from the use of human panellists in the evaluation of odorants.

1. The human sensory response not only varies among individuals but also changes with time for a given individual.

2. Sensitive individuals can detect odours at concentrations below those readily measured by advanced analytical techniques.

3. The human sensory response to an odorant suffers from fatigue and adaptation effects.

4. Environmental effects, such as temperature, humidity and odour background,[80] can have important influences on odour evaluation.

5. Many personal attributes of an individual can influence the evaluation and assessment of odours. In this context age, sex, ethnic and social grouping, smoking and eating habits all influence the response of the panellist.

Despite these complications, it has been stated[81] that the human observer can, under carefully planned and controlled experimental conditions, respond as well as an excellent analytical instrument.

Dravnieks,[77] who has carried out much research into odour assessment, states that the number of panellists per panel should exceed 7, so that some simple statistical tests can be applied to the results; 9 or 10 panellists are preferable. This aspect of panel design, together with other considerations are discussed in the papers of Dravnieks[77] and Turk.[82] Despite the recommendation of at least 7 panellists, the work reported by many researchers who used only 1 to 3 individuals, is of much value in providing relative judgment data.

1.5.1 Odour Intensity and Detectability

Often the intensity of a particular odorant is expressed in units which are related to the threshold concentration. This quantitative assessment suffers from many inadequacies, not the least being an inability to predict the perceived odour intensities above the threshold limit. At

lower intensity levels, odours become difficult to perceive and therefore the odour threshold is expressed as a range of concentrations. The actual values depend on the type of test, panellist selection, detectability criterion etc. and can be defined only in the context of these parameters. The detection of an odour involves a decision process - the panellist may be absolutely certain that the odour is present, or feel fairly certain, or be not so sure etc. The criterion for a yes/no decision is influenced by his willingness to make an erroneous decision, which in turn depends on the consequences of 'yes' and 'no' judgments.[82-85]

Several researchers[76, 86-88] have used the threshold dilution technique to assess diesel exhaust odour intensity. It is sufficient to say that the absolute values produced must be viewed in the light of the foregoing discussion.

Several methods have been developed to measure the intensity of an odour. The simplest involves the assignment of a numerical or word scale to the odour sensation. Typically 4 - 7 categories are used. More categories, especially beyond 10, do not improve the intensity resolution, since the scatter in the judgments increases. A typical category[89] scale which is as good as any is :-

0 - No odour

1 - Just perceptible

2 - Faint

3 - Easily noticeable

4 - Strong

5 - Very strong

The numbers do not indicate how much stronger the sensation is, and once an odour has reached the fifth category no further intensity differentation is possible, ie: two odours rated at '5' can differ greatly in their intensities when compared directly.

Two laws, empirically deduced from odour panel studies, serve to relate the intensity of the odour stimulus to the concentration odorant. The

first of these laws, the Weber-Fechner law, states that the ratio of the intensity of the applied stimulus to the incremental change in intensity of the stimulus which is necessary to produce a 'just noticeable difference' in response, is independent of the original intensity of the stimulus. This law has been found to have widespread applicability[90] to sense perception.

Steven's law, which also is applicable to other physiological response patterns,[91,92] can be expressed mathematically:-

$$I \text{ (perceived)} = k X^{n}$$

$$\text{or } \log I = \log k + n \log X$$

where I is the intensity of the sensation, X is the concentration of the odorant and k and n are coefficients.

Odour intensity ratings are greatly assisted by odour intensity reference scales.[82,93-95] The intensity of the test odour is characterised by that concentration of a reference odorant which smells equally as strong. This technique obviates the difficulties inherent in the semantic and number scales and permits better intensity discrimination even with novice panellists. In a typical test routine the panellists smell the sample odour, X, and compare it with a set of prepared samples of scaled intensity. Turk[82] suggested a binary scale of 12 reference samples in which each successive bottle in the series contained twice the concentration of the odorant as the previous bottle. Comparisons are simplest when X and the reference odorant are similar in quality. However judgments are quite satisfactory even if the odour quality is very different.[93,94] The use of this technique to assess diesel exhaust odour requires the cooperation of a carefully trained panel of observers and the use of a special exhaust dilution—presentation facility.

In 1949 Arthur D. Little Inc. reported[96] the development of a sensory method for the qualitative assessment of an odorant. This technique enabled ADL to carry out an extensive research programme into diesel engine exhaust culminating in the development of the instrumental odour analysis system, which is also central to this particular study.

The ADL method produced qualitative and quantitative descriptions of the odour sensations, reported in terms of reference standards. The composite written description was reproducible and defined the effects of process changes on the odour of the exhaust as compared with the standard operating conditions of the engine.[97] The total odour sensation was described, generally by four to six character notes. The method was qualitative, since a verbal description of the odour qualities was given and the order of the odour character notes indicated their detection as a function of time.

The intensity of each character note as well as the total intensity of aroma (TIA) was rated on a four point intensity scale: not detectable (0), slight (1), moderate (2) and strong (3) intensities. With experienced panellists, the basic four point intensity scale can be extended to a seven point scale by the use of one-half ratings ie:

Numerical Rating	Intensity
0	Not detectable
½	Very slight
1	Slight
1½	Slight to moderate
2	Moderate
2½	Moderate to strong
3	Strong

Two feeling sensations, ie: nose and irritation, were indicated if present by a check mark (✓) without attempting to describe their intensity.

Each ofthe four trained panellists, forming the odour profile panel, entered an odorised static test chamber, and sniffed the air three times. Each panellist recorded his observations on the TIA, odour character notes perceived, and the order of appearance and intensity of the notes. After the observations in the test room, the panellists gathered to report their results. Reference was made to odour standards to assist agreement

on the various verbal descriptions used and to aid the development of a common language for describing the odour quality. The panels' results were then composed in an odour profile which summarised the odour observations of the four panellists and indicated the odour quality, the order of appearance of the character notes, and their relative intensities.

The profile description of the diesel exhaust odour in the test room at a dilution of 600:1 is summarised below:

TIA	2
Smoky burnt	2
Oxidised oil	1½
Kerosene	1½
Nose irritation	✓
Eye irritation	✓

Owing to the inherent variability in odour intensity measurements, particularly over an extended period of time; combined with the difficulty in distinguishing small differences in intensity based on recalled standards, ADL devised a second method of odour measurement.

The dose/response method initially involved the use of the static test chamber, but was later refined into a kinetic odour measurement method. In this technique, the exhaust was presented in five concentrations ie: 0.2, 0.4, 0.8, 1.6 and 3.2 $/m^3$ or dilutions of 6000:1 to 300:1. These were presented first in increasing order, then in random order. The primary response for each of the four panel members at each test condition was the TIA value, although profile descriptions were also reported. The TIA values ranged from barely detectable to strong. The advantage of this method of presentation is that all of the individual intensity values obtained for five concentrations, in two sets, can be summarised by averaging the intensity responses for each concentration. The intensity vs. log concentration data can then be plotted and the regression line can be fitted.

Thus $I = a + b \log_{10} C$

Where C is the concentration of exhaust, ℓ/m^3 of dilution air, I, is the intensity of that exhaust at ℓ/m^3 and b is the slope of the line. The intercept value, a, (ie: exhaust diluted to 1000:1) describes the intensity of the exhaust sample with the most reliability. The calculated intensity, (I), has become the numerical value used in developing correlations with and calibration of the oxygenates expressed as $\mu g / \ell$ of exhaust.

Organic fractions, isolated by liquid chromatography from the trapped exhaust, were also presented and assessed in a manner similar to that just described for the exhaust gas odour assessment, One refinement which was necessary for the presentation of these fractions involved the use of a moving air stream to carry the evaporated fraction to the panellist. The organic fractions were dissolved in nonane and injected by means of a motor driven syringe into the air stream. One advantage of this presentation system over the static test lay in the covert manner of sample presentation to the panellist thus enabling an unbiased report for the detection of low concentrations. The odorised air stream was mixed uniformly in a Kinex static mixer, before it entered the aluminium-clad odour test chamber. Using this procedure, the total organic extract (TOE), of the exhaust, and the aromatic and oxygenate fractions could be presented to the panellists for the dose/response assessment. Figure1·14 shows the odour intensity of the TOE and the separated aromatic and oxygenate fractions vs presented exhaust concentrations. It is clear that the oxygenate fraction is more representative of the total exhaust odour. The separation and characterisation of the aromatic and oxygenate fractions will be described in some deatil in section 1.5.5.2

1.5.2 Odour Quality

Odour character or quality is a difficult concept to define.

Figure 1.14

Odour Intensity vs. Concentration of TOE, Aromatic and Oxygenate Fraction of Diesel Exhaust

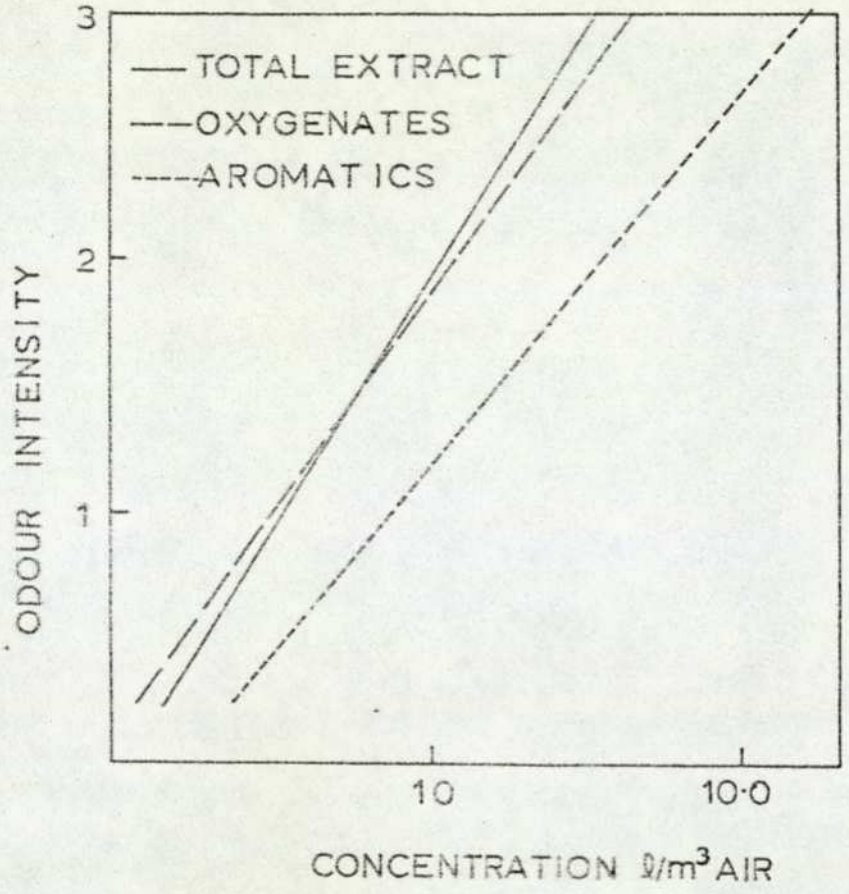

Researchers are now convinced that odours cannot be neatly fitted into a limited number of odour 'types'. Instead, an odour can be characterised in terms of its similarity to other odours or by listing appropriate sensory attributes.

Turk[82] has suggested that diesel exhaust possesses four essential quality 'notes'-burnt, oily, pungent and aldehydic. In order to assess whether these notes are present in a particular exhaust sample, the Turk reference odour kit contains 16 bottles consisting of four concentrations of each of the four quality standards. Each reference odorant consists of a number of carefully blended components mixed in specified proportions, to give an overall odour which is similar to each identifiable quality descriptor. The sample odour is then compared with each of the four quality reference standards to ascertain which descriptors are applicable and then to establish, by means of the concentration series, the contribution of each descriptor to the total odour character.

1.5.3 Odour Acceptability

Odour acceptability is strongly dependent upon the context in which it is perceived. An odour which 'does not belong' is much less acceptable than the same odour arising within its expected environment. However, studies[98] have shown that there are many odours which are almost universally accepted as unpleasant. The same also applies to some 'obviously pleasant'odours, although the diversity of opinion is broader. In addition, many other odours fall in between these extremes and tend to be reported as neutral, pleasant or unpleasant with much inconsistency.

A seven point hedonic scale has been devised to categorise the pleasantness/unpleasantness of an odour:-

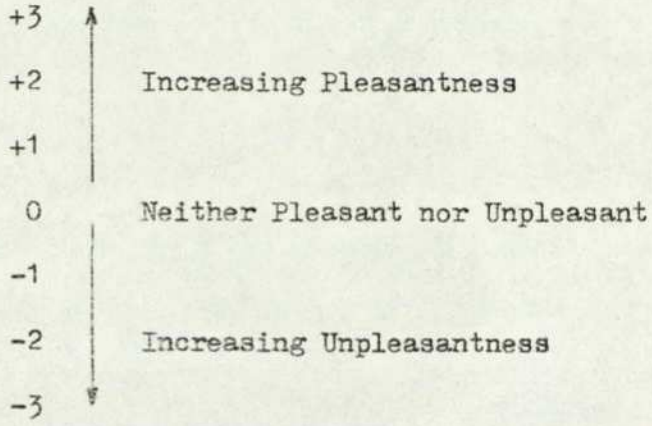

All strongly unpleasant odours will be rated -3, although some may be more unpleasant than others. An example[98] of the use of this scale in classifying eight organic odorants is given below:-

Odorant	Hedonic Value
Thiophene	-2.9
Hexanethiol	-2.9
Pyridine	-2.7
Propionaldehyde	-1.5
Styrene	-1.1
Butan-1-ol	-0.9
Butanone	-0.6
Butyl Acetate	+1.2

Hare et al[99] have reported the findings from their investigations into the public objectionability to diesel exhaust, using a mobile test laboratory. The odour was presented without identification and was assessed using five hedonic descriptors: pleasant, neutral, unpleasant, very unpleasant and unbearable. The main conclusion emanating from the statistical treatment of the results was that the public objectionability ratings could be directly related to the quality and intensity data produced by a trained odour evaluation panel. The survey showed that the objectionability of the diesel exhaust odour increased with odour intensity, although the linearity and the strength of the relationship depended on the manner in

which the objectionability response was elicited from the participants.

1.5.4 Objective Assessment of Odour

By definition, 'odour' can never be objectively assessed since it is the subjective response of a human being to an external stimulus. Nevertheless, instrumental techniques for measuring those particular properties of air samples which can be related to the odour intensity or possibly to the odour quality (as determined by a human panel) have been developed for some well-defined applications. The instruments available vary immensely in design and concept and reviews have been published[100, 101] which describe the respective merits of these potentially useful devices. One technique, for example, uses gas chromatographs equipped with computerised analysis capabilities to classify complex odours.[102]

One of the major problems associated with the design and development of instrumental techniques for odour assessment concerns the degree of sensitivity required from the objective technique, which should ideally compare favourably with the capabilities of the human nose. A number of odorants are known which produce significant odours at concentrations below p.p.b. by volume in air. This corresponds to 10^{-9} g/l, which necessitates either very sensitive detectors or enrichment of the sample while avoiding interference by excess atmospheric moisture or other contaminants.

Many attempts have been made to correlate the perceived odour of a complex mixture with a specific class of chemical substance contained within the sample. Thus for diesel engine exhaust the carbonyl class, or more specifically the aldehyde class, of compounds has been frequently measured in an attempt to establish a quantitative relationship with the odour. Such attempts are often negated by the fact that compounds which belong to the same homologous series but, have different molecular weights usually exhibit widely different odours. For instance, dimethyl and diethyl

sulphides are strikingly unpleasant, but the threshold begins to increase with an increase in molecular weight and the odour quality changes until, with hexasulphide, the threshold is much higher and the odour is not objectionable. Thus analysis by chemical groups, eg: % aldehydes, % sulphides or % mercaptans etc. has little relevance to the quantification of the odour unless only one chemical compound or one class of chemical compound is the principal odorant. The effectiveness of instrumental odour assessment methods is also reduced by synergistic effects which may exist in a compound odour. With synergism, the odour of one compound is modified by the interaction with another odorant and in these circumstances a correlation between the perceived odour intensity and a single chemical class is highly improbable.

1.5.5 The Characterisation of Odour Components in Diesel Exhaust

In 1968, the Coordinating Research Council and the Environmental Protection Agency jointly sponsored two major diesel odour research programmes carried out by ADL Inc.[103-107] and the Illinois Institute of Technology.[108-109] These two programmes have contributed a great deal to the large volume of published information regarding the nature of diesel exhaust odour species and their measurement. The results obtained from both of these studies, during the first three years of the contract have been summarised in a report produced by their sponsors.[110] Owing to the importance of the reported findings and because the results published form the basis of the present study, a brief resumé will be given of the information emanating from the research programmes.

1.5.5.1 The IITRI Research Programme

In order to collect samples for the detailed chemical and odour analysis programme, IITRI developed a unique method of trapping samples of diesel engine exhaust using a solid polymer matrix. The sample traps consisted of stainless steel tubes packed with a hydrophobic cross-linked styrene

polymer which adsorbed practically all hydrocarbons and partial oxidation products while allowing the escape of the odour-irrelevant substances such as: CO, CO_2, H_2O and CH_4 and the permanent gases. By careful application of heat, the compounds were desorbed into a stream of helium which was passed through the trap, and were carried into a gas chromatograph equipped with dual capillary columns. The column effluent was evaluated for its odour by a trained analyst and, whenever possible, the odour of each compound eluted was described qualitatively using the four odour descriptors specified by the Turk kit. The exhaust sample was resolved by the dual column chromatography technique into over 1000 components, about 100 of which were found to be odour-relevant. The odour-relevant peaks appeared to represent individual compounds and these were identified by comparison of retention-time data with those of known compounds and by mass spectroscopy.

The IITRI programme emphasised the identification of chemical classes of substances and the results obtained are listed in Table 1·2

Many high molecular weight cyclic and aromatic hydrocarbon classes, including naphthalenes, indans, tetralins and cycloparaffins were isolated as strong contributors to a 'burnt odour note'. Various non-aromatic hydrocarbons, containing more than one double or triple bond, contributed to the 'burnt odour note' of the overall odour. Aromatic aldehydes containing the benzene or furan structures were found to have varied odours ranging from pleasant to pungent and were considered to be important odour contributors. Some heterocyclic sulpher compounds, such as thiophene and its derivatives, were isolated as odorants. These compound classes are summarised in the above Table.

Those classes of compound, identified but considered to be odour irrelevant, included the lower alcohols, simple alkylbenzenes and alkanes (mostly C_{10} to C_{14}). All these compounds were found in significant amounts, but were generally present at concentrations below their relatively high odour thresholds. Indication of the presence of some n-alkanoic acids

Table 1•2

Classes of Odour Relevant Compounds as Identified by IITRI

General Class	Specific Class	Odour Note
Aromatic hydrocarbons	Alkyl benzenes	Pungent, burnt
	Alkenyl benzenes	Burnt
	Methyl indans	Burnt-fuel
	Naphthalenes	Naphthalene
	Tetralins	Burnt
Nonaromatic hydrocarbons	Alkenes / alkynes	Burnt
Sulfur heterocycles	Thiophenes	Foul-burnt
	Benzothiophenes	Burnt
Aldehydes	Paraffinic aldehydes	Aldehyde
	Aromatic aldehydes	Pleasant
	Furan aldehyde	Pungent

were found, but these were considered not to contribute greatly to the overall odour.

After two years of research, the IITRI programme was terminated in favour of the ADL programme since, the two studies were complementary and the ADL procedure produced more significant information for a given level of effort.

1.5.5.2 The ADL Research Programme

The objectives of the ADL research programme were to identify the odorous compounds present in diesel exhaust and to develop an instrumental technique for their rapid estimation.

As a result of the integrated application of analytical chemistry and sensory methods outlined in Section 1.5.1, ADL have reported the identification of major odorous species in diesel exhaust. The odour is described as having two major odour notes; oily-kerosene and smoky-burnt. The oily kerosene odours are principally due to the alkyl-substituted indans, tetralins and alkylbenzene in the aromatic portion of the unburnt hydrocarbons. The smoky-burnt character is primarily due to the partial oxidation products of these same aromatic species, plus a smaller contribution from the paraffin oxidation products, specifically: alkyl, hydroxy and/or methoxy substituted indanones, phenols, benzaldehyde and alkenones.

The assignment of these odour notes to specific chemical classes was achieved by collecting large volumes of exhaust by condensation, separation of the non-odorous and odorous fractions by liquid chromatography, followed by resolution into individual species by the application of two-stage gas chromatography and final detection by high-resolution mass-spectrometry. Each of the steps in this procedure were guided by odour analysis of the fractions and by determining how well they represented the original exhaust odour. Odour studies showed that the total organic extract (TOE) had the odour intensity and character of the original

exhaust. Using liquid column chromatography, the TOE was resolved into three fractions, the major fraction (80%) consisting of paraffins which had no odour when examined at the appropriate concentration. The exhaust odour was associated with the fractions containing the aromatic species (17%) which exibited the oily-kerosene odour and the oxygenated species (3%) which had the smoky-burnt odour.

Tables 1·3 and 1·4 show the odour-structure correlation for the oily-kerosene odour complex and the smoky-burnt odour complex. In summary, it was found[6] that,

1. The smoky odour character was most consistently associated with hydroxy and methoxy indanones with some contribution from methyl and methoxy phenols.
2. Burnt odours were associated with furans and alkylbenzaldehydes.
3. The oxidised oily character was usually ascribed to alkenones, dienones hydroxycyclocarbonyles and indanones.
4. Irritation factors most frequently associated with lower molecular weight phenols. Some benzaldehydes and methoxy benzenes may also have contributed to this irritaion.
5. While some unsaturated aldehydes contributed to the exhaust odour complex the most abundant exhaust aldehydes did not appear to make a significant contribution.
6. Neither sulpher-nor nitrogen-containing species contributed to the smoky-burnt odour complex. Although such species were observed during analysis none were associated with exhaust odour.
7. Naphthalenes, which constituted 50% of the aromatic fraction, were considered to have irritant properties in addition to enhancing the perceived odour character of the indans and tetralins, ie: the naphthalenes exhibited a synogistic effect rather than being important odorants themselves.

With regard to the origin of the most significant odour contributors, ADL concluded that the aromatic portion of the fuel appeared to be the source,

Table 1·3

Odour-Structure Correlation for the Oily-Kerosene Odour Complex

Odour Type	Associated Structures
Oily	Alkyl benzenes (1)
	Alkyl indenes (2)
Kerosene	Alkyl indans (3)
	Alkyl tetralins (4)
Sensation (feel, irritation)	Methyl napthalenes (5)

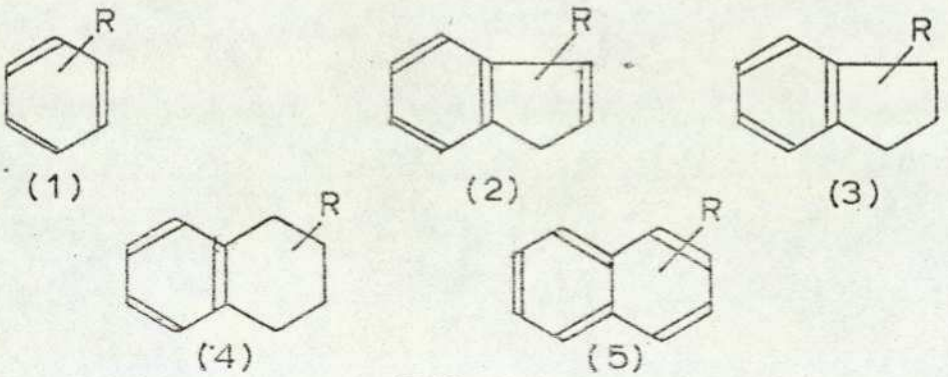

Table 1·4

Odour-Structure Correlation for the Smoky-Burnt Odour Complex

Structure Type	Odour
Alkenone	Oxidised oily
Dienone	Oxidised oily
Furan	Irritation
Furfural	Burnt
Benzenes	
Methoxy	Smoky, pungent
Phenol	Burnt, irritation
Aldehyde	Burnt, pungent
Benzofuran	Particle size
Indanone	Smoky metallic
Idenone	Leathery tarry burnt
Naphthaldehyde	Particle size

although some contribution from the paraffin portion was evident. The estimated concentrations of odour species were thought to be:-

	Total ppm	Individual ppb
Oily-kerosene Aromatics	20	40 - 400
Smoky-burnt Oxygenates	5	0.1- 10

It was also estimated[6] that about 200 different distinct chemical species may be responsible for the oily-kerosene odour, while approximately 2000 species contribute to the smoky-burnt odour. The engine exhaust, under the test condition employed had a total hydrocarbon level (HC) typically at 500 ppmC, from which it can be seen that the odorous species are a very small portion of the exhaust HC's.

By using liquid chromatography, all of the aromatic components which produced the oily-kerosene odour and all of the oxygenates which contributed to the smoky-burnt odour were resolved into just two separate fractions, the former labelled, liquid chromatographic aromatics, LCA and the latter, liquid chromatographic oxygenates, LCO. The resolution of all of the exhaust components into two odour relevant fractions enabled ADL to develop a correlation between the intensity of the exhaust odour and the concentrations of the LCA and the LCO fractions in the exhaust. More specifically ADL found that a particularly good correlation existed between the total odour intensity of the exhaust, expressed in TIA units, and the concentration of the LCO fraction expressed in $\mu g/l$ of exhaust. Mathematically this correlation may be expressed in the form:-

$$TIA = 1.0 + 1.0 \log_{10} LCO(\mu g/l)$$

and was found to be effective down to TIA values of 0·5.

Figure 1·15 shows a plot of observed odour intensity, vs. predicted odour intensity using the above correlation, and indicates that the 1/1 correlation is statistically very good, $2\sigma = 0{\cdot}3$. The TIA values have been determined using various operating conditions, and these data in conjunction with those obtained from field studies have indicated that the TIA

Figure 1·15

Observed Odour Intensity vs. Predicted Odour Intensity

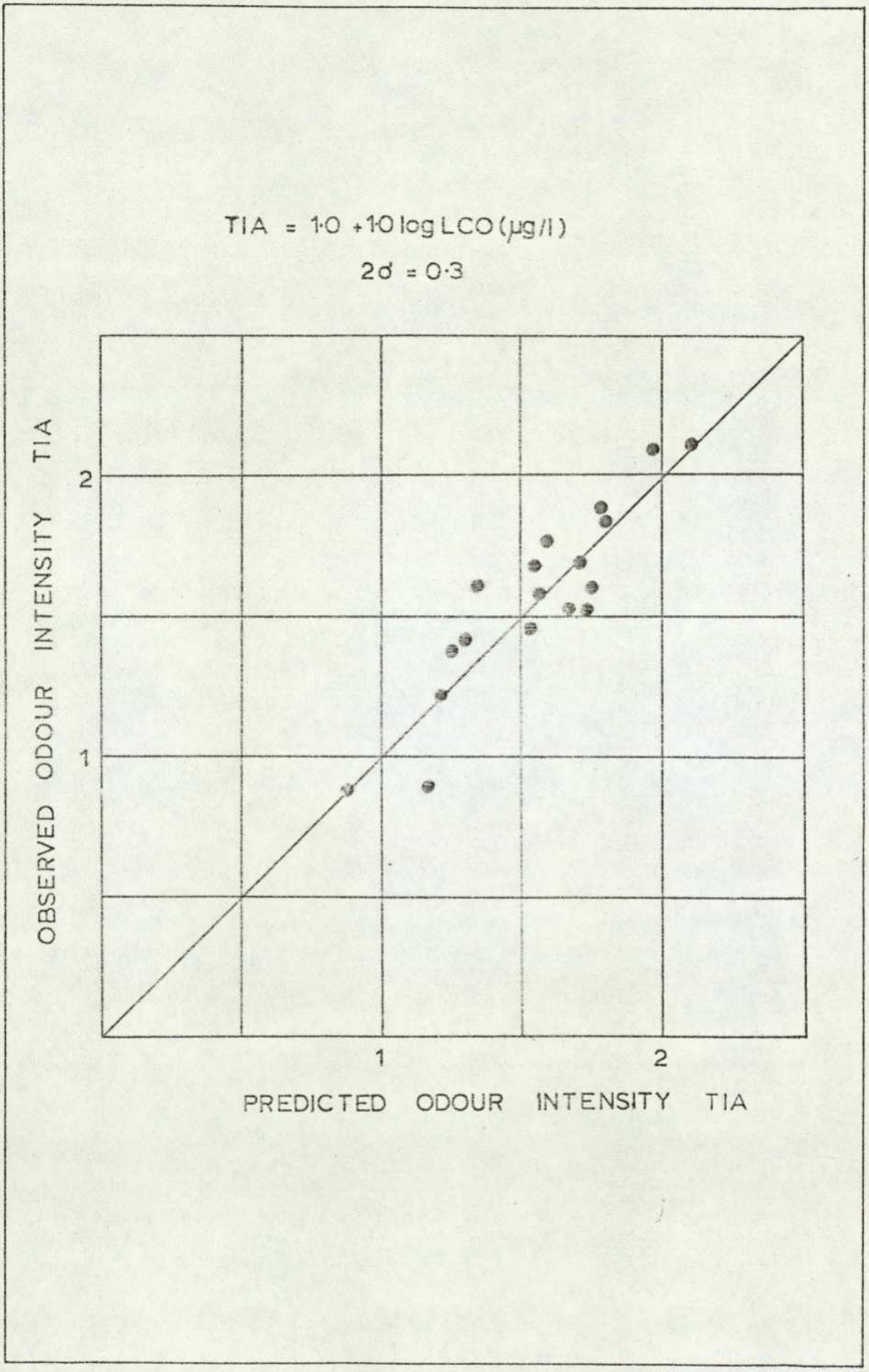

relationship holds for all the conditions tested. On the basis of these results ADL have developed a prototype instrument which uses high pressure liquid chromatography to resolve trapped exhaust samples into the LCA and LCO fractions.

The ADL instrument, known by the nmemonic DOAS, (Diesel Odour Analysis System) is the only instrument of its type available, at present, for diesel exhaust odour measurement. Its development has been followed with interest by diesel engine manufacturers and government organisations, both in America and in Europe, since its universal acceptance could result in odour legislation.

Prior to analysis, diesel exhaust samples are collected in stainless-steel traps packed with Chromosorb 102, a crosslinked polystyrene polymer with a large surface area for adsorption. This particular material is hydrophobic but retains exhaust hydrocarbons with 95-98% efficiency, allowing only 10 ppm of the light hydrocarbons such as methane to escape. The total organic extract (TOE) is recovered for analysis by elution of the trap using cyclohexane. The ADL procedure collects about 25 l of exhaust, although 15 l samples have been found adequate. The exhaust odour species collected may be stored in the traps for about 12 days without incurring significant loss of odour.

The DOAS is shown scematically in Figure 1.16 . It consists basically of a high pressure liquid chromatograph modified to make it specifically suitable for diesel exhaust analysis. A high pressure pump is used to cycle cyclohexane continuously through the system which includes a 15cm x 0.64cm stainless-steel column packed with Corasil II. The column effluent is monitored by a UV detector operating at 254nm. A 10µl vloume of TOE is injected onto the polar column. The LCA fraction is not retained and is eluted to produce the first peak of the chromatogram. The oxygenated species, because of their polarity, are retained on the column and to affect their elution, the polarity of the cyclohexane solvent is increased by

Figure 1·16

Schematic Diagram of Diesel Exhaust Odour Instrument (ADL)

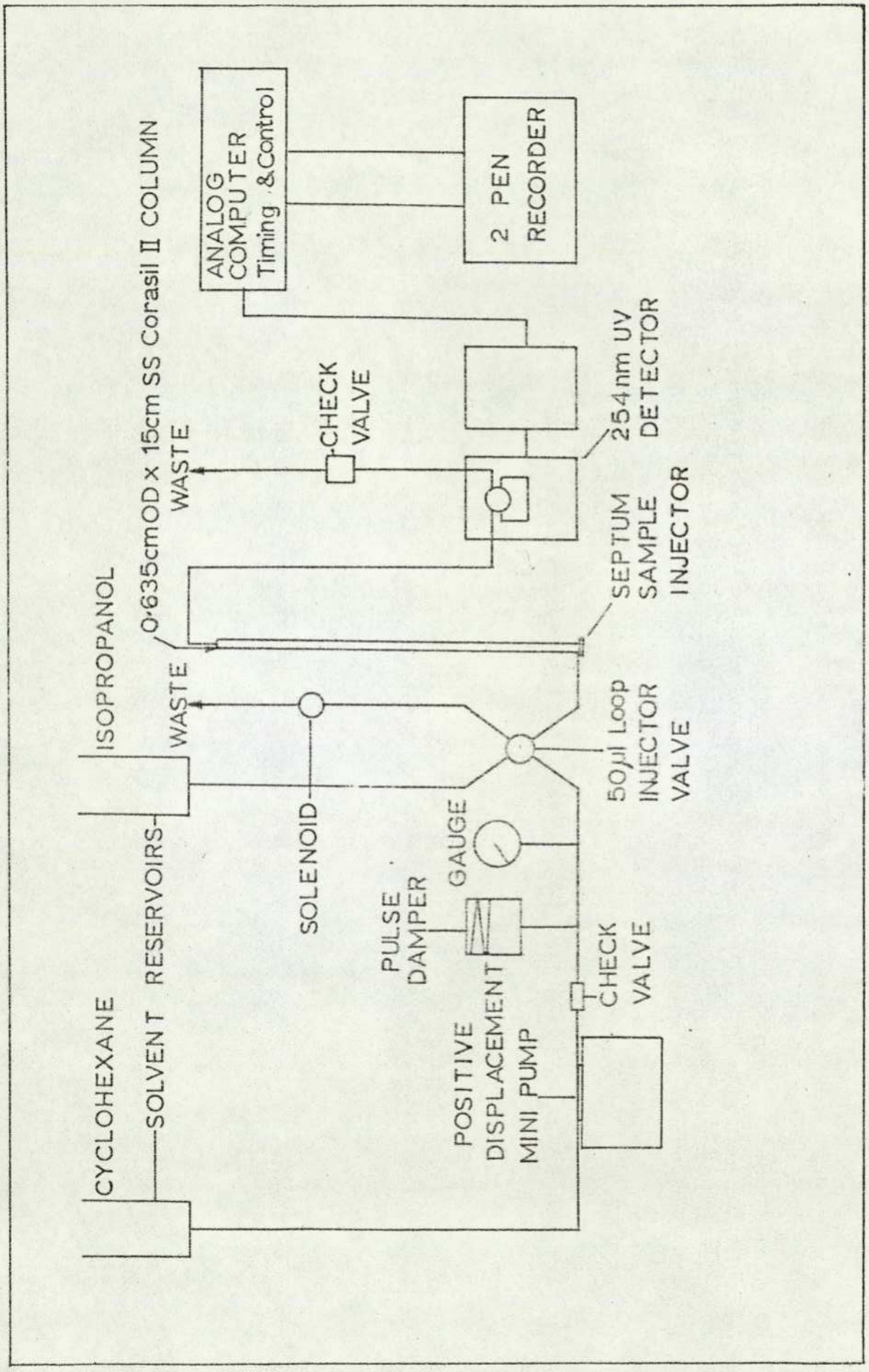

addition of 50µl of isopropanol. The LCO fraction is eluted as the second peak in the chromatogram, an example of which is shown in Figure 1·17

Integrated circuits are used to control the operation of the system, ie: the switching of the isopropanol injection valve and the timing of the sequence of events after injection. The area underneath the chromatogram is processed by additional electronic circuitry which converts the LCO area into µg of LCO and then to the appropriate TIA value using the empirically determined relationship described above. The area of the LCO peak is calibrated against standard solutions of 2-methoxy 4,-hydroxyacetophenone, the relationship between the instrumental response for the LCO fraction and the standard having been previously established. The instrumental technique, therefore, produces a quantitative assessment of diesel exhaust odour eliminating the very costly and time-consuming method of odour panel assessment.

In conclusion, it should be noted that, although the IITRI and ADL programmes produced results which were largely complementary, some differences of opinion exist regarding the nature of some of the odour relevant classes. IITRI obtained evidence which indicated that the aliphatic aldehydes, particularly those possessing unsaturated molecular structures, were important odorants. ADL, however, only confirmed the presence of these compounds in the exhaust, stating that they were less important odorants than many other classes. A similar disagreement concerned the odour relevance of the sulpher-containing heterocycles; IITRI claimed that these compounds were important, while ADL rejected this conclusion. Despite these, and one or two less important discrepancies, the two studies certainly contributed much useful information to the fields of diesel exhaust analysis and the nature of the odorants. It is important to note that the ADL instrumental technique for odour measurement, unlike many other proposed techniques, does not assume that the diesel exhaust odour is due to the presence of a single chemical substance or chemical class in the exhaust. Thus the

Figure 1.17

A Typical HPLC Chromatogram of Diesel Exhaust

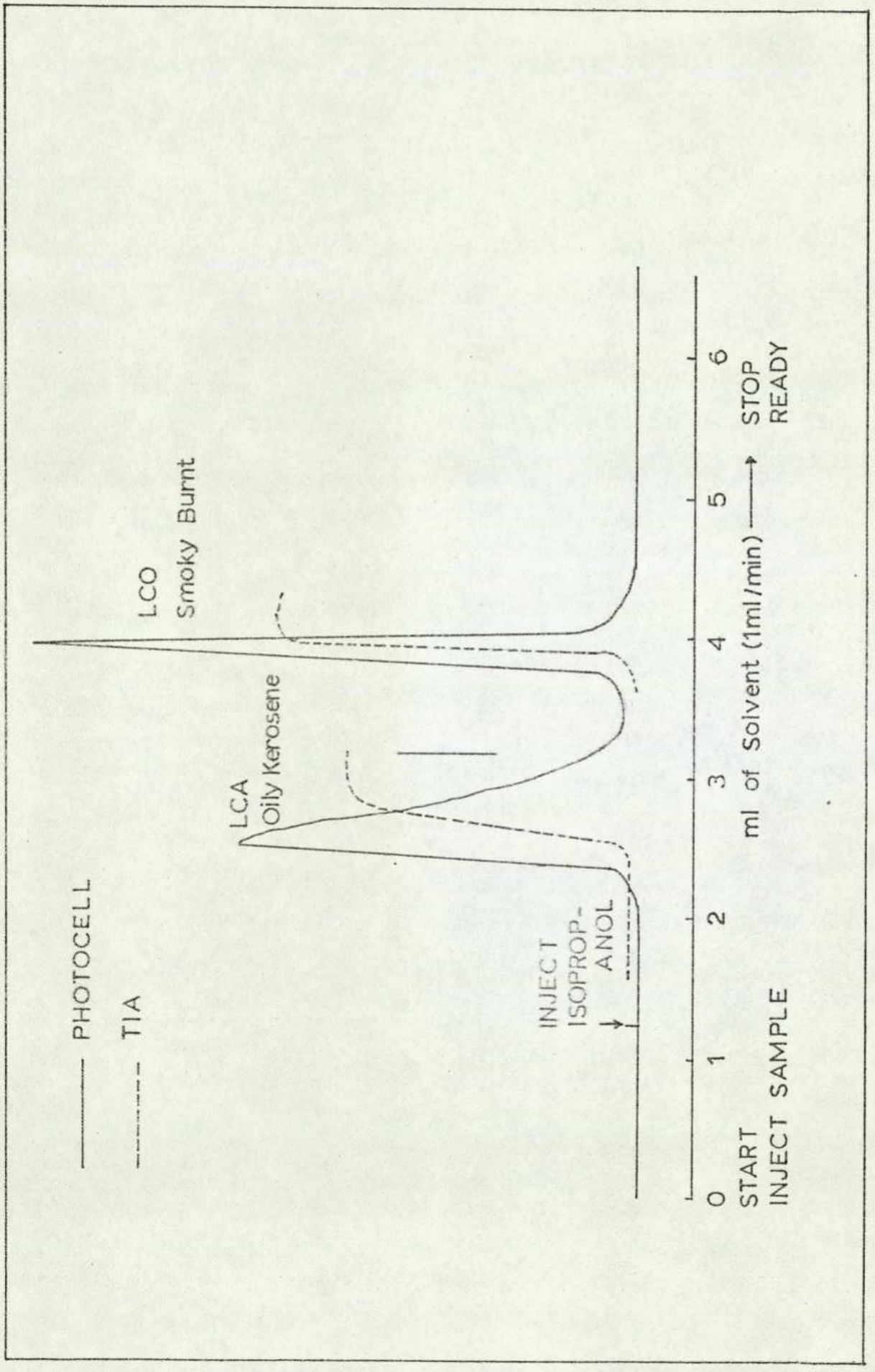

resolution of the discrepancies mentioned above is unimportant to the functioning and reliability of the measurement method.

1.5.5.3 A Comparison of the Subjective and Objective Assessment Techniques

The most consistent and reliable techniques for diesel exhaust odour assessment are those devised by Turk and ADL, both of which have been previously described. The only objective method for diesel exhaust odour assessment is the ADL DOAS which has been developed through correlations with the ADL odour panel. The only test available for checking the validity of the DOAS odour measurements is therefore a comparison with the odour data produced by application of the Turk method. Such a comparison has been performed and reported.[111]

Diesel exhaust samples were collected for odour analysis from four different diesel powered passenger cars. The Turk odour reference kit was used by a trained panel of odour analysts to generate a 'D' value for each exhaust sample. Simultaneously, the ADL DOAS instrument was used to quantify in terms of TIA values a similar set of samples. Figure 1·18 shows the two sets of data obtained and the high degree of correlation which exists between them. This study indicates that the DOAS instrument is capable of quantifying diesel exhaust odour with a degree of accuracy comparable with that obtained from a panel of trained observers.

Figure 1·18

TIA vs. D Rating for the Exhaust Odour of Four Diesel Powered Passenger Cars

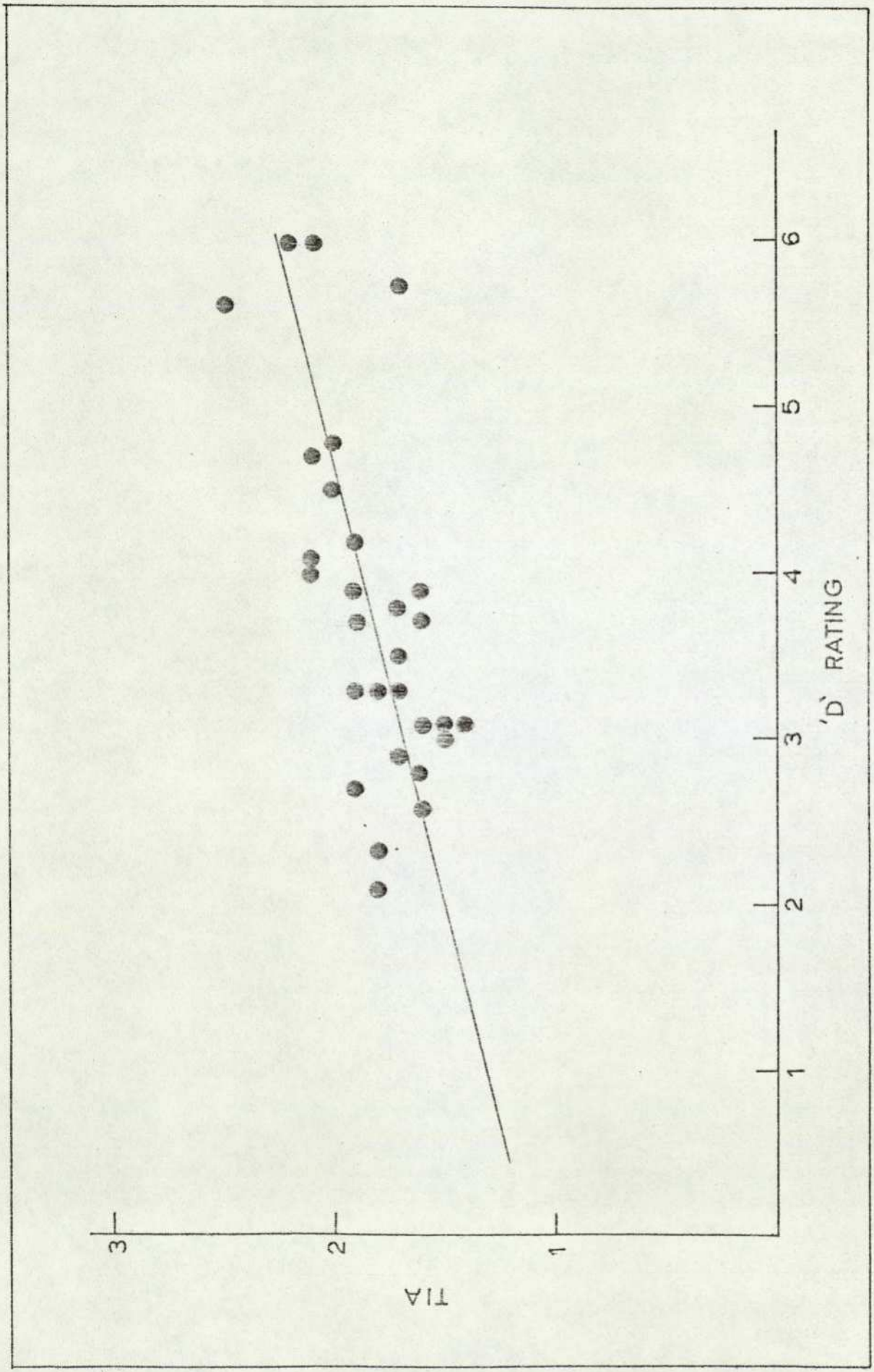

1.6 Present Work

One of the most complex reactions known to chemical science is the combustion of hydrocarbon fuels. Some aspects of the oxidation mechanism have been elucidated as a result of countless studies performed during the last two decades. Measurements of important kinetic parameters such as the rate constants, activation energies and the pre-exponential factors has made possible the development of overall reaction schemes. moreover, the advent of modern analytical instrumentation has resulted in the identification of the intermediates and final products of the reaction.

These developments in combustion science have resulted in an understanding of the processes by which oxidation products are formed. The intention of the present study was to use these well-established techniques to investigate the oxidation of diesel fuel in a static vacuum system and to monitor the formation of odorants during the combustion process.

During the combustion of single component hydrocarbon fuels, various oxidation phenomena, such as slow combustion, cool-flames and two-stage ignition, have been observed. Many partial oxidation products are formed during the slow combustion and cool-flame oxidation processes, and these compounds are very similar to the diesel exhaust odorants characterised by IITRI and ADL. The present study was therefore designed to elucidate the conditions under which a multicomponent diesel fuel exhibits the aforementioned combustion phenomena. Samples were withdrawn during the combustion process for odour analysis using a technique similar to that devised by ADL. Simultaneous gas chromatographic analysis of the samples provided additional information regarding the nature of the components constituting the odour fractions and the efficiency of the collection procedures.

The objective of these analytical studies was to define the conditions favouring odorant formation and to establish the mechanism by which odour relevant compounds are formed from diesel fuel. In pursuit of

this aim, the combustion experiments were performed under various initial pressures and temperatures and with a range of stoichiometries of fuel-air mixtures.

Owing to the complexity of the ADL technique compared with the procedures now employed for the measurement of 'standard emissions', ie: NOx, CO, HC and smoke it was also intended that the possibilities of developing a simple, objective odour measurement technique should be briefly investigated.

SECTION 2

EXPERIMENTAL

SECTION 2

2.1 Objective Odour Assessment

In an attempt to devise an objective method for the qualitative and quantitative assessment of diesel exhaust odour, a literature search was carried out under the following titles: odour, olfaction and olfactometry. The literature contained some reports of research into the development of odour-assessing devices (olfactometers) which varied in complexity and mode of operation. Adsorption of the odorant onto a substrate was frequently cited as the potential basis for an olfactometer. Two devices which employed adsorption as the fundamental operating mechanism differed widely in the emphasis placed on the respective aspects of the adsorption process. One device used the exothermic heat release which arose from the adsorption process as a means of detecting and characterising the odorant. The other device concentrated on the electronic effects emanating from the adsorption of a vapour onto an organic layer sandwiched between two metallic layers, i.e. in the form of an organic analogue of an inorganic semiconductor. This latter device has been patented and forms the detector section of a commercially available hydrocarbon vapour monitor.

These two detectors were chosen for further investigation in order to determine their potential applicability to diesel exhaust odour assessment. The construction of the two types of olfactometer together with the responses produced by these devices to standard odorants will be described. Finally their usefulness in assessing diesel exhaust odour in situ will be analysed.

2.1.1 Adsorption Olfactometry

2.1.1.1 The Development and Construction of an Adsorption Olfactometer

Initially, the concept of assessing an odorant by detecting the heat evolved during the adsorption of its vapour on a substrate was suggested by Moncrieff,[112] who indicated that this physicochemical process was possibly fundamental to the perception of odours in biological systems. Moncrieff used two thermistors in a Wheatstone bridge cicuit as the basis for his olfactometer. One of the thermistors was coated with an organic or inorganic film on which the odorant would be adsorbed;the other thermistor was uncoated but subjected to the same environment as the coated one. Adsorption of the odorant vapour on the film produced a resistance differential between the two thermistors resulting in the generation of a signal at the Wheatstone bridge output. The amplitude of the differential signal was found to be a function of the chemical structure of both the vapour and the film and the vapour concentration in the air stream. The apparatus developed differed from Moncrieff's design in that it was possible to measure electronically the heat of adsorption of vapours on comparatively large quantities of organic and inorganic gas chromatographic packing materials over a range of temperature, pressure and flow rate conditions.

The apparatus is shown schematically in Figure 2.1. The complete system was housed in a thermally insulated box constructed from hardboard and expanded polystyrene, a design which permitted isothermal measurements to be made within the range 25 to 35°C. Compressed air from a cylinder was first purified by passing it through a column of activated carbon and then humidified by bubbling it through a drechsel bottle containing distilled water. Once inside the box the air stream was passed through a

Key to Figure 2.1

A	Inlet for Purified and Humidified Air
B	Glass Coil for Temperature Equilibration
C1-3	Flowmeters for Streams 1 - 3
D	Mixing Chamber
E	Odorant Vaporiser
F	Pressure and Temperature Measurement Globe
G	Thermistor (THB12)
H	0-15p.s.i. Pressure Transducer
I	Detector in Conditioning Position
J	Detector in Sensing Position
K	Syringe
L	Outlet to Vacuum Pump
M	Recording Thermistor (THB12)

Figure 2.1

Odorimeter Apparatus Flow Scheme

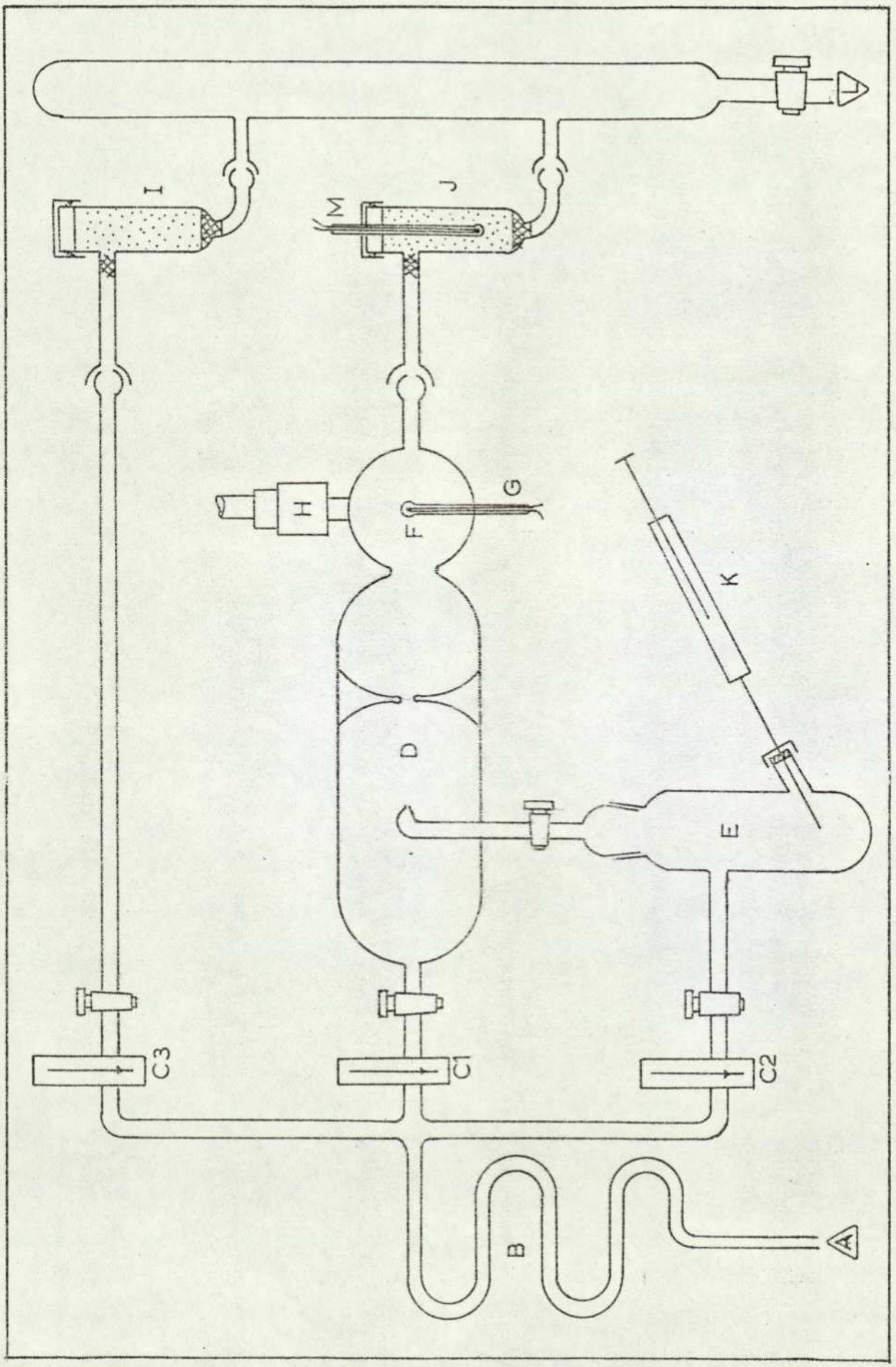

glass coil to achieve thermal equilibrium between the air stream and the box atmosphere. The stream was then split into three separate streams, each monitored by a flowmeter. Stream (1) entered the mixing chamber and constituted the diluting air for the odorant which was injected into the reservoir. The vapour from the odorant was carried to the mixing chamber by stream (2). Stream (3) was used to condition the detector prior to an odour assessment run. The mixed odorant and diluent gases then passed into a sphere situated at the end of the mixing chamber where the temperature of the air stream was measured by thermistor G. The gas finally passed into the detector, shown in Figure 2.2, which consisted of a glass cell containing 1 g of adsorbent packed around a second thermistor M. The back pressure resulting from restriction of the gas flow by the packing was measured by a pressure transducer,H, situated in the globe. The pressure thus recorded was then nullified by attaching a vacuum pump to the outlet of the detector, thus assisting the gas flow through the cell. Adsorption of the odorants was therefore effectively performed at atmospheric pressure.

The circuit for the thermistor Wheatstone bridge network is shown in Figure 2.3. The THB12 negative temperature thermistors were of the miniature glass encapsulated germanium bead type, activated by a 2 volt stabilised d.c. power supply. The low heat capacity of these particular thermistors rendered them especially suitable for the application in hand. The output of the network was recorded on a Bryans X-Y plotter operating with an internal time base signal.

The detector was tested with three types of adsorbent: activated charcoal, Chromosorb 102 and 20% Dinonyl phthalate on Chromosorb W. The packing was conditioned with air stream (3) for 30 minutes at the flow rate selected for the'odour' assessment, normally 0.5 l min^{-1}

Figures 2.2 and 2.3

Figure 2.2 Detector Cell

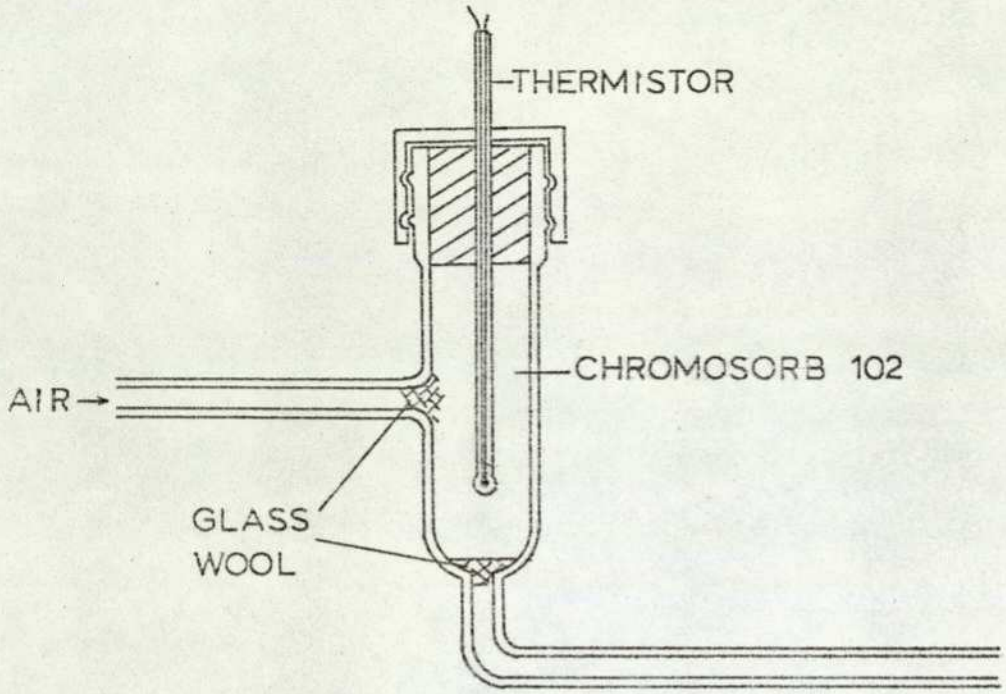

Figure 2.3 Wheatstone Bridge Network

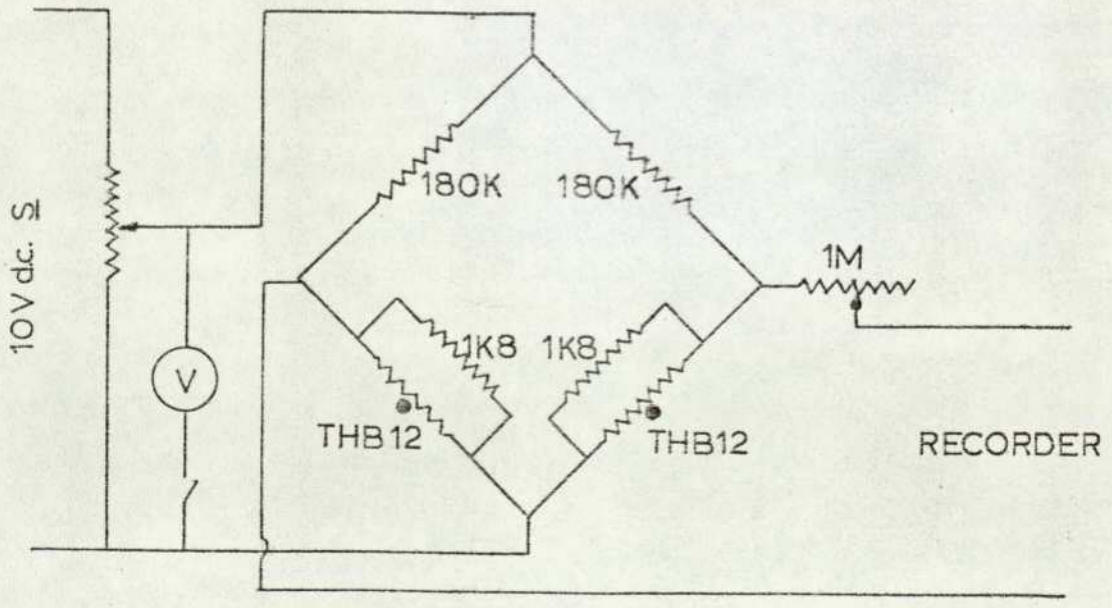

Three odorants; acetone, methanol and propanol were chosen for preliminary tests on the device, followed by many other compounds of the aldehyde, ketone and ether classes. The adsorption and desorption curves were found to be essentially similar in shape, but the differences which did arise such as base width, rise time and peak height were found to be sufficiently reproducible and unique to permit the qualitative differentiation between the odorants used.

2.1.1.2 Procedure for Testing the Response with Various Odorants

A typical operating procedure using Chromosorb 102 as the adsorbent and methanol as the odorant was as follows. The detector cell was packed with 1 g of the adsorbent after silanised glass wool plugs were fitted to the inlet and outlet ports of the cell in order to retain the packing particles. The cell was then capped and conditioned by air stream (3) for 30 minutes at 0.5 l min^{-1}; see Figure 2.2.After this period, the cell was removed from the conditioning position and a thermistor was placed in the cell, which was then attached to the outlet of the mixing chamber. The flow rate of streams (1) and (2) were adjusted, together with the vacuum pump, to give the desired total flow rate, dilution ratio and null pressure point. The temperature of the air stream was then measured by recording the output of thermistor G in a separate Wheatstone bridge network, the output of which was recorded on a milliammeter calibrated in degrees centigrade. After the system had been allowed to equilibrate for 5 minutes, 0.25 ml of odorant was injected into the reservoir through the rubber septum, and the differential signal of thermistor M with respect to thermistor G was recorded. Typical curves thus produced are shown in Figure 2.4.

The conclusions which can be drawn from the many experiments

Figure 2.4

Typical Response Curves Obtained with Packed Detector

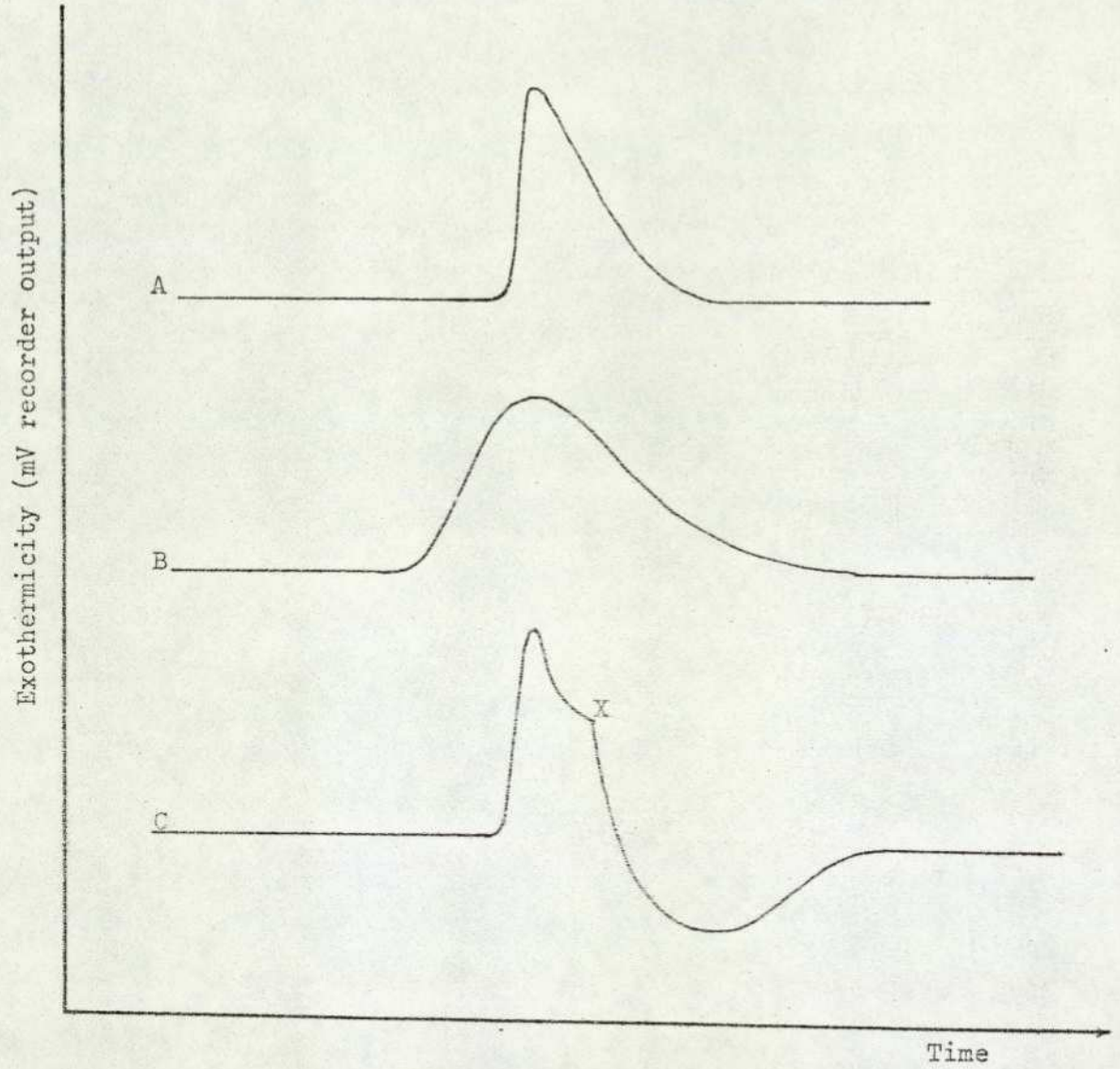

A. Adsorption of Acetone on Chromosorb 102 at 0.51 /min.

B. As A but at 0.12 l/min.

C. As A but desorption started at X.

Note: In all cases except curve C the sample vapour was in contact with the adsorbant throughout the time period shown.

carried out are:-

1. The apparatus was capable of measuring kinetically the heats of adsorption of vapours on activated solids.

2. The quantitative response at a given flow rate and temperature was proportional to:-

(i) the concentration of the odorant irrespective of whether this was determined by the volume injected or the dilution ratio used,

(ii) the chemical composition of the odorant and

(iii) the chemical nature of the adsorbent.

The above observations were reproducible for concentrations of odorant below a critical value unique to each odorant. Above this critical concentration the adsorbent became saturated and insensitive to further increases in odorant concentration. This process appeared to be analogous to olfactory fatigue which occurs in the organoleptic perception of odour.

3. Curve characteristics such as base width, rise time, desorption time and peak height were all dependent on the chemical nature of the odorant and and adsobent. Thus under the same conditions of temperature, pressure, flow rate, sample concentration and adsorbent, the curve characteristics were unique to each odorant tested i.e. the apparatus had qualitative discernment capabilities.

With regard to the functioning of the apparatus, it was found that the reproducibility of the response depended on the use of freshly activated adsorbent for each test unless lengthy in situ reconditioning at elevated temperatures was performed. In addition heat loss from the cell to the surrounding atmosphere and the excessive quantity of ineffective adsorbent surrounding the thermistor were considered to reduce the sensitivity of the apparatus. For these reasons, further modifications were made together with an attempt to reduce the size of the apparatus.

The modified detector cell shown in Figure 2.5 was housed in a detector block, Figure 2.6, which was machined from aluminium - a material which has been chosen and reported [103] as suitable for the lining of odour assessment chambers. The reference cell was housed in a fixed compartment of the detector block, while the sample cell was removable to permit the rapid interchange with a freshly packed cell and to assist with the cleaning and packing. Both the reference and the parallel sample cell consisted of two chambers. The first chamber in the reference cell contained only a thermistor and the second only the adsorbent. In the sample cell the first chamber contained both thermistor and adsorbent whilst the second acted as a dummy chamber. This configuration allowed equalisation of the air flows through the parallel sample and reference cells, the resistance to air flow afforded by the packing in the sample cell being compensated by the ineffective packing in the reference cell.

Air was drawn through the detector by a vacuum pump and passed through a flowmeter attached to the outlet. In order to test the response of the detector to various odorants, the inlet tube was inserted into the neck of a test tube containing the odorant. The response produced was recorded on the Bryans X-Y plotter and Figure 2.7 illustrates the typical responses achieved with isopropanol and acetone with 20% dinonyl phthalate adsorbent packing.

2.1.1.3 The Applicability to Diesel Exhaust Odour Assessment

After prolonged testing of this device, it was appreciated that, although its potential for detecting chemical vapours under idealised conditions was confirmed, its suitability in its present form for the assessment of diesel odours was extremely limited. Specific aspects of its design which would need modifying include the attainment of isothermal

Figure 2.5

Detector Cell Construction

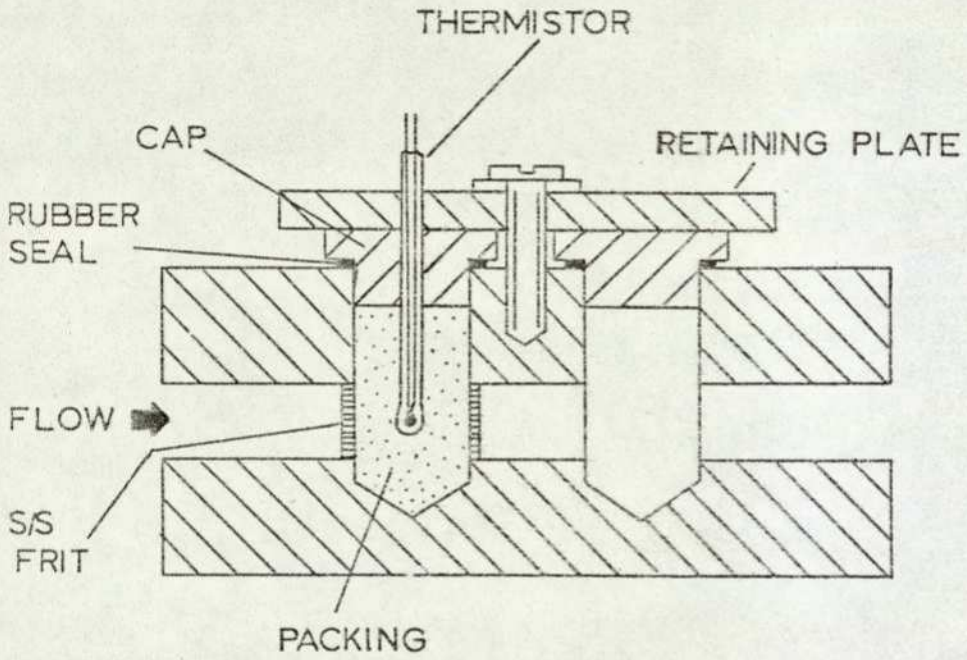

Figure 2.6

Complete Detector Block Assembly

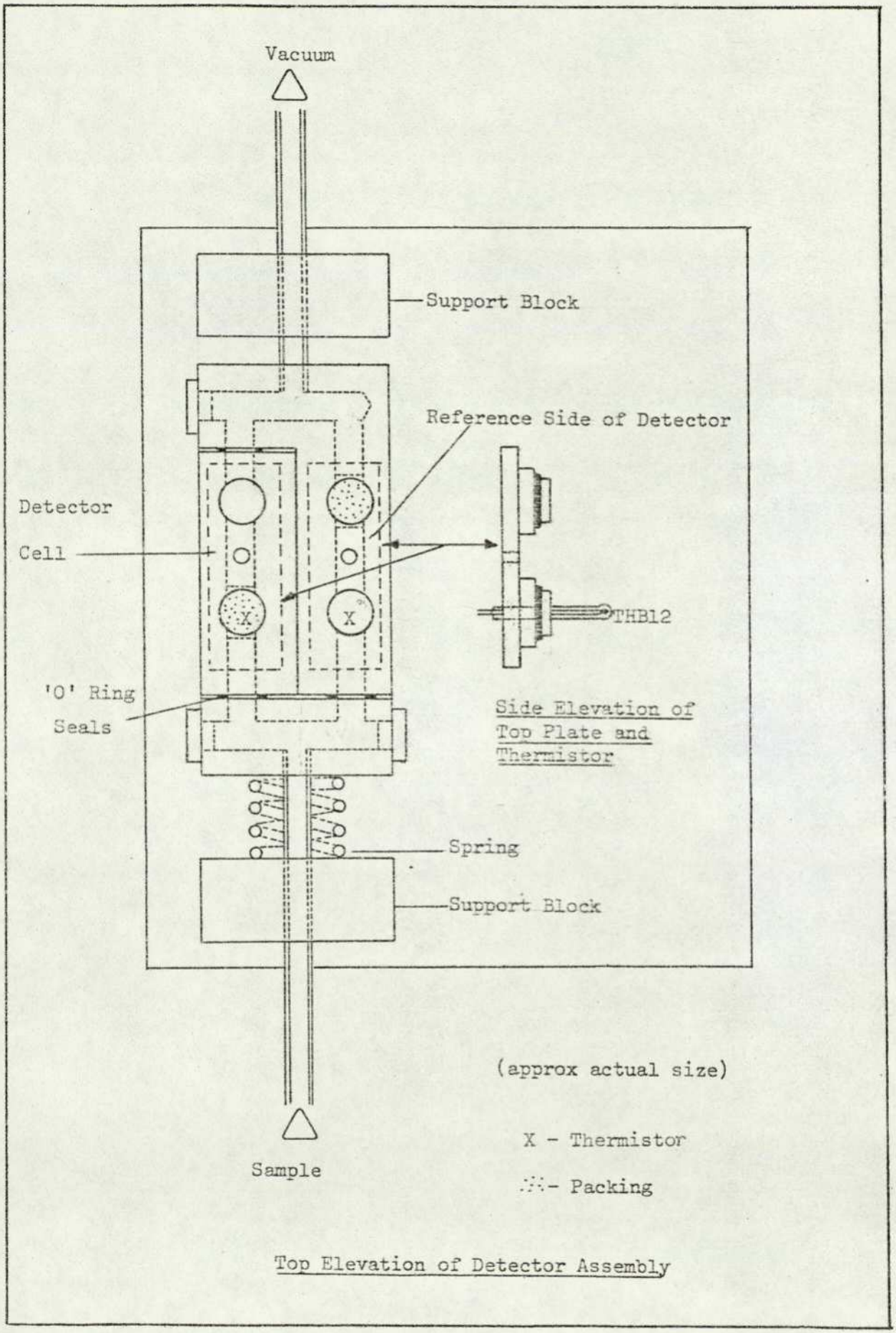

Figure 2.7

Detector Response Characteristics

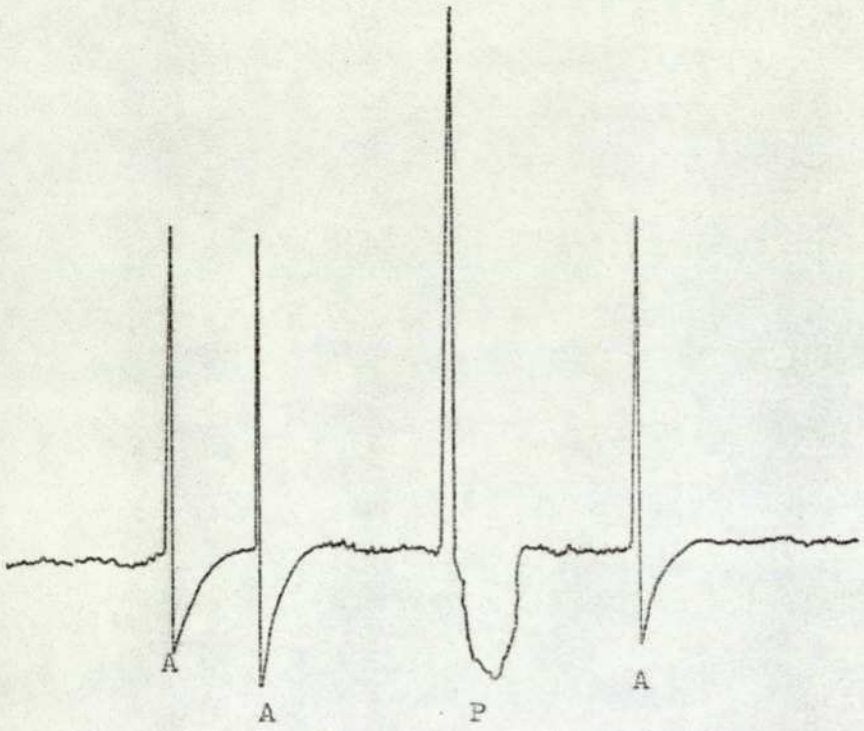

Adsorption Curve Characteristics of Acetone (A) and Propanol (P) on 20% Dinonyl phthalate on 80/100// Chromosorb W.

conditions for the detector and gas streams since temperature greatly affects the adsorption process. The thermistors were low-temperature types, requiring that the ambient temperature should not exceed 100°C. In order to achieve these conditions for diesel odour testing, the exhaust would need to be cooled and possibly diluted with nitrogen to prevent condensation of some of the higher-boiling components. This would result in greatly reducing the concentration of the actual odorant components of the exhaust making it essential that higher standards of electrical stability and sensitivity should be achieved. A correlation of the detector response pattern with a human odour judging panel would also have to be performed in order to achieve meaningful results from the objective method.

The recognition of the amount of experimental work and the specialised facilities required to render the device a viable proposition made termination of the investigation into the adsorption device inevitable.

Although some of the conclusions listed here are also applicable to the organic semiconductor detector, the work on these two devices was performed simultaneously. Therefore, a brief description of the work carried out on the organic semiconductor detector will be given, since it will assist in the appreciation of an overall picture in objective odour assessment techniques.

2.1.1 Organic Semiconductor Olfactometry

2.1.2.1 The Theory of Organic Semiconductor Operation

The idea of a completely electronic analogue of the olfactory process is not new. In addition to the device described above, which was developed from Moncrieff's pioneering work, Wilkins and Hartman[113]

suggested the possibility of detecting odours by the change induced in the electrical potential of an exposed wire whilst Meinhard[114] devised and patented the construction of an organic semiconductor which he claimed could form the basis of an olfactometer. This latter device was chosen for further investigation into its applicability to the assessment of diesel exhaust odour.

Meinhard[114] showed that various odorants could be qualitatively and quantitatively estimated by the use of semiconductor devices which employed organic materials as their constituent parts as opposed to the traditional inorganic compounds. Using layers of carefully chosen organic compounds between metallic electrodes, Meinhard produced a device that displayed the characteristics of a conventional diode. Different organic materials produced similar properties to those exhibited by P,N,P^+ and N^+ inorganic materials.

Adsorption of odorants at the interface between the two organic layers resulted in a change in the I - V characteristics of the device, especially when operating in the reversed bias mode. Figure 2.8 illustrates the characteristics displayed by a conventional inorganic P N function diode and for comparison the lower section of the Figure shows the I - V characteristics of a phenazine (N) and a fluorescein (P) diode under the influence of increasing sulphur dioxide concentrations in the ambient atmosphere. The magnitude of the change in the I - V characteristics is proportional to the concentration of the odorant and to the area of the junction exposed, thus giving the detector quantitative estimation capabilities. The response to a particular odorant is unique for a given combination of organic layer materials. Thus if several different combinations were to be used in separate diodes operating simultaneously then a 'finger print' may be obtained for a given odorant making qualitative

Figure 2.8

Inorganic and Organic Semi-conductor Characteristics

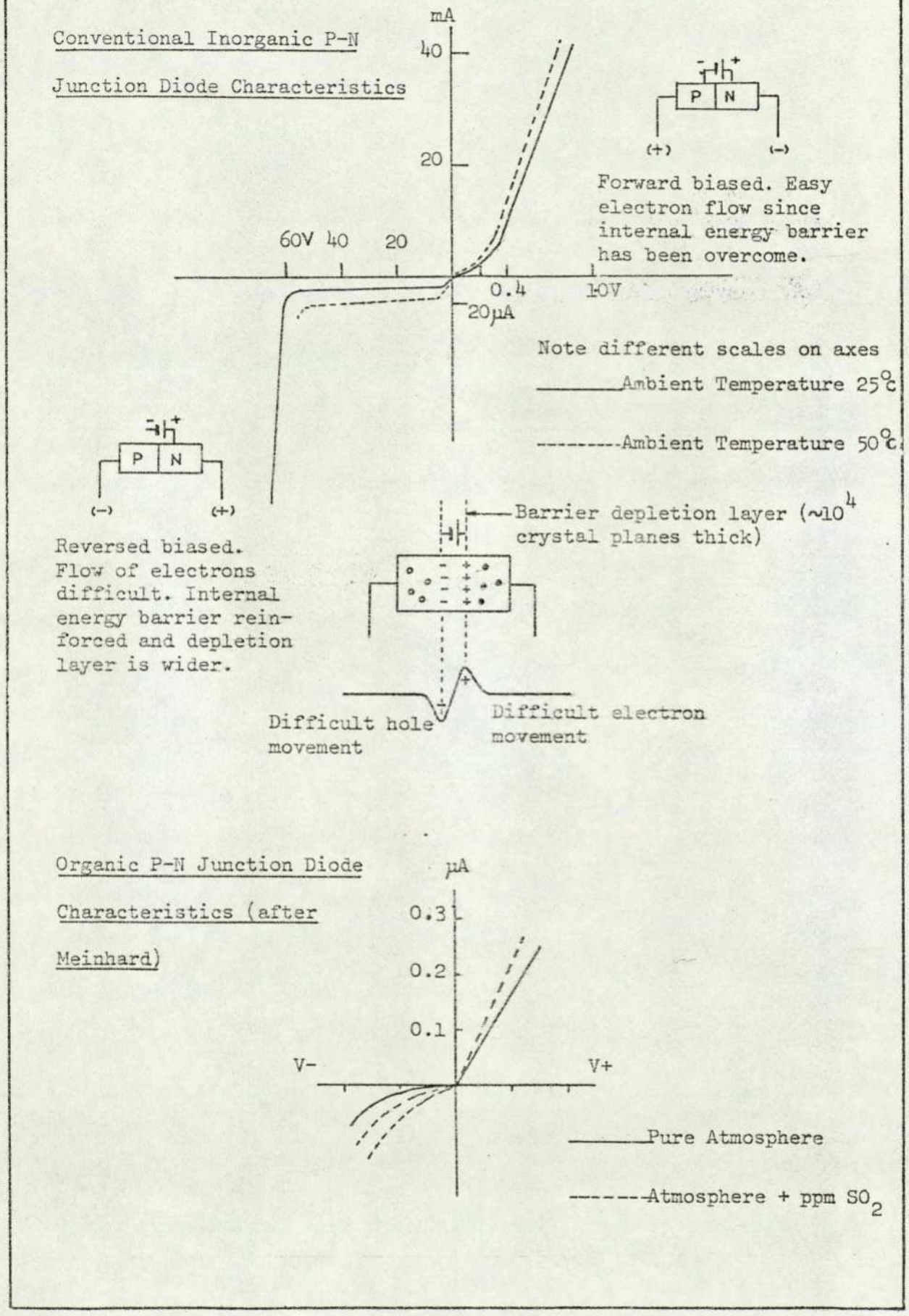

discernment possible.

Table 2.1 gives a list of possible organic materials which could be used in the construction of these devices. The combinations of urea/ naphthalene, naphthalene/sodium salt of fluorescein and fluorescein/ phenazine were investigated.

2.1.2.2 The Construction of an Organic Semiconductor

Two methods of producing the organic layers were investigated. The first method employed the compression of the various layers in a miniature opposed plunger machine, and the second involved the deposition of the organic compounds from solution by evaporation of the solvents.

For compression, a thin layer of copper powder was placed on the top of a plunger in a cylindrical stainless-steel die. The second plunger was then placed in the die and the plungers were compressed together in a vice. One plunger was then removed and a layer of crystals of the organic compound was placed on the copper disc and tapped to distribute the material evenly. This layer was then compressed. This first coated electrode was then expelled from the die and the procedure was repeated with more copper powder and the second organic compound forming the opposing electrode. To complete the semiconductor, the first coated electrode was reintroduced into the die so that the two organic layers were face to face. Hand pressure on the two plungers was then sufficient to compress the layers together.Electrical leads were attached to the electrode faces using conductive silver paint.

In the solvent deposition method, fluorescein was dissolved in a minimum quantity of methanol and the solution was poured over the copper face of a 25 x 25 mm piece of printed circuit board. The solvent was then evaporated at room temperature and the plate was dried in a vacuum oven at

Table 2.1

Organic Materials Suitable for Organic Semi-Conductor Construction

(after Meinhard)[114]

Type		Examples
N	Reducing Agents	Phenazine
	Lewis bases	Charge Transfer Complexes
	Soft bases	
P	Oxidising Agents	Biradical Acceptors e.g.
	Lewis Acids	PNA's
	Soft Acids	Pyrolysed Polymers
		Charge Transfer Complexes
		Chloranil + p-phenylenediamine
		Iodine + Anthracene
		Aromatics, Dyestuffs etc.
		Quinones and Derivatives
		Highly Conjugated Aromatic and
		Aliphatics

Examples of Junctions

N + P	Phenazine/chloranil + p-phenylenediamine
	Phenazine/Fluorescein
P + P	Indigo/Chloranil
	Indigo/Chloranil + p-phenylenediamine
	Chloranil/Chloranil + p-phenylenediamine
	Indigo/Fluorescein

50°C. Phenazine was dissolved in cyclohexane to form a saturated solution at 80°C and after deposition on another electrode the above drying procedure was repeated. When dry, electrical leads were attached to the two film-covered electrodes which were then placed face to face.

Using the circuit shown in Figure 2.9, I - V characteristics were obtained as shown in the lower part of the Figure. The semiconductors produced by solvent deposition were far more successful than the compressed layer devices. This was probably due to the uniformity and thinness of the organic layers produced by the former procedure.

2.1.2.3 Testing the Response to an Odorant

In order to test the effect of an odorant on the device, it was necessary to expose the organic layer interface to the vapour under test. Meinhard suggested that this could be achieved by drilling holes through the top electrode, perforating the two organic layers and terminating at the surface of the bottom electrode. In practice, this was found to be difficult without the use of specialised engineering equipment. In the case of the compressed semiconductors, the drilling action disintegrated the top electrode, indicating the inefficiency of the compression machine in compressing the metallic powder into a coherent mass. It was therefore impossible to test the response of the devices made without resorting to more technically complex methods of exposing greater areas of the organic layer interface, possibly by chemical etching processes used in the photographic and electronic industries. Exposing the junction along the edge of the electrode to odorants did not produce any observable change in the I - V characteristics, but this was not unexpected owing to the small area thus exposed. Continuation of the investigation into the semiconductor devices was therefore abandoned for the following

Figure 2.9

Semi-conductor Testing Circuit and Characteristics

Semiconductor Testing Circuit

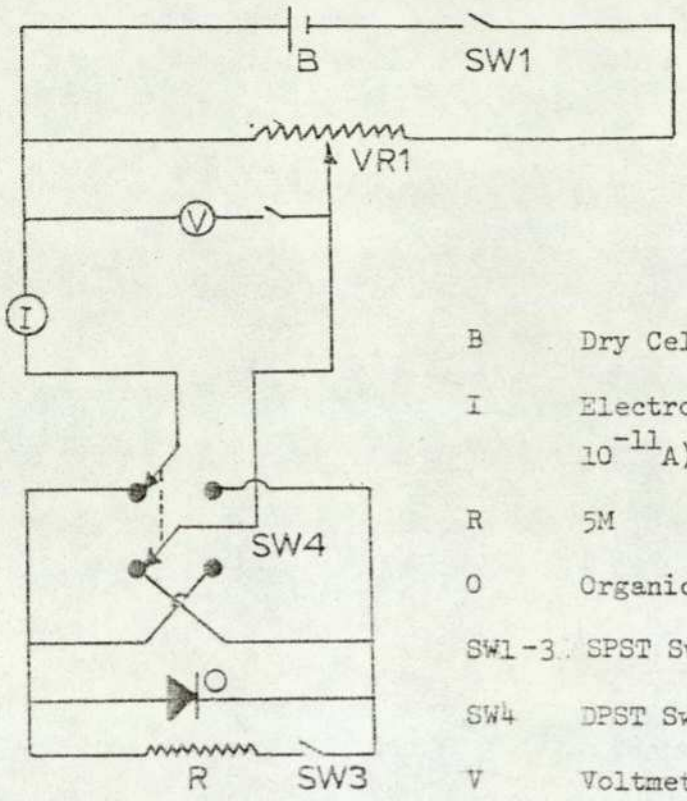

B	Dry Cell 1.5V
I	Electrometer (Sensitivity 10^{-11}A)
R	5M
O	Organic Semiconductor
SW1-3	SPST Switches
SW4	DPST Switch
V	Voltmeter
VR1	5M Potentiometer.

Semiconductor Characteristics

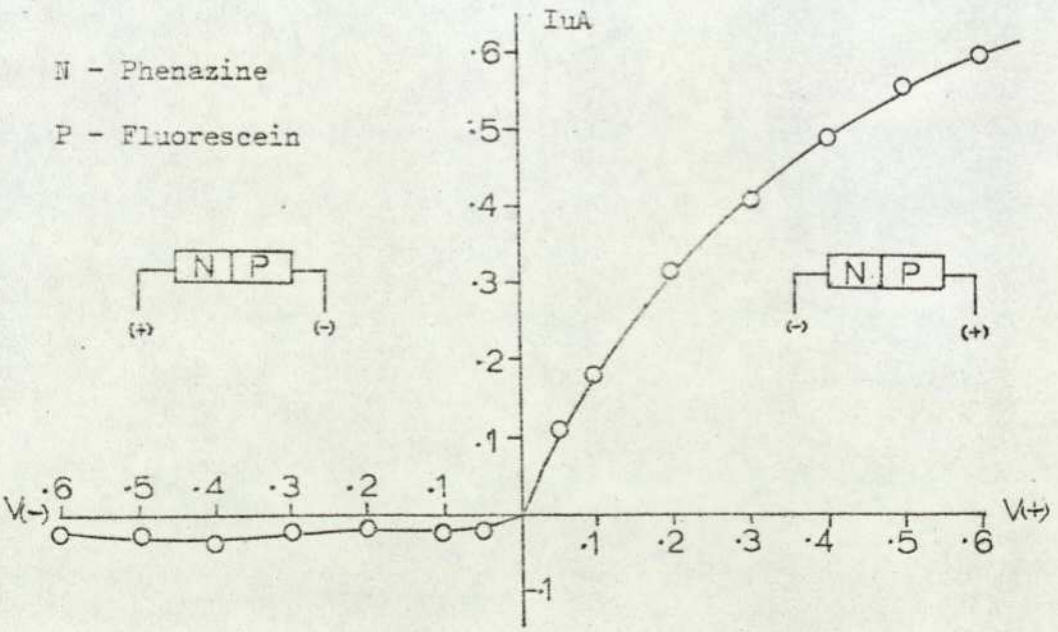

reasons:-

1. Highly specialised construction techniques would be needed for the production of functioning devices.

2. The response of the device to many odorants would have to be correlated with the response of a human odour-judging panel, the prohibitive nature of this aspect being the complexity and expense in both time and finance needed to obtain meaningful results.

3. Dehydration of diesel exhaust would be a necessary prerequisite to testing with the semiconductor device, since condensed water vapour would result in a short circuit of the two electrodes. The dehydration process would undoubtedly irreversibly change the qualitative and quantitative characteristics of the exhaust odour.

2.1.3 The Applicability of Objective Odour Assessment Techniques to Diesel Exhaust Odour

Of the two objective instrumental techniques described above, the adsorption device appeared to be the most promising, owing to its simple construction and the fact that results were forthcoming in terms of response to chemical environments presented to it. In addition, the problem concerning the water vapour content of the exhaust might be avoided by the use of packings, similar to Chromosorb 102, which are unaffected by water vapour. However, the amount of experimental work involved in producing the device (or combination of devices) together with the correct packing materials which would enable a correlation to be established with a human odour judging panel, was considered prohibitive.

Since an objective method developed by Arthur D. Little inc. had been reported[106-107] together with substantial evidence to support its

applicability to the diesel exhaust odour problem, a decision was made to concentrate on this apparently viable objective method. However, the advantages of the two objective methods investigated lay in their potential compactness and ease of operation, making direct in field measurements possible. Continued investigation may be justified if future legislation necessitates a quantitative assessment of exhaust odour and if the advantages mentioned above are considered sufficiently important.

As a note of interest, the organic semiconductor device has been produced commercially under the acronym MACOR[115] (Molecular Adsorption Controlled Organic Rectifier).

2.2 The Static Vacuum Apparatus

2.2.1 The Vacuum System

The static vacuum apparatus differed from the conventional all-Pyrex glass system in that the reactor consisted of a cylindrical stainless-steel bomb. A schematic diagram of the system is shown in Figure 2.10 from which it can be seen that greaseless Rotaflo taps were used in all line sections through which the reaction products passed. These sections of the line were maintained at 100°C using Electrothermal heating tape to prevent product condensation.

The air used for the majority of the oxidation experiments was drawn from the laboratory atmosphere through two packed columns, one containing activated charcoal and the other molecular sieve. These columns removed water and other contaminants, the efficiency of removal being reflected in the highly reproducible nature of the combustion data collected. The gas storage globes were reserved for the volumes of oxygen and nitrogen which were used in the preparation of specific atmospheres.

Some difficulty was encountered in constructing a vacuum-tight connection between the reactor and the glass apparatus. A rigid glass-to-Kovar metal seal was initially employed with a $\frac{1}{4}$ to $\frac{1}{4}$ inch Swagelok coupling connecting the metal section of the seal to the reactor inlet/outlet port. This seal did not however, withstand the thermal stress arising from a change in reactor temperature and therefore eventually fractured. The connector was modified to introduce a degree of flexibility by using a convoluted stainless-steel tube connected to a glass-to-stainless-steel seal. This proved satisfactory for some time before failing once again at the seal. The final modification dispensed with the seal altogether and replaced it with a Swagelok union and a p.t.f.e. ferrule, the convoluted

Key to Figure 2.10

BV	Baffle Valve
C1	Activated Carbon Column
C2	Molecular Sieve Column
DP	Diffusion Pump
F11	Perkin-Elmer F11 Gas Chromatograph
F	Furnace
G1	Penning Gauge
G2	Piranni Gauge
GCL	Gas Chromatography Loop
I	Injection Ports
LCT	Liquid Chromatography Trap
M1,2	Mercury Manometers
O	Observation Port
PT	Pressure Transducer
PV	Pressure Release Valve
RP	Rotary Pump
RV	Reaction Vessel
SV	Solenoid Valve
T1-4	Cold Traps
V1-3	Gas Storage Globes
V4	Product Sharing Globe

Figure 2.10

The Static Vacuum Apparatus

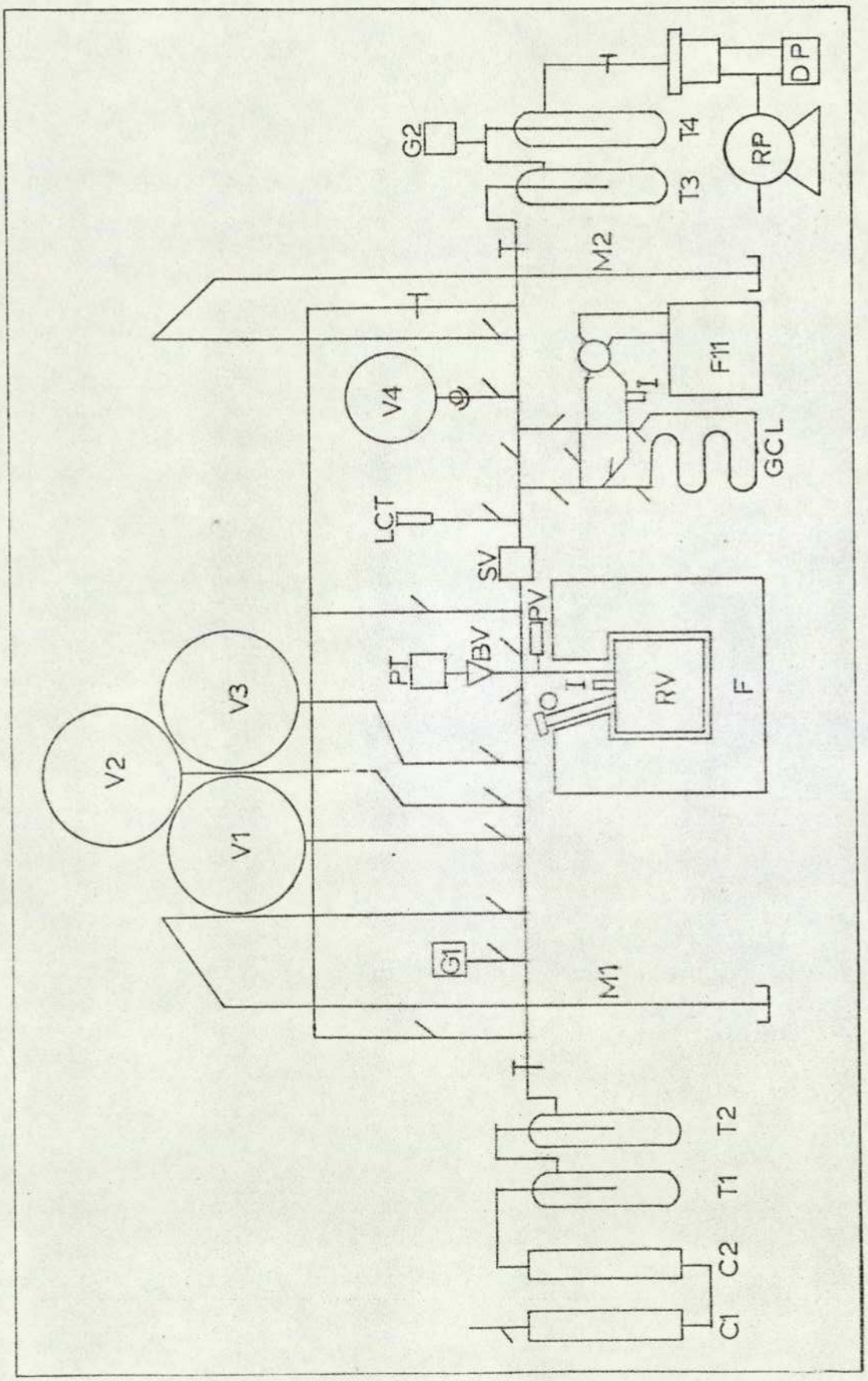

stainless-steel tube thus being connected directly to the glass apparatus. This connection withstood furnace temperature changes and allowed a vacuum of 2×10^{-4} torr to be achieved in the system. Figure 2.11 illustrated the successful design of the connector.

In order to protect the pressure transducer from excessive pressure pulses resulting from hot ignitions, a glass baffle containing a glass float was incorporated into the system below the pressure transducer orifice. Pressure changes accompanying slow combustion and cool-flames were recorded unhindered, but under an excessive pressure surge the float would seal off the transducer orifice.

2.2.2 The Reaction Vessel Design

Figure 2.12 shows a vertical cross-section of the stainless-steel reactor which was constructed in two parts, both enveloped by a 1 cm. thick copper jacket. The lower section contained the 325 ml reaction volume which was cylindrical in geometry; 10.26 cm. deep and 6.35 cm. in diameter, with stainless-steel walls 2.82 cm. thick. The reaction volume was enclosed in the lower section by an upper plate which bolted down with eight screw studs. The three ports which penetrated the reaction volume were located on this upper plate. One port, equipped with a Perspex window enabled observations of light-emitting combustion phenomena; the inclusion of this port increased the reaction volume to 341.5 ml. Fuel injection through a silicon-rubber septum was facilitated by a second port centred on the vertical axis of the reaction volume and the remaining port was the stainless-steel inlet/outlet port through which the reaction atmospheres were admitted and the reaction products were withdrawn. A pressure release valve was incorporated into this last port to vent any explosive pressure surges which might occur. The valve was set with a cracking pressure of

Figure 2.11

The Flexible Stainless Steel Connector

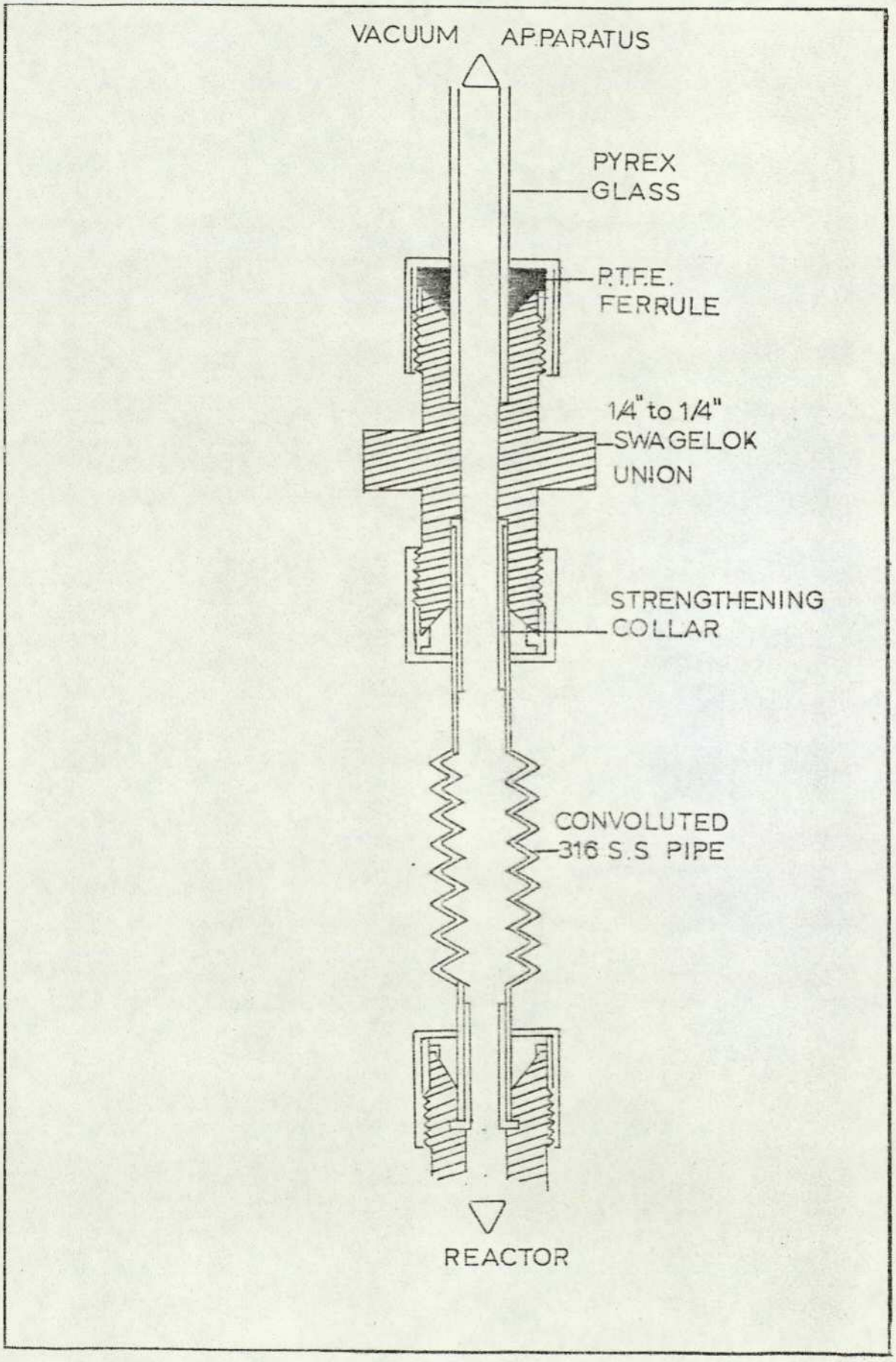

Key to Figure 2.12

AG	Aluminium Gasket
I	Injection Port
O	Observation Port
P	Perspex Window
PV	Pressure Release Valve
RV	Reaction Volume
S	Screw Studs
SS	Silicon Septum
TH	Thermocouple Bore Hole

Figure 2.12

The Reaction Vessel

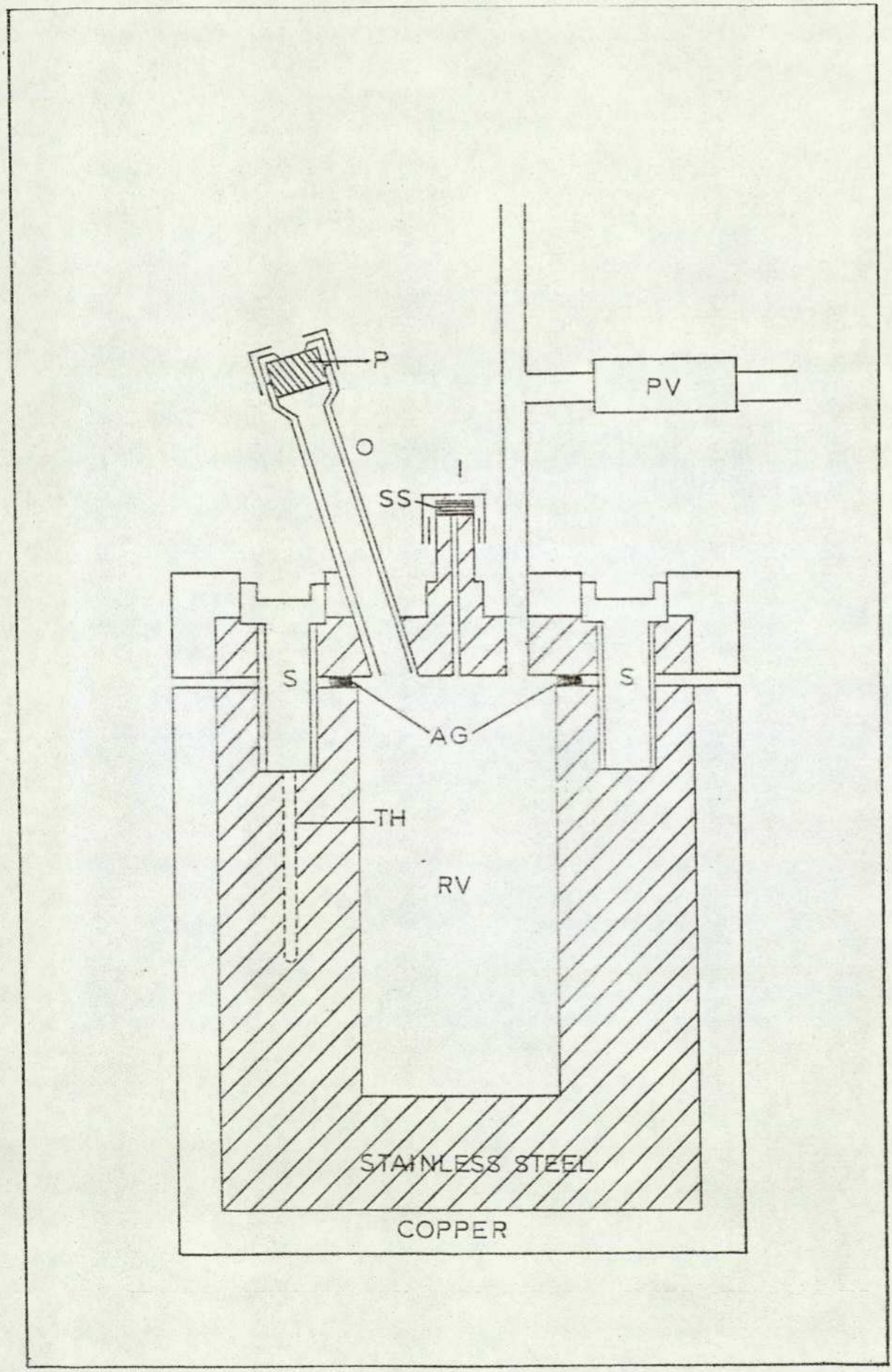

25 to 30 psig. A nitrogen envelope surrounded the whole reaction vessel at all times, thus minimising atmospheric oxidation of the outer surface.

Initially, some difficulty was encountered in making the interface between the two sections of the reaction vessel vacuum-tight. As a first attempt the two faces were polished using a very fine grade of polishing paper supported on a plate-glass table. The two sections were then bolted down with a torque of 80 ft lbs. The failure to hold a vacuum made it apparent that an interfacing gasket was essential. Indium, a material frequently used in high vacuum applications, was an obvious first choice, but its low melting point excluded it from the application in hand. The problem was solved by using a jointless aluminium ring gasket and with this in place a vacuum of 2×10^{-4} torr was achieved.

The internal surface of the reactor was cleaned with acetone and cyclohexane prior to being closed and was found to be conditioned after only three or four runs under cool flame conditions.

The heating equipment consisted of a Stabilag furnace containing four heating elements. The top of the furnace was in the form of a split collar, each half of the collar housing a heating element. This design allowed the reactor to be easily removed for servicing when required.

The heating circuit is shown in Figure 2.13 and was developed so that each of the housing elements could be balanced to give an even temperature distribution.

Temperature control was achieved using a platinum resistance thermometer which supplied signal feedback to an A.E.I. RT3R/MK2 proportional temperature controller. The platinum resistance thermometer (see Figure 2.14) was modified from a C.N.S. model so that it could be accommodated by the 3 mm diameter drilling in the reaction vessel wall. The output from the controller supplied the total current requirement of

Key to Figure 2·13

A	0 - 10 Amp Ammeters
C1,2,3	Heating Circuits
CR	Current Regulator
PTC	Platinum Resistance Temperature Controller
PRT	Platinum Resistance Thermometer

Figure 2.13

The Furnace Heating Circuit

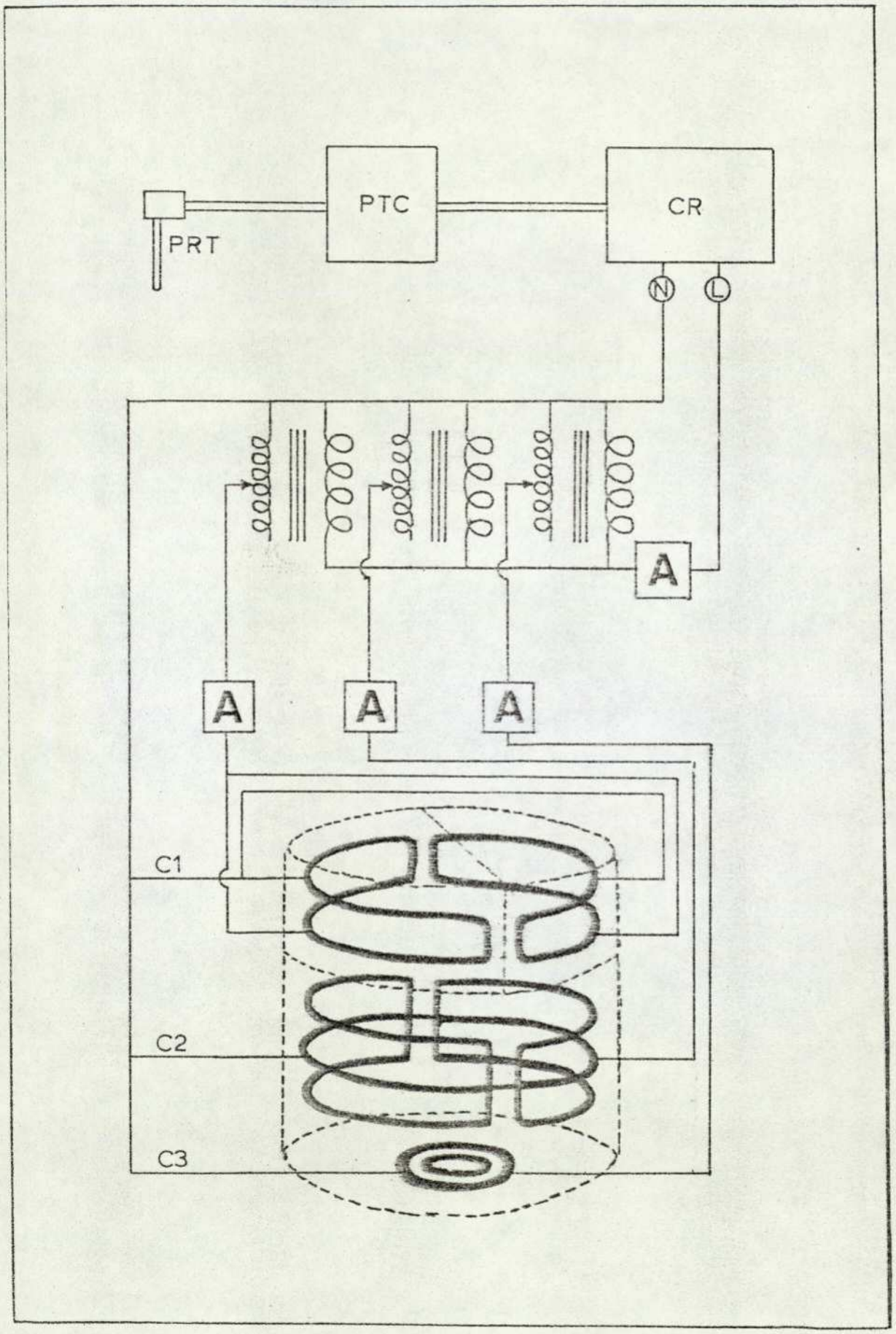

Figure 2.14

The Construction of the Platinum Resistance Thermometer

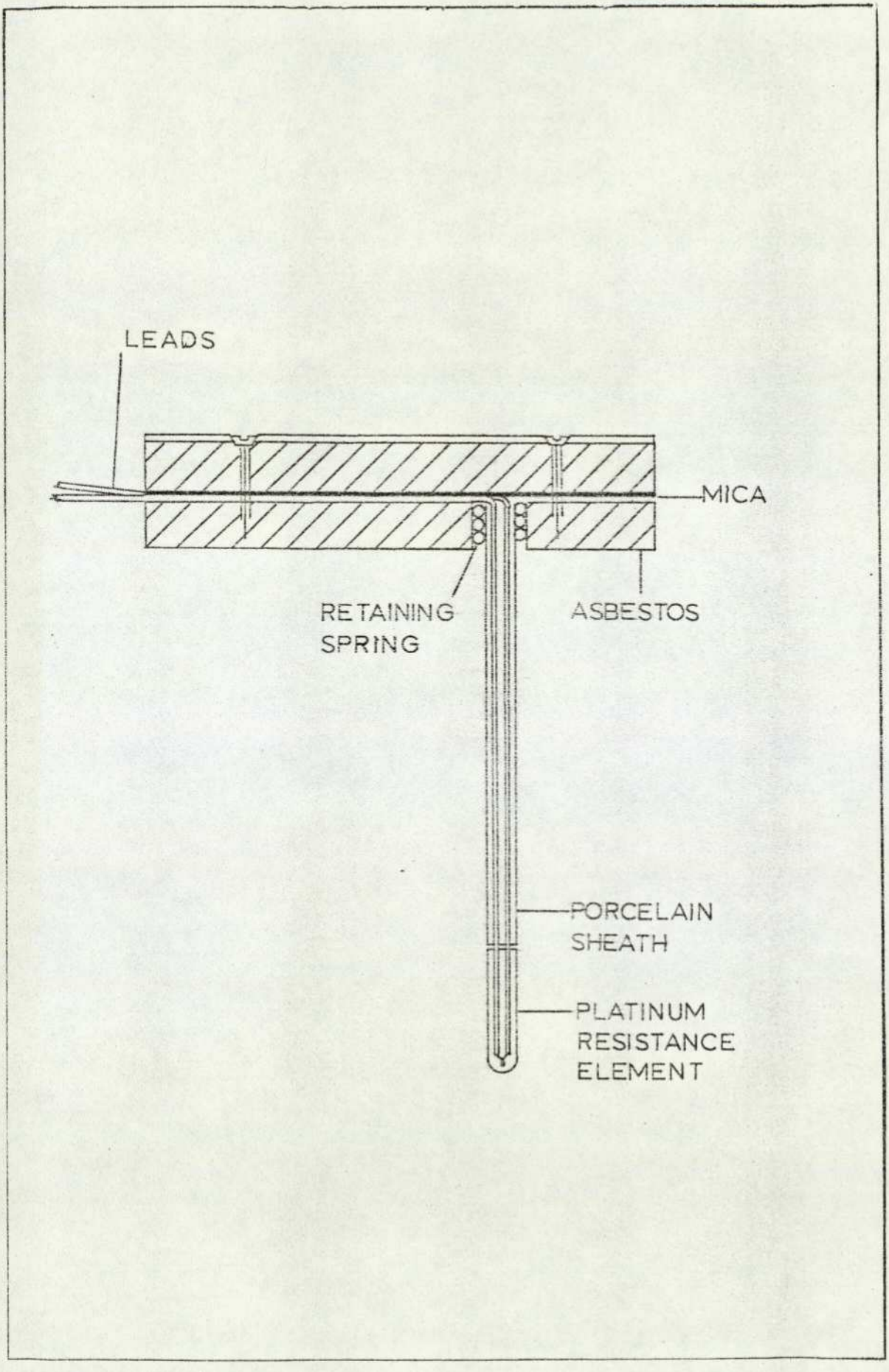

the furnace. The proportion of this current selected for each heating element was determined using heavy-duty voltage regulators. The required temperature of the furnace could be maintained to within $\pm 1^{\circ}C$ and was measured using standardised chromel-alumel thermocouples placed to varying depths in vertical hole borings in the reaction vessel wall.

2.2.3 Fuel Injection

Fuel was introduced into the reaction vessel through a silicon-rubber septum housed in the injection port situated in the centre of the reaction vessel head. The required quantities were delivered from micro-syringes designed for high pressure liquid chromatography. All the syringes were equipped with needle guides, since the injection port was not easily accessible and rapid injection was essential. With fuel volumes less than 5 μl, the pressure variation which accompanied injection was so small that it was necessary to have a fast responding marking system to record the point of fuel injection on the pressure chart. The simple device developed for this purpose is shown in Figure 2.15. The $1\frac{1}{2}$-volt charge from the battery was stored by the capacitor until it was discharged at the required instant across a spare galvanometer in the Honeywell 1706 Visicorder. To synchronise the discharge with the end of injection, a micro-switch was attached to the syringe barrel in such a position that it was operated by the finger at the end of the syringe plunger stroke. The single deflection produced and recorded on the chart thus defined the zero-time point with respect to the subsequent pressure-time trace.

2.2.4 Pressure Measurement

The pressure changes accompanying the course of a reaction were monitored using a 0 to 50 psia unbonded strain gauge transducer supplied

Figure 2.15

The Injection Marker Apparatus

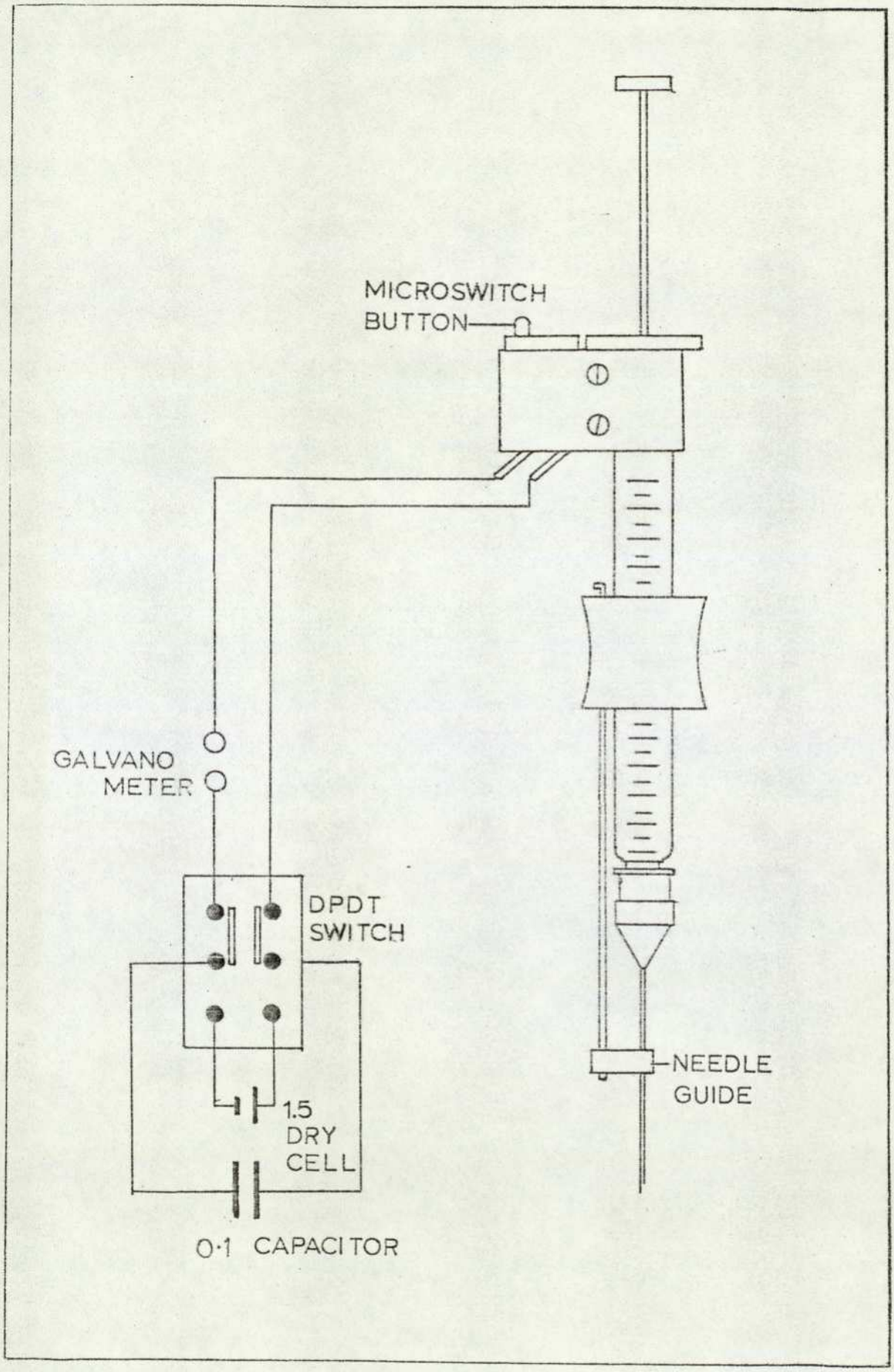

by Bell and Howell (type 4.306-0242-03MO). The 10 volts DC required for excitation of the transducer bridge was obtained from a Belix TSS65 stabilised power supply.

The output signal from the transducer was amplified using an LM201 operational amplifier functioning in the inverting mode and the signal thus produced was recorded using a Honeywell 1706 Visicorder equipped with a 130A miniature galvanometer. The circuit for the LM201 operational amplifier is shown in Figure 2.16.

2.2.5 Product Analysis

2.2.5.1 Product Sampling Valve and Timing Gate

An essential prerequisite for monitoring the formation of odorants during the oxidation reaction was a facility which enabled the instantaneous sampling of the products at any desired time after injection. Previous devices have employed a solenoid-operated valve activated by a transistor-based time-delay circuit. In order to take advantage of the recent advances in solid-state electronics, particularly the widespread application of monolithic integrated circuits, a circuit design employing such devices was developed. Two 555 Timer A chips were incorporated into the circuit, the remaining auxiliary external components simply being the resistor-capacitator networks and associated switching apparatus. One of the timers determined the initial delay period, i.e. the time interval between injection and valve opening. The second timer controlled the time period for which the solenoid valve remained open. The first timer was set in operation by closing the same set of contacts on the syringe barrel, which were used as part of the injection marker system. The second timer was directly coupled to the output of the first, so that the two time

Figure 2.16

The Operational Amplifier

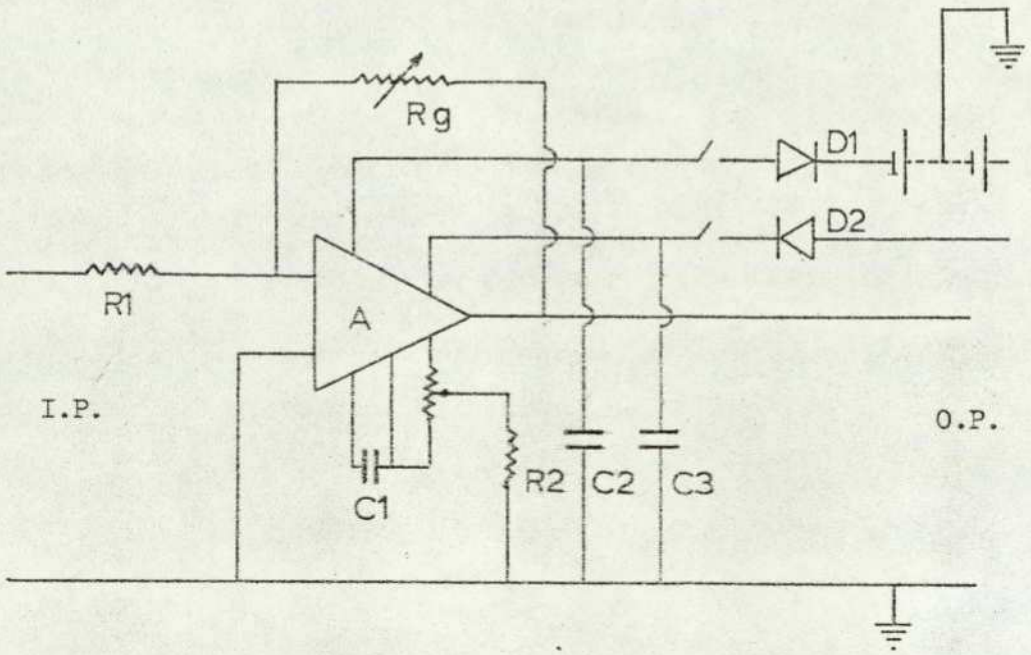

COMPONENTS

A	LM201 Operational Amplifier
C1	30 pf
C2,C3	0.22μF
R1	10k
R2	5.6M
Rg	10k, 20k, 30k, 40k, 50k, 100k, 200k
I.P.	Input Signal from Transducer
O.P.	Output Signal to Galvanometer
D1,D2	IN4001 diodes

periods were consecutive. Manual operation of both first and second timers was possible using pulses generated through bias switches. The advantages of using a timing network such as this were the reproducibility of the time intervals and the semi-automatic nature of the sampling operation. Both time periods, which were independently set, were selected using a particular resistor-capacitor network. Thus, once these networks were selected, the sampling procedure was automated from the moment of closing the syringe contacts on injection. This dispensed with the inherently cumbersome use of a stopwatch which for short time periods, would have been most inconvenient.

The circuit was constructed on copper strip board, the external components to the chips being carefully selected to attain the manufacturers quoted reproducibility for the timing periods of $\pm$ 0.5 % for 100μs and $\pm$ 2 % for 3 minutes. Capacitor leakage is obviously a factor which seriously influences the timing reproducibility and thus care was excercised in the construction to minimise leakage through grease or flux. Supply voltage for the timer chips was obtained from a Kingshill stabilised power supply which delivered 12 volts DC to the parallel voltage rails. Figure 2.17 illustrates the complete solenoid-timer network.

External indication of the timer states was achieved using two small filament bulbs powered directly from the output of each timer. This arrangement was particularly useful when the timer periods were set up prior to operation during an experimental run.

A cross-section of the solenoid valve is shown in Figure 2.18 which illustrates the very simple mode of operation. On activation of the coil, the iron rod lifts rapidly under the effect of the induced magnetic field, thus opening the valve orifice and permitting free gas flow. Products are then instantaneously withdrawn under vacuum from the reactor

Key to Figure 2.17

Integrated Circuits

A	Timer A Operational Amplifier RS

Capacitors

C1,6,12,15,16	Polyester 400V d.c.
C5,6,7,10	Polyester 400V d.c.
C3,8	Polycarbonate 630V d.c.
C4,9	Polycarbonate 63V d.c.

Diodes

D1,2	IN4002

Resistors (All Metal Oxide Tol ±2%)

R1-10	1-10M (Prefered Values)
R11-20	1-10M (Prefered Values)
R21,23	300k
R22,24	15k
R25,26,27	10k

Transistors

TR1	BFY50

Miscellaneous

RY	Relay 12V d.c. 300 ohms
SV	Solenoid Valve
SW1,2	Switches, bias to off (240V 3A)

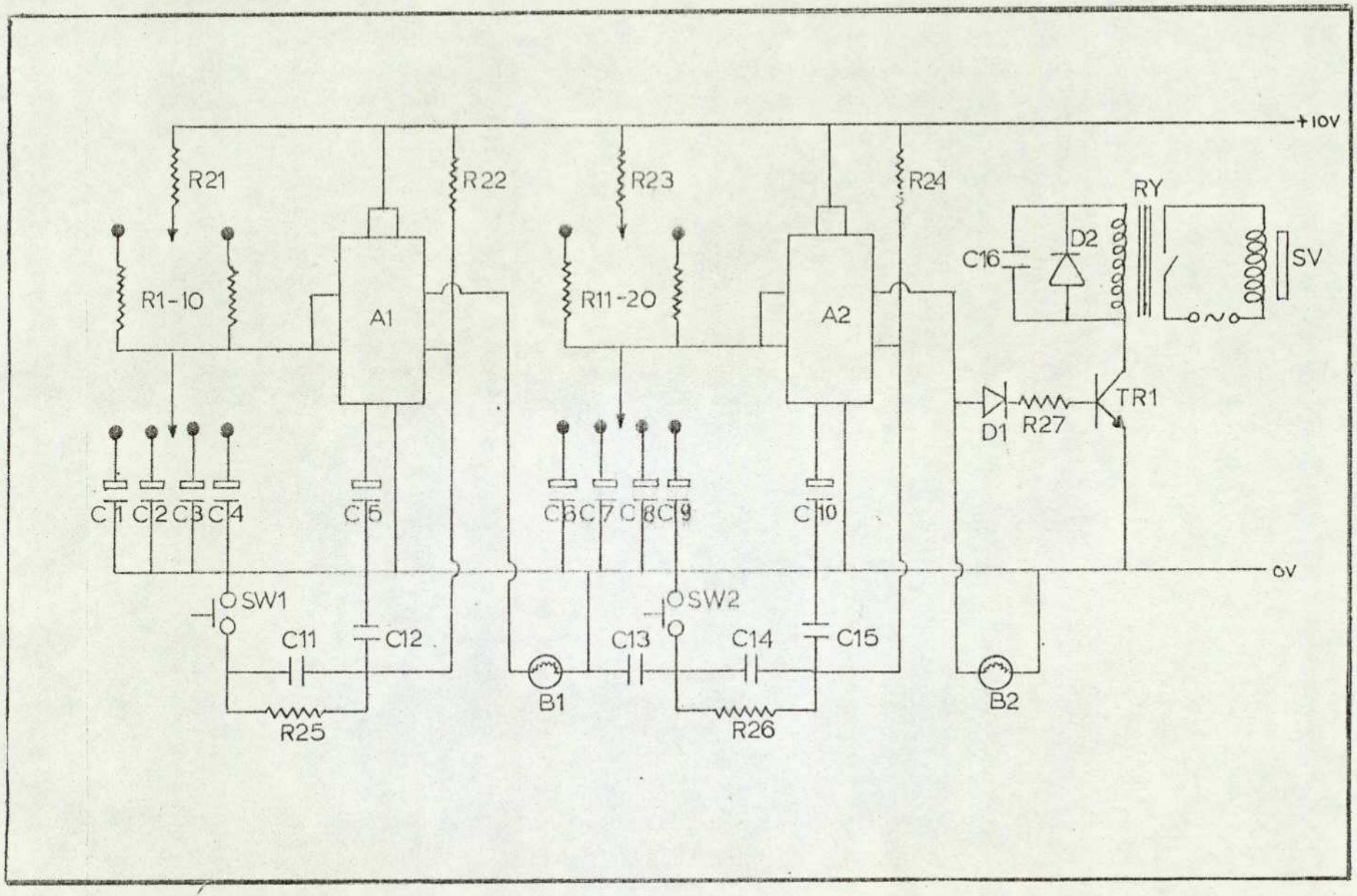

Figure 2.17

The Solenoid Valve Timer

Figure 2.18

The Solenoid Valve

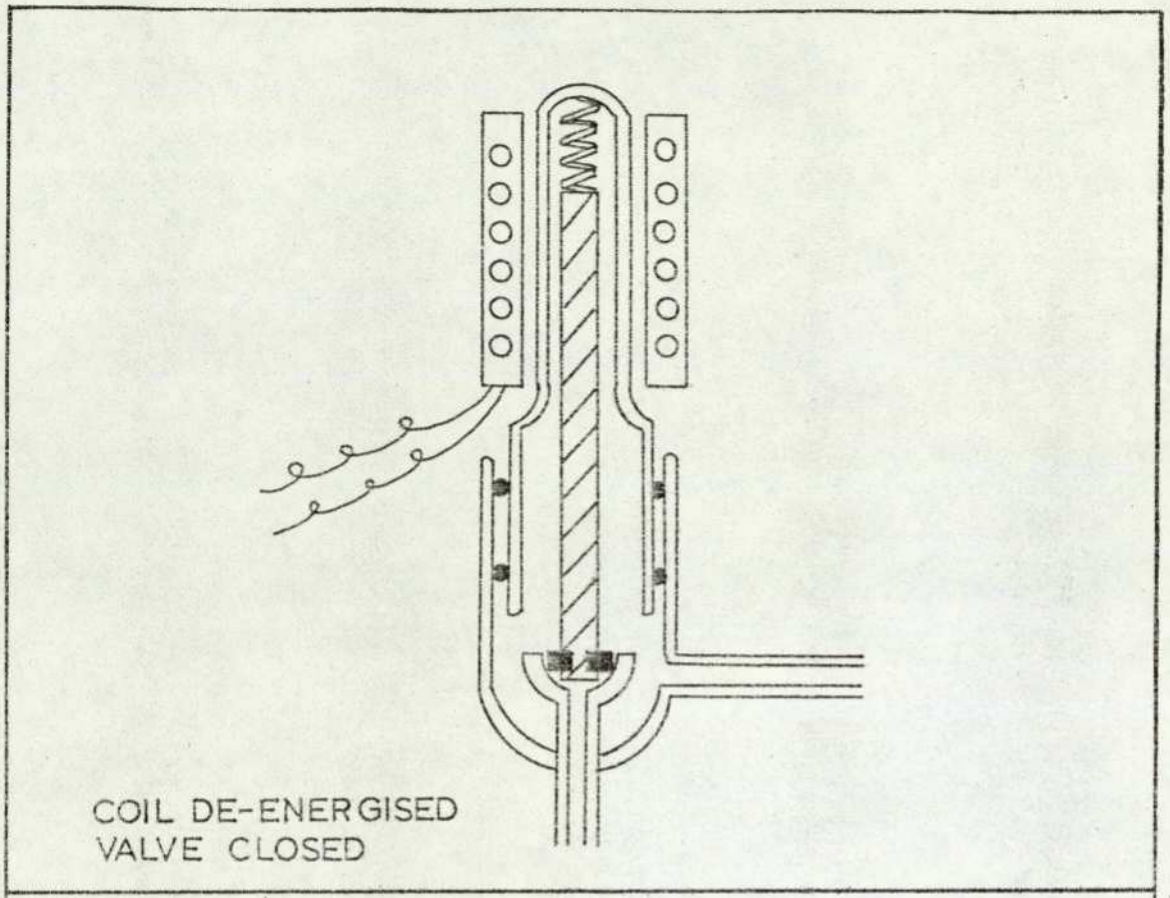

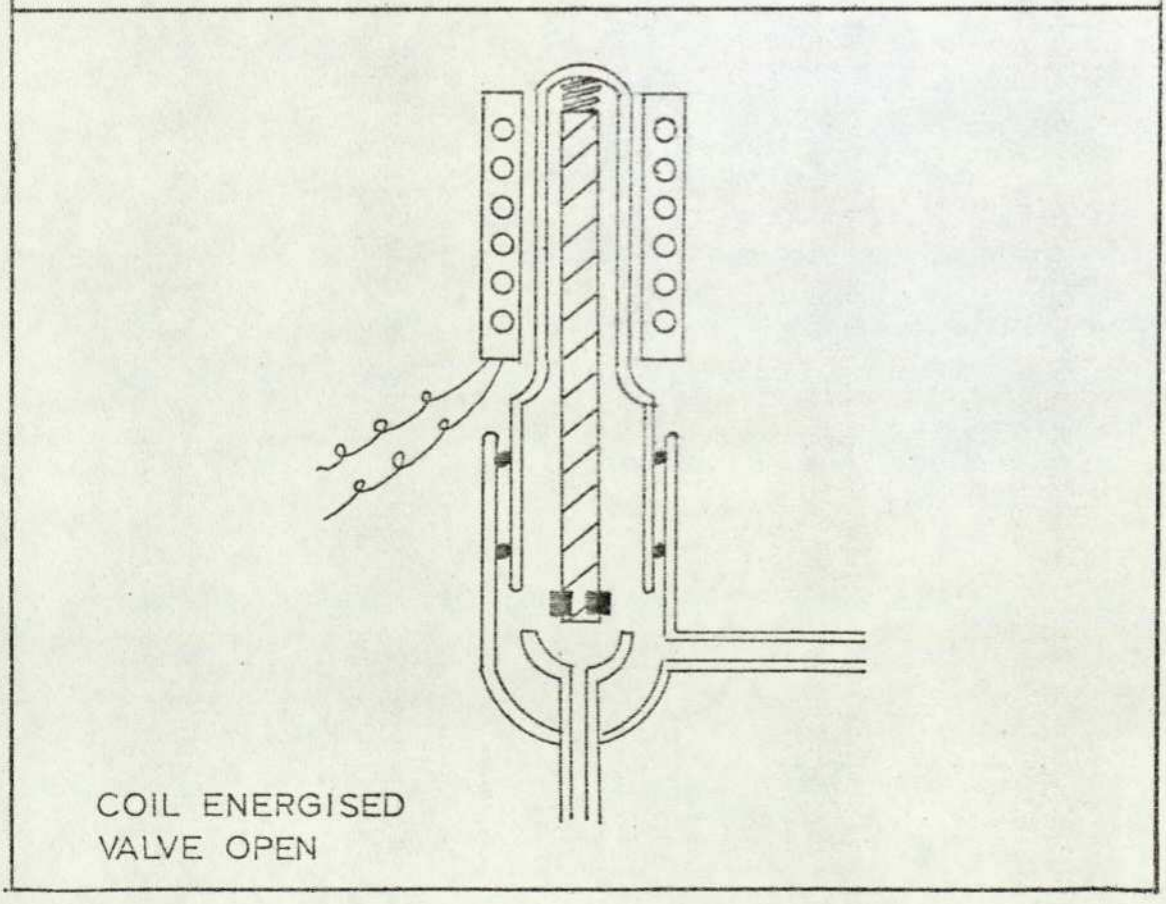

into either the stainless-steel liquid chromatography traps or the glass gas chromatography loop.

2.2.5.2 Gas Chromatography

The Sample Loop

Much experimental work went into the development of the on-line gas chromatographic sampling system. Initially the F11 GC was linked to the combustion rig by a four-way rotary valve and $\frac{1}{8}$ inch bore Pyrex glass tubing, a system which together with the injection port incorporated into the loop, had a total volume of 10 ml. The loop was maintained at 100°C with Electro-thermal heating tape. With this design, however, only trace quantities of products were actually transferred to the capillary column for analysis. Modifications to this system were made and a glass coil was added to the loop, increasing its volume to 25 ml. and simultaneously permitting the trap to be cooled using liquid nitrogen for the purpose of condensing the gaseous products. These modifications were made in conjunction with a reduction in the volume of the product-sharing globe to 250 ml., which also assisted in increasing the volume of sample trapped. Good chromatograms resulted from these modifications even without cold trapping of products.

The final design of the loop is shown in Figure 2.19. The stainless-steel valve employed to redirect the carrier gas through the loop was initially connected to the loop by Drallim brass couplings and silicon-rubber washers. However, it was discovered that the trace chromatograms produced as background were due to the products being retained within these couplings. This problem was eliminated by using stainless-steel Swagelok couplings and p.t.f.e. ferrules. The injection

Figure 2.19

Product Sample Loop for Gas Chromatographic Analysis

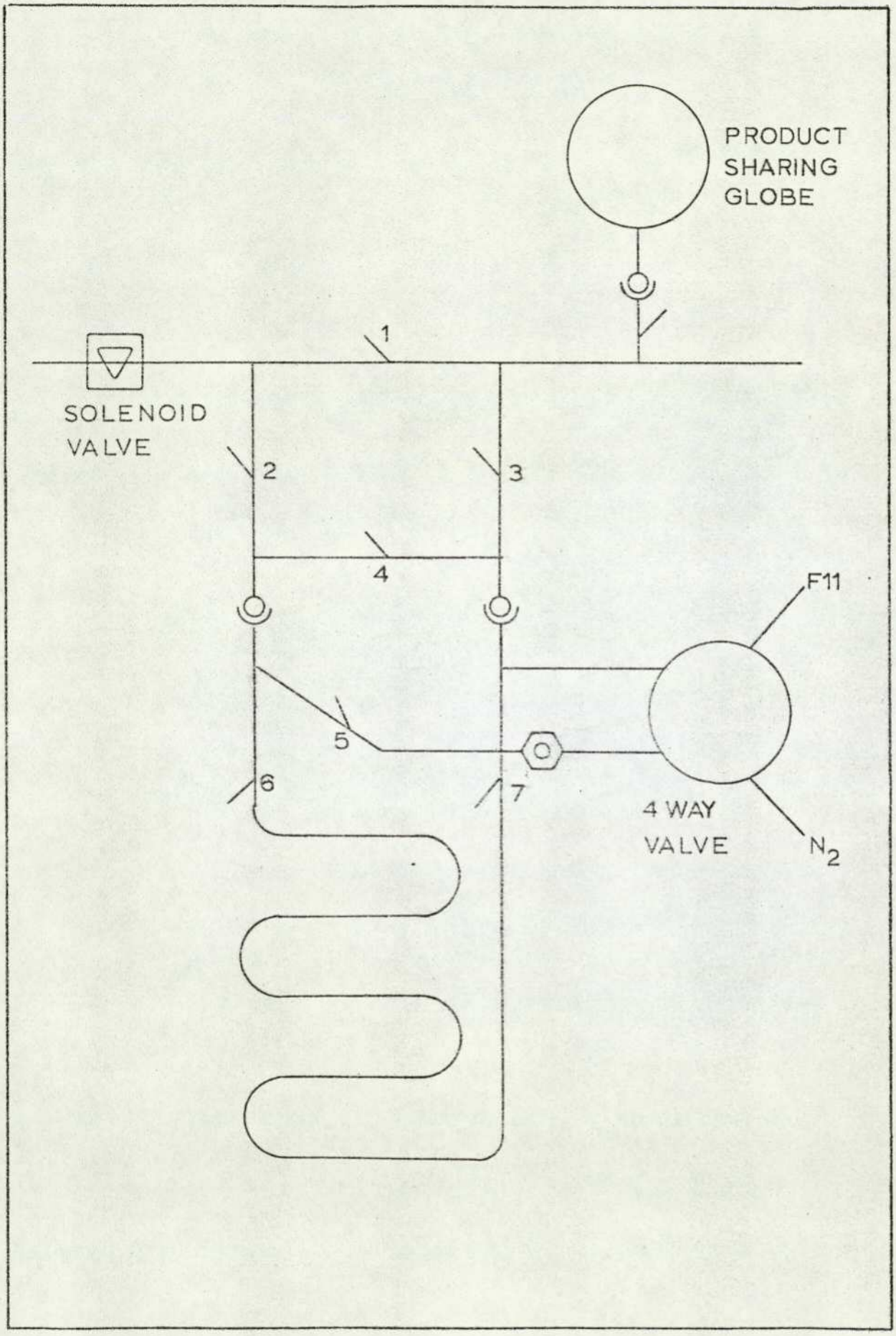

port incorporated into the loop enabled the accurate measurement of retention times for standard compounds which were directly injected into the loop and also permitted the doping of the product sample trapped in the loop with known compounds.

The Gas Chromatograph

A Perkin-Elmer F11 Gas Chromatograph, equipped with flame ionisation detector and linear temperature programmer, was used for on-line gas chromatographic analysis of the oxidation products from the various fuels and also of the fuels themselves. Component separation was achieved using a 50 ft. Carbowax 20M support coated open tubular (SCOT) capillary column. The column was chosen for its particular affinity for polar species and for the high temperature stability of the stationary phase. The column was carefully conditioned using a prolonged step-wise temperature programme and low nitrogen carrier gas-flow rate. Three pre-column splitters were available for use with the column and after some experimentation the medium-flow splitter operating with a 2:1 splitter: column ratio was found to give optimum performance. The splitter was used to reduce the possibility of column overload since sample volumes for capillary column seraration are typically 0.1 μl. The flow rates required are also much less than for packed columns and are normally less than 5 ml. min.$^{-1}$ compared with the 20 or 30 ml. min.$^{-1}$ with packed columns. Flow rates were monitored using a bubble flow meter attached to the splitter vent since the column flow rate/splitter flow rate was found to be constant over a wide range of carrier gas pressures. The carrier gas, together with the hydrogen and compressed air for the f.i.d., were controlled using needle valves and pressure gauges.

Fuel analyses were also carried out using the same chromatograph

equipped with a stainless-steel $\frac{1}{8}$ in.x 12 ft. column packed with 15 % Apiezon L on Chromosorb P 80-100#. Apiezon L is primarily a boiling-point column and the results obtained were compared with those obtained from a simulated distillation. Once again, the high temperature stability of the column packing made the column highly suitable for resolution of the high molecular weight components found in diesel fuel.

Further confirmation of the alkane peak assignments to some of the fuel components was obtained with a Perkin-Elmer F30 Gas Chromatograph attached to a Varian CDS 111 (C) Computing Integrator. Comparisons were made between the chromatograms produced from American test fuel and those from standard diesel fuel. For the analysis a 6 ft. stainless-steel column packed with Carbowax 20M was used with dual flame ionisation detectors. The CDS 111 integrator quantified the results obtained from the two fuels and expressed the data in peak area percent. A standard mixture of nine alkanes from C_5 to C_{16} made identification of these alkanes possible in both fuels. The programme used for this analysis together with the details of all the other fuel analyses is reported in Section 2.4.

2.2.5.3 Liquid Chromatography

The Sample Traps

Combustion products intended for liquid chromatographic analysis were trapped by a method which was developed for diesel exhaust analysis. The miniature traps were identical in design to the large traps employed for the collection of 15 litres of diesel engine exhaust. Figure 2.20 illustrates a cross-sectional view of a typical trap constucted from a 1.18 in. x 3/16 in. O.D. 316 stainless-steel tube with a 3/16 to $\frac{1}{4}$ in. 316 stainless-steel Swagelok reducing union fixed to each end. The

Figure 2.20

Product Sample Trap for Liquid Chromatography

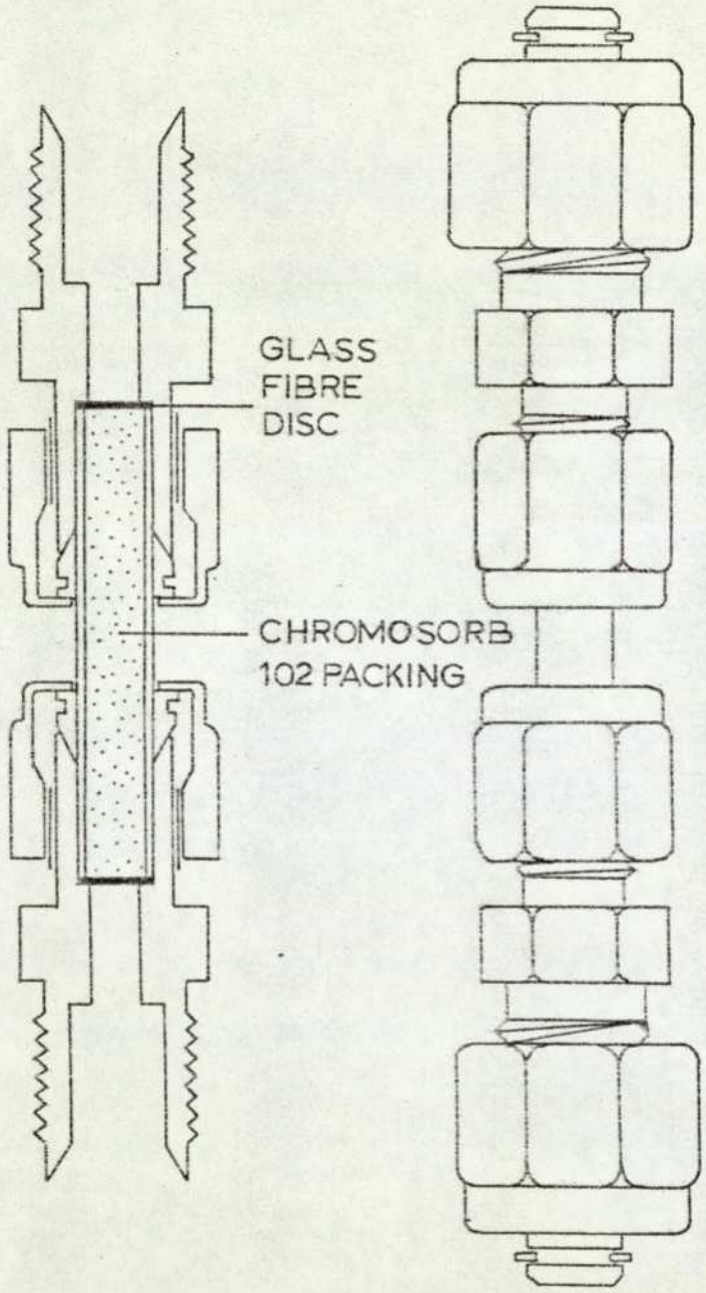

combustion products were trapped on a solid cross-linked polymer packing, Chromosorb 102, the fine particles of which were retained in the tube by discs of silanised glass fibre sheet housed in the Swagelok couplings. Figure 2.21 shows how the traps were located in the static vacuum apparatus prior to sampling. The ball joint at the end of the fexible p.t.f.e. tubing was coupled to the socket situated below the product sharing globe V4, since this part of the apparatus became redundant during the sampling procedure.

Prior to use, the Chromosorb 102 packing material was purified of trace contaminants by careful elution procedure which involved the use of three solvents. 200 grams of the packing material was transferred to a 1 cm. glass column, the lower end of which was restricted and plugged with silanised glass wool. One litre of methanol was passed through the column to remove any polar contaminants, followed by 500 to 800 ml. of pentane. Finally cyclohexane was used to flush out the previous solvents. The Chromosorb 102 was then dried at room temperature by spreading it on a shallow dish placed in a position free from atmospheric contaminants. Information regarding the quality of solvents and the Chromosorb 102 is included in Table 2.2.

The Liquid Chromatograph

Analysis of the cyclohexane eluent from the Chromosorb 102 traps was performed using the technique devised by Arthur D. Little Inc. for the analysis of diesel exhaust samples. A successful attempt was made to faithfully reproduce the essential details of the ADL equipment, the only difference being the manual as opposed to the electronic operation of the events sequence used in the ADL scheme. The basic components of the scheme were available as the Perkin-Elmer 1240 HPLC

Figure 2.21

The in situ Connections of an LC Trap

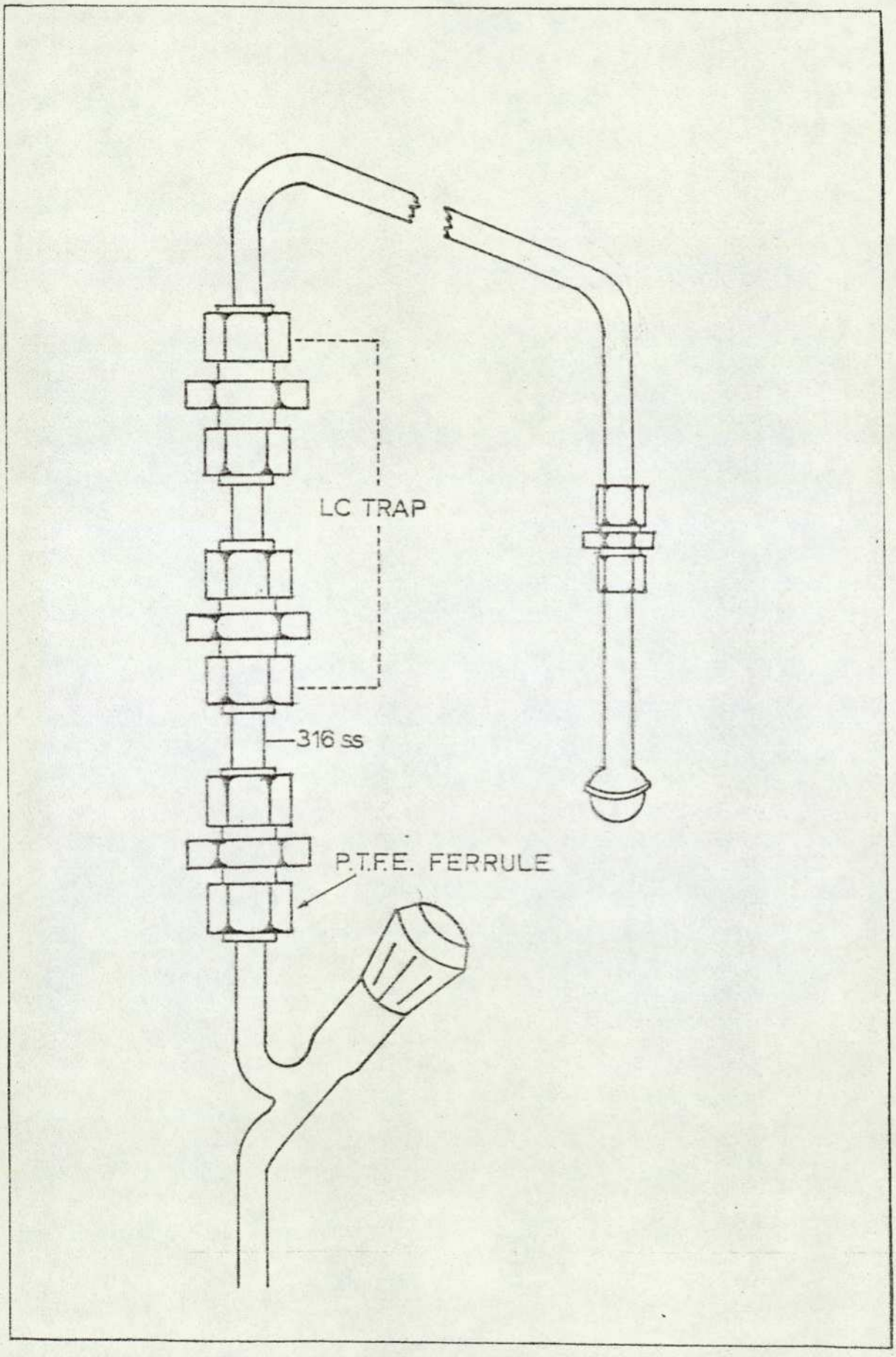

Table 2.2

Specification of Materials Used in Liquid Chromatography

Chemicals	Supplied By	Purity
Chromosorb 102 60-80 mesh	Perkin-Elmer	-
Cyclohexane	BDH	AnalaR
Pentane	BDH	AnalaR
Methanol	BDH	AnalaR
Propan-2-ol	BDH	AnalaR
Silica Gel Adsorption Activity 1	BDH	AnalaR
Aluminium Oxide W 200 Basic Activity Grade Super 1	Koch-Light	-
2'-Hydroxy-4'methoxy acetophenone	Aldrich Chemical Company	99%
Indan	Aldrich Chemical Company	97%

with the additional requirement of a high-pressure fixed volume loop injector valve. The flow scheme is shown in Figure 2.22

The objective of the high-pressure liquid chromatograph (HPLC) analysis of each sample was to resolve the exhaust components contained in the cyclohexane solution into two fractions, one containing the non-oxygenated aromatic and aliphatic species (designated liquid chromatographic aromatic, LCA) and the other the oxygenated compounds (designated liquid chromatographic oxygenates, LCO). This simple resolution was achieved on a 15 cm. x 0.33 cm. stainless-steel column packed with Corasil II. The column was conditioned prior to use by passing a methanol flow at 1 ml. $min.^{-1}$ for 50 minutes followed by cyclohexane under the same conditions. Reconditioning of the column was sometimes necessary and this involved the same procedure.

Samples were injected into the solvent stream at the top of the column using a septum injector and a 10μl syringe designed for high back pressure injection. The septum was constructed of soft silicon-rubber faced with p.t.f.e. on the solvent side.

The resolved peaks emerging from the column were detected by a mercury line U.V. absorbance detector equipped with filters selecting a wavelength of 2537Å. At this particular wavelength the paraffinic species in the sample do not absorb and therefore pass through the detector without contributing to the non-oxygenated component peak. The detector contained two 12μl cells, one for reference and the other for the sample, each with a path length of 10 mm. An absorbing component passing through the detector produced a differential signal which was amplified by an electrometer equipped with a range selector and attenuator. The detector output in the form of optical density units (O.D.) had a maximum sensitivity of 0.01 OD fsd. on a 10 mv. recorder. This degree of

Key to Figure 2.22

C	Column
F	Flowmeter
G	Pressure Gauge
I	Septum Injector
P	Pump
PCO	Pressure Cut-Off Device
PD	Pulse Damper
RC	Reference Cell (Detector)
S1	25ml Polypropylene Syringe
S2	10ul Microsyringe
SC	Sample Cell (Detector)
SR	Solvent Reservoir
V	Fixed Volume Loop Injector Valve
VR	Solvent Reservoir

Figure 2.22

Liquid Chromatograph Flow Scheme

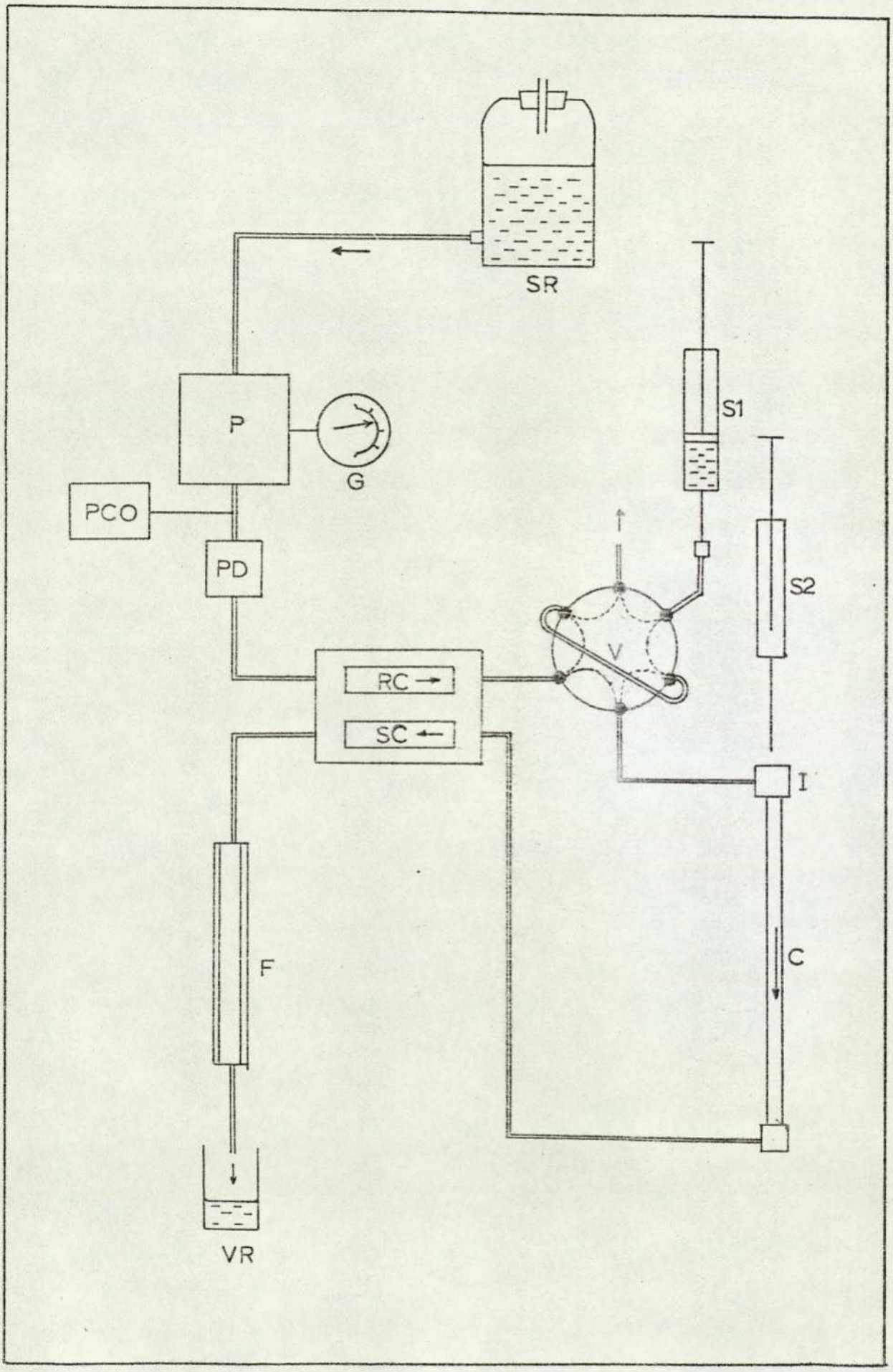

sensitivity was not required, however, and analyses were usually performed on a range of 2.5 OD fsd. for a 10 mv. output. The signal from the electrometer was recorded on a Perkin-Elmer-Hitachi recorder (2.5 mv. fsd.) which, on account of its lower input voltage requirements, responded to a signal of 0.63 OD with 100 % deflection on the aforementioned range setting. The peak areas were quantified by a Kent-Chromalog electronic integrator coupled in parallel to the recorder output.

Solvent flow through the system was generated by a Milton-Roy positive displacement reciprocating pump which delivered solvent with a quoted repeatability of $\pm$ 0.3 % at flow rates from 0.6 ml. min^{-1} to 4.6 ml. min^{-1} and pressures up to 1000 psi. All analyses were performed at a flow rate of 1 ml. min^{-1}. The pump was operated in conjunction with a Nester-Faust pulse damper which minimised solvent flow fluctuations well below the detector response level when set at 2.5 OD fsd.

A gradient elution and degasser unit was used as a reservoir for the cyclohexane. The solvent was continually stirred in the reservoir and could be heated under reflux to remove dissolved gases which might otherwise form bubbles in the detector giving rise to spurious signals. The gradient elution unit was not used for the generation of a solvent polarity gradient, since the analytical procedure necessitated the introduction of a discrete solvent slug rather than a continuously increasing polarity scheme. Isopropanol was used as the high polarity solvent which enabled the elution of the polar components retained by the Corasil II column. A volume of 50 μl was injected into the solvent stream using a Perkin-Elmer fixed volumn loop injector valve specifically designed for this purpose.

The necessity for using solvents of very high purity for the analysis procedure was very evident. Fresh aliquots of AnalaR cyclohexane

taken from the storage bottle were found to give the best results. If, however, the reagent had been allowed to stand in contact with air for any length of time, then it was found necessary to purify it by passing it through a 1 in. column, the upper portion containing 100 g. of silica gel (Woelm Activity 1) and the lower portion containing 100 g. of aluminium oxide (W basic Activity super 1). The first 50 ml. of eluent was discarded and the next 500 ml. was retained. Fresh isopropanol was also used throughout the analysis since use of the aged reagent resulted in peak-tailing of the LCO peak.

By modification of the gradient elution former unit, a convenient method for eluting the LC traps of the bomb exhaust was achieved. The gradient elution unit consisted of a synchronous-motor driven syringe which delivered a high polarity solvent into the continuously stirred degasser reservoir. As described previously, the generation of such a gradient was not warrented and therefore the syringe mechanism lent itself to the controlled elution of the traps. To facilitate elution, a Swagelok coupling and a length of p.v.c. tubing was used to connect the syringe to the trap. Cyclohexane was delivered at a constant flow rate of 0.5 ml. min^{-1} and the eluent was collected in 1 ml. graduated flasks held at the lower end of the trap. This technique not only rendered the elution reproducible under flow conditions, but also minimised the elution times which under gravity feed conditions might have been sufficiently long to make solvent evaporation a problem.

2.2.6 Fuels

In order to produce results relevant to the production of odorants during diesel engine combustion process, an authentic diesel fuel of the type commercially available to the general public was used

for all the experiments. This fuel was purchased from a retailing garage and the single quantity of fuel obtained served for the complete experimental programme. Variations in fuel composition, which are known to occur with each delivery to the retailer, were thus avoided. The fuel was stored in a cool atmosphere in opaque glass containers, since under these conditions diesel fuel is known to exhibit high stability. Gas chromatographic analysis of the fuel directly after purchase and at regular intervals throughout the experimental period indicated that the fuel suffered no changes in composition.

The exact specifications relating to the analysis of the diesel fuel used are related in Section 2.4. The specifications concerning the other compounds used for fuel are given in Table 2.3.

Table 2·3

Fuels (Other Than Diesel) Used in Combustion Studies

Chemicals	Supplied by:-	Purity
n-Hexadecane	BDH	Minimum assay GLC 99%
Ethylbenzene	BDH	Minimum assay GLC 99%
n-Butylbenzene	BDH	Minimum assay GLC 99%
Xylene	BDH	AnalaR
Indan	Ralph N-Emmanuel	97%
1-decene	BDH	Boiling Range (95) 167 - 171°C

2.3 Experimental Techniques

2.3.1 Calibration of the Pressure Transducer and Pressure Recording

The outputs of the pressure transducer and the electronic amplification equipment together with the galvanometer response were calibrated against a mercury manometer. Various pressures of dry nitrogen were admitted to the reaction vessel and the galvanometer spot displacement corresponding to each pressure was recorded. A linear relationship with minimum hysteresis was recorded for the pressure range 0 to 600 torr. Attenuation changes affected only the gradient of the relationship, not the linearity. Prior to each set of experiments at a given temperature and pressure, the calibration procedure was carried out; repeated calibrations were then performed during and after the same set of experiments or whenever attenuation changes were made. The reproducibility throughout the experimentation and indeed over a long period of time was found to be extremely good.

To record the pressure-time trace corresponding to each fuel oxidation, the following technique was used. The required pressure of gas acting as the atmosphere for the experiment was admitted to the bomb, the pressure of the gas being measured by the manometer M1. The 1706 Visicorder galvanometer spot was then displaced by the zero potentiometer on the LM201 amplifier to give a trace approximately 1 cm. from the bottom of the chart. Once this had been set, the same pressure of gas would always return the galvanometer spot to the same position on the chart. The chart drive was then set in motion and the fuel was injected into the bomb. The pressure rise accompanying the combustion process was then recorded as the galvanometer spot was displaced. If necessary, adjustments were made to the amplifier attenuation in order to produce the maximum galvanometer deflection

for a given pressure rise, whilst keeping the spot to the limits of the 12 cm. wide chart. The calibration procedure for the chosen attenuation setting was then performed.

2.3.2 Fuel Injection

A study of diesel engine combustion reveals the important role played by fuel injection characteristics in determining the form of the resulting combustion process. Spray atomisation and penetration are two critical factors which affect the nature and completeness of combustion. However, in the experiments conducted with the static vacuum apparatus, no useful purpose would have been served in attempting to simulate the diesel engine injection process, since sub-atmospheric pressures and comparatively low temperatures were employed, both of which affect the spray characteristics. The injection technique used to introduce the desired quantity of fuel into the bomb was similar to that employed in gas chromatography, i.e. rapid, clean injection with quick withdrawal of the syringe needle.This technique produced results of high reproducibility.

Two types of septa were tested for their durability. The first type consisted of a rubber-teflon-rubber sandwich construction, specifically recommended for extreme temperature conditions. The second type consisted of a soft white silicon rubber which was, however, found to be more durable, lasting for more than 25 injections before replacement became necessary.

2.3.3 Product Sampling and Analysis

2.3.3.1 Gas Chromatography

Analysis of the contents of the bomb at any instant after injection was facilitated by rapid withdrawal of the gases under vacuum through the solenoid valve into a sampling loop. The sequence of events for this process will be related with reference to Figures 2.11 and 2.20, the tap identification numbers being common to both Figures. As an example of a typical analysis, the sampling of the pre-cool flame oxidation of diesel fuel at 500 torr pressure and 280°C will be cited.

The time for analysis was chosen to be approximately two seconds after injection. The timing circuit was therefore set to give two seconds as the initial delay period and five seconds as the valve-opening time, since this would allow pressure equilisation within the loop. The bomb was then conditioned with five runs each consisting of one 5 μl. injection of fuel into 500 torr of air, ten minutes being allowed to elapse between each run during which time the bomb was evacuated. After the last ten minute period, taps 13 and 22 were closed, isolating the bomb from the vacuum system. Tap 21 was slowly opened allowing 500 torr of air, measured on manometer M1, to fill the bomb. Tap 15 was then closed leaving tap 14 in the open position. Evacuation of the loop, sample sharing volume V4, and the line including manometer M2 now being complete, taps 10 and 11 were closed. In order to direct the gas flow through the loop, taps 1,4,5 and 12 were closed. With the system in this condition only the solenoid valve restricted the bomb contents from enetering the evacuated sample loop. The Visicorder galvanometer spot was checked to read P_o and the chart drive was set in motion. Injection of the 5 μl of fuel resulted in the syringe contacts starting the initial delay period of the timer. After two seconds the solenoid valve automatically opened to allow the partially oxidised fuel products to escape and fill the loop, V4 and the manometer M2. After

five seconds, taps 2 and 3 were closed, tap 5 was opened and the rotary valve on the F11 was turned to redirect the carrier gas through the loop. The carrier gas was allowed to flow through the loop for 15 minutes before being returned to its original position. The whole system was then evacuated in preparation for further runs.

Prior to analysis the gas chromatograph was set with the required initial conditions and the baseline checked for stability. The programme used for the analysis of the oxidation products of all the fuels was as follows:-

N_2 carrier gas	3 psi split with vent: column ratio as 2:1; 4 ml./min through column
H_2 (FID)	17 psi
Air(FID)	25 psi
Initial Temp.	60 ^{o}C
Initial Period	5 minutes
Final Temp.	195 ^{o}C
Prog. Rate	5 ^{o}C/min.

Under these conditions, 40 minutes was sufficient to elute all the peaks.

For the major part of the analytical work, low fuel volumes were injected into the bomb as determined by the stoichiometric equation for oxidation. In addition the fuel lean region was of particular interest requiring even smaller quantities of fuel. The conditions, therefore, forced the use of low attenuation settings, since the actual quantities of products formed were so small. The ionisation amplifier was therefore operated with the attenuator set between 10 and 50 which resulted in the baseline drift originating from column bleed being very significant, even after careful and lengthy conditioning of the column.

This baseline drift excluded the possibility of using an electronic integrator for quantifying the peak areas. The quantification of components being eluted from a capillary column is known to be a more complex task than for packed column assessment, since the splitting ratio and other factors have to be taken into consideration. With the chromatograms being so complex in nature together with the high degree of baseline drift, the problem becomes virtually insoluble. A capillary column was chosen for the particular application in hand for its ability to produce an extremely high degree of component resolution together with its low sample volume requirements.

It was possible to formulate very useful conclusions from the qualitative data produced by the capillary chromatography and the shortage of quantitative data was compensated for by the results obtained from the liquid chromatographic analysis, the two techniques complementing each other in a very favourable manner.

2.3.3.2 Liquid Chromatography

In a manner very similar to that described for the collection of bomb products for gas chromatographic analysis, it was possible to collect samples for liquid chromatographic analysis. The essential difference between the sampling methods was that the samples for LC analysis were adsorbed on to a solid stationary phase and therefore did not remain in the gas phase as for the GC analysis. The solid adsorbent used for this purpose was Chromosorb 102, since its efficiency in the collection of such components has been reported.[108,109] The traps were placed prior to sampling in the vacuum line above tap 12. The flexible p.t.f.e. tubing terminating in a ball joint was located in the cup section above tap 8, the product sharing volume V4 being redundant for this

sampling operation. The sequence of events leading to the actual time of sampling was identical to that employed for GC analysis. Taps 1,2, 3,9 and 10 remained closed, and taps 2 and 8 were opened allowing evacuation of the trap through tap 11. When the solenoid valve was opened the gaseous contents of the bomb were drawn under vacuum through the traps. The sampling section of the line was open to the vacuum system throughout the sampling period. The solenoid valve remained open for 1 minute, which was sufficient to evacuate all the contents through the sampling trap. After the sampling period, taps 12 and 8 were closed and the trap was removed and capped with stainless-steel plugs.

It has been reported that the samples thus collected are stable for some considerable period of time. However, although experiments did not disprove this claim, an attempt was made to analyse the samples within 24 hours from collection.

Preparation of the traps before sampling and their cleaning after use involved the careful washing of the couplings and tubes with water followed by acetone and finally cyclohexane. The interior surfaces of the traps were cleaned with the assistance of a small diameter GC column cleaning brush.After this washing procedure, the traps were dried in an oven at 200°C for 24 hours.

Silanised glass fibre matting was used to retain Chromosorb 102 packing within the tubes. To ensure an exact fit of the glass fibre retaining disc within the Swagelok union, the following technique for fitting the discs was developed. The Swagelok reducing union was placed upright on a flat surface with the 3/16 ID end uppermost. The glass fibre sheet, previously washed in cyclohexane and dried, was placed flat over the Swagelok opening and a disc of the material punched out of the sheet directly into the coupling using a length of 3/16 in. steel-tube specially

sharpened for the purpose. The trap was then located in the union, the fibre disc thus being retained. In order to pack the tubes, they were placed upright in a retort clamp and the lower end sealed with the fibre disc was attached to a vacuum line. The Chromosorb 102 was then firmly packed into the tubes accompanied by tapping. When full, the open end was closed by another Swagelok coupling complete with fibre disc. For storage, both before and after use, the traps were capped with stainless-steel Swagelok plugs.

Each trap was stamped with a number at one end which fulfilled the dual role of enabling identification of each sample and also affording a means of indicating which way up the trap was placed in the combustion apparatus during sampling. It was important that elution of the traps should be performed in a manner such that the sample was eluted from the same end of the trap from which it entered. This reverse elution eliminated the possibility of the sample undergoing a chromatographic elution with perhaps the retention of some of the trapped components.

Elution of the traps using the motor driven syringe has already been described. The trap was connected to the syringe using a coupling adaptor which enabled the connection of a length of narrow bore p.t.f.e. tubing to the trap and to the end of the syringe needle.

Once eluted the sample solutions were stable only for a relatively short period and analysis was always performed within three hours of elution. If the samples were left for a period in excess of 24 hours, then there was a noticeable decrease in the LCO peak area indicating the instability of some of the components.

The 1240 HPLC was prepared for analysis by filling the reservoir with 200 ml. of cyclohexane solvent and setting the flow rate to 1 ml./min. The detector was calibrated using the internal calibration filter and the

baseline was corrected if necessary. The syringe holding the isopropanol in the fixed volume loop injector was filled with fresh reagent. After pumping for 1 minute, 50 µl of isopropanol was injected and simultaneously a stopwatch was started. After 1 min. 40 seconds, the isopropanol passed through the detector and although the pure reagent does not absorb at 254 nm, a response was recorded. This signal was due to a number of factors. First, the introduction of a second solvent into the main solvent stream is known to produce a detector response, since there is a loss of transmitted light due to a change in the angle of refraction of the liquid in the detector cell. This effect, however, is expected to be rather small. Secondly, an unknown impurity possibly originating in the cyclohexane has been observed to accumulate on the column. This impurity is polar in nature and is therefore retained on the column until the passage of the isopropanol. The size of the peak thus produced is proportional to the volume of cyclohexane which has passed through the column, and for this reason it was essential to inject the isopropanol at regular timed intervals in order to quantify the background peak and to make it reproducible. Isopropanol was therefore injected every 5 minutes which allowed sufficient time for the resolution of the LCA and LCO peaks.

After 5 or 6 isopropanol injections the background peak area assumed a minimum and reproducible level. 10 µl injections of the cyclohexane samples were made 30 seconds prior to the next isopropanol injection. This time scale permitted the complete elution of the LCA peak before the emergence of the LCO. One 50 µl injection of isopropanol was sufficient to elute all the LCO contained in one 10 µl injection sample. The Kent-Chromalog integrator quantified each peak, several injections of each sample being made to ascertain the average area and the percent standard deviation (δ%) for the data.

Calibration of the LCA and LCO peak areas was achieved by using two standard solutions. For the LCA peak area indan was recommended by ADL as a calibration standard. A solution of 0.608 g./100 ml. cyclohexane was made, a 2 μl injection of this solution thus containing 12.04 μg. of indan. The Chromalog gave an average respose of 18.6 counts/ μg. indan. The ratio of the detector response per μg. of indan to that per μg. of LCA depends on the fuel type. GC/MS facilities were not available to establish this ratio for the fuel used so that quantities of LCA had to be expressed as μg of indan. For the LCO peak, 4-methoxy, 2-hydroxy acetophenone was recommended as the standard. A solution containing 139 mg/ 100 ml. of cyclohexane was made; a 1 μl aliquot of this solution therefore contained 1.39 μg HMA. Since the ratio of the detector response to LCO compared to an equal quantity of HMA is known to be constant at 0.72, a 1 μl injection of the standard solution gives the same response as 1 μg. of LCO. 3 μl injections of HMA were made for each set of samples to calibrate for the LCO response. The Chromalog integrator gave an average response of 133 counts μl. HMA.

To establish the background peak originating from the trap alone, one trap from every batch of traps prepared was set aside before sampling and was then eluted with the rest of the traps containing samples. The traps did contribute a very small amount to the LCO peak and this contribution, typically less than 2 % of the smallest LCO peak of the samples, was deducted from the area of each LCO peak.

2.4 Fuel Analysis

Diesel fuel is a complex mixture of organic compounds containing species with carbon numbers from C_5 to C_{32+}. The majority of the fuel consists of alkanes but aromatic and olefinic species are also present to varying degrees depending on the origin and blending of the fuel.

A complete analysis of the fuel would prove to be a very difficult task and in fact no such attempt has been reported in the literature. The aim of the gas chromatographic analyses which were carried out was therefore to:-

a. characterise the fuel used in the oxidation experiments;
b. to determine the molecular weight spread of the components;
c. to compare the chromatograms of the standard diesel fuel to those of the American test fuel;
d. to obtain a fingerprint chromatogram of the fuel for comparison with those obtained for the oxidation products;
e. to divide the chromatograms into molecular weight bands thus permitting comparisons with published data to be made;
f. to check for any changes in fuel composition which may have ocurred during the experimental period.

The gas chromatographs and the respective operating conditions used are summarised in table 2.4

In addition to the GC data collected, a sample was analysed by

Table 2·4

Details Pertaining to the Gas Chromatographic Analyses

Chromatograph	Microtek 2000	Perkin Elmer F11	Perkin Elmer F11	Perkin Elmer F30	Hewlett Packard 5700A
Detector	H_2 FID	H_2 FID	H_2FID	H_2FID	H_2FID
Column	6' x 1/8"	Am x 1/8"	50' Scot capillary	6' x 1/8"	6' x 0·09" ID
Packing	Carbowax 20M	15% Apiezon L Chromosorb P	Carbowax 20M	Carbowax 20M	Diatomite C (AW-DMCS)+10% SE-30
Carrier Gas	N_2	N_2	N_2	N_2	N_2
C.G. Flow Rate (ml / min)	30	24	4	30	30
Initial Temp.(^{o}C)	60	70	60	70	60
Initial Period(min)	0	25	5	10	0
Final Temp. (^{o}C)	220	250	195	200	300
Programme Rate (^{o}C / min)	10	10	5	10	8
Sample Volume (ul)	1	1	1	1	1
Objectives and Results	Preliminary Investigation into Fuel Composition	Characterisation of Alkanes in Fuel and Products	Characterisation of Alkanes in Fuel and Products under High Resolution Conditions	Characterisation of Alkanes in Fuel with measurement of relative peak areas	Simulated Distillation of Diesel Fuel (Courtesy of ADL)

Admiralty Oil Laboratory who kindly established the elemental composition of the fuel and also specified some of the physical characteristics, i.e. colour, flash point and viscosity. The results are given in Table 2.5. AOL also supplied results from a simulated distillation of a typical diesel fuel using a method similar to the ASTM method[116]. This data has proved most useful for comparison with the GC data collected.

From the data in Table 2.5, it can be seen that the C:H ratio of hexadecadiene approximates very closely to that of diesel fuel. In addition, hexadecadiene has a molecular weight which can be considered representative of the 'average' molecular weight of diesel fuel. For these reasons, the stoichiometric equation for the oxidation of diesel fuel was established using the molecular weight of hexadecadiene as an approximation.

$$C_{16}H_{30} + 23.5O_2 \rightarrow 16CO_2 + 15H_2O$$
$$222 + 752 \rightarrow 704 + 270$$

i.e. 752g of O_2 = 23.4% Air (Wt)

752g of O2 is contained in 3204g Air

F/A ratio = 222/3204 = 0.069

This value is within the range often quoted in the literature i.e. 0.067 to 0.07, the variations arising from the differing values that the authors attribute to the C:H ratio and the weight % of oxygen in the air.

Using the above value for the stoichiometric F/A ratio, the measured density of the fuel (0.827), and the hexadecadiene approximation for the molecular weight, a computer programme was devised to calculate the volume of fuel which was required to comply with the stoichiometric equation for oxidation over a range of initial temperature and pressure conditions. The programme also calculated the pressure rise produced solely by vaporisation of the fuel under these same conditions. This

Table 2·5

AOL Analysis of Diesel Fuel Used in the Present Work

Elemental

C%	86·40,	86·70
H%	13·77,	13·61
N%	ND*	ND*
O%	ND*	ND*

Characteristics

Appearance:	Clear and Bright
Colour:	1·0
Flash Point (PMC):	150°F (65·56°C)
Viscosity @ 100°F:	4·5 cS

Comparison of Molecular Weight and C:H Ratio with Alkanes

Hydrocarbon	M.Wt.	C:H Ratio (WT)
Diesel Fuel	—	0·157 - 0·159
Hexadecadiene	222	0·156
Hexadecane	226	0·150
Heptadecane	228	0·176

* ND = Not Detected

calculation assumed the applicability of the ideal gas laws to the completely vaporised fuel.

The fuel lean regions of combustion were of particular interest, since they represented the gross F/A ratios effective in the diesel engine under normal running conditions. Inspection of the fuel volumes calculated revealed that a 10 μl syringe could be used for the injection process with reasonable accuracy. Larger fuel volumes, i.e. for $\delta > 1$, were infrequently injected with a 25 μl syringe since under conditions of high temperature and pressure, hot ignitions invariably resulted.

Using the same computer programme format, calculations were made for the various fuel types investigated and data was obtained in this manner for 1-decene, n-butyl benzene and hexadecane fuels.

SECTION 3

RESULTS

SECTION 3

3.1 Gas Chromatographic Analysis of Diesel Fuel

3.1.1 Simulated Distillation

The results obtained from a simulated distillation of a typical diesel fuel under the conditions listed in Table 2.4 are graphically shown in Figures 3.1 and 3.2. The percent distillation data in Figure 3.1 were calculated from the total area underneath the chromatogram while adhering to the conditions and method explicitly defined in the ASTM procedure[116]. Figure 3.2 illustrates the component distribution by boiling point, showing the total number of peaks in each block of the histogram from Figure 3.1, together with the number of peaks each of which had an area greater than 0.05% and 0.1% respectively of the total.

Elution of C_{20} (eicosane) marked the 85% distillation point containing 139 resolved peaks from a total of 229. Of these, 23 components were present in quantities between 1 and 2% area and four peaks were between 2 and 3% area. The straight chain alkanes formed 20.37% of the total chromatogram area up to and including C_{20}. The individual alkanes constituted some of the largest single component peaks in the chromatogram.

Table 3·1 contains data relating to the aromatic content and boiling point ranges of several types of European and American diesel fuels. The ASTM[117] has specified three grades of diesel fuel for use in American engines: the ASTM No1-D fuel, used principally in automotive power units, is considerably more volatile than the British Class A fuel and has a lower boiling range i.e. 175 to 285°C (cff. 180 to 360°C), the ASTM-2-D is similar to BS Class A fuel and is used for heavier engines, and the ASTM-4-D is similar to BS Class B but is much more viscous. These data would indicate that, in general, American fuels have lower final boiling ranges than their European counter-parts. The fact that fuel characteristics effect the nature of the exhaust emitted is discussed in Section 4.

Figure 3·1

Distillation and Composition Data for a Typical Diesel Fuel

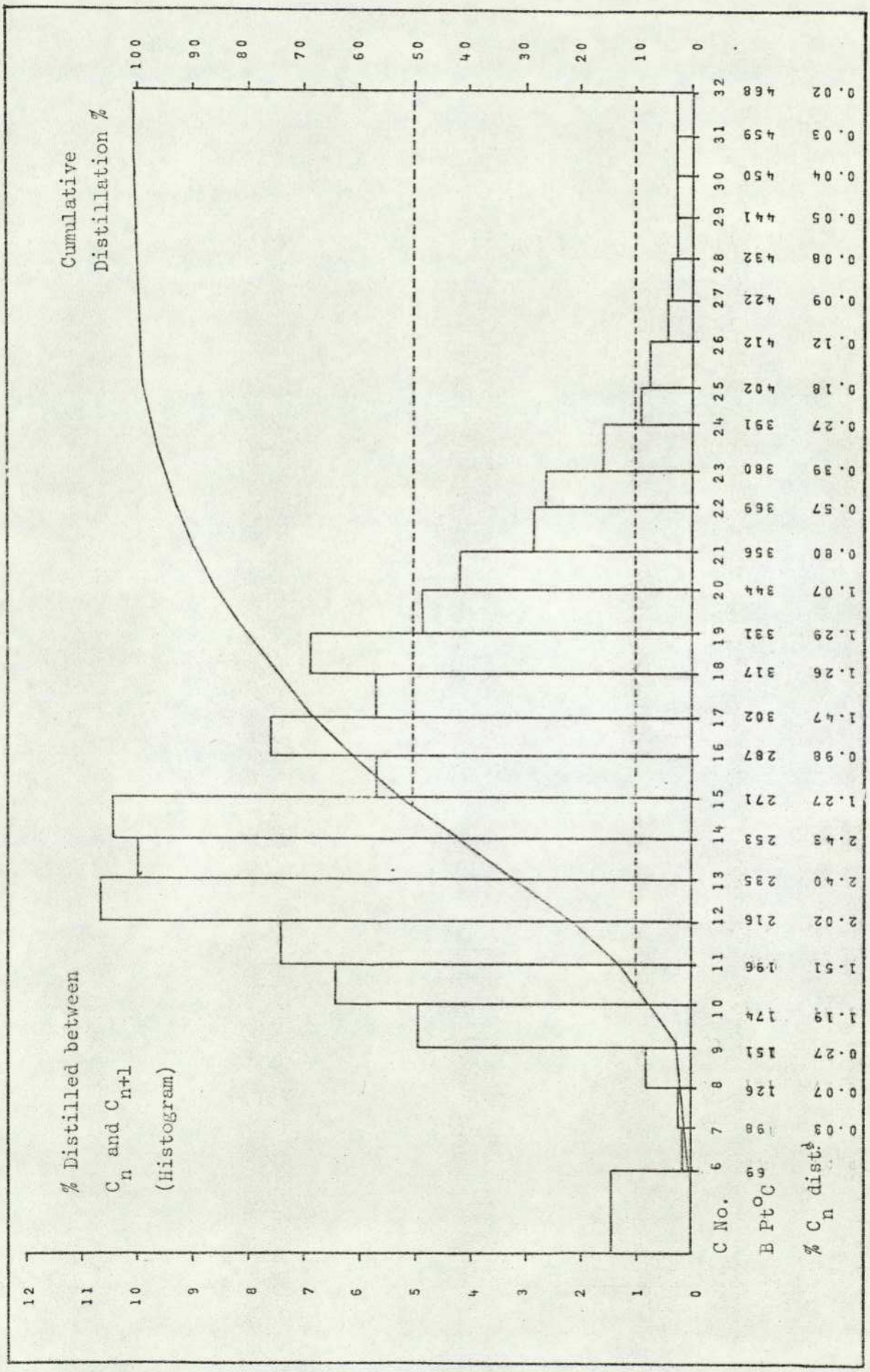

Figure 3.2

Composition Data for a Typical Diesel Fuel

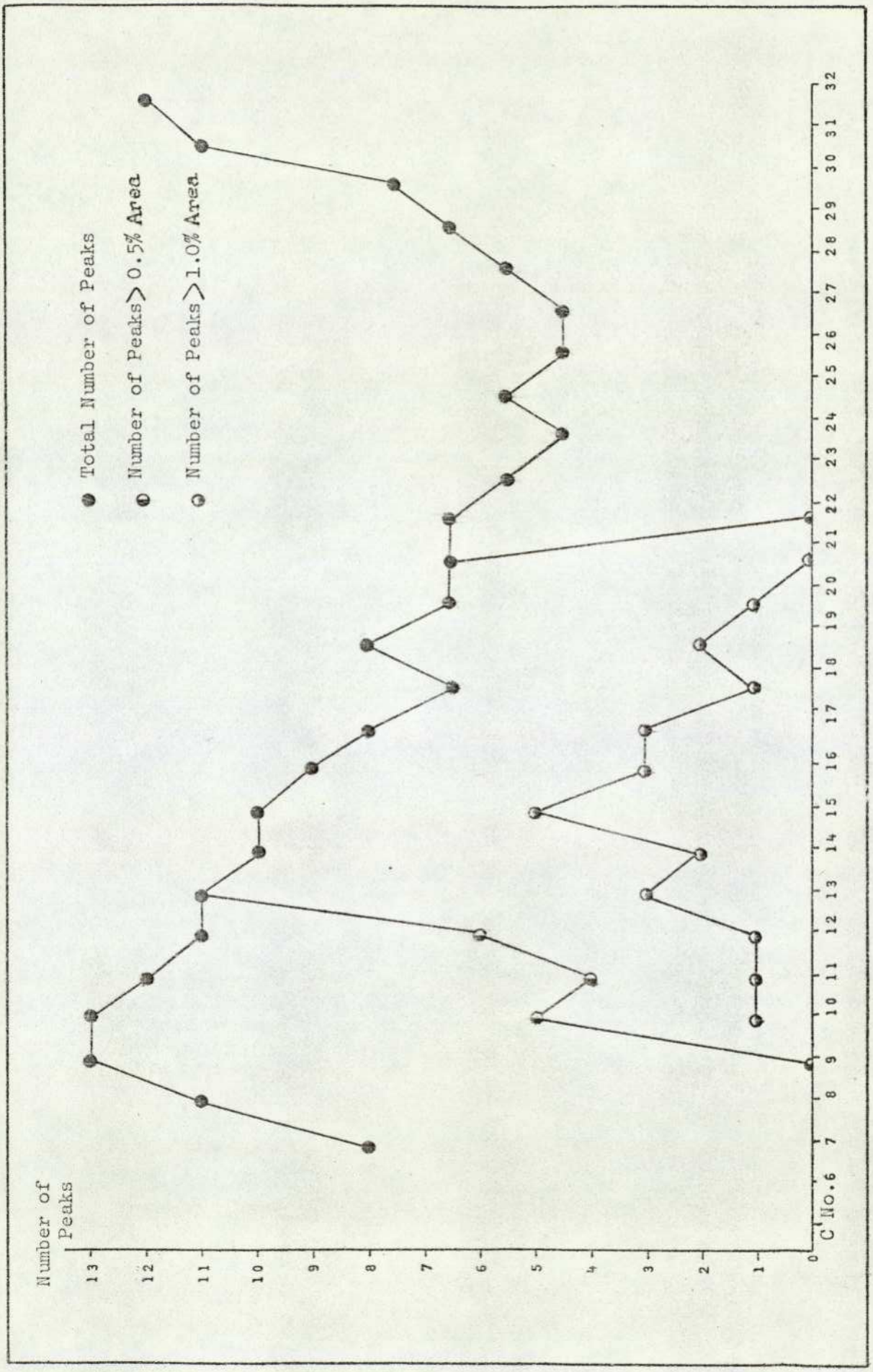

Table 3·1

Boiling Point and Aromatic Content Data for American and European Fuels

Fuel	Aromatics	Distillation °C		
		10%	50%	90%
DIESO - AOL Data European	No Data	185	265	356
No1 DEF 2405 A(1) 47 - cetane European	20·4	203	251	324
No2 DEF 2405 A(1) European (low temp.)	32·0	231	260	293
Soltrol low aromatics American	1·3	237	247	257
Midwest No2 American	34·7	214	263	307
No1 Diesel American	20·8	202	224	258
No2 Diesel East Coast American	24·1	218	250	297
EM-70-F American	15·0	184	202	232

3.1.2 Carbowax 20M Packed Column Chromatography

Analysis using a packed Carbowax 20M column (6 metres) in the PEF30GC enabled the C5 to C20 alkanes to be identified by comparison of the peak retention times with those of the pure compounds. Elution of eicosane marked the point at which 82% of the total area under the chromatogram had been recorded. The alkanes from C5 to C20 accounted for 43% of the area but before these results are compared with those derived from the distillation data it should be stated that the degree of fuel component resolution obtained under the packed C20M conditions was not as good as that achieved under the prolonged temperature programme involved in the distillation procedure. This was shown also by the fact that only 30% of the peaks recorded under the distillation conditions were detected on the F30GC. However it was observed that straight-chain alkanes particularly those between C_{12} and C_{20}, were again present as the predominant fuel components.

Analysis of an American test fuel under the same conditions produced a chromatogram with an overall distribution of fuel components similar to that obtained with the European fuel. Undecane appeared to be the principal fuel component in the chromatogram, but this conclusion might need to be modified if the detector response were calibrated for individual components.

3.1.3 Apiezon L Packed Column Chromatography

Using a packed Apiezon L column under the conditions outlined in Section 2.4, the diesel fuel was resolved into 83 peaks with a distribution pattern very similar to that achieved by the distillation procedure. Apiezon L separates components in order of boiling-point and this column was particularly effective at separating the low molecular weight components eluted at the front of the chromatogram. For example, pentane and hexane were separated by four minutes under the programme used, whereas, with C20M,

these components were virtually superimposed on one another which made cryogenic cooling a necessary experimental prerequisite for improvement of the resolution.

Figures 3.3 and 3.4 together show the first 48 minutes of a typical chromatogram obtained for the fuel. The alkane peaks from C_5 to C_{14} are eluted in this period but after C_{14} the chromatogram spreads out and C_{20} is eluted after 125 minutes. It is evident from Figure 3.4 that this complex section of the chromatogram is only partially resolved.

3.1.4 Carbowax 20M Capillary Column Chromatography

Fuel analysed on the F11 GC capillary column produced chromatograms that exhibited a higher degree of resolution than that achieved with any of the packed columns, except under the distillation procedure. Figures 3.5 and 3.6 show the first 48 minutes of the chromatogram, which was sufficient to elute all the major components including the high molecular weight alkanes. Carbowax 20M separates components in order of boiling point and polarity, so that the components eluted at the front of the chromatogram were low polarity, low boiling point species. Diesel fuel does not contain oxygenated organic compounds and therefore high polarity components of the carbonyl type for example, would not be expected to be present. Instead, variations in polarity arising from the molecular configuration of the many isomeric alkanes and aromatic hydrocarbons present, together with individual component boiling points will determine the order of elution.

Many fuel chromatograms were run in order to establish a 'finger-print' of the fuel. Oxidation of the fuel in the static vacuum apparatus was studied to a large extent in the regions of incomplete combustion. It was therefore necessary to determine which components in the product chromatograms were original fuel components and which were formed during the oxidation reactions. It can be seen from the examples of the chromatograms included here that this was a difficult task. For this reason, oxidation

Figure 3·3

Apiezon L Packed Column Chromatogram of Diesel Fuel

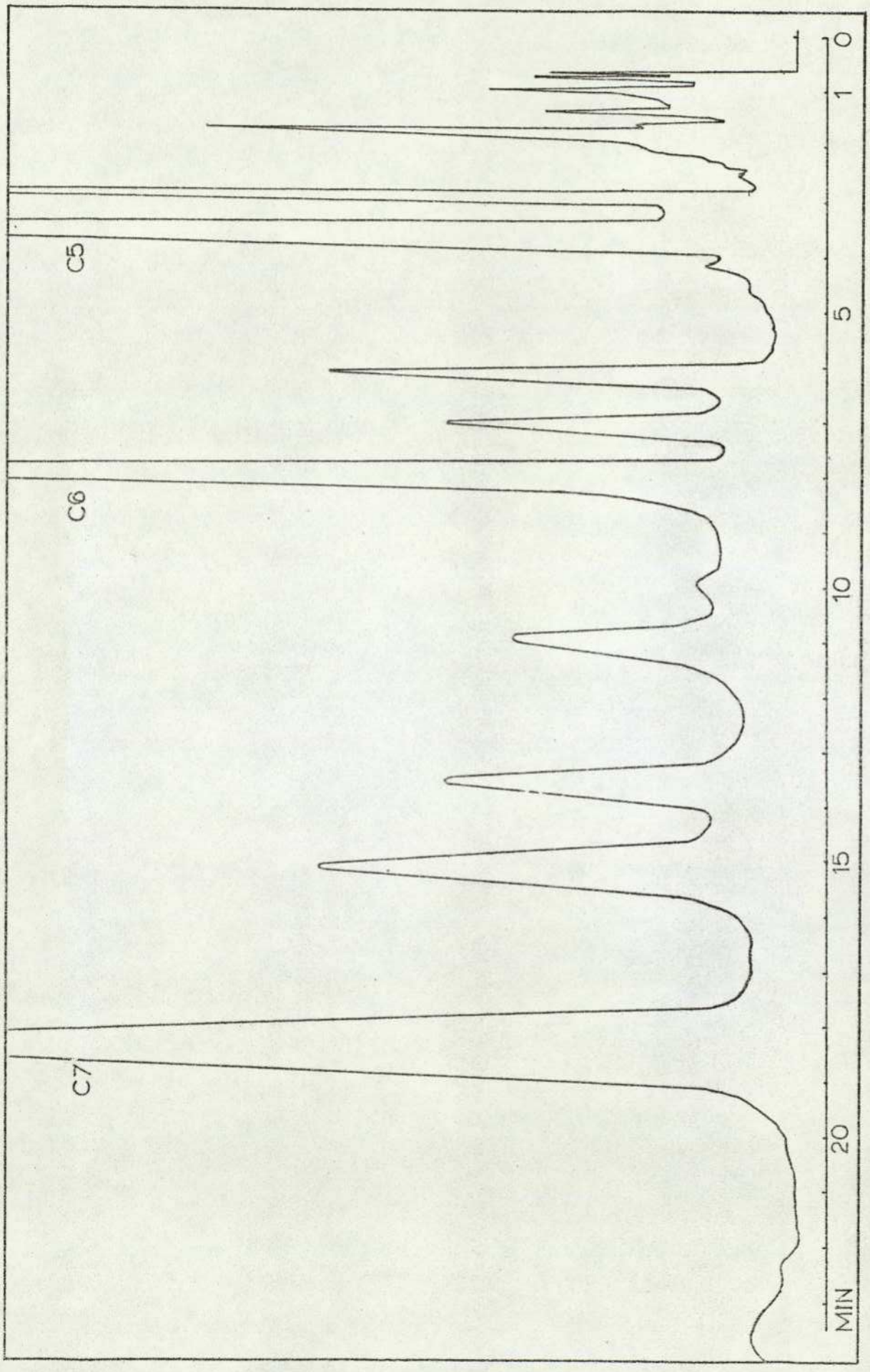

Figure 3·4

Apiezon L Packed Column Chromatogram of Diesel Fuel (Cont.)

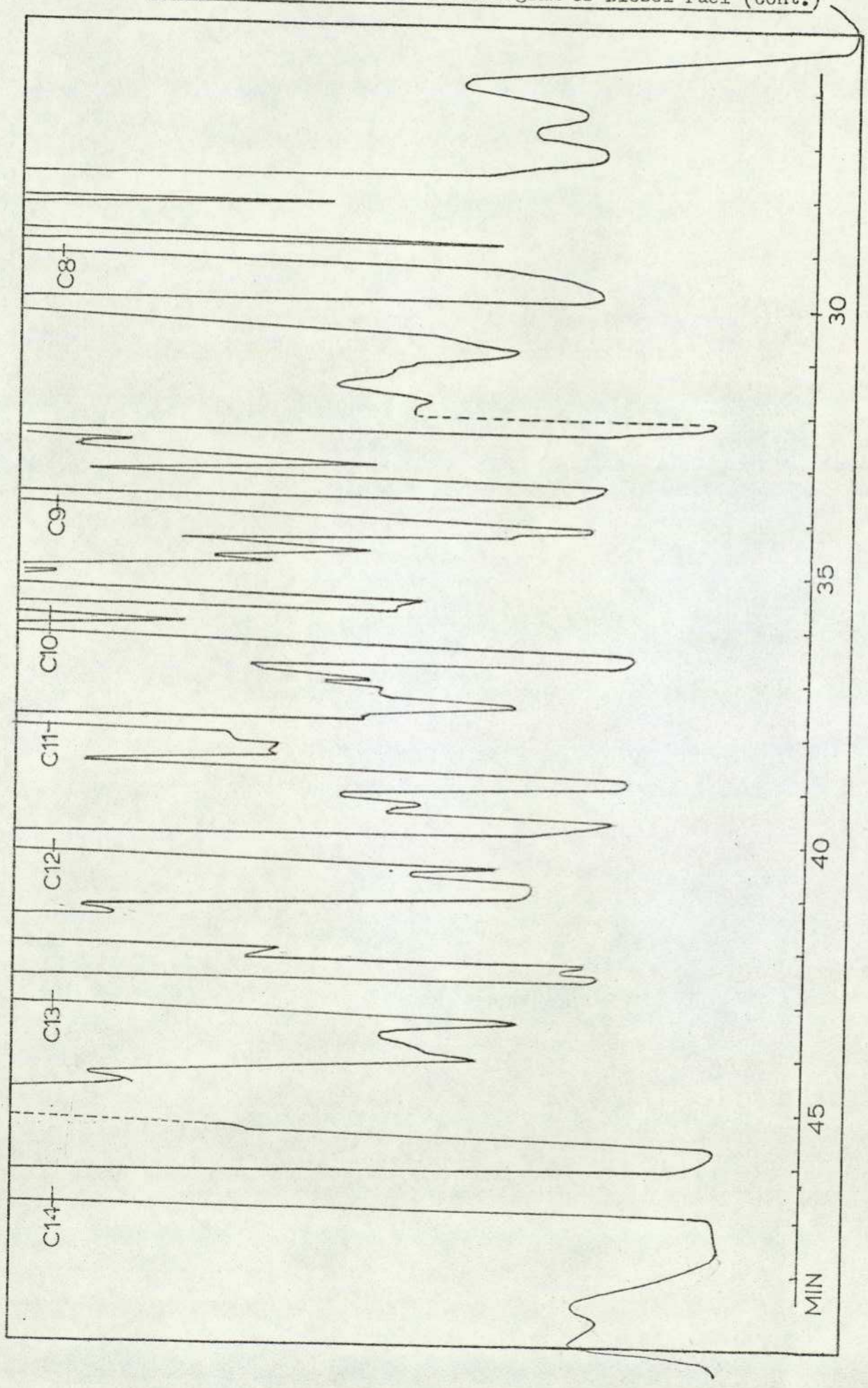

Figure 3·5

Carbowax 20M Capillary Column Chromatogram of Diesel Fuel

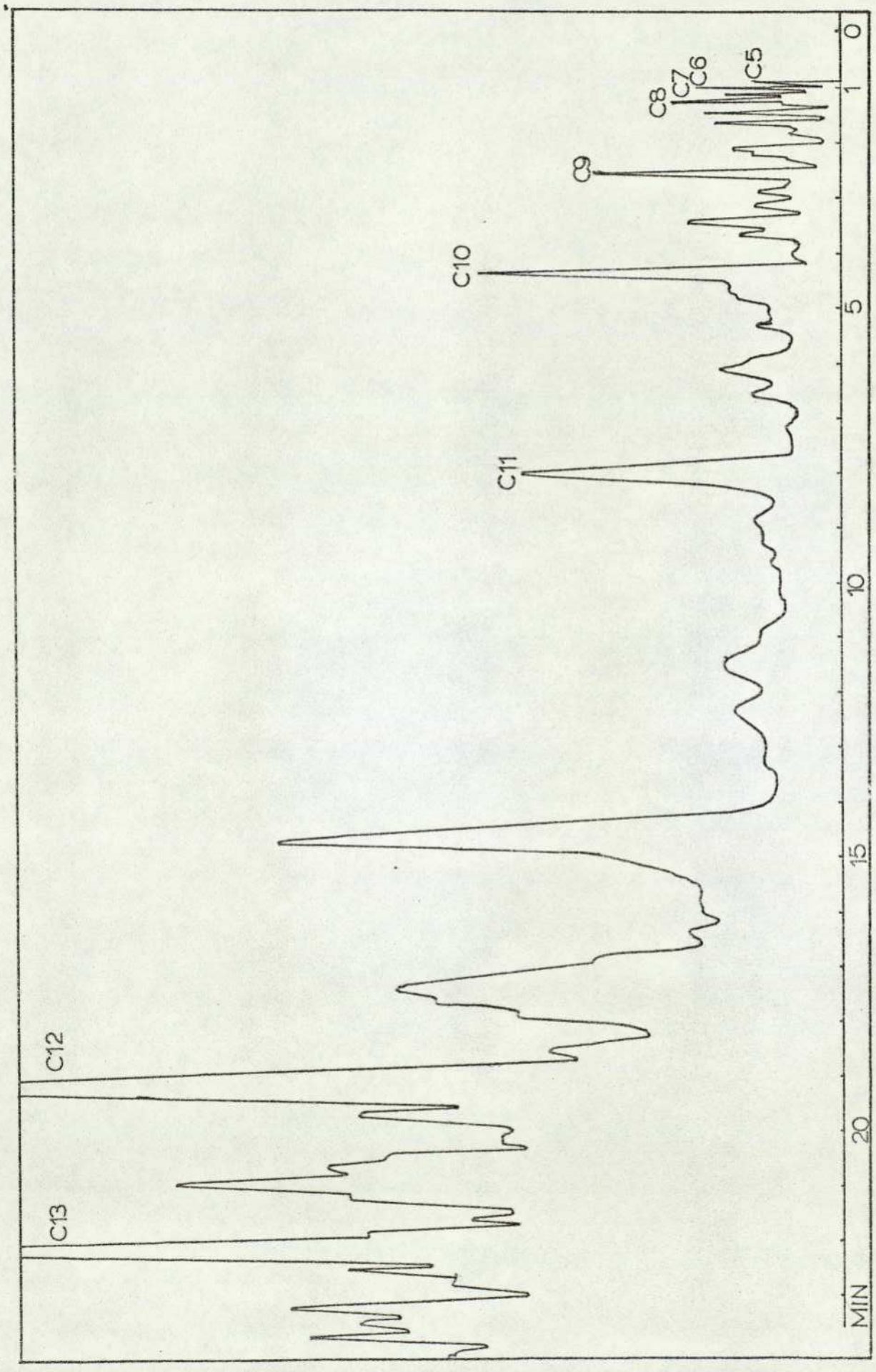

Figure 3·6

Carbowax 20M capillary Column Chromatogram of Diesel Fuel (Cont.)

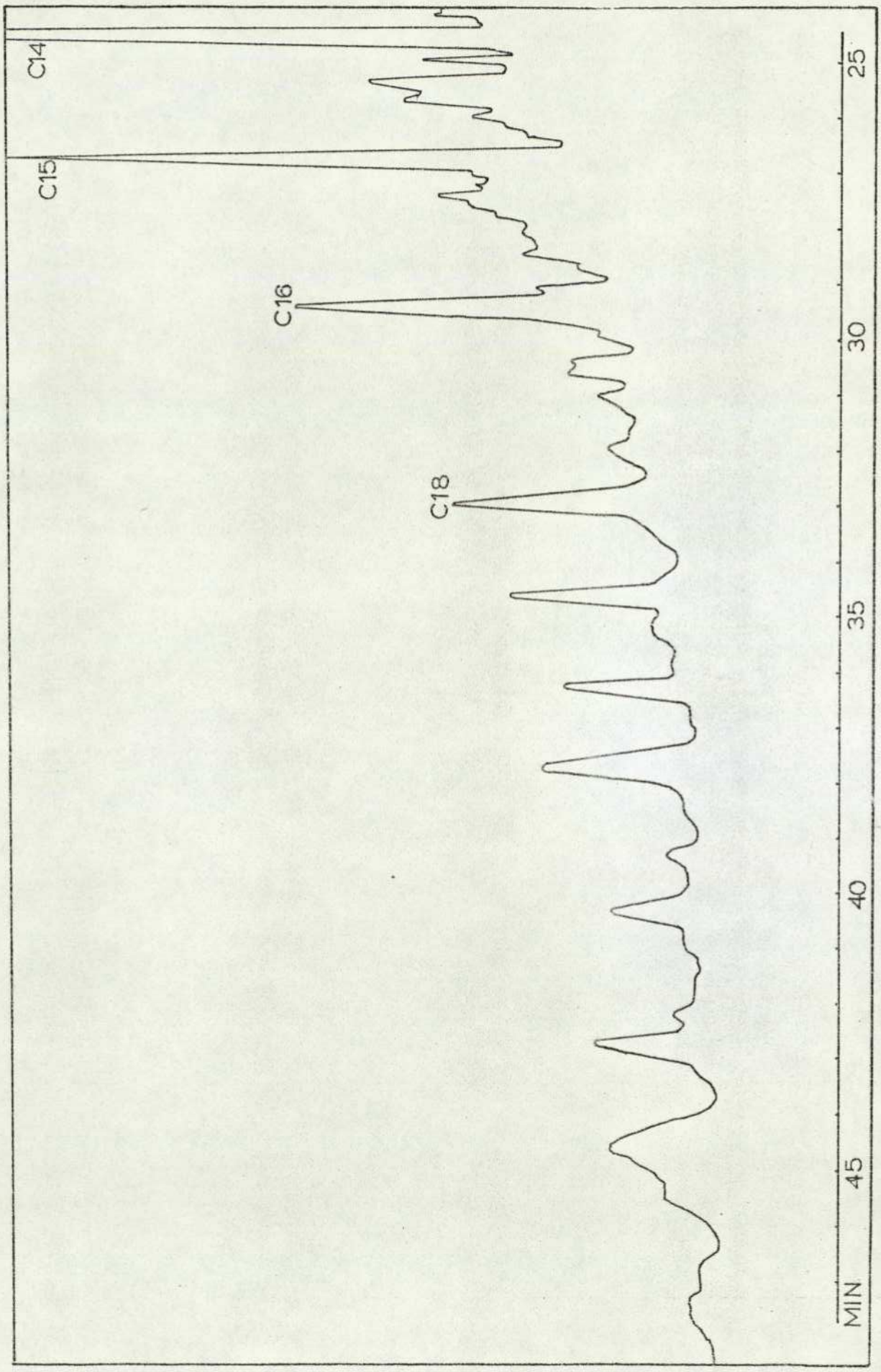

experiments were also carried out using hexadecane as a single component fuel, since the interpretation of the product chromatograms was simplified. Hexadecane is sufficiently similar to diesel fuel to enable significant comparisons to be made of the ensuing combustion mechanisms.

3.2 Static Vacuum Studies

3.2.1 Fuel Vaporisation

Fuel vaporisation is a necessary prerequisite to gas phase oxidation. It was therefore considered necessary to establish the characteristics of the vaporisation process for several reasons. First, the pressure rise due to fuel vaporisation alone had been calculated using a computer programme and it was clear that empiricle verification of the pressure data obtained would indicate the validity of the assumptions made in the calculations. Secondly, the nature of the vaporisation process was important in determining the characteristics of the combustion process, possibly being a rate-determining step during short induction periods. Thirdly, further information regarding the cooling effect of fuel vaporisation on the atmosphere contained in the bomb was needed.

In order to check the validity of the computer calculated fuel vapour pressures at given temperatures in the bomb, increasing volumes of fuel were injected into nitrogen atmospheres and the resultant pressure rises were recorded. Figure 3.7 illustrates a typical set of data for the vaporisation of diesel fuel at 295°C (568°K) and at various initial pressures within the bomb. It can be seen that, as expected, the initial pressure of nitrogen has no effect on the vapour pressure attained in the bomb. An increase in the initial pressure served as a check on the electronic recording equipment, since recalibration had to be carried out for each new pressure. For low fuel volumes and low temperatures the pressure rise accompanying vaporisation was small (~3 torr) rendering the observed pressure data more susceptible to experimental error. Nevertheless it can be seen that a high degree of correlation exists between the calculated and the experimentally determined vapour pressures, thus indicating the applicability of the computer data to the present system.

Figure 3·7

Comparison of Experimental and Calculated Values for the Vapour Pressure of Diesel Fuel at 295°C

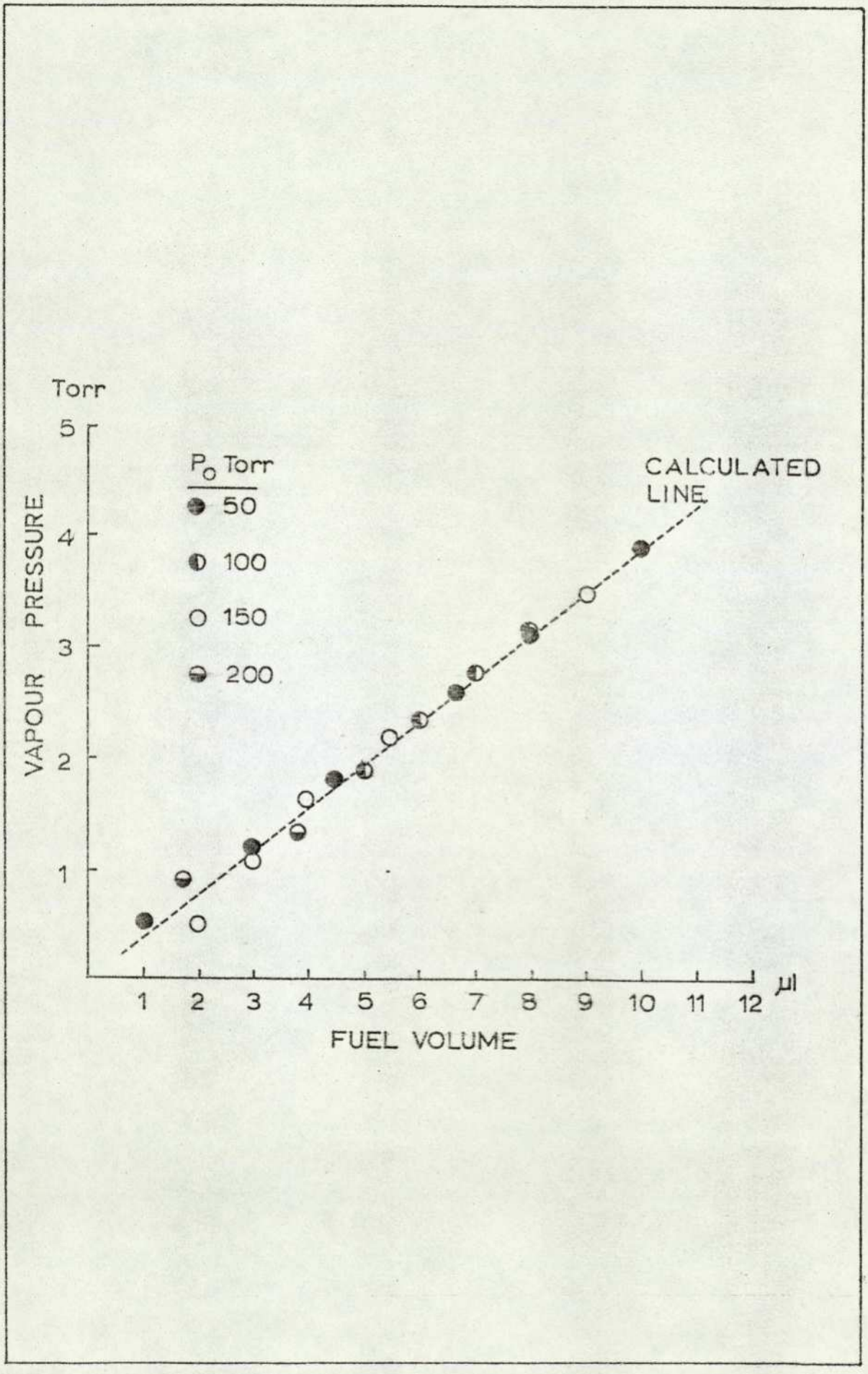

At 250°C (523°K) the vaporisation of the fuel produced vapour pressures that were of the order of 63% less than the calculated values. Reference to Figure 3.1 provides an explanation for this behaviour since it is apparent from boiling point considerations that only 42% of the fuel distils at a temperature of 250°C. This temperature was therefore adopted as the lowest temperature at which oxidation experiments could be carried out, since below this temperature only low concentrations of the higher boiling components would be present in the gas phase. In addition temperatures below 250°C have little relevance to the actual conditions found in the diesel engine combustion chamber.

Figure 3.8 shows the pressure time data recorded during the vaporisation of volumes of diesel fuel injected into 600 torr of nitrogen at 310°C (583°K). Figure 3.9 compares the effect of increasing the initial nitrogen pressure on the pressure drop caused by the cooling effect of diesel fuel and n-butylbenzene on the atmosphere in the bomb. It can be seen from Figure 3.9 that n-butylbenzene has a much greater cooling effect than diesel fuel as would be expected from specific heat and latent heat considerations.

Studies of the physical factors involved during the admission of cool gasses into heated reaction vessels have shown[118] that the subsequent rise in temperature lays significantly behind the recorded pressure rise as measured by a piezo-electric pressure transducer. The significance of this observation is that, although the pressure equilibrium point has apparently been reached, the actual temperature in the reaction vessel is appreciably lower that the equilibrium temperature. This effect becomes more pronounced as the fuel concentration, initial pressure and reaction vessel temperature are increased. An additional aspect to consider with respect to the injection of liquid fuels is that the rate of vaporisation for a given hydrocarbon fuel is also affected by the prevailing conditions.

Figure 3·8

Variation in Pressure Recorded after Injection of Fuel into an Atmosphere of Nitrogen

Pressure-Time Trace Recorded During Vaporisation of Diesel Fuel

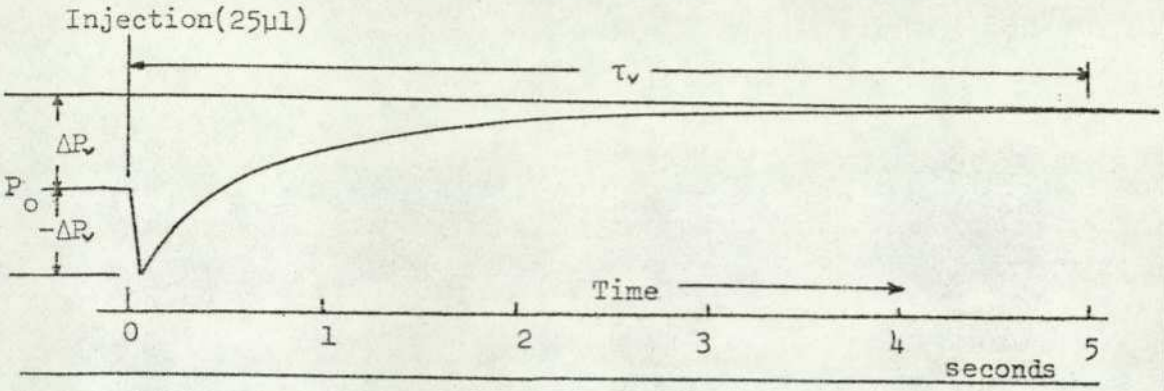

$-\Delta P_v$ and ΔP_v vs. µl fuel injected at 600 torr and 310°C

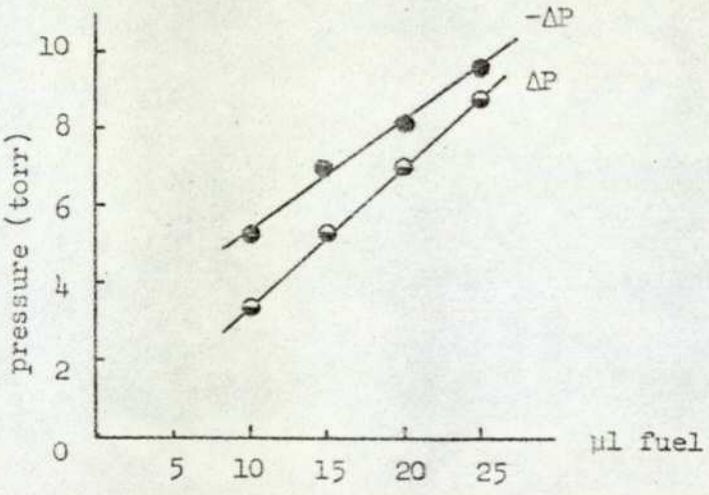

τ_v vs.µl fuel injected at 600 torr and 310°C

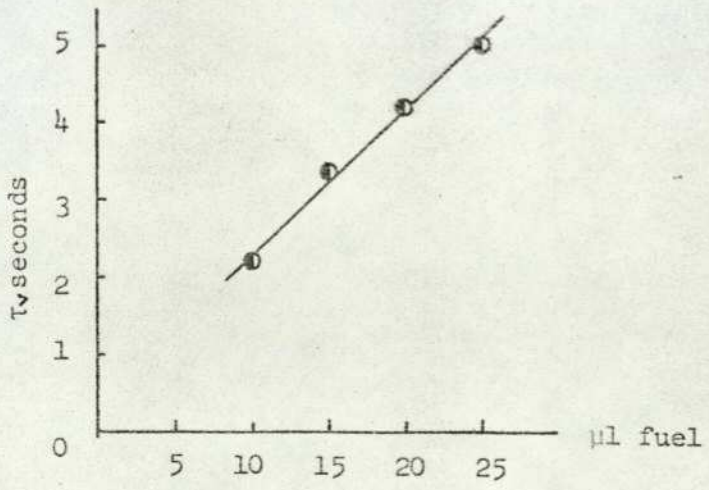

Figure 3·9

-ΔP vs.ΔPo Data for n-butylbenzene and Diesel Fuel (25ul injections at 310°C)

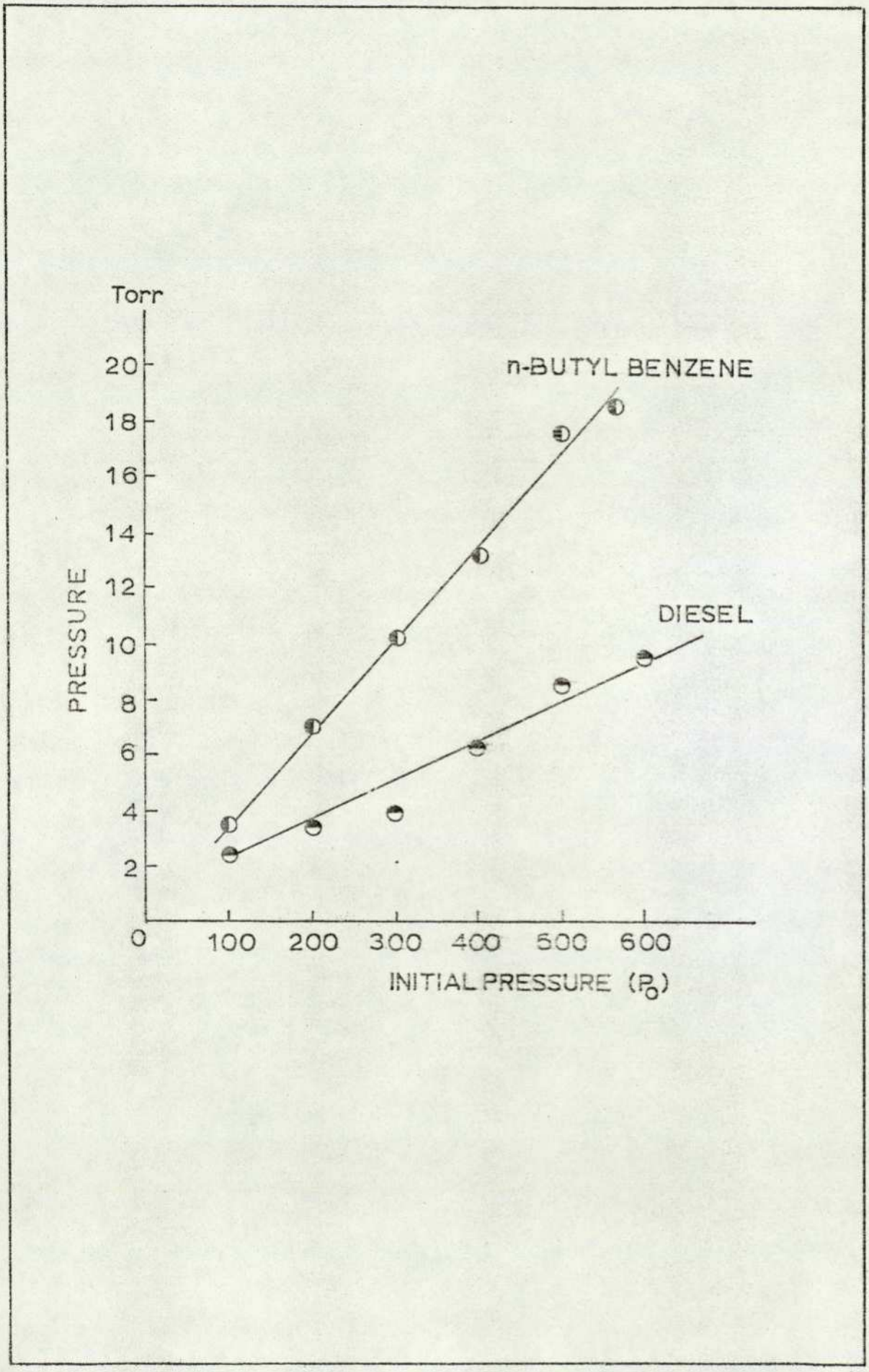

Evidently it is important that combustion data collected from static vacuum systems should be interpreted with due consideration for the actual conditions existing in the reaction vessel.

In order to assess the extent to which the temperature of the atmosphere in the reaction vessel was affected by injection of the liquid fuel, the apparent reduction in temperature was calculated from the observed pressure drop and application of the ideal gas equation. For example at 310°C a 25µl injection of diesel fuel into 600 torr of nitrogen produced a calculated fall in temperature of 9°C (3%) from the equilibrium temperature. This corresponds to a drop of 0.4°C/µl of fuel injected. For smaller volumes of fuel, the fall in temperature was not so great but the temperature drop of the reaction vessel atmosphere dropped to a rate of 0.51°C/µl for a 10µl injection. This observation is consistent with the heat balance and heat transfer mechanisms operating in the system. The 3% drop in temperature represents the maximum extent to which the temperature deviated from the equilibrium value as a result of fuel vaporisation. Under most conditions the fuel volumes rarely exceeded 10µl and were never greater than 25µl.

As a summary of this particular aspect, the following observations can be made regarding the results obtained during the vaporisation experiments.

1. An increase in the initial pressure Po, while the temperature and fuel volume remained unaltered;
   - (i) increased $-\Delta P$
   - (ii) increased τ_v
   - (iii) had no effect on ΔP_v
2. An increase in the fuel volume while P_o and T_o remained unaltered;
   - (i) increased $-\Delta P$
   - (ii) increased τ_v
   - (iii) increased ΔP_v
3. An increase in temperature while the fuel volume and P_o remained

unaltered;

(i) decreased $-\Delta P_v$

(ii) decreased τ_v

(iii) increased ΔP_v

3.2.2 Fuel Oxidation Kinetics

Figure 3.10 shows the types of pressure-time trace which were recorded together with the kinetic parameters measured during the various combustion phenomena. The final pressure reached in the bomb after reaction was complete was designated as ΔP_∞ . The amplitude of the pressure pulse accompanying the passage of the first cool flame, ΔP_1 was measured together with the induction period, $\tau_{c.f}$. ΔP_v was deducted from both ΔP_∞ and ΔP_1 before plots of these parameters were constructed.

The single and multiple cool flames which were readily produced in the fuel vapour-oxidant mixtures are shown in Figure 3.10 as traces (b) and (c) respectively. Under certain conditions, single (d) and two-stage (e) ignitions were recorded. However, the typical slow combustion (f) curves so frequently reported in the literature on hydrocarbon oxidation were not observed. In the absence of any cool-flames, the traces recorded closely resembled the vaporisation curve (a), produced in an inert nitrogen atmosphere. Under the conditions leading to slow oxidation the only indication that reaction had occured was that ΔP_∞ was greater than the value recorded in an inert atmosphere.

The oxidation experiments were carried out for two reasons; first to establish the type of combustion behaviour which could be expected for various diesel fuel / oxidant ratios under a variety of temperature and pressure conditions, and secondly to determine the extent to which diesel fuel combustion paralleled that of other hydrocarbon fuels. A

Figure 3·10

Examples of Pressure - Time Oscillograph Recordings

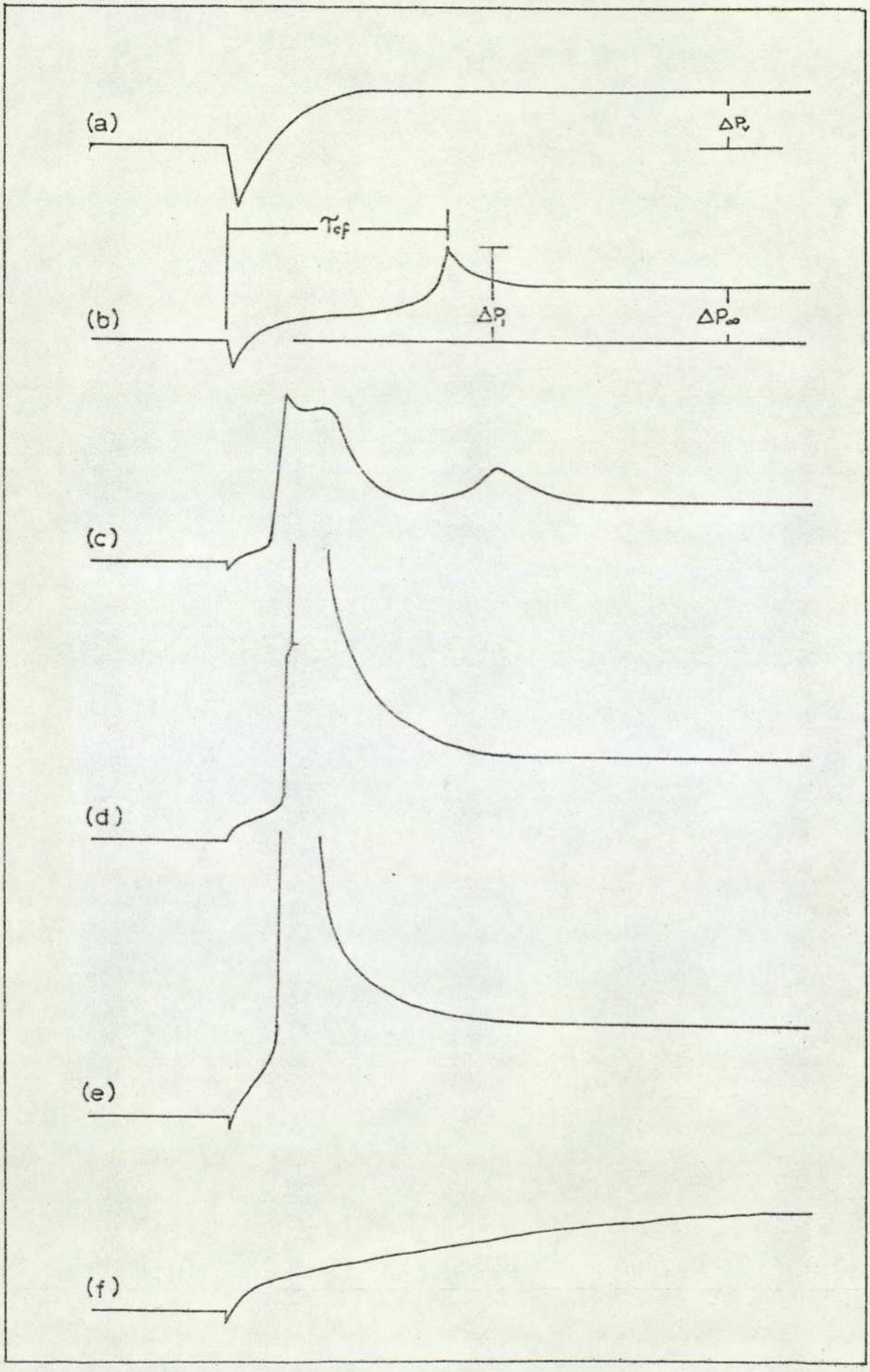

complete and qualitative kinetic investigation of diesel fuel combustion in the system used was precluded by the complexity of the fuel and the practical limitations of the system. Besides these aspects the determination of kinetic parameters in such a system is of academic interest only and the data so obtained would have been of little practical significance.

From the data collected, specific conditions were selected for analysis of the oxidation products.

Throughout the following pages the fuel concentration is expressed in terms of the eqivalence ratio σ, which is defined as the volume of fuel actually injected into the oxidant atmosphere divided by the volume of fuel required for complete combustion according to the stoichiometric equation. Thus, for an equivalence ratio of unity i.e. $\sigma=1.0$, the stoichiometric quantity of fuel was added to the oxidant and for $\sigma=0.5$, only half the stoichiometric quantity of fuel was injected. Alternatively the equivalence ratio may be expressed in the following manner:-

$$\sigma = \frac{\text{F/A ratio used}}{\text{stoichiometric F/A ratio}}$$

3.2.2.1 Kinetic Measurements at 250°C

At 250°C the measured vapour pressure of the fuel was smaller than the calculated value; an explanation of this has already been given. Despite this observation, a brief study was made of the types of combustion occuring at this relatively low temperature.

Single cool flames were observed at pressures between 50 and 250 torr for rich fuel-oxidant mixtures in which σ exceeded 1.0. Above 250 torr cool flames were observed in leaner mixtures where $\sigma<1.0$, their intensity, ΔP_1, increasing and the preceding induction period, τ_{cf}, decreasing as σ was increased. At 600 torr a hot ignition was observed when $\sigma = 0.6$. Figure 3.11 (A) shows the σ vs ΔP_∞ and vs ΔP_1 relationships determined at 600 torr and figure 3.11 (B) shows decrease in the induction period with

Figure 3·11

Kinetic Data for Diesel Fuel Oxidation at 600 torr and 250°C

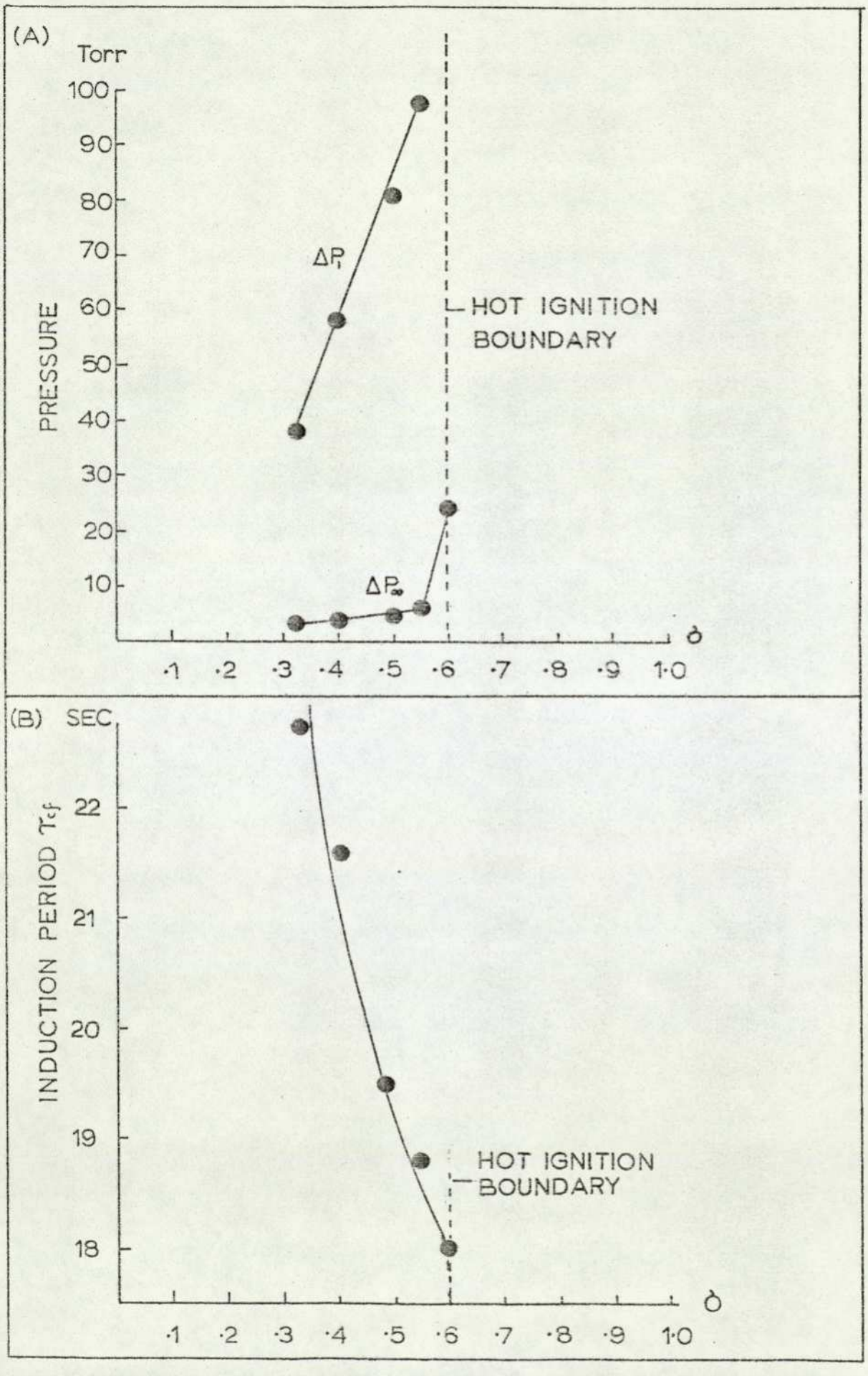

an increase in σ. The observations and data collected established that a multicomponent fuel such as diesel fuel behaves in a manner similar to that established for many single component hydrocarbon fuels.

If equilibrium of the pressure, temperature and concentration of the contents of the bomb occurred prior to sampling, then the analytical results obtained would be of greater value and less ambiguous. In order for equilibrium to be established, the induction period must be of sufficient duration to allow the heat and mass transfer mechanisms to be optimised. Inspection of Figure 3.11(B) indicates that 18 seconds or more were available for equilibration but it was doubtful whether complete vaporisation of the injected fuel had occurred. This condition may have resulted in higher concentrations of the lighter components of the fuel being present in the gas phase, thus representing a somewhat artificial environment for the preignition reactions. An increase in the temperature of the bomb was therefore necessary, although a large reduction in the induction period would then be expected due to its exponential decrease with increasing temperature.

3.2.2.2 Kinetic Measurements at 280°C

At 280°C the measured fuel vapour pressure equalled the calculated value of 0.38 torr / µl fuel.

Preliminary investigations at this temperature revealed that many of the combustion phenomena considered to be of interest occurred if a specific value for σ of 0.42 was selected, and the initial pressure Po was then increased. Figure 3.12(A) shows the variation of ΔP_∞ and ΔP_1 with increasing Po. Figure 3.12(B) illustrates the exponential decrease in the induction period, τ_{cf}, with increasing values of Po. This relationship is expressed mathematically as: $\tau_{cf} = KPo^{-n} + C$, and is found to be applicable to many hydrocarbon + oxygen systems.

Figure 3.13 shows the development of a cool flame and traces its

Figure 3·12

Kinetic Data for Diesel Fuel Oxidation at 280°C

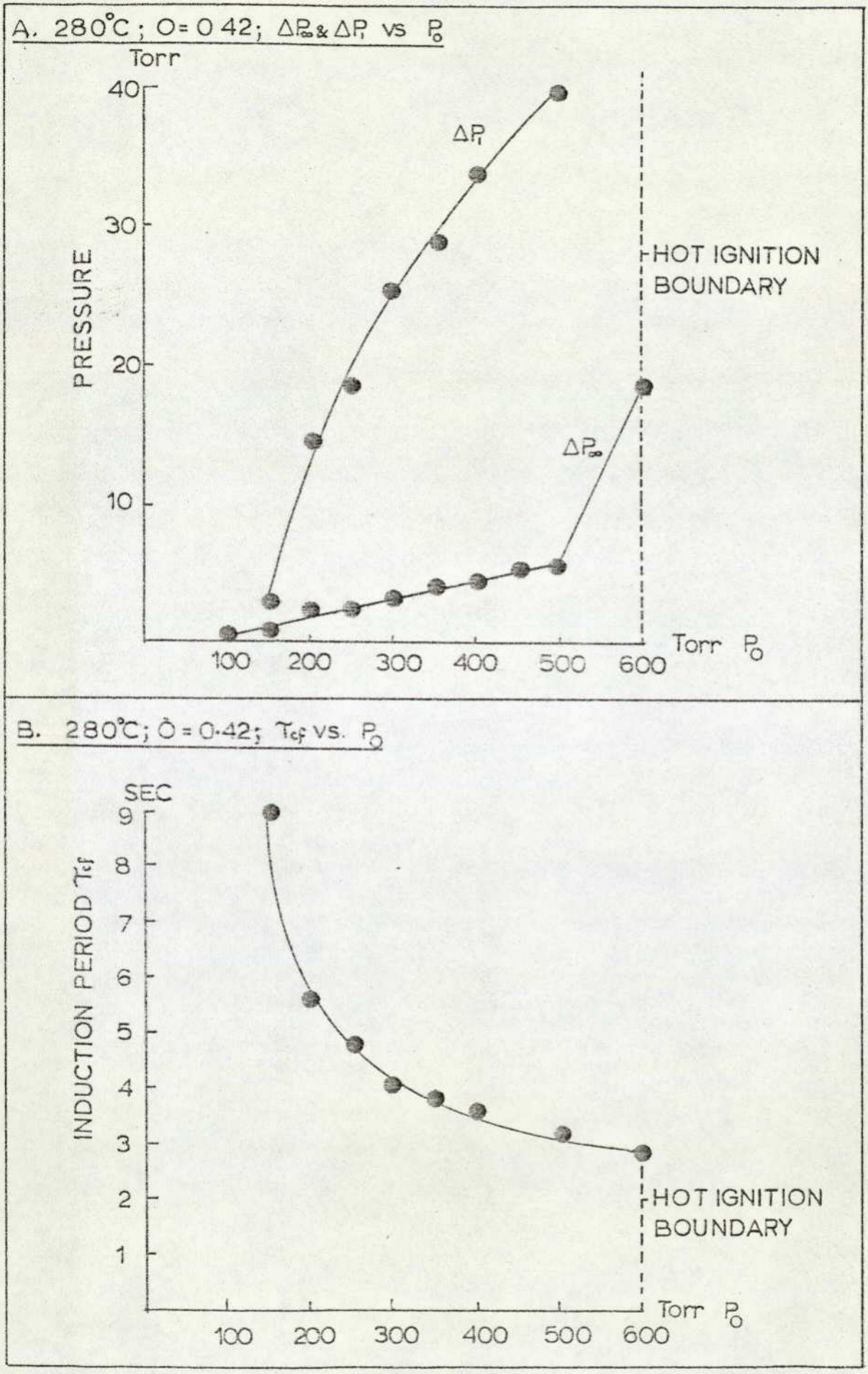

Figure 3·13

Pressure - Time Oscillographs Recorded During Fuel Oxidation (δ=0·42; To=280°C)

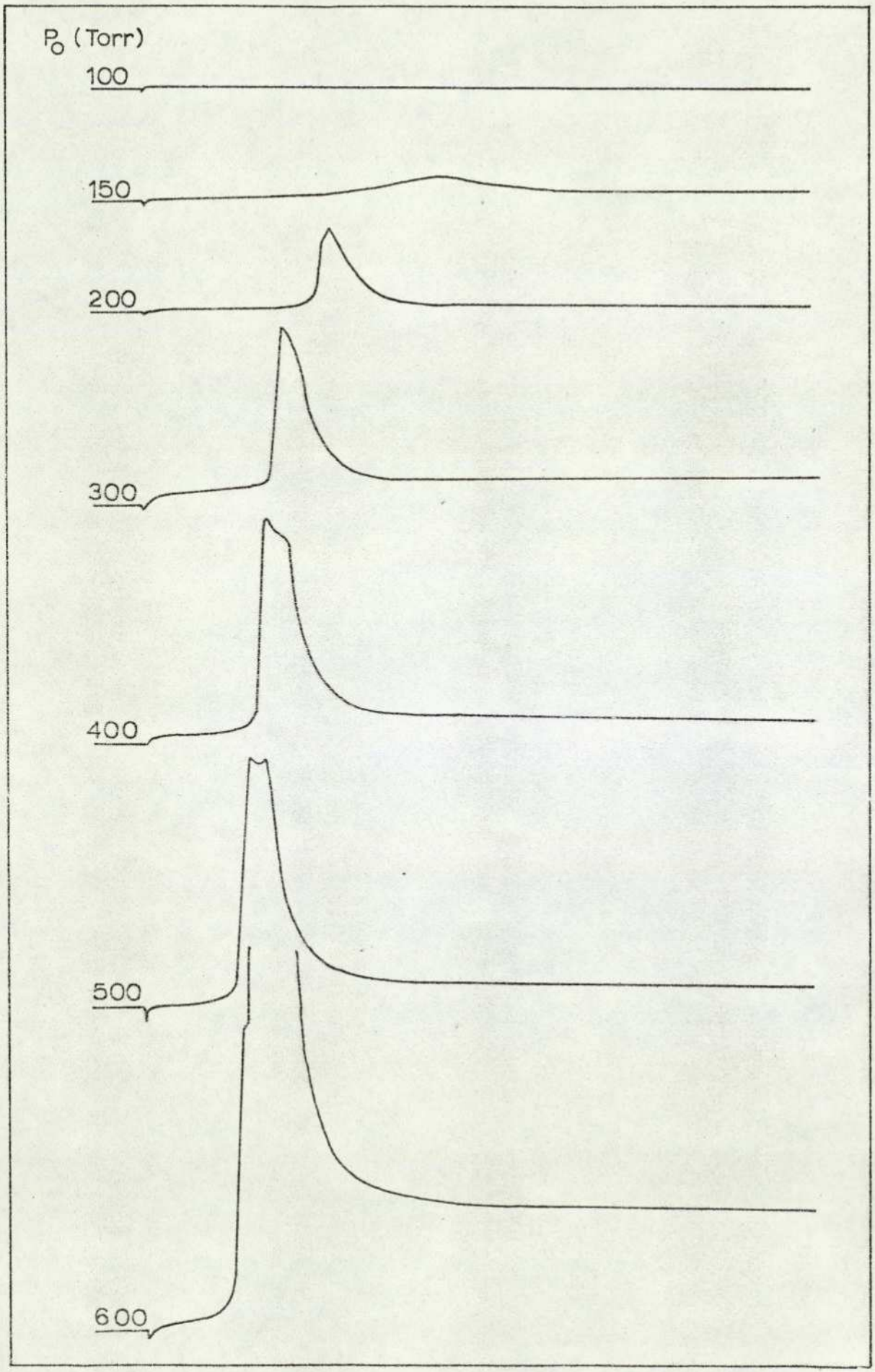

progression through increasing ΔP_1 and ΔP_∞ values to a two stage hot ignition. These recordings were made for $\sigma = 0.42$ and increasing values of Po as indicated in this Figure.

Comparison of Figures 3.11(B) and 3.12(B) reveals that the induction period leading to hot ignition at 280°C was much shorter than that at 250°C ie. 3 seconds compared with 18 seconds. For short induction periods, other factors such as fuel injection rate, fuel vaporisation rate and heterogenicity of reactants become relevant. An attempt was therefore made to lengthen the induction period by adding nitrogen as a diluent and thus reduce the importance of these factors.

To observe the effect of added nitrogen on the induction period various pressures of air, P_A, were admitted to the bomb. The pressure was then increased by adding nitrogen to give a total pressure, P_{TOT}, of 600 torr. Fuel volumes corresponding to $\sigma = 0.42$ for each particular value of P_A were then injected and τ_{cf} was measured. For comparison, the τ_{cf} values were also obtained for the same set of P_A values for air alone, ie: when $P_A = P_{TOT}$.

Figure 3.14 shows the relationship between τ_{cf} and P_A for both sets of experiments. The effect of the nitrogen diluent is greatest when the partial pressure of air in the reactant atmosphere is below 0.5, when the maximum effect recorded was a 20 % increase in the induction period. When the partial pressure of air exceeds 0.5 the two curves are indistinguishable within the limits of experimental error. The addition of nitrogen is evidently thus not a practical method of increasing the induction period at high air pressures.

From Table 3.1 it can be seen that diesel fuel contains a high percentage of aromatic species. In order to establish whether aromatic compounds typical of those present in diesel fuel would undergo oxidation at 280°C, xylene, indan, ethylbenzene and n-butylbenzene were injected into 600 torr of air. No evidence of oxidation was observed for any of

Figure 3·14

Effect of Nitrogen Diluent on the Induction Period

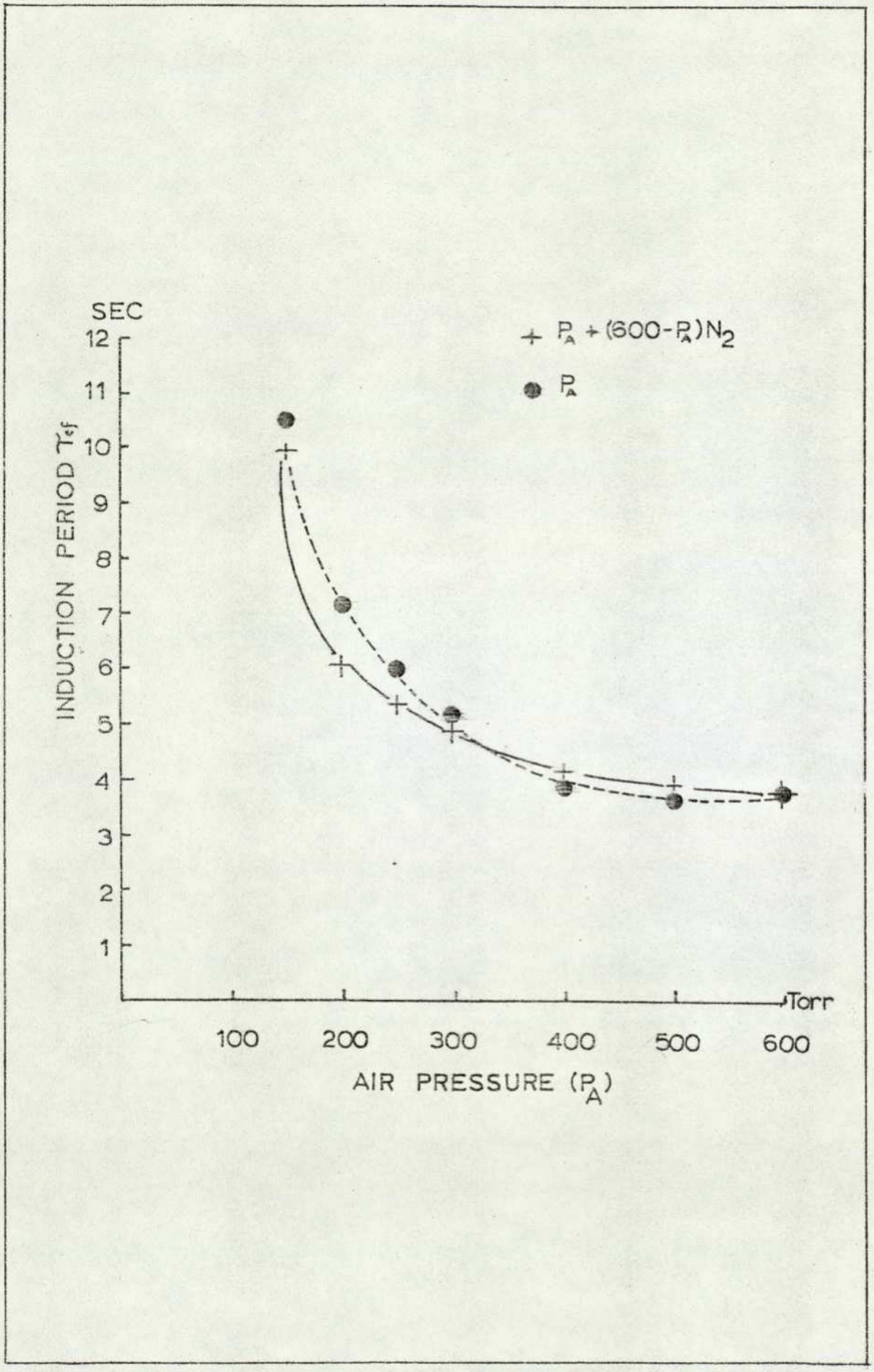

these compounds over the range $\sigma = 0.1$ to 2. The temperature of the bomb was then increased to 295°C in an attempt to induce oxidation of the aromatic compounds and to bring the temperature of investigation into line with the wall temperatures encountered in the diesel engine combustion chamber.

3.2.2.3 Kinetic Measurements at 295°C

Extensive kinetic studies of diesel fuel oxidation were carried out at 295°C since this temperature produced interesting combustion phenomena, including oscillatory cool-flames.

Figures 3.15(A) and (B) show the trends exhibited by ΔP_∞ and ΔP_1 vs P_0 for a range of σ values. Figure 3.16 shows how ΔP_∞ varies with σ for increasing P_0 values, straight line relationships being observed throughout the pressure range. The variation of ΔP_1 with σ for increasing P_0 (Figure 3.17) is however more complex, the plots exhibiting decreasing degrees of curvature with increasing P_0 until at 600 torr a straight line is obtained.

Multiple cool-flames were readily produced at 295°C and up to five were recorded with injections of 9 and 10 µl of fuel ($\sigma = 0.79$ and 0.87 respectively) into 500 torr of air. Two typical traces which were recorded are shown in Figure 3.18; these illustrate the oscillatory cool-flames found at two P_0 and σ values.

Hexadecane was used as a fuel in brief comparison studies which revealed that combustion phenomena analogous to those encountered with diesel fuel, were produced under similar conditions. The ΔP_∞ and ΔP_1 values for hexadecane were of the same order of magnitude as those of diesel fuel but the induction periods were always shorter, e.g. at 500 torr and $\sigma = 0.42$ for both fuels, τc.f. is 2.3 seconds for diesel fuel and 0.8 seconds for hexadecane. For comparison with results for diesel fuel at 200 torr, (Figures 3.16 and 3.17) the ΔP_∞ and ΔP_1 values for hexadecane with increasing σ are shown in Figure 3.19. The trends characteristic of

Figure 3·15

P_∞ and ΔP_1 vs. ΔP_o Data for Diesel Fuel Oxidation at 295°C

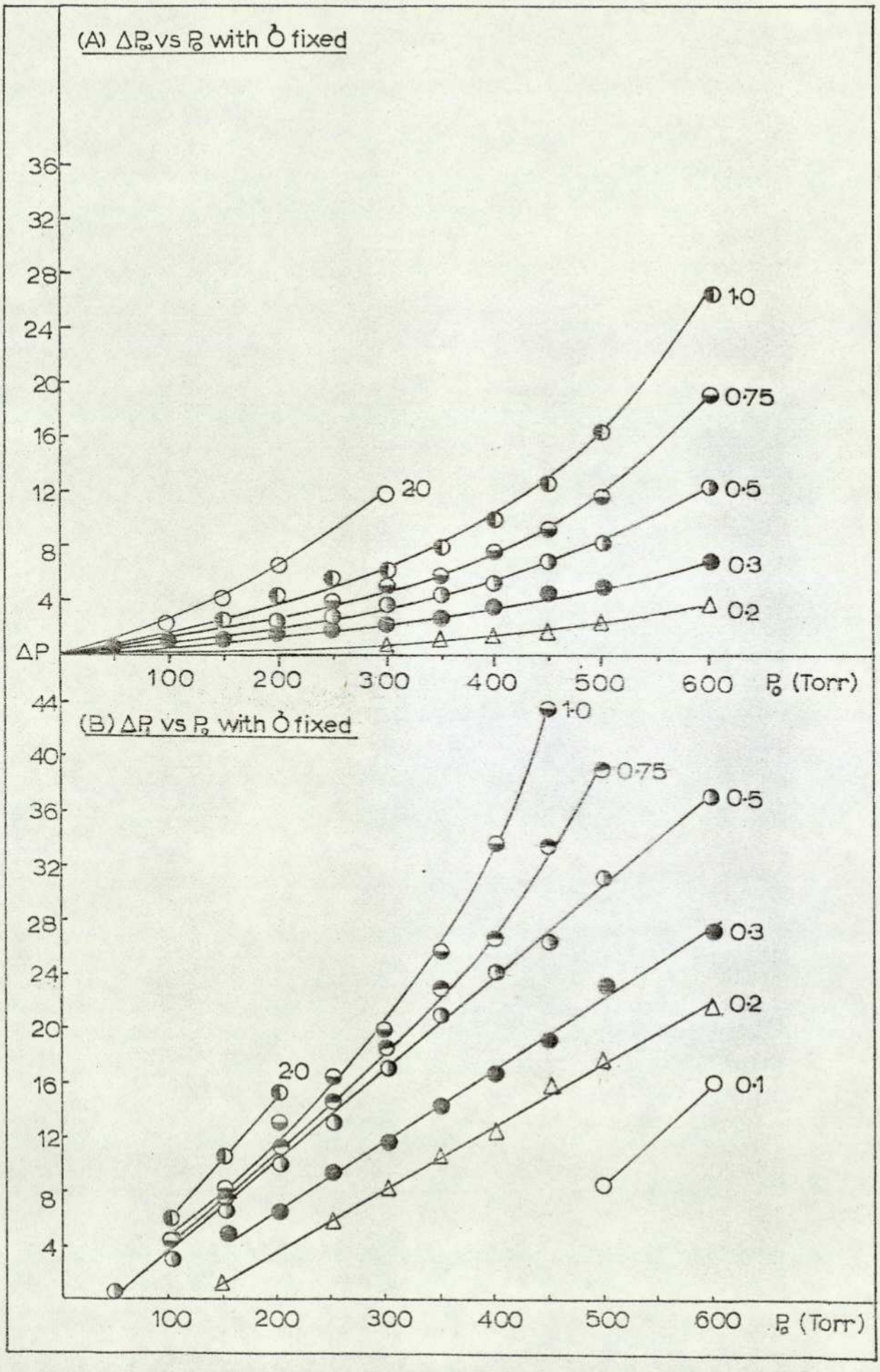

Figure 3·16

P_∞ vs. δ at Various Initial Pressures for Diesel Fuel Oxidation at 295°C

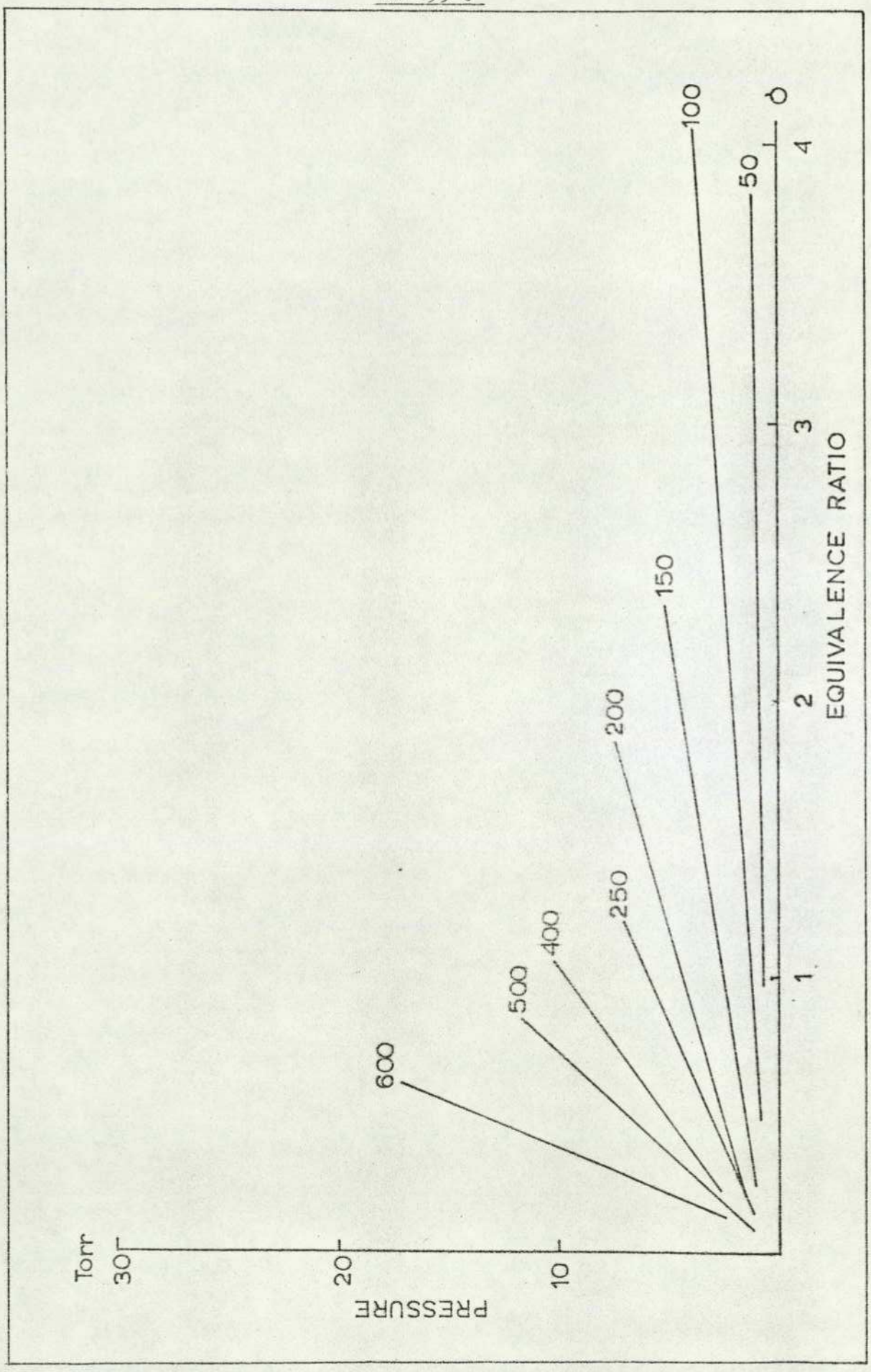

Figure 3·17

ΔP_1 vs. δ at Various Initial Pressures for Diesel Fuel Oxidation at 295°C

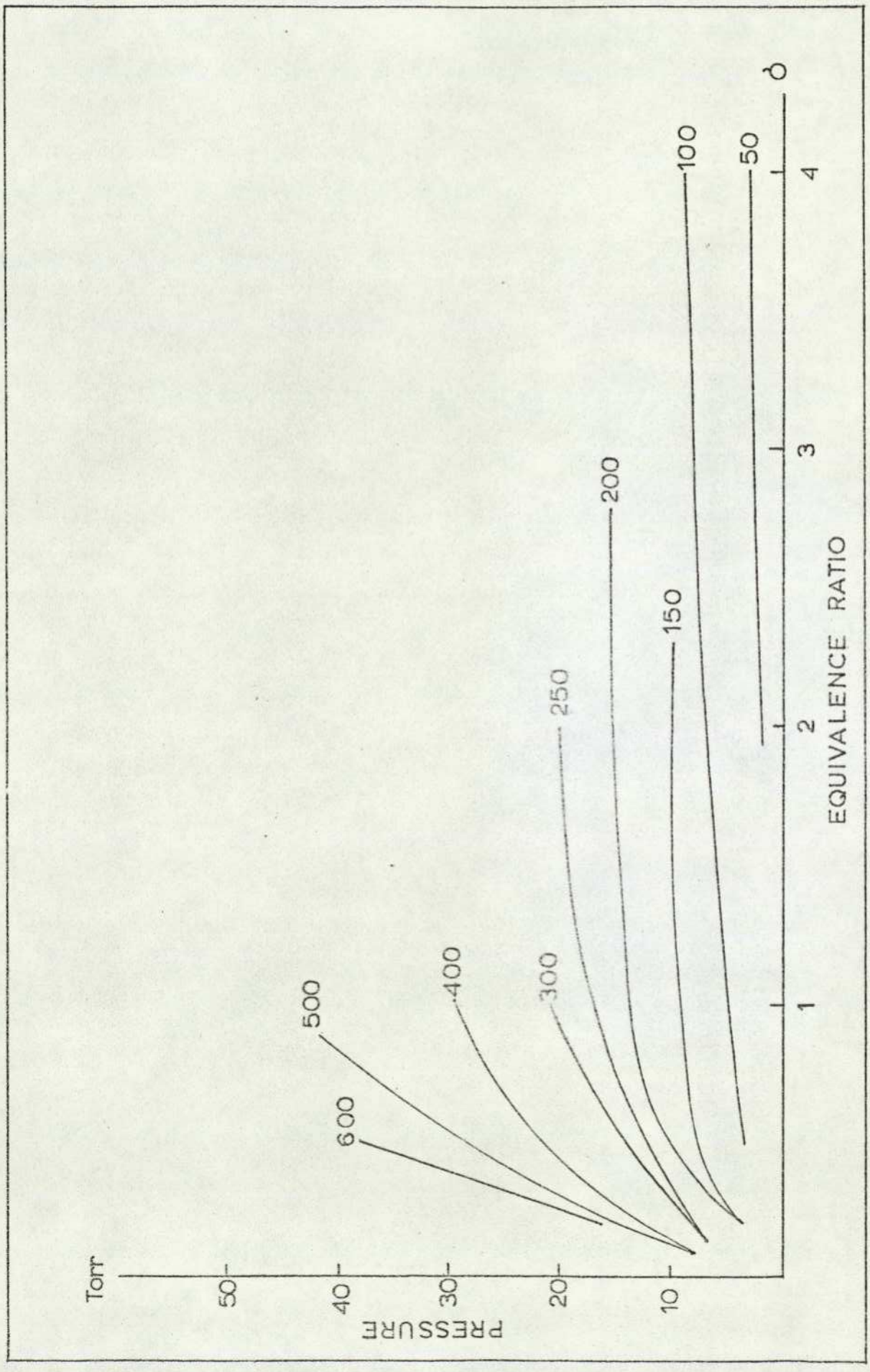

Figure 3·18

Oscillatory Cool Flame Recordings for Diesel Fuel Oxidation at 295°C

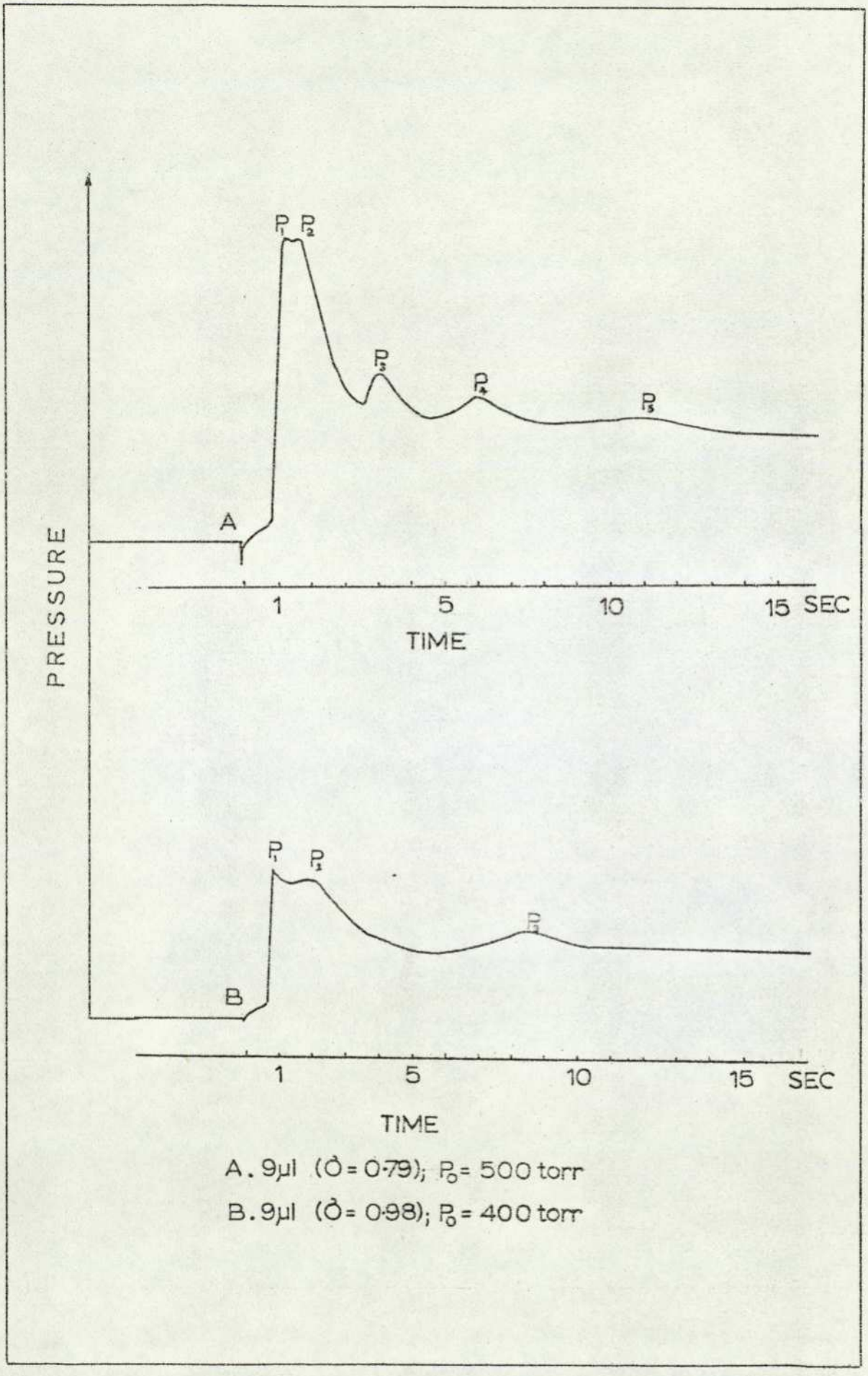

A. 9µl ($\dot{O}$ = 0·79); P_0 = 500 torr

B. 9µl ($\dot{O}$ = 0·98); P_0 = 400 torr

Figure 3·19

ΔP_∞ and ΔP_1 vs. δ for Hexadecane Fuel Oxidation at 200 torr and 295°C

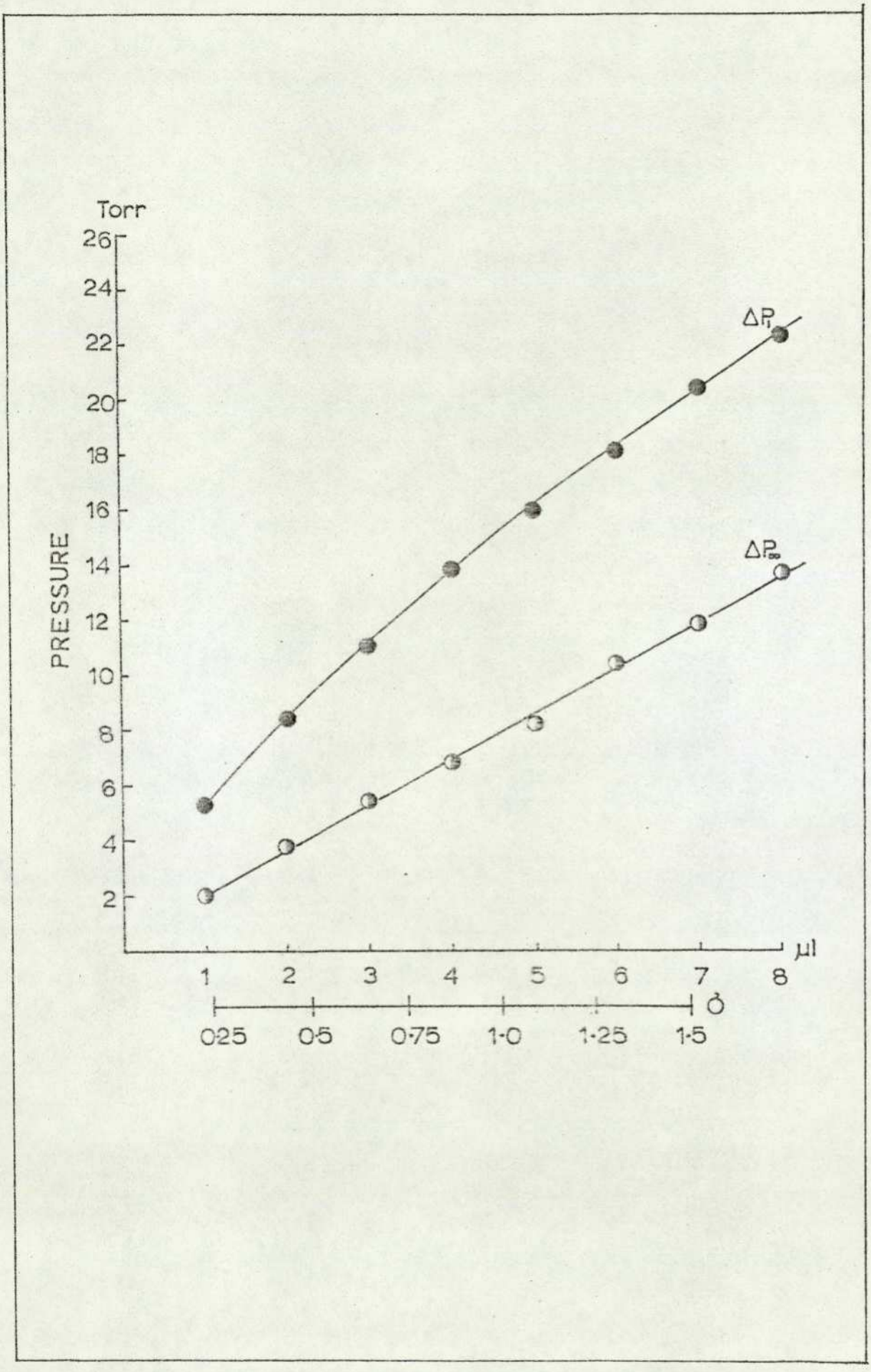

diesel fuel are again encountered with hexadecane. The pressure time traces recorded indicated the close similarity which existed between the two fuels in that the shape of the cool-flame pressure profiles were very similar in comparable regions in the respective ignition diagrams.

Injection of the same aromatic compounds mentioned in the previous section once again resulted in no detectable oxidation at 295°C. The lack of chemical reactivity of the compounds under investigation thus made it necessary to raise further the temperature of the bomb.

3.2.2.4 Kinetic Measurements at 310°C

This temperature was the highest to which the bomb was raised in these studies. The induction periods for diesel fuel were very short ie. $\tau_{cf} < 0.8$ seconds at all pressures. Measurements of kinetic parameters was thus considered to be of little value since the rate of vaporisation would have been comparable with the rate of the pre-cool flame reactions. Figure 3.20 shows the effect of initial temperature on the induction period leading to the passage of the first cool-flame in fuel oxidant mixtures of increasing equivalence ratio at 600 torr total pressure. The exponential decrease in τ_{cf} with T_o anticipated from the form of the Arrhenius equation governing the reactions leading to the cool flame is found to apply to the data collected.

Out of the list of aromatic compounds injected as fuels only n-butylbenzene produced a cool-flame. Figure 3.21(A) shows the decrease in τ_{cf} with σ for this hydrocarbon at 600 torr and Figure 3.21(B) shows the variation of ΔP_∞ and ΔP_1 with σ once again at 600 torr. After the type of combustion expected of the three fuels had been established, analysis of the contents of the bomb could be carried out under comparable conditions throughout the pressure-time profile. Section 3.3 presents the LC trapping and analysis results for the oxidation products from the bomb; these are important with regard to odorant formation during combustion. Section 4.4

Figure 3·20

τ_{cf} vs.To for Diesel Fuel Oxidation at 600 torr and for Various Equivalence Ratios

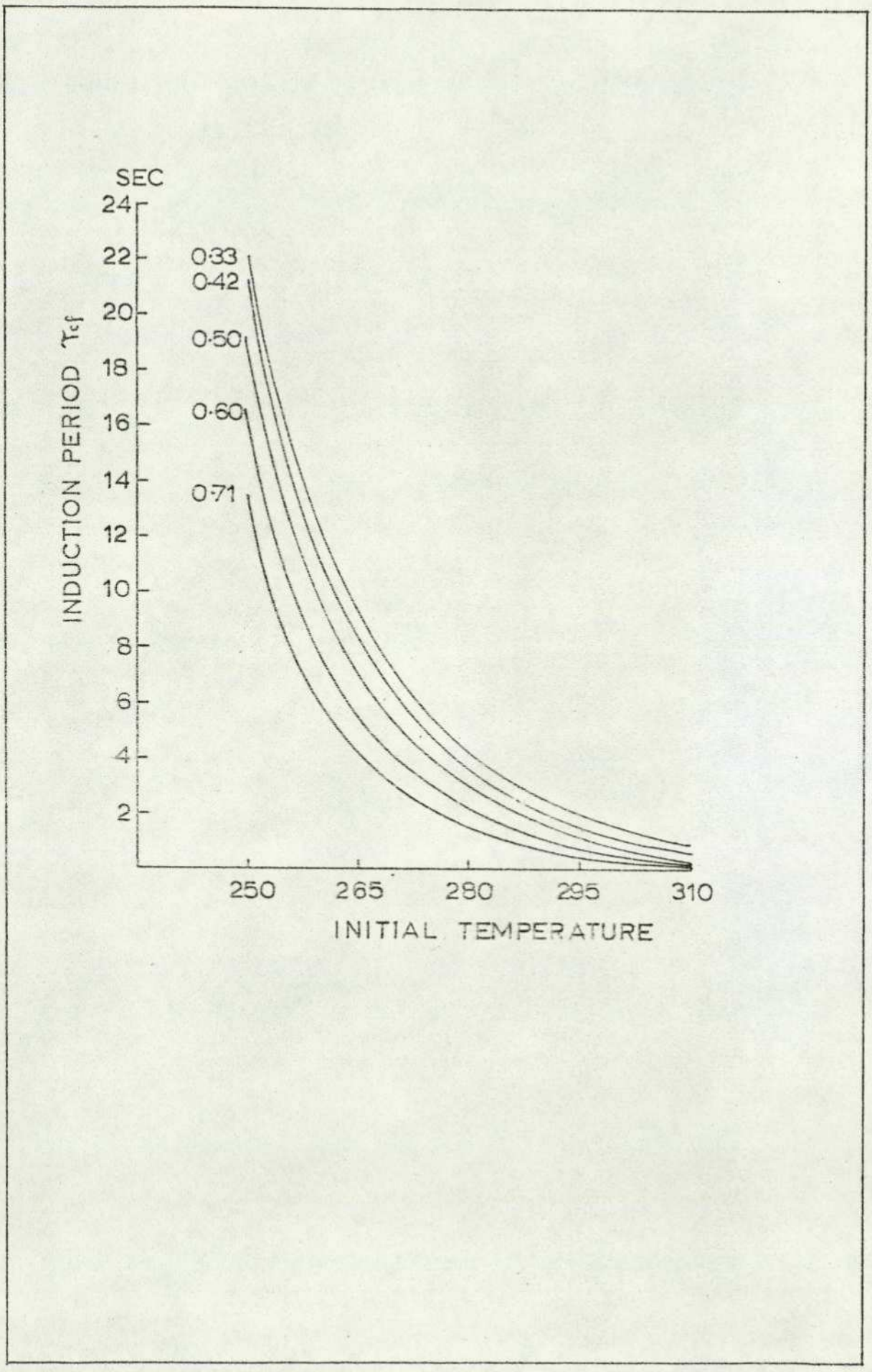

Figure 3·21

Kinetic Data for n-butylbenzene Oxidation at 600 torr and 310°C

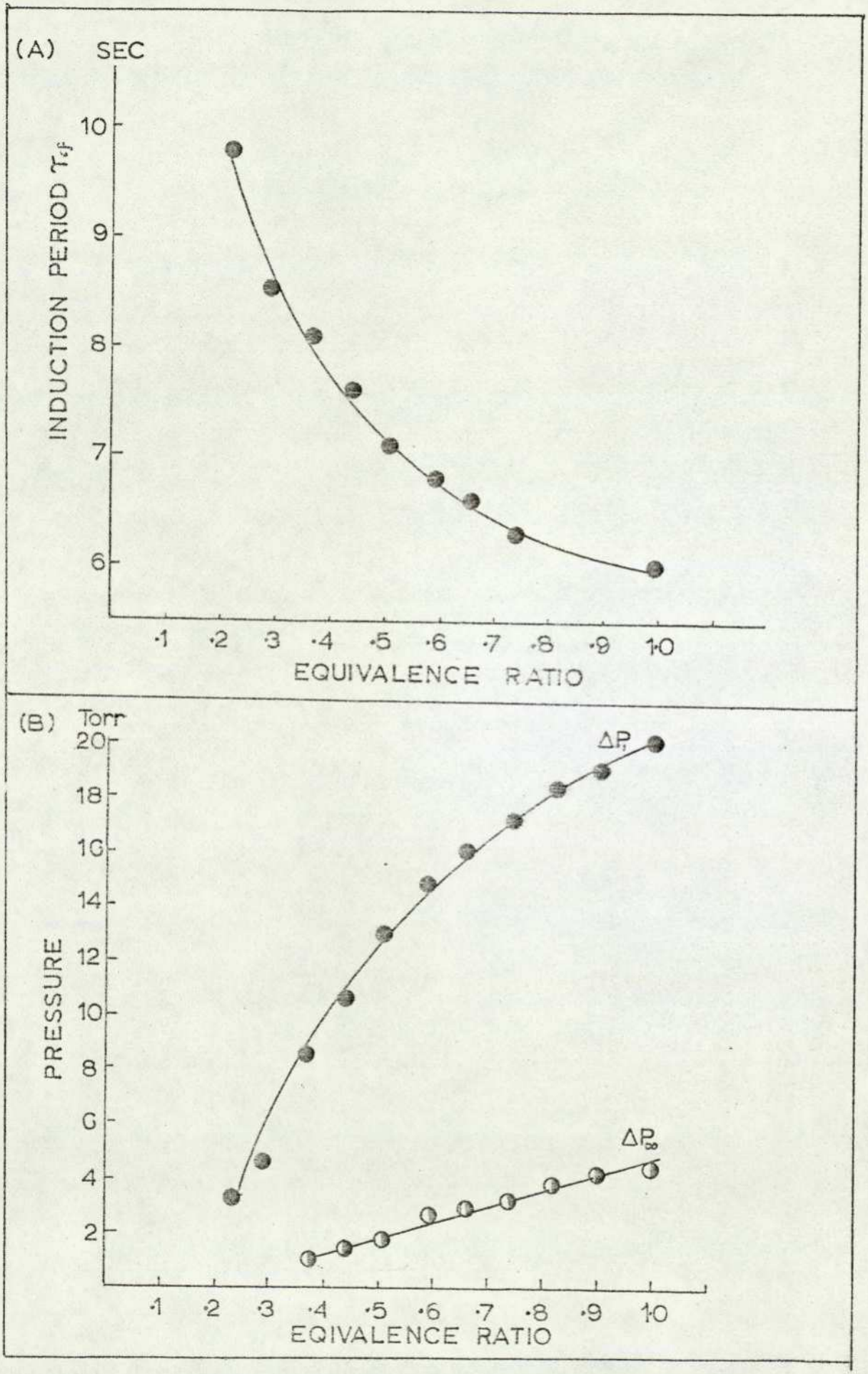

gives an account of GC analysis under similar conditions, the results providing further information on the chemical processes involved.

3.3 Liquid Chromatographic Analysis of Fuel Oxidation Products

3.3.1 Analysis of Products Formed at 280°C

The oxidation products of the fuels were were withdrawn for analysis by the method described in Section 2.2.5.3 and under the conditions listed in Table 3.2

Each Figure shows the pressure time trace recorded under the stated initial conditions and serves to relate the analysis point to the oxidation pressure-profile. Table 3.3 includes the percent standard deviations ($\%\sigma$) for the LCA and LCO areas measured by the integrator for four sample injections. The degree of dispersion in the peak areas listed ie: $\%\sigma$ = 0.00 to 6.00, applied to all the data contained in the subsequent tables.

Figure 3.22 shows the changes observed in the LCO and LCA levels of the samples taken at the indicated times. The number located in the Figure directly above each pair of points is the trap identification number and indicates the order in which the samples were taken for analysis.

The kinetic background to the emission of cool-flames has been described in Section 3.2.2.2. Figure 3.13 summarises the development of the pressure-time traces with increasing values of P_o from 500 to 600 torr. It was under these conditions that the LCA and LCO levels were determined.

In order to determine the LCA and LCO background levels of the fuel system, 5 µl of diesel fuel were injected into 500 torr of nitrogen and after 5 seconds the contents were withdrawn into trap 9. The LCA and LCO levels recorded are shown in the Figure at the point prior to injection since the sampling time used for the background measurement was of little significance. Further confirmation of the very low LCO value recorded in the background was obtained by injecting into the HPLC a sample of diesel fuel in cyclohexane. The presence of LCO components in the fuel was so low that even with undiluted fuel no LCO peak was recorded.

Table 3.2

Conditions under which the Fuels were Oxidised at 280°C

Fuel Used	Initial Pressure	Fuel Volume Injected μl	Equivalence Ratio	Combustion Phenomena Observed	Table	Figure
Diesel	500	5	0.42	Two Cool Flames	3.3	3.22
Diesel	600	6	0.42	Two-Stage Ignition	3.4	3.23
Diesel	600	4.5	0.32	Two Cool Flames	3.5	3.24
Hexadecane	500	5.0	0.42	Two Cool Flames	3.6	3.25
1-Decene	500	5.8	0.42	Two-Stage Ignition	3.7	3.26

Table 3.3

Data Pertaining to the LCA and LCO Levels Taken During Diesel Fuel Oxidation at 280°C, 500 torr Pressure and with an Equivalence Ratio of 0.42

Trap No.	Analysis Time (sec)	σ% LCA	LCA (µg)[1] per µl fuel	LCA (µg)[1] per Trap	σ% LCO	LCO (µg)[2] per µl fuel	LCO (µg)[2] per Trap	TIA
5	0.2	5.66	537.6	107.5	1.50	81.0	16.2	3.9
3	1.4	3.20	539.3	107.9	2.91	77.0	15.4	3.8
4	3.2	0.00	747.3	149.5	2.07	124.0	24.8	4.0
6	3.3	1.95	779.6	155.9	1.95	116.0	23.2	4.0
1	3.4	5.17	621.0	124.2	6.9	93.5	18.7	3.9
7	4.0	0.47	670.3	134.1	3.86	154.8	31.0	4.1
2	5.6	3.29	804.7	160.9	4.0	135.0	27.0	4.1
8	26.5	1.32	512.1	102.4	3.54	145.7	29.1	4.1
9		2.18	174.7	35.0	3.29	18.0	3.6	3.2

1. Concentration of LCA in ug expressed in terms of Indan equivalent

2. Concentration of LCO in ug expressed in terms of 4-methoxy,2-hydroxyacetophenone equivalent.

Figure 3·22

LCA and LCO Levels Recorded During the Oxidation of Diesel Fuel at 280°C, 500 torr and with δ = 0·42

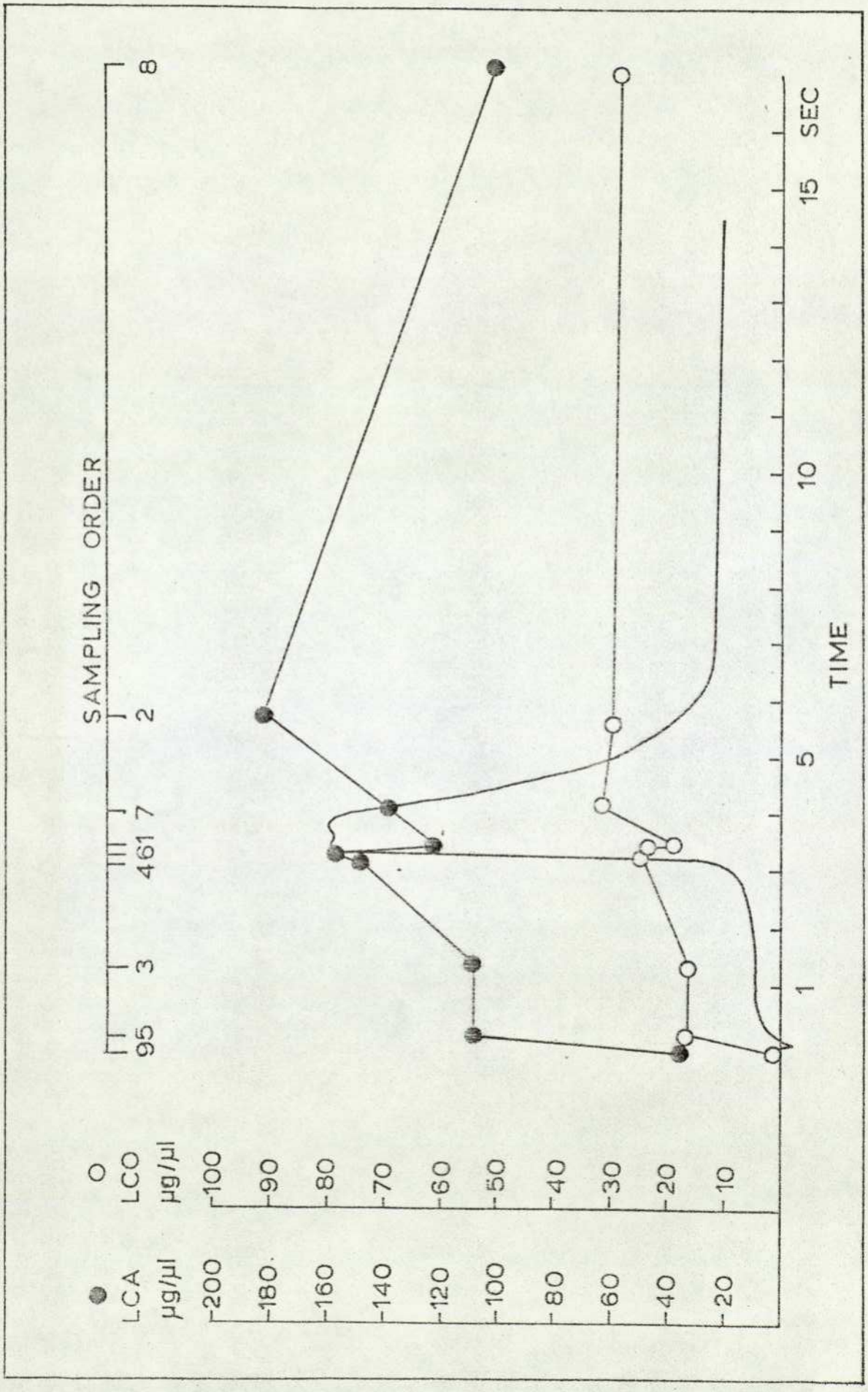

Inspection of Figure 3.22 shows that the LCA and LCO levels rise to relatively high values within a very short time. This observation is exemplified by the levels in trap 5, the contents of which were collected 0.2 seconds after injection. There is then a parallel rise in both LCA and LCO as the cool-flame front is approached, followed by a drop in both levels as the flame passes through the reactant volume. A further rise then occurs before the levels decrease as ΔP_∞ is approached. Although the time interval between injection and the analysis point could be accurately measured, ie: $\pm$0.04 seconds, the reaction may not undergo instantaneous quenching. Further reactions may therefore occur even during the short analysis period. These reactions could result in a slight delay between the point of analysis on the pressure time trace and the observed change in LCA and LCO levels. Evidence of further reactions taking place during analysis was obtained at high pressures and certain σ values. Under these conditions, the recording of the instantaneous pressure drop on activation of the solenoid valve indicated that a slight increase in pressure caused the trace to deviate from the vertical. This suggested that the reaction was still continuing in those circumstances owing to the increased reaction rate.

The data in Table 3.3 and Figure 3.22 were were collected as the two-stage ignition boundary was approached. An increase in the initial pressure to 600 torr produced an ignition at the same equivalence ratio (Table 3.4 and Figure 3.23). The increase in LCA and LCO as the cool-flame front is approached is again observed and this is followed by a severe reduction in both levels to trace quantities as the hot ignition occurs. The LCA then appears to make a partial recovery to its pre-ignition value while the increase in LCO is more gradual.

A reduction in fuel volume to 4.5 μl (σ = 0.32) enabled data to be collected at 600 torr for the passage of two cool flames (Table 3.5 and Figure 3.24)

Two other fuels, hexadecane and 1-decene were oxidised for

Table 3.4

Data Pertaining to the LCA and LCO Levels Recorded During Diesel Fuel Oxidation at 280°C, 600 torr Pressure and with an Equivalence Ratio of 0.42

Trap	Analysis Time	LCA (μg) per Trap	LCA (μg) per μl Fuel	LCO (μg) per Trap	LCO (μg) per μl Fuel	TIA
2	1.3	99.5	16.6	0.0	0.0	0.0
3	2.3	483.9	80.7	104.2	17.4	3.9
1	2.8	317.2	52.9	61.6	10.3	3.7
4	3.3	21.5	3.6	0.0	0.0	0.0
5	5.5	48.4	8.1	0.0	0.0	0.0
6	11.6	45.7	7.6	9.4	1.6	2.8

Figure 3·23

LCA and LCO Levels Recorded During the Oxidation of Diesel Fuel at 280°C, 600 torr and with σ = 0·42

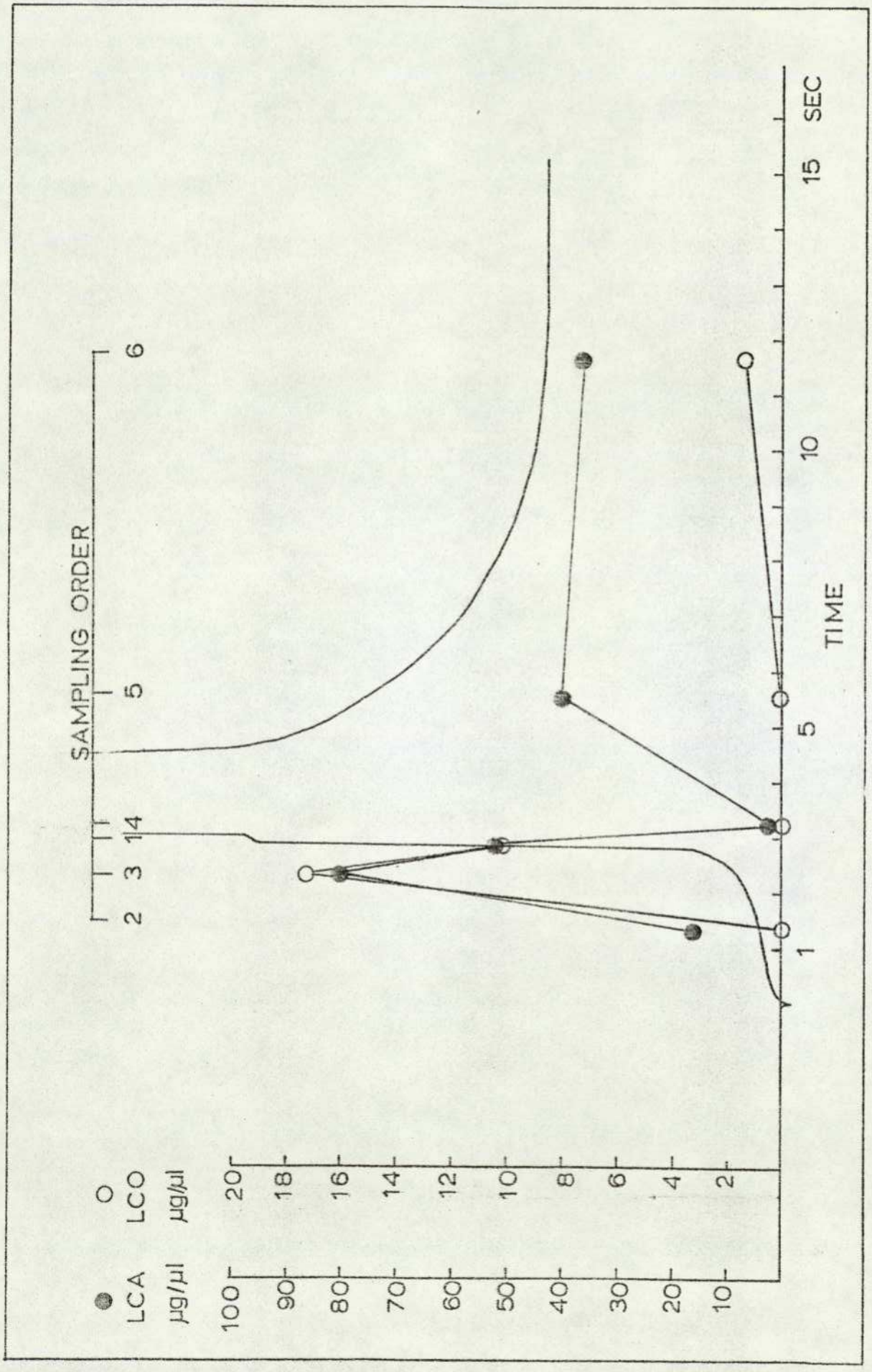

Table 3.5

Data Pertaining to the LCA and LCO Levels Recorded During Diesel Fuel Oxidation at 280°C, 600 torr Pressure and with an Equivalence Ratio of 0.32

Trap	Analysis Time	LCA (μg) per Trap	LCA (μg) per μl Fuel	LCO (μg) per Trap	LCO (μg) per μl Fuel	TIA
3	1.3	81.1	16.2	28.9	6.4	3.3
2	4.2	316.2	63.2	87.1	19.4	3.8
4	3.8	270.3	54.1	70.2	15.6	3.7
1	8.3	317.2	63.4	88.3	19.6	3.8
*5	4.6	43.2	8.7	17.0	3.78	3.1

* Sample Taken During Ignition

Figure 3·24

LCA and LCO Levels Recorded During the Oxidation of Diesel Fuel at 280°C, 600 torr and with σ = 0·32

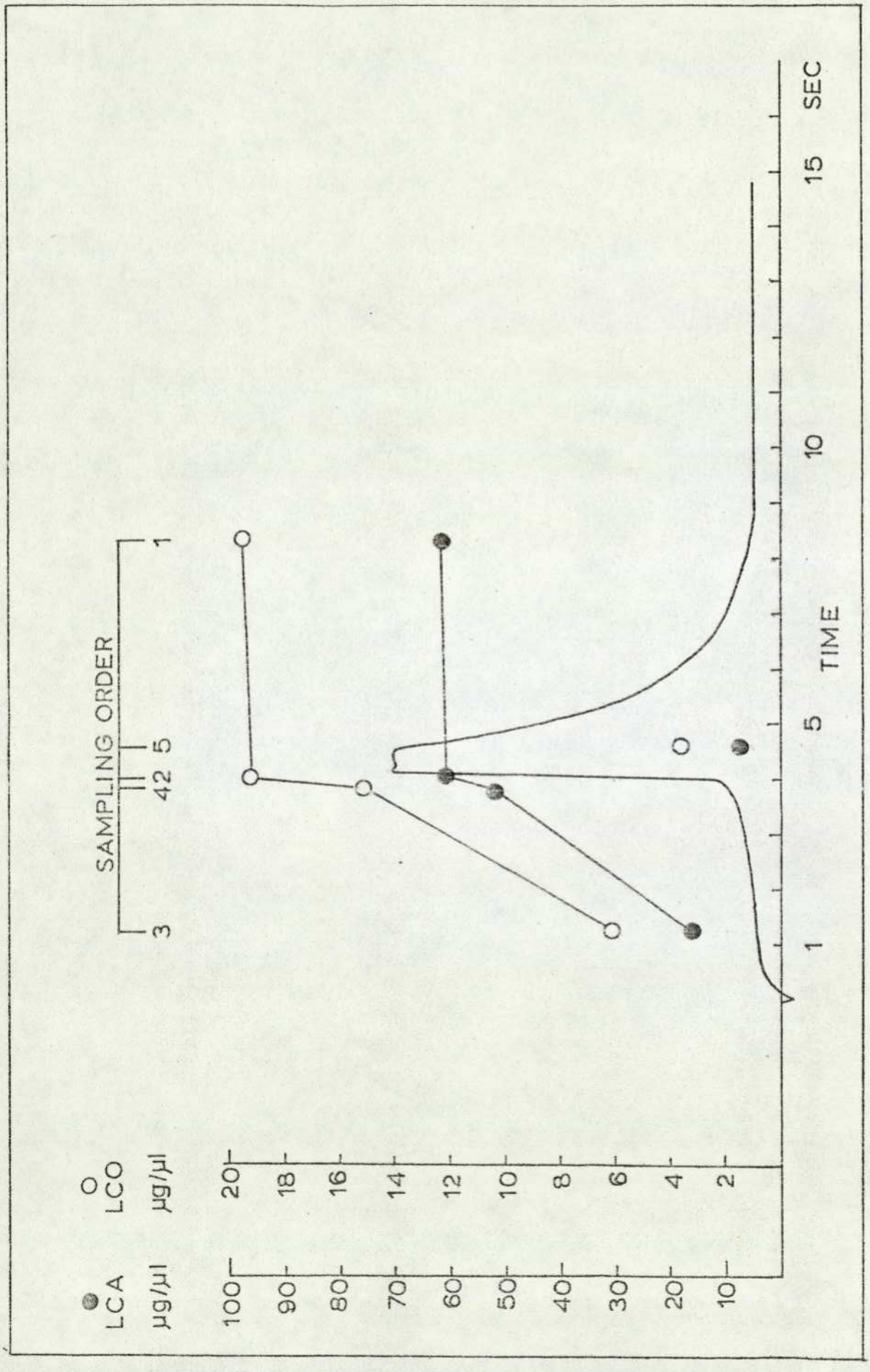

comparison under the same conditions as one of the diesel fuel experiments ie: σ = 0.42 and P_o = 500 torr. Hexadecane exhibited cool-flames (Figure 3.25) while 1-decene produced a two-stage ignition (Figure 3.26). Tables 3.6 and 3.7 contain complete analysis data for these two systems. The conditions used for the oxidation of hexadecane and the diesel fuel at σ = 0.32 were on the boundary between the two-stage ignition and cool-flame regions. The balance between the conditions leading to either of these phenomena was so fine that the evacuation time of the bomb between injections determined the nature of the resulting combustion. If the evacuation time was no greater than 10 minutes minutes, then two-stage ignition invariably resulted for injections of fuel under conditions apparently similar to those inducing two cool-flames. Table 3.5 shows that trap 5 contained the products of a hot-ignition induced by injecting the fuel after only five minutes of evacuation. Similarly, traps 6 and 8 (Table 3.6) contained samples from hot-ignitions generated by the same procedure. All the other points in these Figures were obtained under the same conditions but allowing 10 minutes evacuation between each injection. The same drastic reduction in the LCA and LCO levels was observed following these hot-ignitions as was recorded in Figure 3.23.

One interesting aspect of the results obtained with the two non-aromatic fuels, ie: hexadecane and 1-decene, is the LCA levels recorded. Although these levels were very low, some of the LCA components were found with hexadecane. Injection of undiluted 1-decene into the HPLC gave 9.27μg LCA / μl of fuel, which was very similar to the initial LCA levels recorded for traps 5, 4, 1 and 6. However, the LCA levels in hexadecane fuel was zero as determined by the above procedure but it increased significantly during oxidation rising to a maximum of 6.5 μg / μl of fuel prior to the first cool flame.

Table 3.6

Data Pertaining to the LCA and LCO Levels Recorded During Hexadecane Oxidation at 280°C, 500 torr Pressure and with an Equivalence Ratio of 0.42

Trap	Analysis Time	LCA (μg) per Trap	LCA (μg) per μl Fuel	LCO (μg) per Trap	LCO (μg) per μl Fuel	TIA
4	0.56	18.8	3.8	34.7	6.9	3.5
3	1.12	26.9	5.4	50.0	10.0	3.7
5	1.32	29.6	5.9	30.2	6.0	3.4
2	1.52	32.3	6.5	45.5	9.1	3.6
1	5.84	21.5	4.3	45.5	9.1	3.6
6*	1.8	5.4	1.1	0.0	0.0	0.0
8*	1.6	5.4	1.1	0.5	0.1	1.7
9 N_2	3.4	0.0	0.0	3.2	0.6	2.5

*Samples Taken During Ignition

Figure 3·25

LCA and LCO Levels Recorded During the Oxidation of n-hexadecane at 280°C, 500 torr and with $\sigma = 0{\cdot}42$

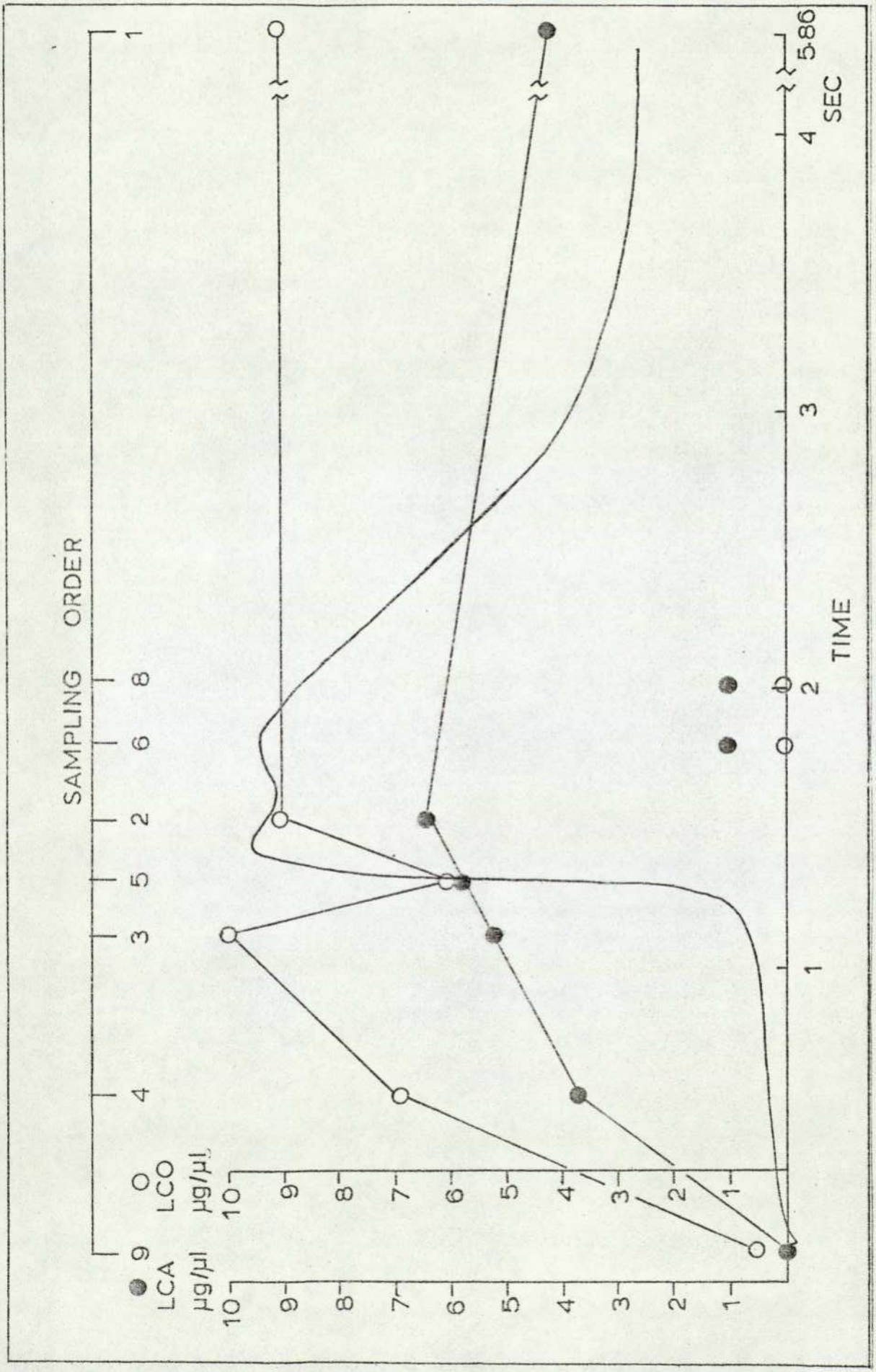

Table 3.7

Data Pertaining to the LCA and LCO Levels Recorded During 1-Decene Oxidation at 280°C, 600 torr Pressure and with an Equivalence Ratio of 0.42

Trap	Analysis Time	LCA (μg) per Trap	LCA (μg) per μl Fuel	LCA (μg) per Trap	LCO (μg) per μl Fuel	TIA
5	1.0	61.8	10.7	51.5	8.9	3.7
4	1.14	56.5	9.7	39.5	6.8	3.6
1	1.16	60.9	10.5	53.5	9.2	3.7
6	2.28	59.1	10.2	49.6	8.6	3.7
7	2.32	10.8	1.9	13.2	2.3	3.1
2	2.40	5.4	0.9	5.9	1.0	2.7
3	5.44	2.7	0.5	0.0	0.0	0.0

Figure 3·26

LCA and LCO Levels Recorded During the Oxidation of 1-decene at 280°C, 500 torr and with $\sigma = 0{\cdot}42$

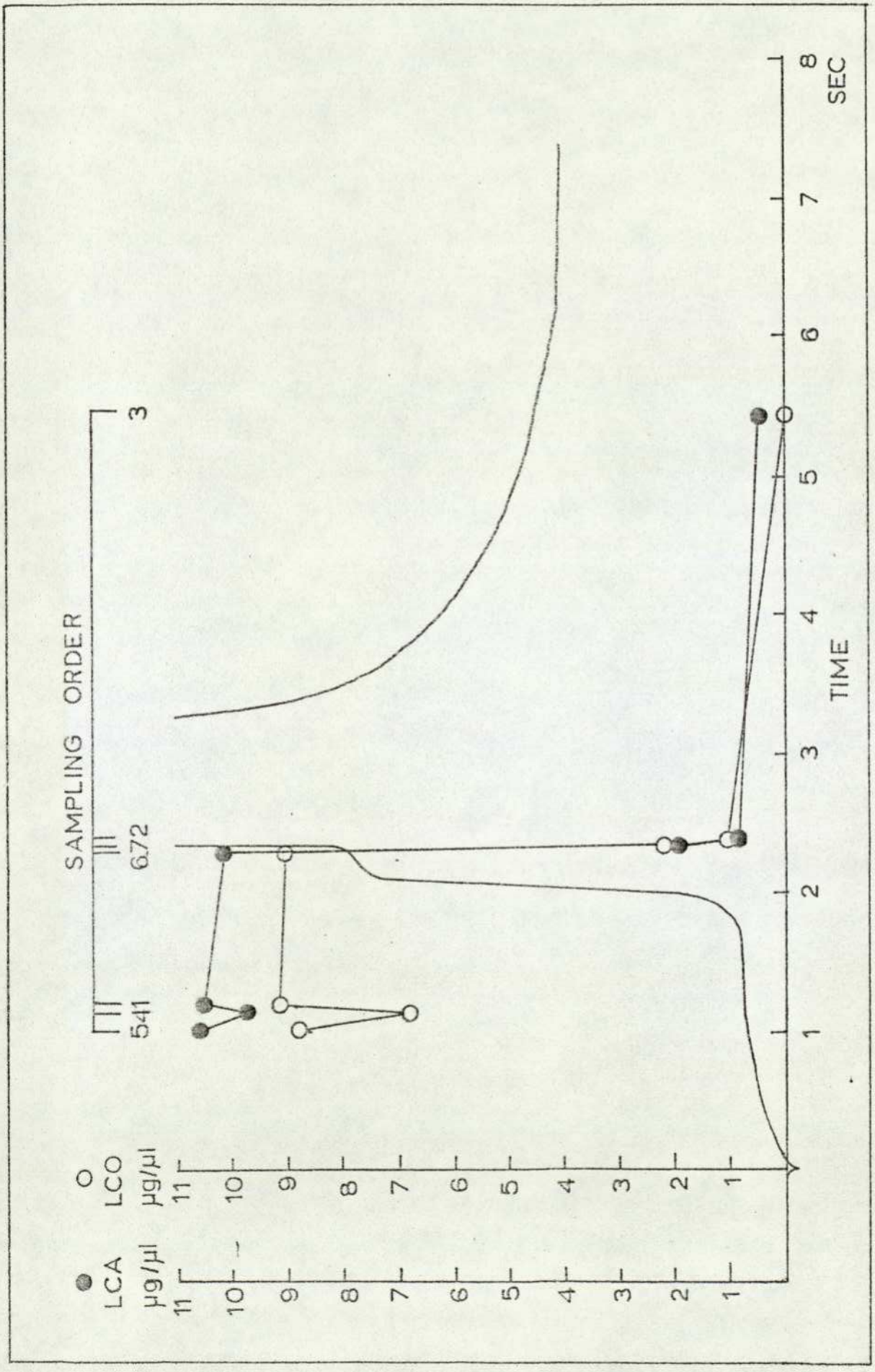

3.3.2 Analysis of Products Formed at 295°C

Investigations were continued at the above temperature using the conditions and fuels summarised in Table3.8.

The variation in LCA and LCO levels found at 280°C were also observed at 295°C, (Figure 3.27) To ascertain the relationship between the LCA and LCO levels and the equivalence ratio, the products were analysed at P_∞ for each σ value used. In practice this required sampling of the contents of the bomb six seconds after injection of the fuel. Reference to Figure 3.27 serves as an example to show that P_∞ had been reached during this six second period. The LCA and LCO values determined are shown in Figure 3.28.

Hexadecane was again used for comparison with diesel fuel and the results obtained from oxidations carried out under similar conditions are shown in Figure 3.29. The LCA and LCO levels are within the same order of magnitude as those measured at 280°C. Once again very low LCA levels are observed.

3.3.3 Analysis of Products Formed at 310°C

As described in Section 3.2.2.4, n-butylbenzene was the only aromatic compound found to undergo oxidation at these temperatures. Figure 3.30 shows a typical cool-flame profile obtained during oxidation and the LCA and LCO trends. As expected the LCA and LCO levels were very high compared with those for standard diesel fuel. The LCO levels measured were also much higher, showing a 60% increase above those obtained from diesel fuel.

Analysis of the oxidation products at P_∞ for n-butylbenzene showed a more complex variation of the LCA and LCO levels with σ than for diesel fuel, as a comparison between Figures 3.31 and 3.28 indicates. The degree of reproducibility of the n-butylbenzene data is typified by the two points in Figure 3.31, relating to injections of 9.8 and 10 µl of fuel

Table 3.8

Conditions under which Fuels were Oxidised at 295°C

Fuel Used	Initial Pressure	Fuel Volume Injected µl	Equivalence Ratio	Combustion Phenomena Observed	Table	Figure
Diesel	500	5.0	0.42	Two Cool-Flames	3.9	3.27
Diesel	600	1.7	0.12	Two Cool-Flames	3.10	3.28
		3.0	0.22	" " "	"	"
		4.4	0.32	" " "	"	"
		4.9	0.37	" " "	"	"
		5.8	0.42	" " "	"	"
		6.5	0.47	" " "	"	"
		7.2	0.52	" " "	"	"
		8.5	0.62	Two-Stage Ignition	"	"
Hexadecane	500	5.0	0.42	Two Cool-Flames	3.29	3.11

Table 3.9

Data Pertaining to the LCA and LCO Levels Recorded During Diesel Fuel Oxidation at 295°C, 500 torr Pressure and with an Equivalence Ratio of 0.4

Trap No.	Analysis Time	LCA (µg) per Trap	LCA (µg) per µl Fuel	LCO (µg) per Trap	LCO (µg) per µl Fuel	TIA
4	0.16	439.1	87.8	94.0	18.8	3.9
3	1.0	587.4	117.5	152.7	30.5	4.2
2	1.36	727.2	145.4	155.0	31.0	4.2
5	1.90	676.1	135.2	150.1	30.0	4.1
6,8	1.92	618.3	123.7	142.3	31.7	4.1
7	3.0	739.3	147.9	169.7	33.9	4.2
1	4.36	607.5	121.5	154.3	30.9	4.2
9 N_2	-	94.1	18.8	14.2	2.9	3.1

Figure 3·27

LCA and LCO Levels Recorded During the Oxidation of Diesel Fuel at 295°C, 500 torr and with σ = 0·42

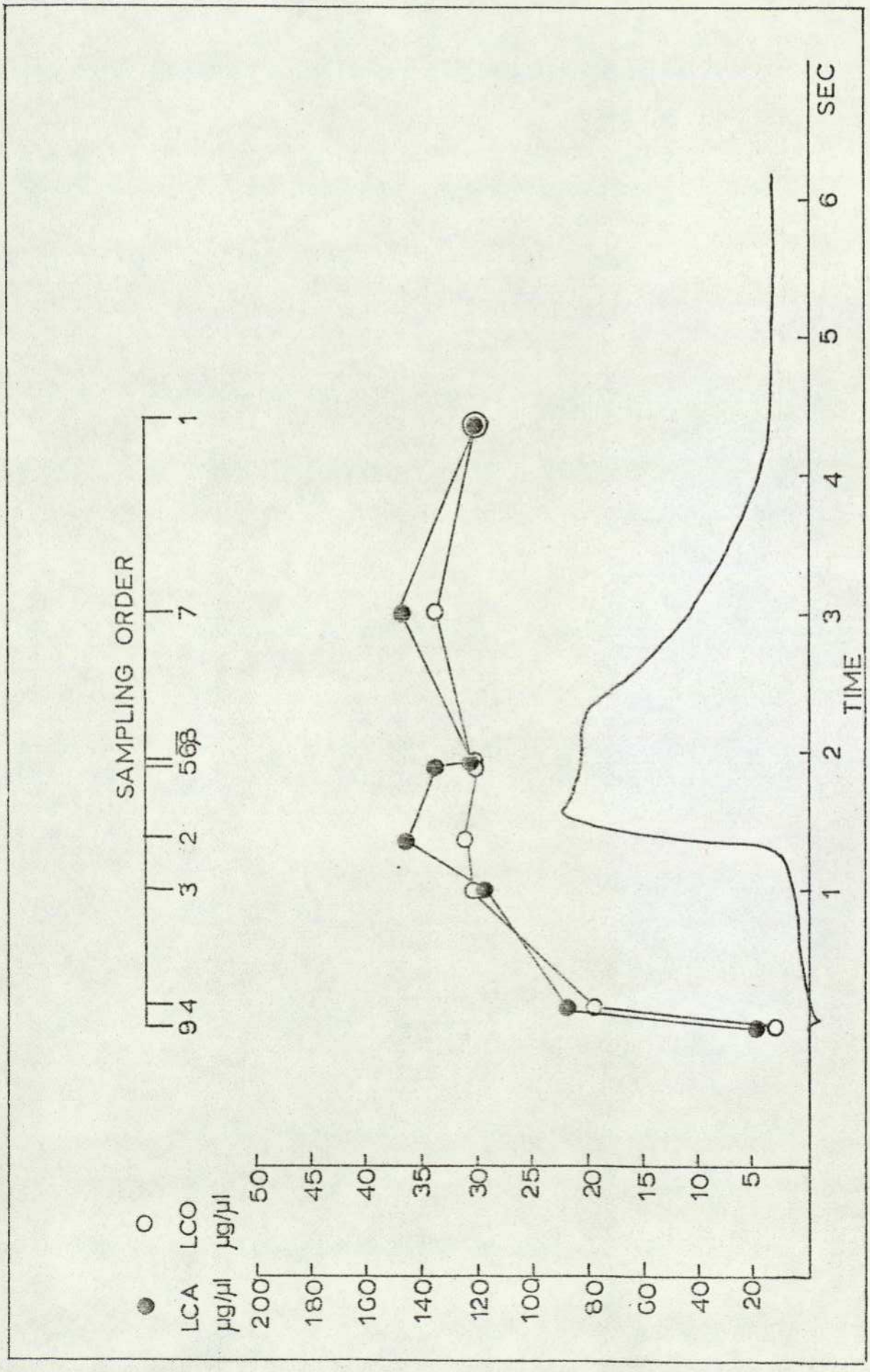

Table 3.10

Data Pertaining to the LCA and LCO Levels Recorded at P_∞ During Diesel Fuel Oxidation at 295°C 600 torr Pressure and for Various Equivalence Ratios

Fuel Volume Injected µl	Equivalence Ratio	LCA (µg) per Trap	LCA (µg) per µl Fuel	LCO (µg) per Trap	LCO (µg) per µl Fuel	TIA
1.7	0.12	207.9	122.3	43.0	25.3	3.5
3.0	0.22	489.3	163.1	117.3	39.1	4.0
4.4	0.32	790.3	179.6	204.1	46.4	4.2
4.9	0.37	960.4	196.0	235.2	48.0	4.3
5.8	0.42	1090.4	188.0	278.4	48.0	4.3
6.5	0.47	1235.0	190.0	299.0	46.0	4.4
7.2	0.52	1360.2	188.9	317.7	44.1	4.4
8.5	0.62	333.3	39.2	20.7	2.4	3.2

Figure 3·28

LCA and LCO Levels Recorded During the Oxidation of Diesel Fuel at 295°C, 600 torr and with Various Equivalence Ratios

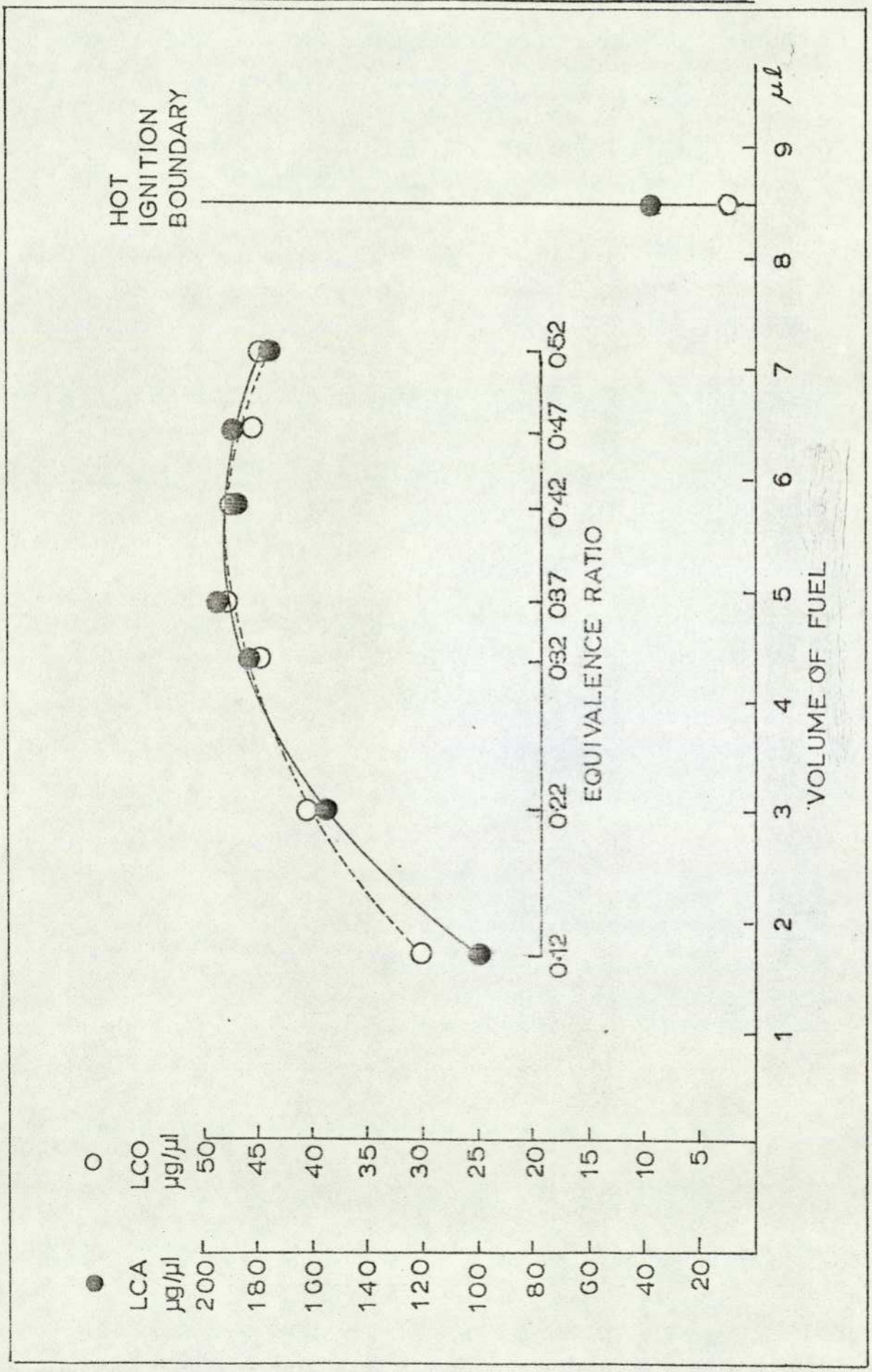

Table 3.11

Data Pertaining to the LCA and LCO Levels Recorded During Hexadecane Oxidation at 295°C 500 torr Pressure and with an Equivalence Ratio of 0.42

Trap	Analysis Time	LCA (μg) per Trap	LCA (μg) per μl Fuel	LCA (μg) per Trap	LCO (μg) per μl Fuel	TIA
7	0.12	16.1	3.4	0.0	0.0	0.0
2	0.6	8.1	1.7	22.1	4.6	3.3
3	0.72	0.0	0.0	23.6	4.9	3.3
5	1.04	8.1	1.7	26.7	5.6	3.4
4	1.44	13.4	2.8	23.3	4.9	3.3
6	6.4	8.2	1.7	30.7	6.4	3.5
1	15.0	14.4	3.0	11.5	2.4	3.0
8 N_2	-	0.0	0.0	0.0	0.0	0.0

Figure 3·29

LCA and LCO Levels Recorded During the Oxidation of n-hexadecane at 295°C, 500 torr and with α = 0·42

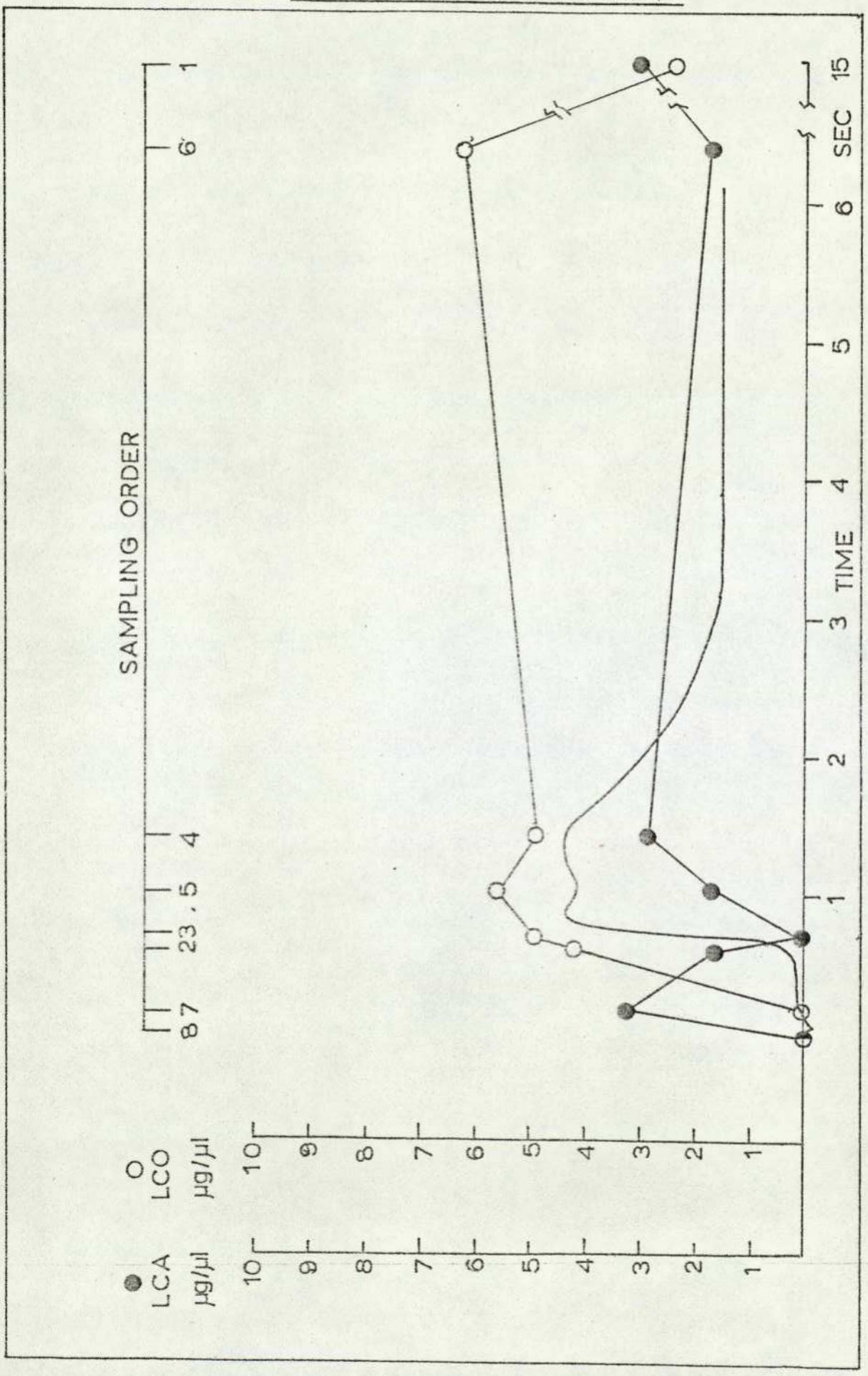

Table 3.12

Data Pertaining to the LCA and LCO Levels Recorded During n-Butylbenzene Oxidation at 310°C, 600 torr Pressure and with an Equivalence Ratio of 0.42

Trap No.	Analysis Time	LCA (μg) per Trap	LCA (μg) per μl Fuel	LCO (μg) per Trap	LCO (μg) per μl Fuel	TIA
4	0.83	2223.0	390.0	114.1	20.0	4.0
5	1.83	2758.8	484.0	148.8	26.1	4.1
7	4.01	2650.5	465.0	198.3	34.8	4.2
6	6.67	3197.7	561.0	270.9	47.5	4.3
2	7.17	4377.6	768.0	335.5	58.8	4.4
8	7.8	4104.0	720.0	356.4	62.5	4.3
1	11.67	3659.4	642.0	327.2	57.4	4.4
3	15.33	4485.9	787.0	431.8	75.8	4.5
9 N_2	-	1886.7	331.0	26.6	4.7	3.3

Figure 3·30

LCA and LCO Levels Recorded During the Oxidation of n-butylbenzene at 310°C, 600 torr and with $\sigma = 0{\cdot}42$

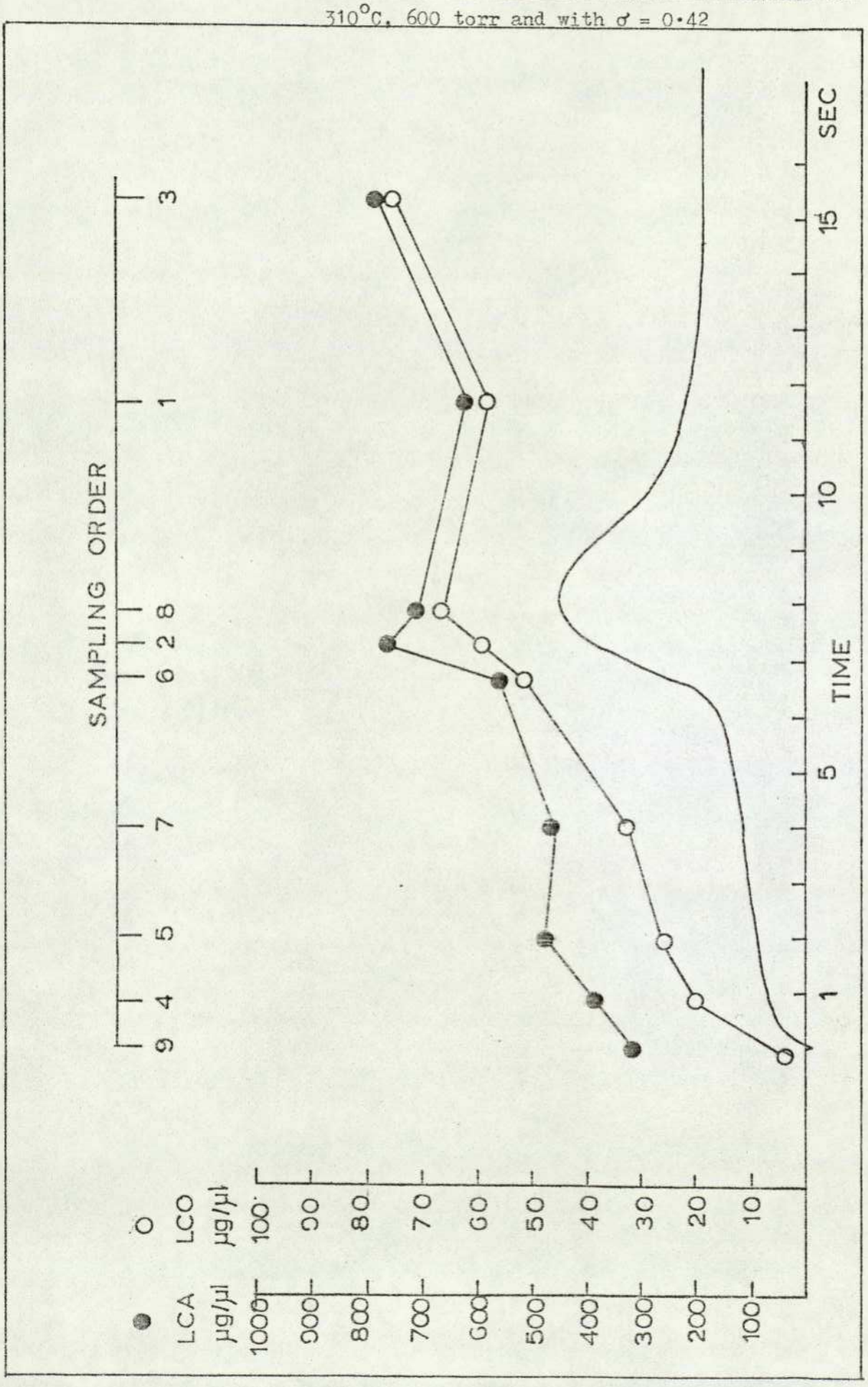

Table 3.13

Data Pertaining to the LCA and LCO Levels Recorded at P_∞ During n-Butylbenzene Oxidation at 310 C, 600 torr Pressure and for Various Equivalence Ratios

Fuel Volume Injected µl	Equivalence Ratio	LCA (µg) per Trap	LCA (µg) per µl Fuel	LCO (µg) per Trap	LCO (µg) per µl Fuel	TIA
1.6	0.12	1518.8	949.3	75.7	47.3	3.8
3.0	0.22	2446.2	815.4	217.2	72.4	4.2
4.4	0.32	3867.4	879.0	325.8	74.0	4.4
5.7	0.42	4301.1	754.6	359.8	63.1	4.5
7.1	0.52	5473.1	770.9	486.7	68.5	4.6
8.4	0.62	6365.6	757.8	537.4	64.0	4.6
9.8	0.72	6666.7	680.3	581.8	59.4	4.7
10.0	0.73	6795.7	679.6	586.5	58.7	4.7

Figure 3·31

LCA and LCO Levels Recorded During the Oxidation of n-butylbenzene at 310°C, 600 torr and with Various Equivalence Ratios

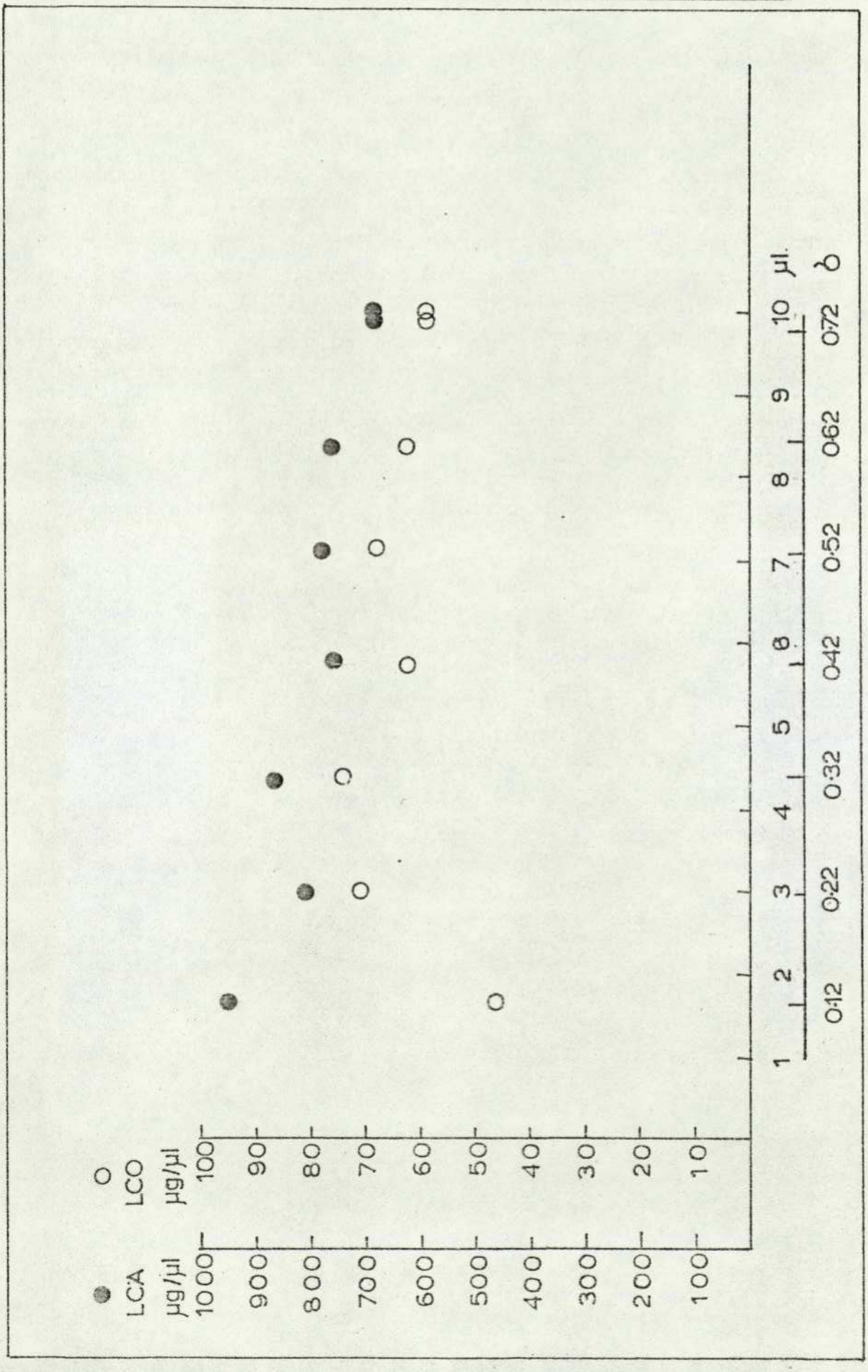

(σ = 0.72 and 0.73).

Further information regarding the reproducibility was obtained from oxidations of standard diesel fuel and American test fuel. Table 3.14 summarises the data obtained at 600 torr and with σ = 0.42, and this shows that the greatest dispersion in the P_∞ analysis data was reflected by a % σ value of 7.13 in the LCO levels for the standard diesel fuel. One important feature of these data is the apparently higher LCA and LCΩ levels of the American test diesel fuel when injected into nitrogen.

Samples of the oxidation products were collected from mixtures containing 600 torr of air and with an equivalence ratio of 0.42. The products were withdrawn 20 seconds after injection, during which period three cool-flames were observed with both fuels. The American fuel prior to oxidation contained 11% more LCA than the standard fuel. After oxidation the difference increased to 32%. The LCO levels after oxidation were very similar despite the fact that the American test fuel had an initial LCO level nearly three times higher than that of the standard fuel.

Table 3.14

Comparison of LCA and LCO Levels in European and American Test Fuels Before and After Oxidation at 310°C, 600 torr Pressure and with an Equivalence Ratio of 0.42

Standard Diesel Fuel

Trap No	LCA (µg) per Trap	LCA (µg) per µl Fuel	LCO (µg) per Trap	LCO (µg) per µl Fuel	TIA
1	758.1	133.0	209.9	36.8	4.2
2	774.2	135.8	232.2	40.7	4.3
σ%	1.49	1.49	7.13	7.13	-
$\bar{x}$	766.1	134.4	221.1	38.8	4.2
3 N_2	467.7	82.1	6.3	1.1	2.7

American Test Fuel

Trap No	LCA (µg) per Trap	LCA (µg) per µl Fuel	LCO (µg) per Trap	LCO (µg) per µl Fuel	TIA
1	1010.8	177.3	211.3	37.1	4.2
2	1010.8	177.3	212.7	37.3	4.2
σ%	0.00	0.00	0.46	0.46	-
$\bar{x}$	1010.8	177.3	212.0	37.2	4.2
3 N_2	521.5	91.5	17.4	3.1	3.1

3.4 U.V. Spectrophotmetric Analysis of LC Trap Eluent

The cyclohexane eluent obtained from each LC trap was subjected to U.V. absorption analysis in order to ascertain the U.V. spectrum in the 200 - 350 nm wave length range. A Pye-Unicam SP 800 double beam spectrophotometer, equipped with matched 2mm quartz cells was used for the analysis which was carried out with cyclohexane in the reference cell.The undiluted exhaust eluent from the LC trap was usually transferred without dilution to the sample cell. The main object of subjecting the LC eluent to liquid chromatography was to separate the oxygenated from the aromatic species. This was necessary since the ADL correlation of odour panel response to LCO concentration was subject to less dispersion than the parallel correlations with either the LCA fraction of the combined LCO plus LCA fractions. Since no such separation was performed in the present study, however, the absorbance at 254 nm resulted from the combined absorbancies of the two fractions.

A typical spectrum of the oxidation products of diesel fuel is shown in Figure 3.32. The rise in absorption at the high energy end of the spectrum is due to the absorbance of the paraffinic portions of the molecules present. The 254 nm fixed wave length monitoring by the HPLC detector does not coincide with a unique absorbance band. ADL chose 254 nm as the monitoring wave length since it was a preferred value for commercially available gratings, the use of which would preclude detection of alkanes.

Figure 3.33 shows the results obtained from the analysis of a selection of fourteen samples of the products of oxidation of diesel fuel. The LCO and LCA content of each sample was known from LC analysis. The samples were selected to give a wide range of LCO and LCA concentrations in order to determine the correlation with absorbance over the whole range investigated ie. 0.0 to 1.0 absorbance units.

The degree of correlation of either LCA or LCO with the total

Figure 3·32

U.V. Spectrum of Diesel Fuel Oxidation Products

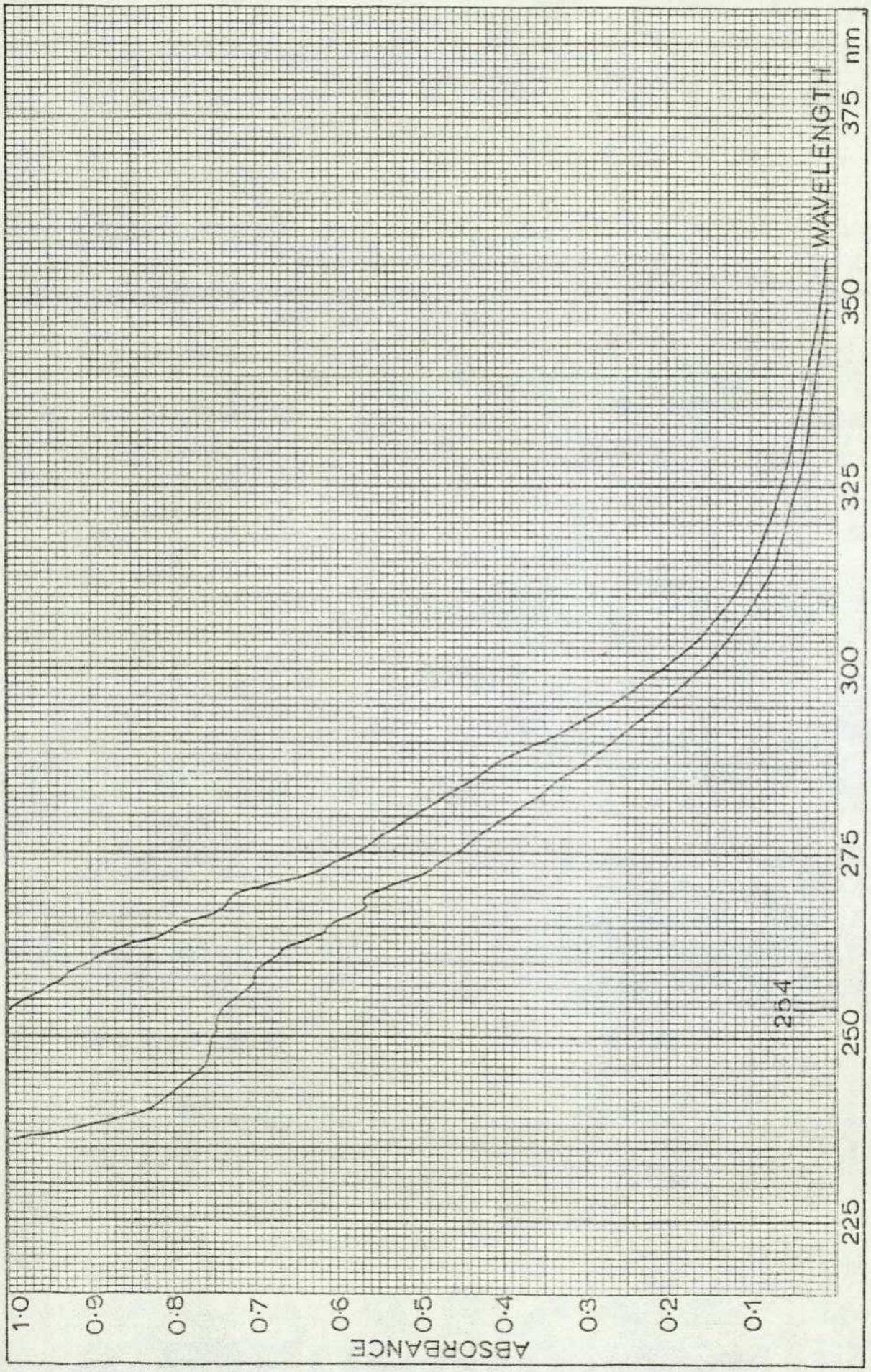

Figure 3·33

LCA and LCO vs. U.V. Absorbances at 254nm for Diesel Fuel Oxidation Samples

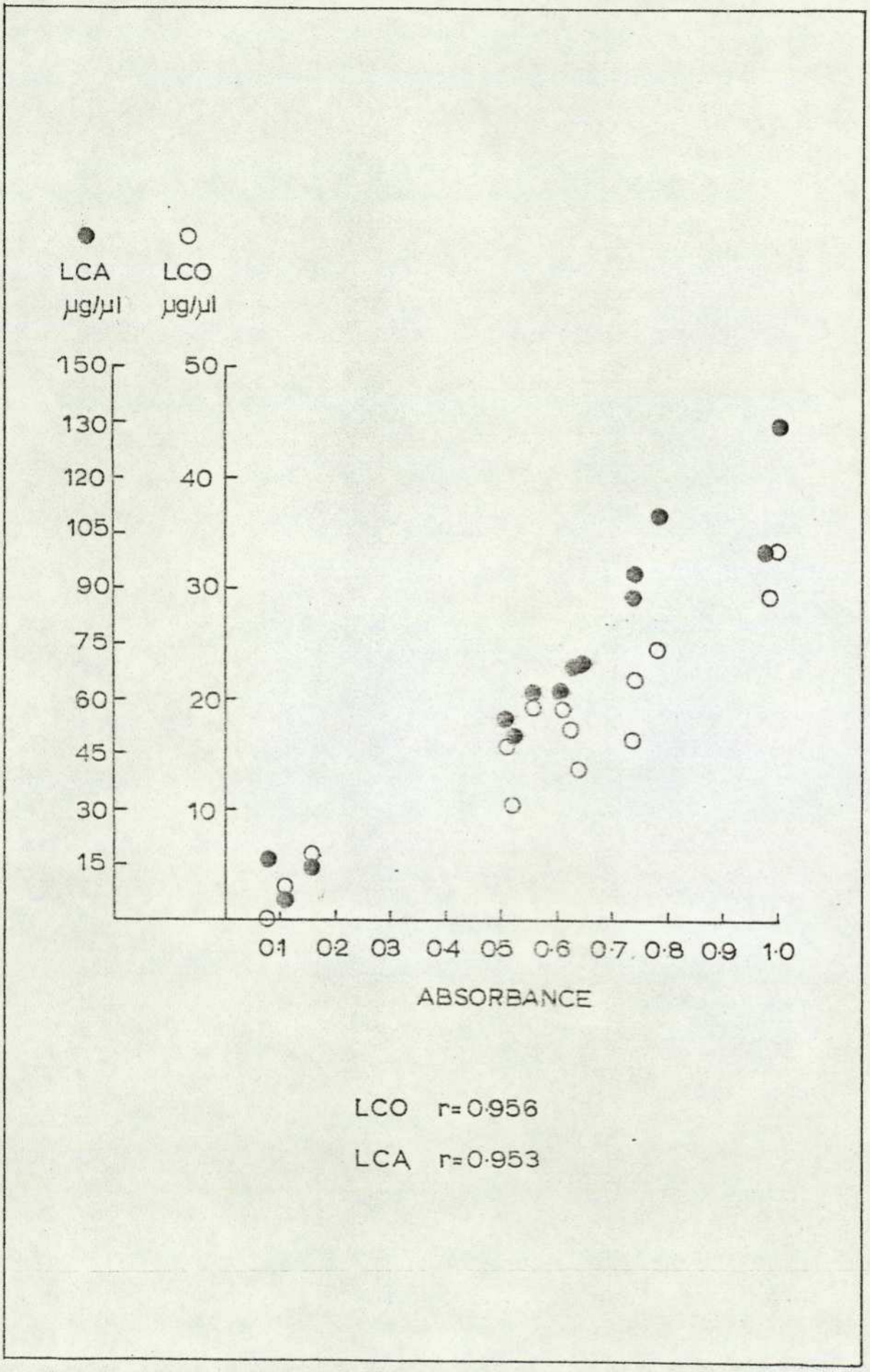

sample absorbance at 254 nm is extremely good, a finding confirmed by the statistical treatment of the two sets of data which give high values for the correlation coefficients (r).

Figure 3.34 shows the spectrum obtained for samples of the products of hexadecane oxidation. The spectra show greater definition than those for diesel fuel samples, with a band centred at 260 nm. Carbonyl groups strongly absorb at 260 nm[119] and the particularly well-defined absorption at this wave length suggests the presence of aldehydic and ketonic groups in the oxidation products. These species are of course also present in the diesel fuel samples but tend to be marked by the vast numbers of other species present, particularly the aromatic compounds. The correlation of the absorbance with LCA and LCO is once again very good as shown by the data in Figure 3.35.

Figure 3·34

U.V. Spectrum for n-hexadecane Oxidation Products

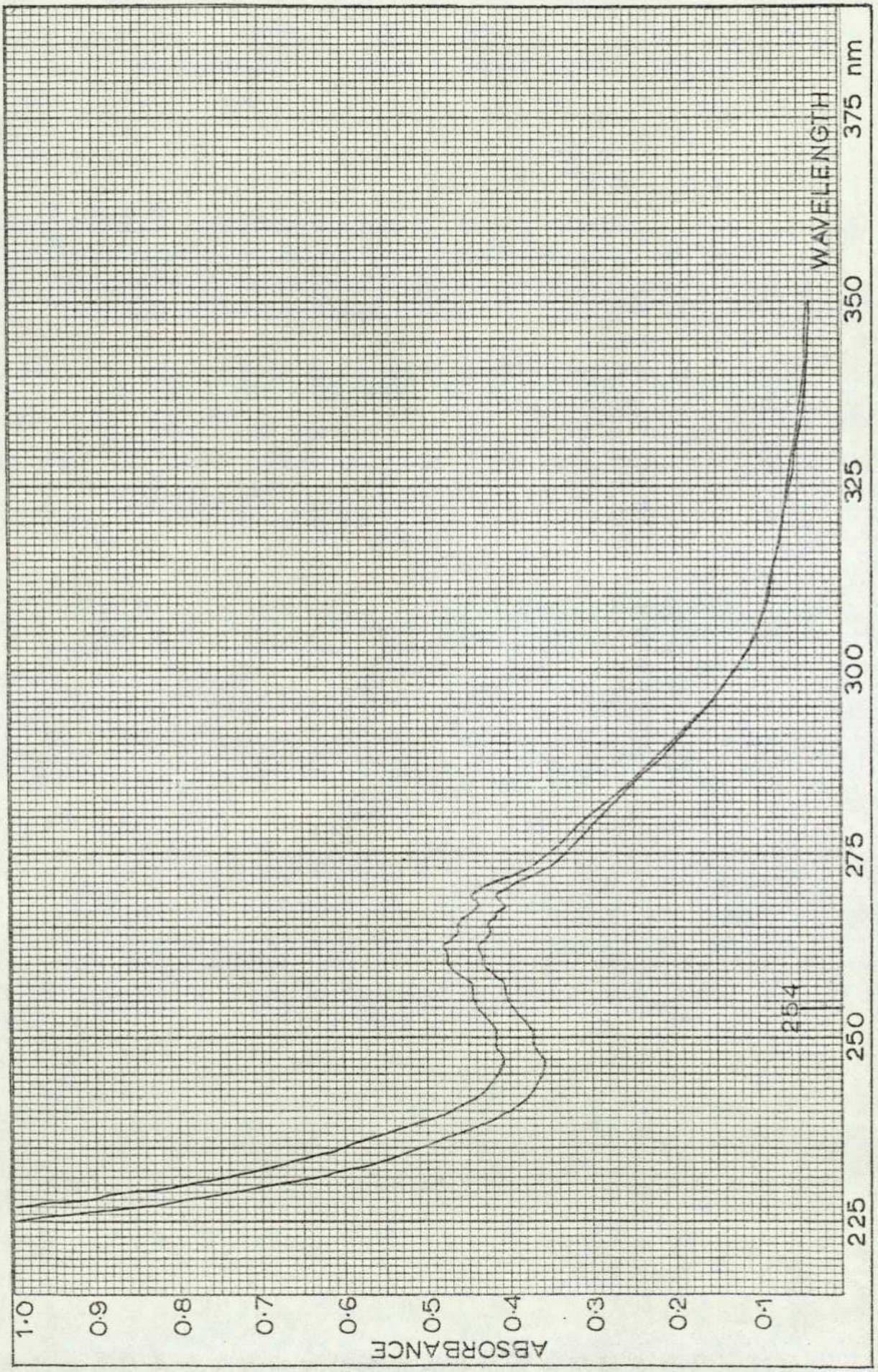

Figure 3·35

LCA and LCO vs. U.V. Absorbance at 254nm for n-hexadecane Oxidation Samples

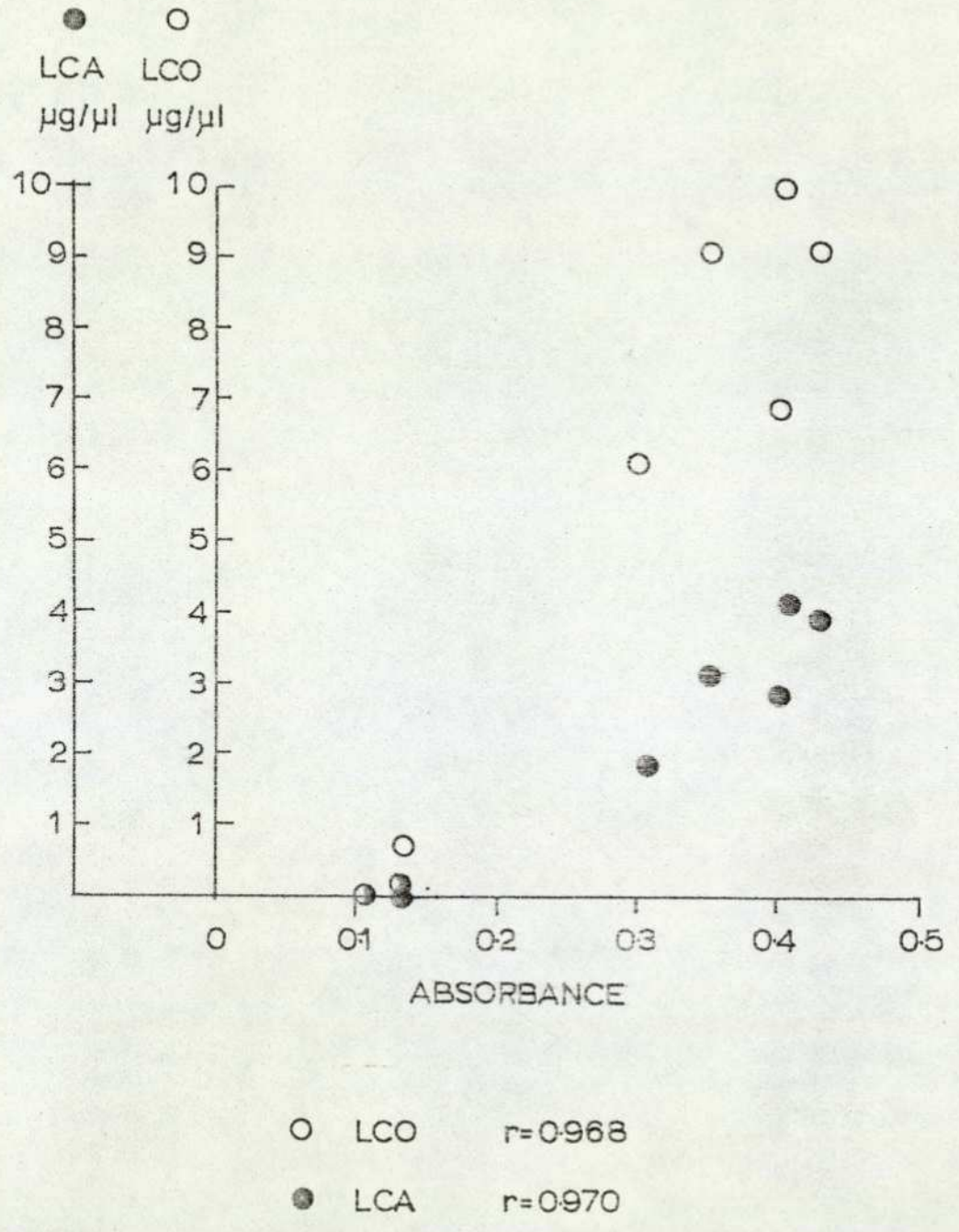

3.5 Gas Chromatographic Analysis of Fuel Oxidation Products

Section 2.3.4.1 describes the method employed for the trapping and analysis of the gaseous oxidation products. In order to evaluate the efficiency of the trapping process, two other techniques were employed to collect samples for GC analysis. In one method, the products from 35 post-cool flame runs were condensed in the evacuated loop by surrounding it with liquid nitrogen. The oxidations were all carried out under the same conditions, ie. 600 torr of air at 310°C and $\sigma = 0.42$; and the samples were withdrawn after the same length of time. The products condensed into droplets which formed two phases, one consisting of an opaque aqueous deposit and the other of a light-brown oily liquid. These deposits were recovered from the loop using a minimum quantity of cyclohexane and the resultant sample was then reduced under vacuum at room temperature to approximately one-third of its original volume. For comparison, other samples were obtained for GC analysis from the LC traps; the cyclohexane eluent containing the oxidation products derived under the same conditions as those above, was again reduced under vacuum and the concentrate was injected on the F11 column.

Chromatograms of samples obtained before and after vacuum concentration indicated that no excessive loss of the lower molecular weight components occurred through preferential evaporation.

As stated previously in Section 2.3.4.1, the results from these analyses were essentially qualitative. Information was obtained concerning the efficiency of the respective trapping techniques and comparisons of the oxidation product chromatograms with those of the original fuel allowed some important deductions to be made.

3.5.1 Diesel Fuel

3.5.1.1 Samples Collected in the Gas Phase

Pre-cool flame product chromatograms indicated the presence of components with Kovats Indices (KI) ranging from ca. 1050 to more than 2,000. The relative peak areas and peak distribution patterns were very similar to those of the original fuel. Figure 3.36 shows one such pre-cool flame chromatogram obtained by injecting 5 μl of diesel fuel into 500 torr of air at 280°C and sampling after 1.5 seconds. Those components in the fuel with KI between 500 and 1050 were not detected in the pre-cool flame chromatograms. These lighter molecular weight components together constitute approximately 11% of the total area of the chromatogram (Figure 3.1), each individual component being present in very low concentrations. For this reason, their presence was not detected.

Post-cool flame product chromatograms did, however, record the elution of low molecular weight low polarity components within the first three minutes. This band of eight resolved components with KI ranging from 500 to 900 was entirely unique to the post-cool flame product chromatograms. Two of the principal peaks in this band had retention times comparable with those of ethanal and propanal (54 and 78 seconds respectively). The post-cool flame chromatograms differed from those of the original fuel in that the alkane peaks displayed shoulders, ie. unresolved components, and the peaks eluted between each alkane showed differences in relative areas and distribution patterns. These sections of the chromatograms have been labelled 1 to 5 in Figure 3.37 to assist in the discussion of their characteristics.

Chromatograms of the products remaining after the occurence of an ignition (Figure 3.38) were completely different from the cool-flame or initial fuel chromatograms. The ignition product chromatograms contained fewer peaks and exhibited a major peak with KI = 1600. The components eluted in the first 3 minutes were present in much lower concentrations than in the post-cool flame product chromatograms.

Figure 3·36

Pre-cool Flame Products Chromatogram on C20M(Diesel Fuel Oxidation at 280°C, 500 torr and with σ=0·42)

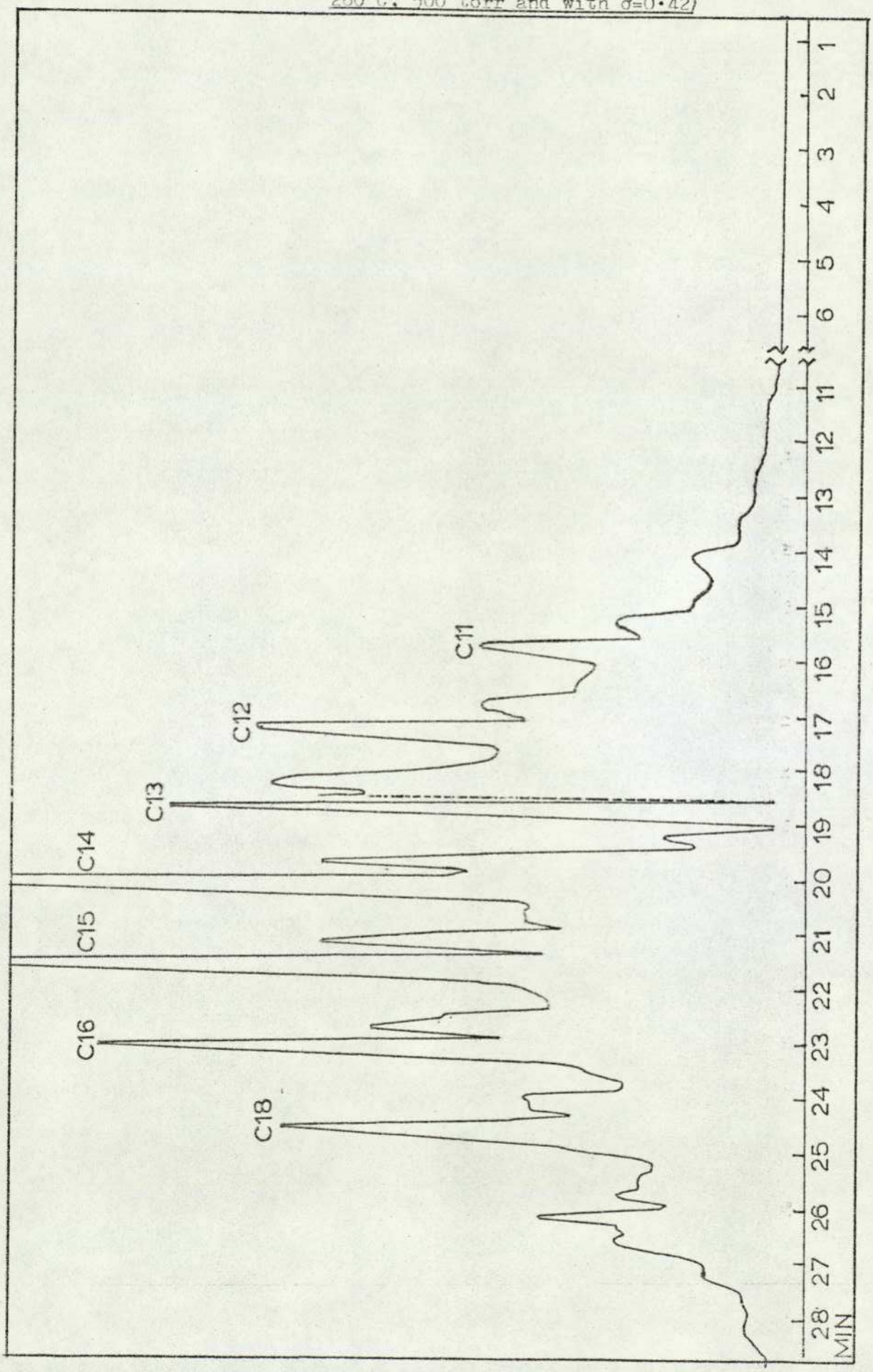

Figure 3·37

Post-cool Flame Product Chromatogram on C20M(Diesel Fuel Oxidation at 280°C, 500 torr and with σ=0·42)

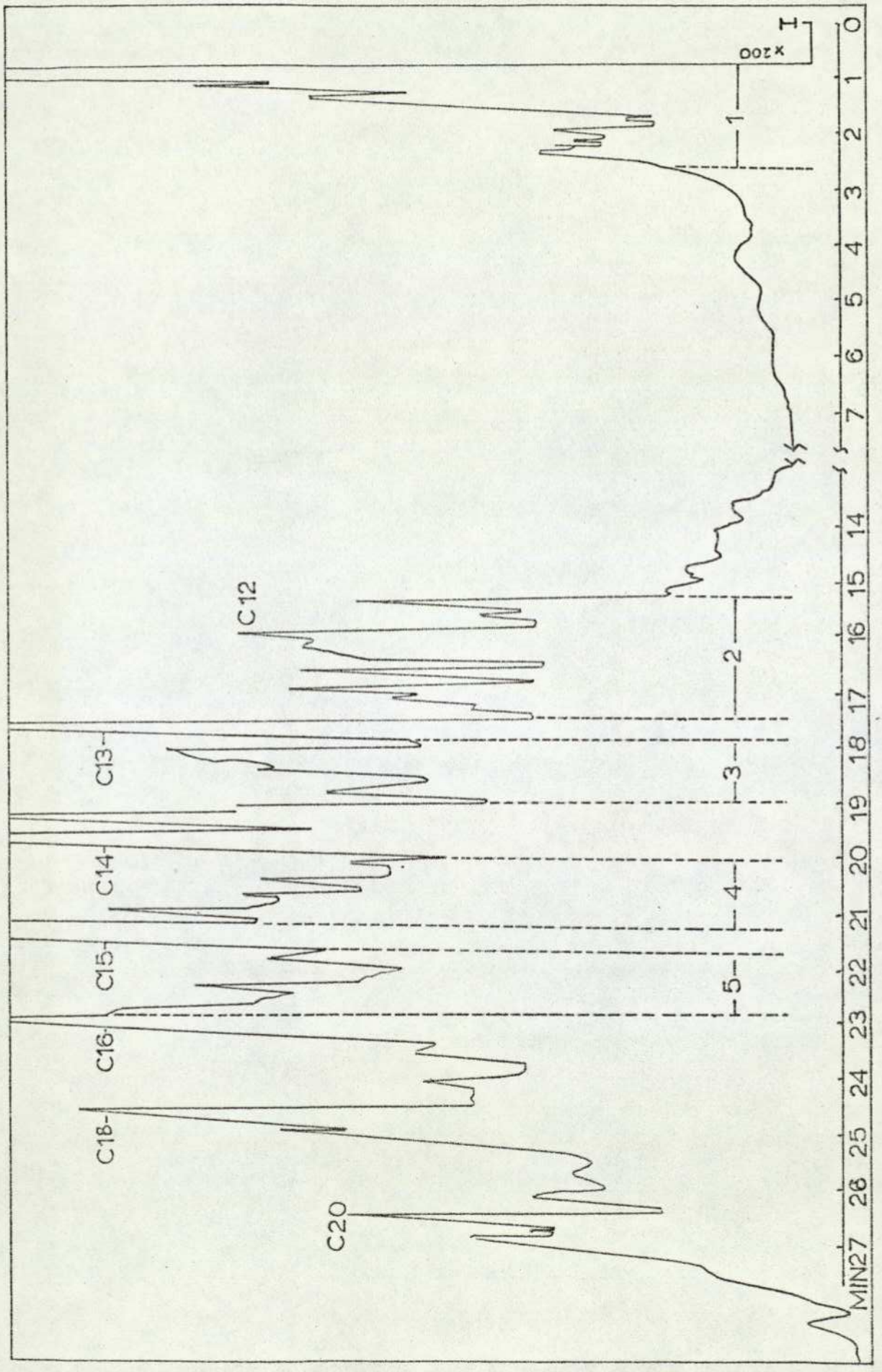

Figure 3·38

Post-hot Ignition Chromatogram on C20M(Diesel Fuel Oxidation at 280°C and 600 torr)

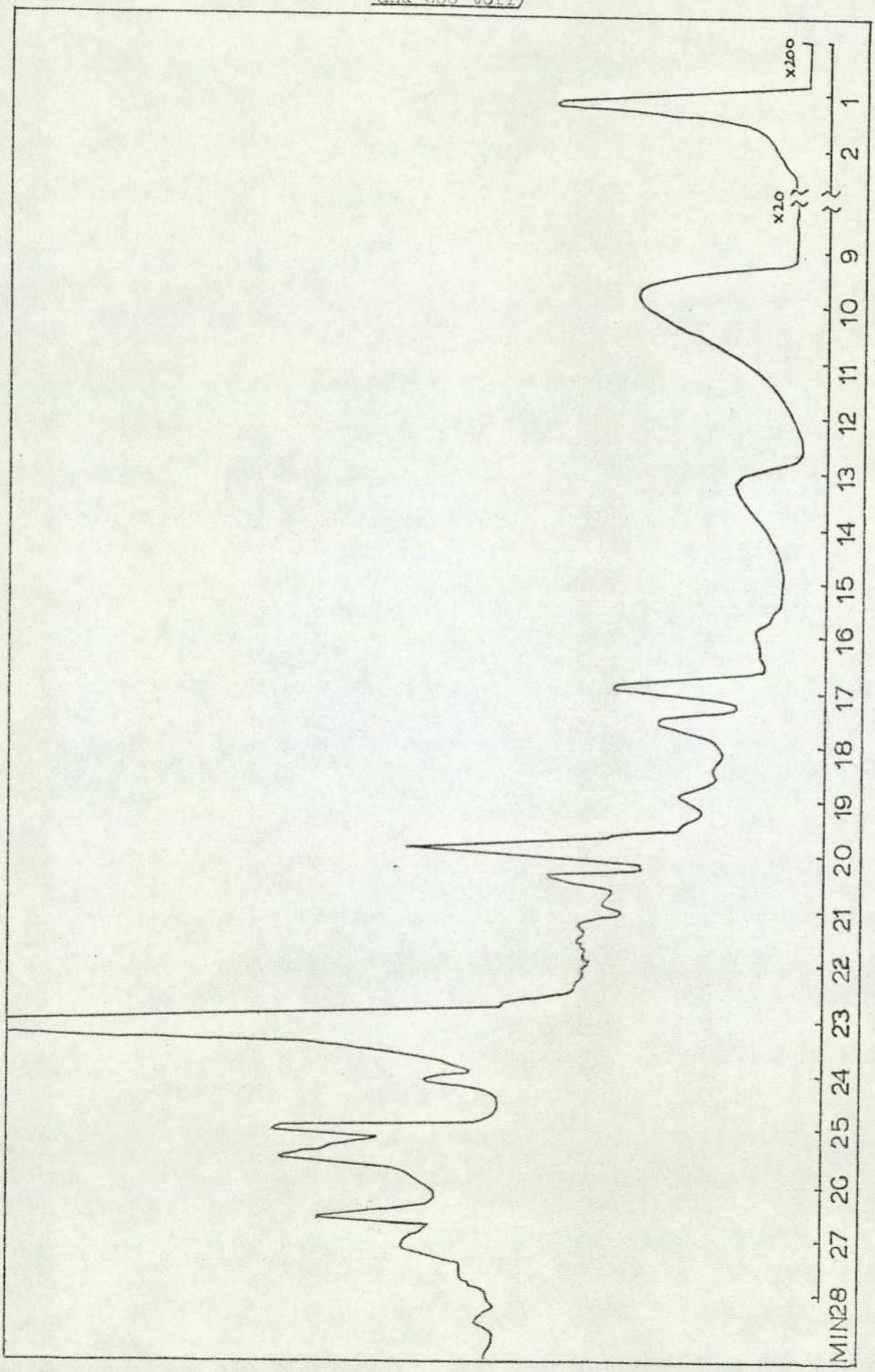

3.5.1.2 Samples Collected in the Chromosorb 102 Traps

Diesel fuel oxidation products trapped on Chromosorb 102, eluted with cyclohexane and injected onto the F11 GC after the eluent had been partially removed under vacuum, produced chromatograms which indicated the efficiency of the trapping process. The cyclohexane solvent peak obliterated the first four minutes of the chromatogram so that the components constituting band 1 in Figure 3.37 were masked. From KI = 1050 to 2000 the chromatograms were similar to those obtained for the gas samples, Figure 3.39. This similarity suggests that the Chromosorb 102 traps were efficient collectors of the oxidation products and that preferential retention of particular chemical groups did not occur, an observation which has been reported by other workers.[108,109]

3.5.1.3 Condensed Gas Phase Samples

Chromatograms of the products collected by condensation in the trap cooled with liquid nitrogen were run on the PE F30 GC using a six metre packed C20M column operating under the conditions listed in Table 2.3.

These chromatograms exhibited greater resolution owing to the larger quantities of individual components present in the samples. There was again partial obliteration of the front of the chromatogram by the solvent peak, nine peaks were nevertheless recorded before the solvent in a chromatogram of post-cool flame products. Figure 3.40 illustrates the improved resolution of this portion of the chromatogram. The retention times for the alkane components are also shown at the bottom of this Figure.

3.5.2 Hexadecane Fuel

Figure 3·39

Post-cool Flame C20M Chromatogram of Diesel Fuel Oxidation Products

Collected in LC Trap

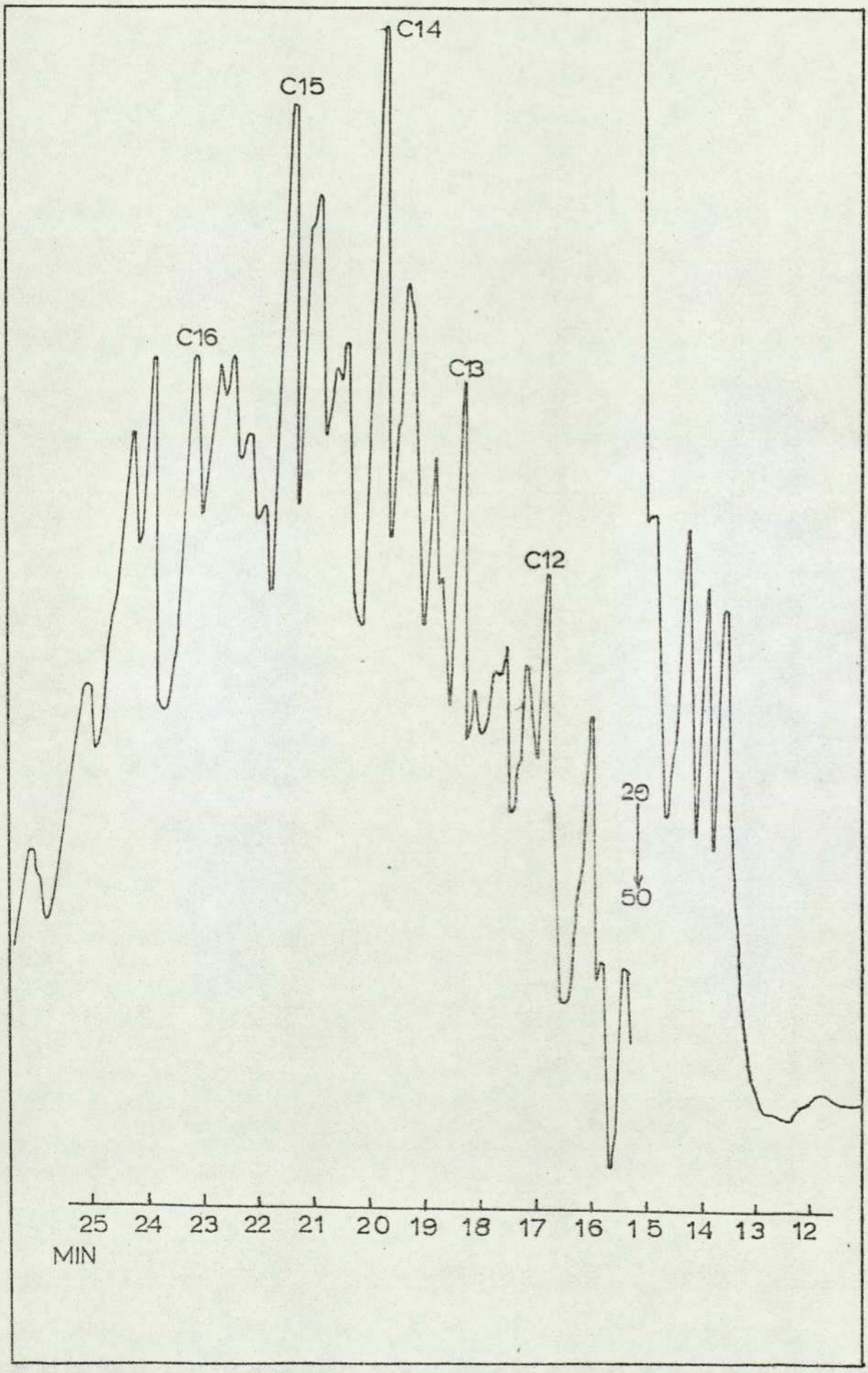

Figure 3·40

Post-cool Flame Products Chromatogram of Diesel Fuel Oxidation Products Collected by Condensation Method

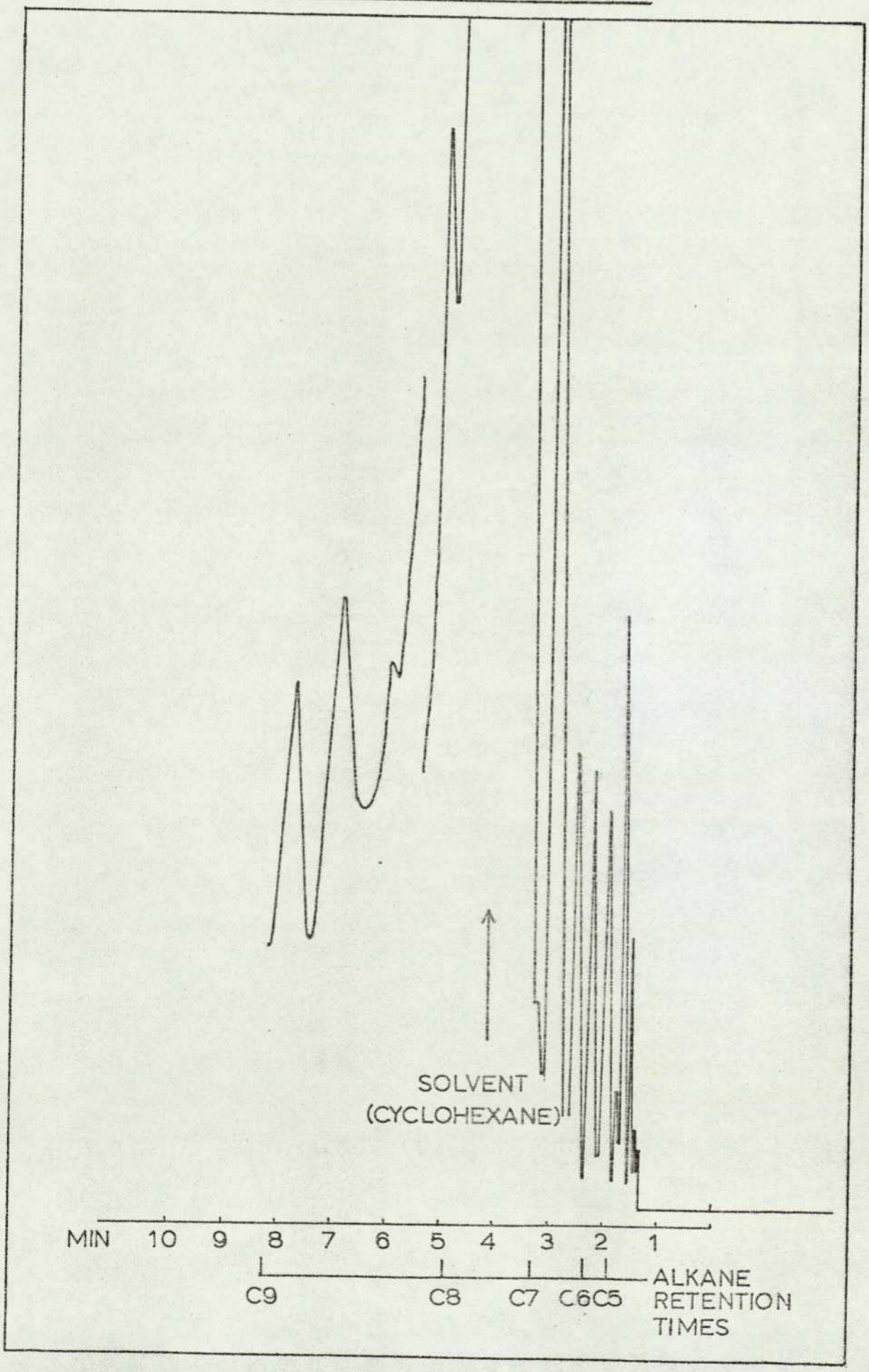

3.5.2.1 Samples Collected in the Gas Phase

The chromatograms of samples of oxidation products of diesel fuel were so complex due to the multicomponent nature of the fuel that the assignment of peaks to the individual components proved to be difficult. In order to resolve this problem, hexadecane was chosen as representative fuel. The reasons for the choice of this compound were its similar kinetic behaviour to diesel fuel and also its molecular attributes mentioned in Section 2.4.

Samples of gas phase products were taken during the oxidation of hexadecane in a manner similar to that used for the oxidation products of diesel fuel. At 280°C and σ = 0.42, hexadecane injected into 500 torr of air produced two cool-flames with high ΔP_1 and ΔP_2 values. Samples were taken throughout the cool flame region. The induction period leading to the first of the cool-flames was shorter than that obtained with diesel fuel under the same conditions ie. 1.4 seconds compared to 3.2 for diesel fuel.

Figures 3.41 and 3.42 show the chromatograms of product samples withdrawn after 1.00 and 1.08 seconds ie. both during the induction period. During this very short time, a large number of oxidation products are rapidly formed. Chromatograms taken after 12 seconds were very similar to those at 1.08 seconds indicating that most of the oxidation products are formed early in the reaction and persist throughout the cool-flame. Attempts were made to take samples which would provide some information regarding the chemical processes occurring between 1.00 and 1.08 seconds, but the practical limitations of the system made this impossible.

Alkane assignments in the product chromatograms were made on the basis of the comparison of retention times of the peaks with those of standard compunds and by "doping" the samples with pure alkane components prior to further GC analysis.

All the oxidation products formed had KI less than 1600 on C20M.

Figure 3·41

C20M Chromatogram of Hexadecane Oxidation Products Recorded 1·0 Seconds After Injection of 5µl of Fuel into 500 torr Air at 280°C

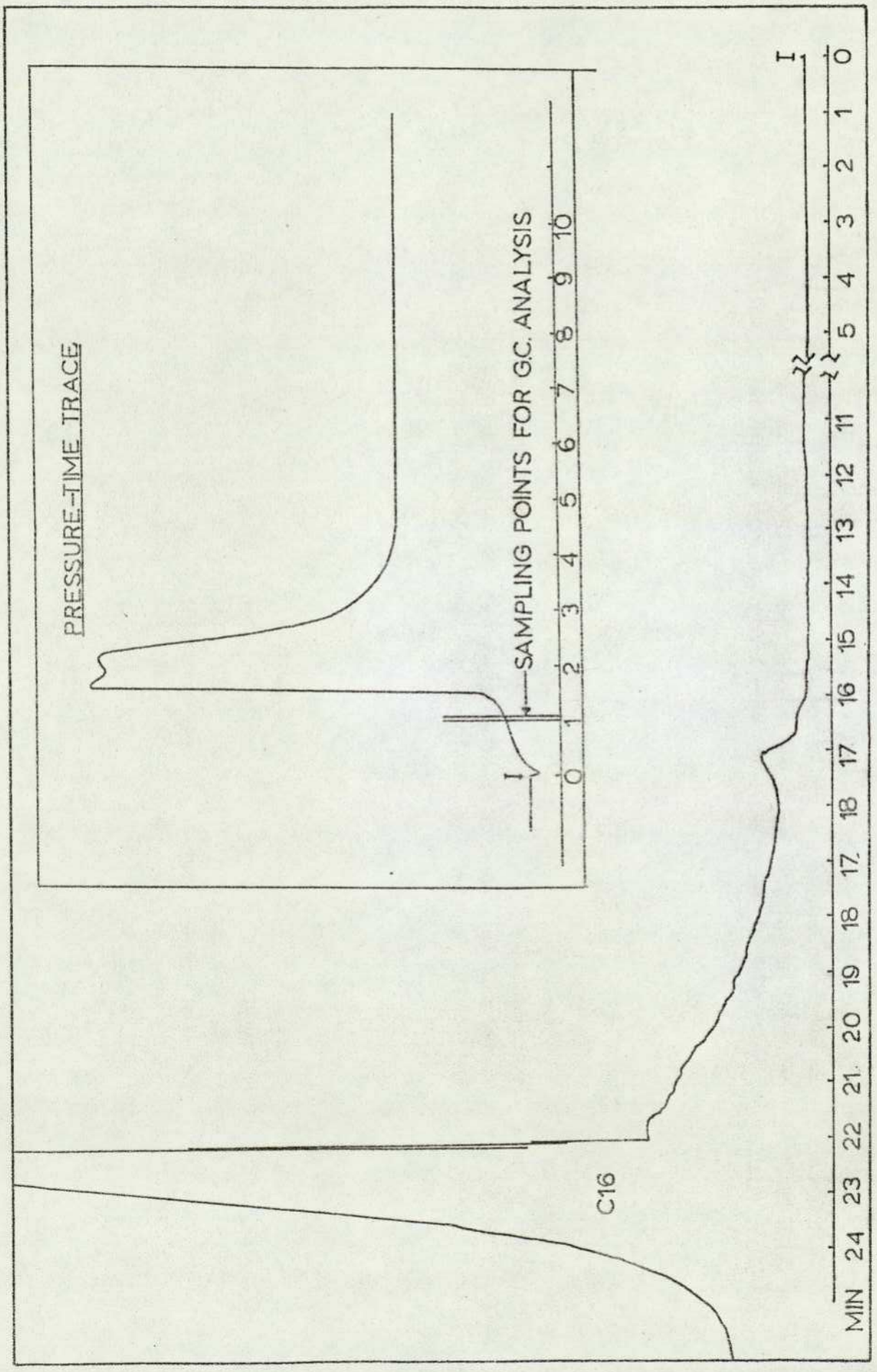

Figure 3·42

C20M Chromatogram of Hexadecane Oxidation Products Recorded 1·08 Seconds After Injection of 5µl of Fuel into 500 torr of Air at 280°C

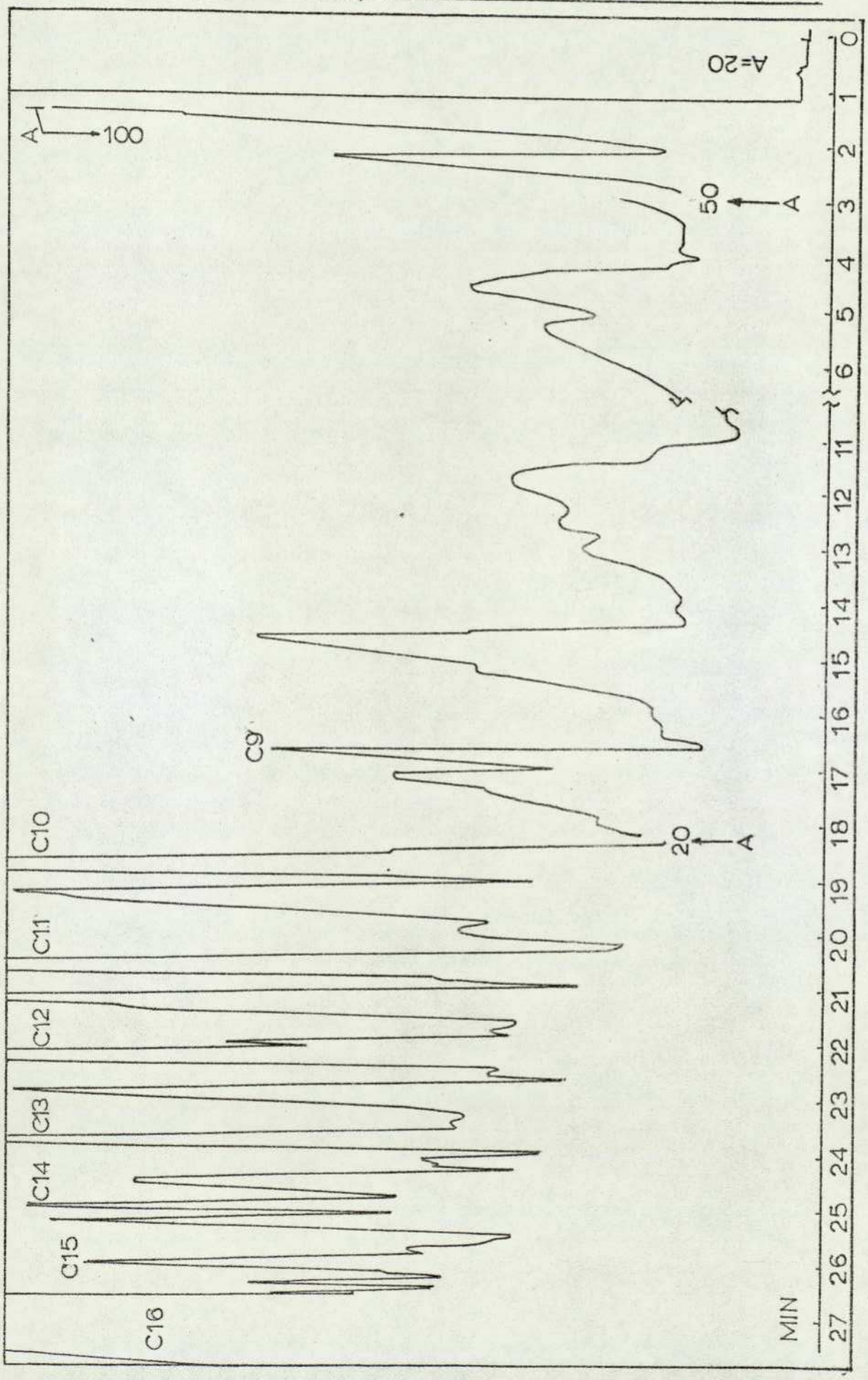

Thus the formation of detectable quantities of compounds such as acetophenone or alkyl-substituted tetralins through cyclisation reactions was precluded.

3.5.2.2 Samples Collected in the Chromosorb 102 Traps

GC analysis of the LC trap eluent containing the oxidation products of hexadecane produced chromatograms which were very similar to those obtained from the gas phase samples. Loss of compound resolution due to reduction in component concentration was evident in all the chromatograms (Figure 3.43). Nevertheless it was possible to make a direct comparison of the gas phase and LC trap sample chromatograms. The efficiency of the LC trap procedure was again confirmed since compounds with KI greater than 500 were present in the chromatograms in similar proportions to those in the gas phase samples. Components of lower KI were obliterated by the cyclohexane peak.

3.5.3 n-Butylbenzene Fuel

3.5.3.1 Samples Collected in the Chromosorb 102 Traps

With the samples taken from the LC trap during the oxidation of n-butylbenzene as described in Section 3.2.3.3 the combined eluent fractions from each trap were partially distilled under vacuum. The concentrated sample solution was then analysed by GC and Figure 3.44 shows the number and distribution of the component peaks. The number of peaks recorded was much smaller than for either diesel fuel or hexadecane post-cool flame oxidation samples, being more comparable with the number found for the ignition samples from diesel fuel.

Figure 3·43

Post-cool Flame C20M Chromatogram of Hexadecane Oxidation Products Collected in LC Trap

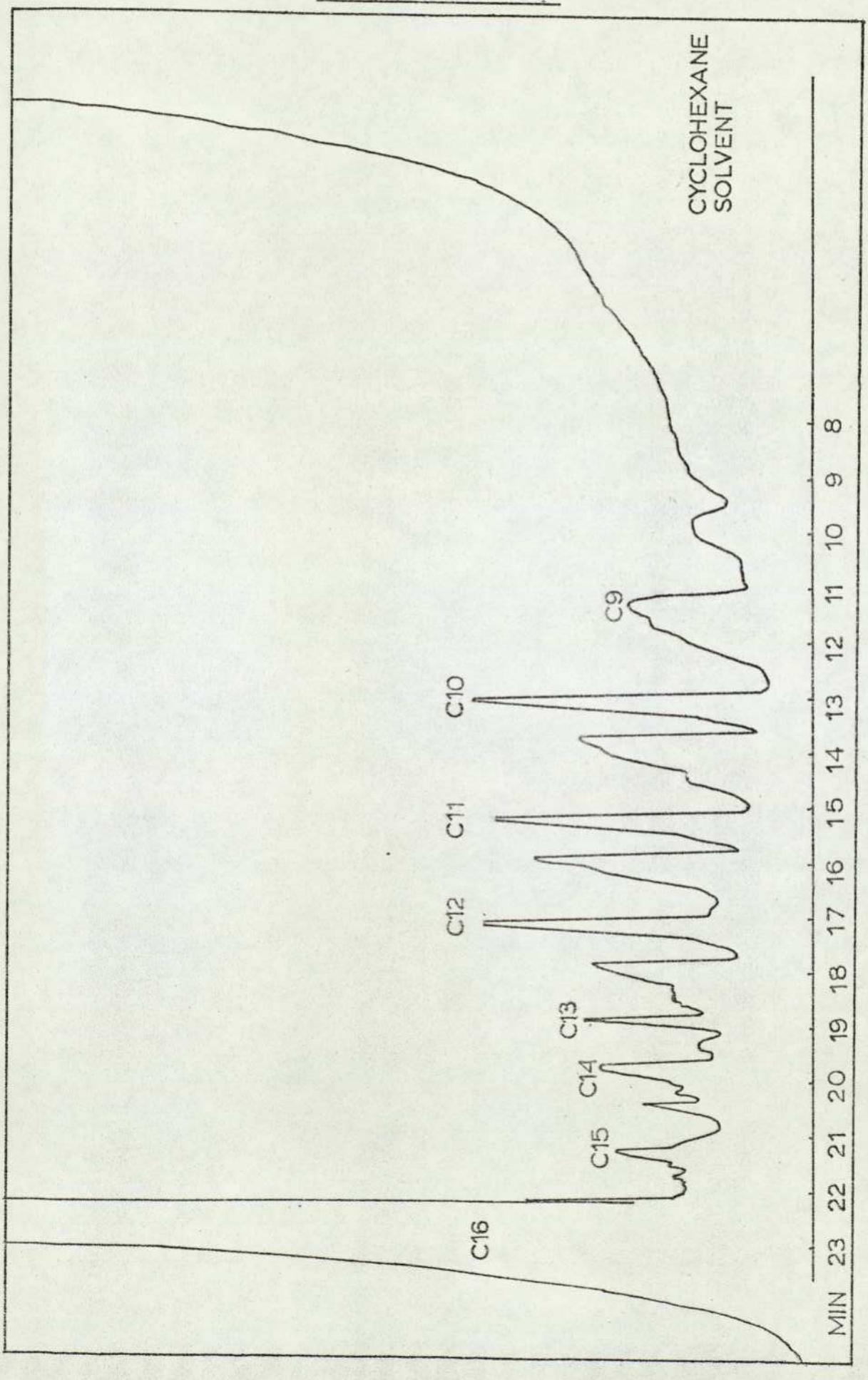

Figure 3·44

Post-cool Flame C20M Chromatogram of n-butylbenzene Oxidation Products Collected in LC Traps

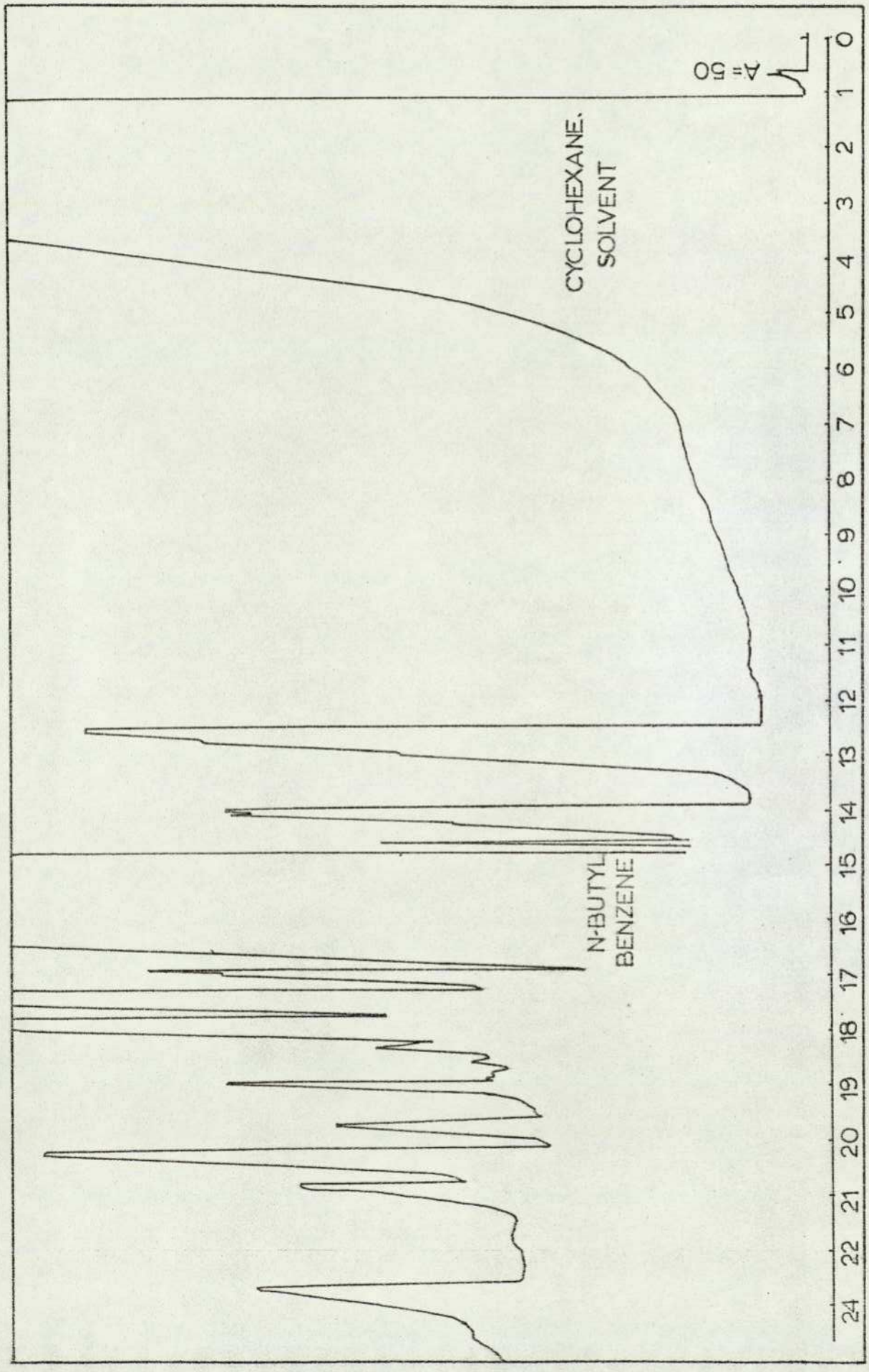

3.5.4 Diesel Engine Exhaust Samples

3.5.4.1 Samples Collected in the Chromosorb 102 Traps

In order to compare the gas chromatograms of the LC trap oxidation products from the static vacuum apparatus with those of diesel engine exhaust, samples were taken from a diesel engine for analysis. The engine was operating at 800 rpm with 8 cu mm of fuel injected per cylinder. The fuel pressure was recorded as 215 at. and the timing was 15° DNIT. Figure 3.45 shows the most important section of the chromatogram obtained. Sample doping with pure alkane components assisted peak assignment.

Figure 3·45

C20M Chromatogram of Diesel Engine Exhaust Collected in LC Trap

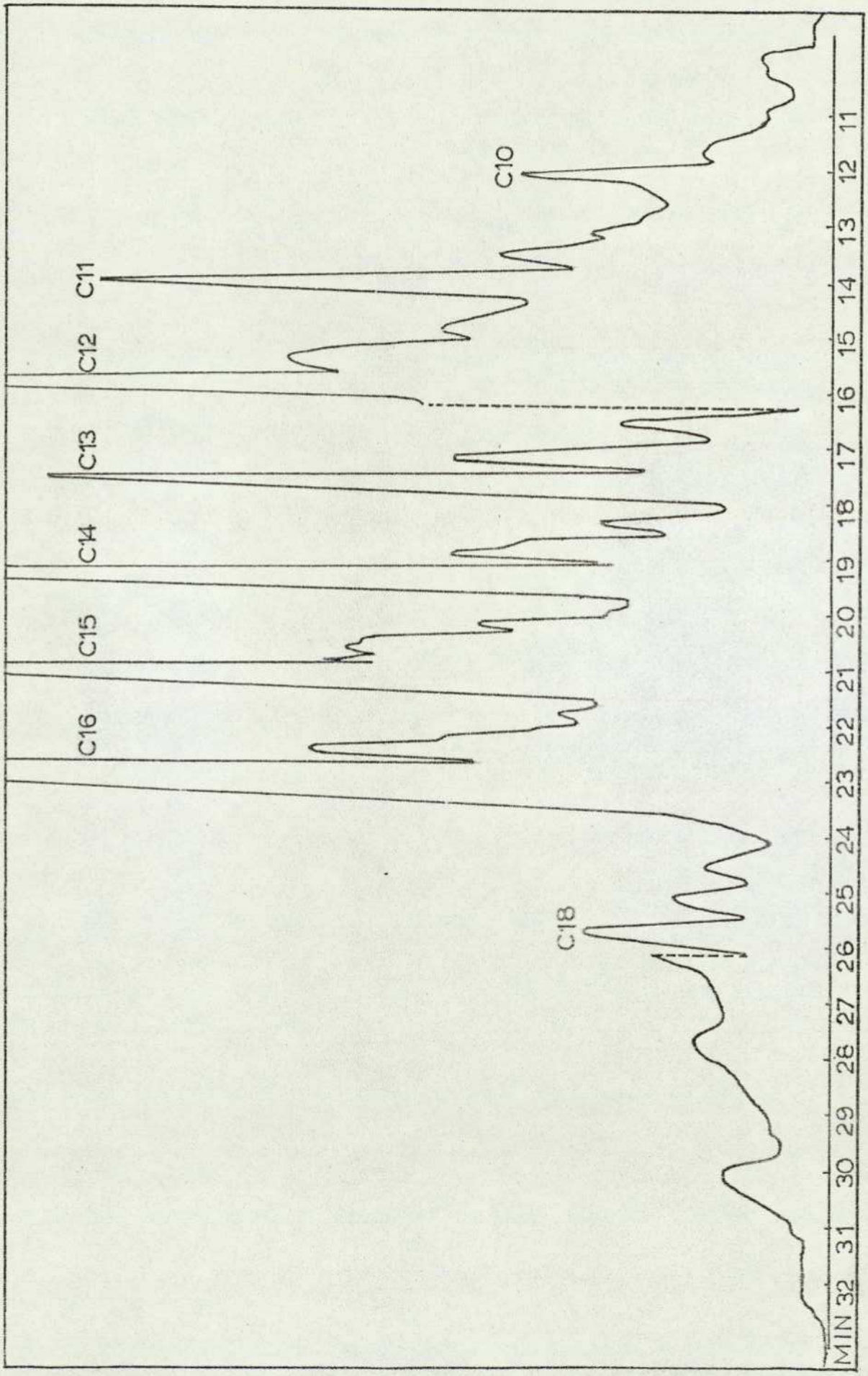

SECTION 4

DISCUSSION

SECTION 4

4.1 The Composition and Combustion of Diesel Fuel

In the petroleum industry the gas-chromatographic analysis of a particular diesel fuel complements physical analysis. In the present work, chromatograms obtained for the fuel were compared with those obtained for the products after the fuel had been oxidised. The chromatographic and other analytical results shown in Figures 3.1-3.6 indicate the diversity of the components to be found in diesel fuel. The extremely complex nature of the combustion process is of course predetermined by the multicomponent nature of the fuel as well as by the mechanisms of fuel injection and mixing in the combustion chamber.

A static vacuum system was chosen for the oxidation experiments in order to obtain some degree of control over the conditions governing the combustion process. The use of such systems for the study of hydrocarbon oxidation is well established, although their application to fuels with a carbon number greater than ten has been very limited.

It was apparent at the outset of this work that results of a quantitative kinetic nature would only be meaningful if the equilibrium condition of temperature, pressure and homogeneously dispersed reactant concentration were obtained prior to reaction. Under such conditions it may be assumed that the fuel undergoing oxidation is representative of a combustion microcosm existing somewhere in the spatial and temporal coordinates of the diesel engine combustion chamber. The considerable pressure differences existing between the real and laboratory systems would not be expected to influence the oxidation mechanism to any significant extent.[21] However, since the regions of the ignition diagram which were of greatest interest were those where the induction period was less than six seconds, the attainment of equilibrium conditions prior to reaction could not be assumed. Nevertheless, the results obtained are useful in a qualitative sense, even though the absolute values of the kinetic parameters are only relevant in the context of the particular system used.

4.1.1 Fuel Vaporisation and Preflame Activity

Figures 3.8 and 3.9 show the effects produced by the endothermic vaporisation of the liquid fuel on the pressure inside the bomb. The extent to which the equilibrium of the system is perturbed was discussed in Section 3.

Cylinder studies of diesel engine combustion have included the examination of the cooling effect caused by fuel vaporisation in the context of investigations into heat release. One of the first comprehensive studies into heat release was reported by Austen and Lyn.[48] Figure 4.1, produced as part of their study, shows a heat release profile of a direct injection engine at two engine speeds. The cooling effect of the fuel vaporisation, particularly at low speed, is quite marked. In a more recent study, Hoelzer[120] has defined two phases of heat release, phase 1 resulting primarily from non-luminous premixed combustion which involves a significant portion of the fuel and phase 2 representing the light-emitting diffusion-controlled process. Austen et al[48] recognise also a third phase (see Fig 4.1) and add that the first phase lasts for only a few crank angle degrees (ca 5°CA), while the diffusion-burning phase continues for ca 40°CA, and constitutes the main heat-release period. These two periods together account for 80% of the total heat release. The third phase, defined by Austen and Lyn,[48] corresponds to the tail in the diagram, in which a small but distinguishable rate of heat release persists throughout the expansion stroke and produces the remaining 20% of liberated heat. These observations are summarised in Figure 4.2 which also indicates the prevailing mechanism of combustion in each of the phases defined. Austen et al[48] were able to correlate the amount of fuel injected during the ignition delay period with the rate of pressure rise and thereby show that the portion of fuel undergoing premixed combustion significantly influences the shape of the cylinder pressure diagram.

Garner et al,[121] from their studies have been able to produce a diagram (Figure 4.3) which shows the differential cylinder pressure profile

Figure 4·1

Analysis of Heat Release : Effect of Engine Speed

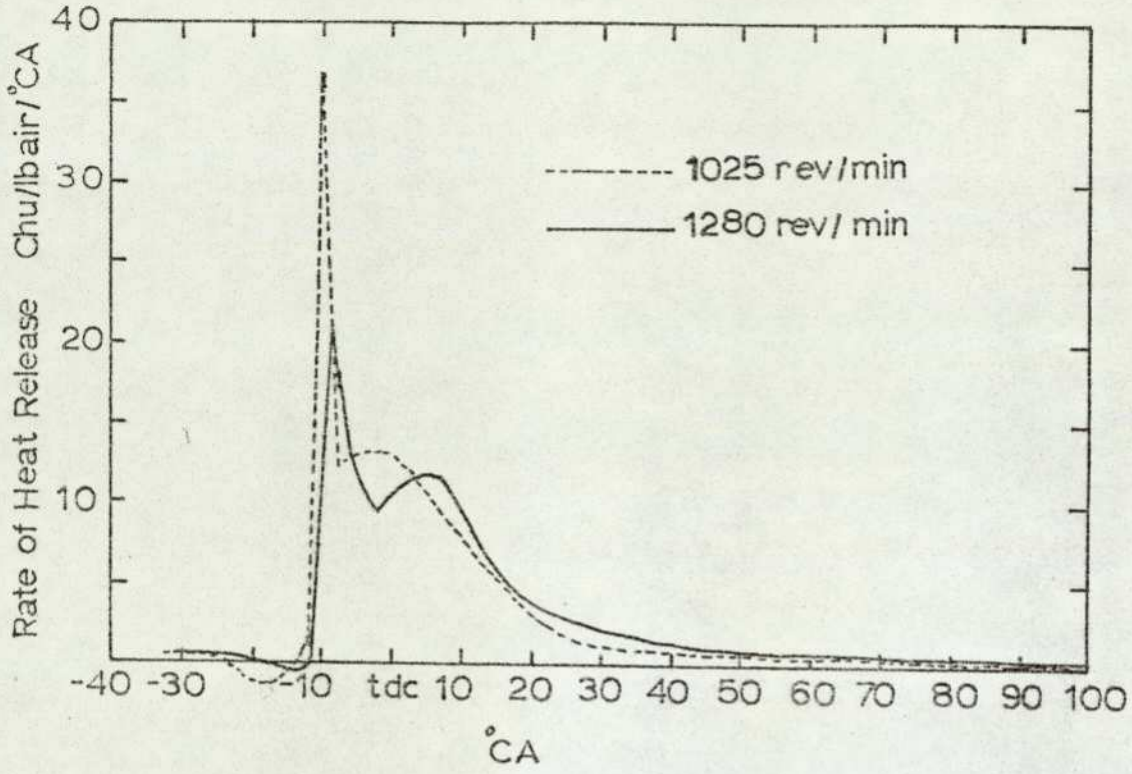

Figure 4·2

The Events which Determine the Rate of Heat Release

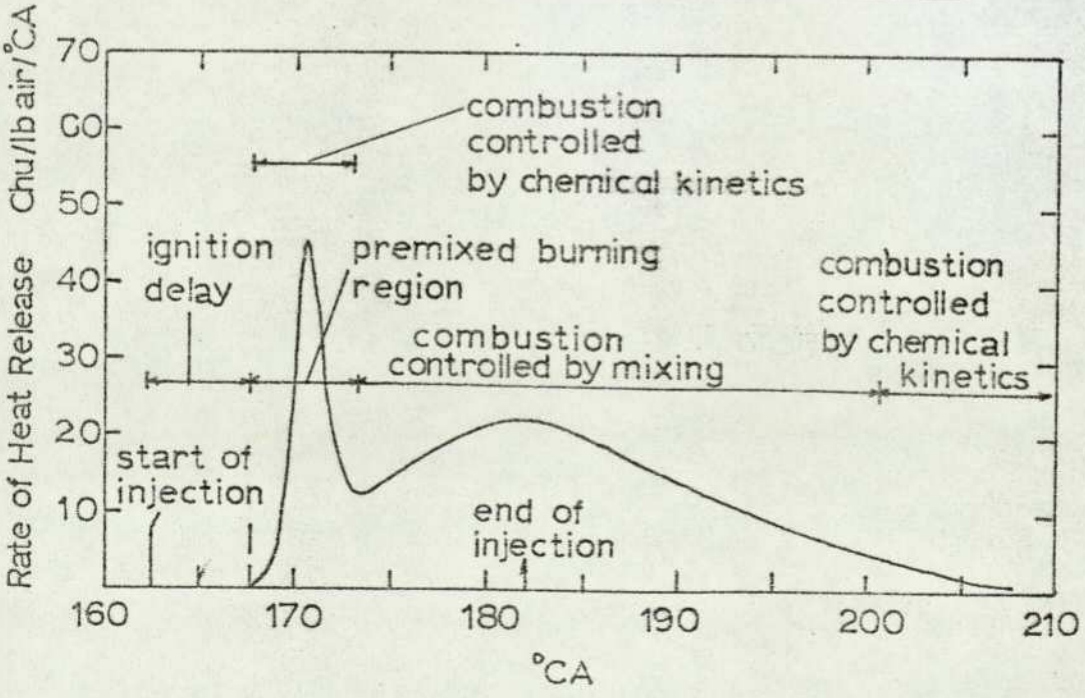

Figure 4·3

Preflame Reactions During the Initial Stages of Diesel Fuel Combustion in an Engine[12]

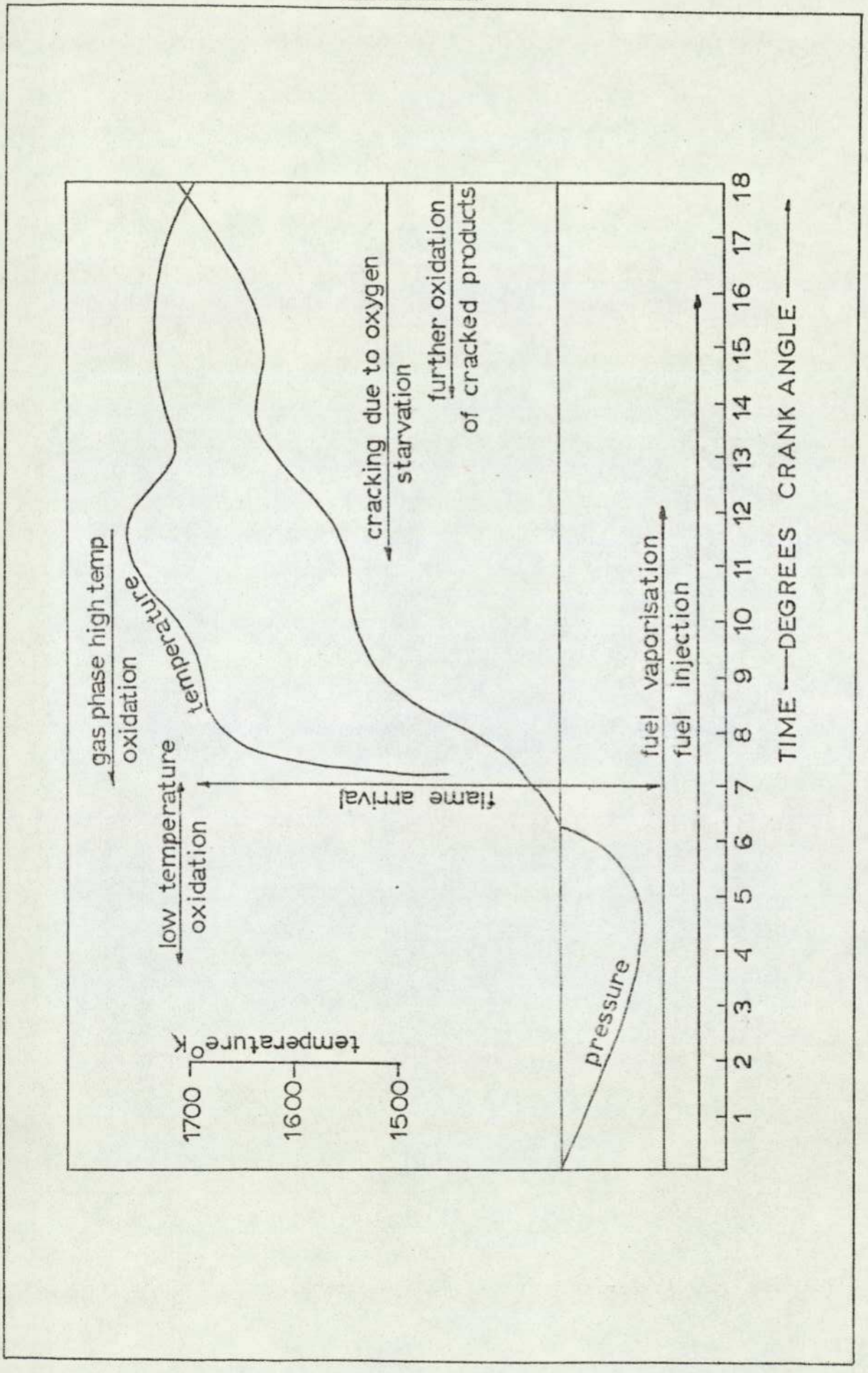

with no engine compression included. The cooling effect of the fuel vaporisation is clearly shown and the oxidation and pyrolysis reaction occurring throughout the different periods are indicated. Fuel injection starts at zero on the time scale and continues for 16°CA. Maund[121], in a discussion of the preflame reactions, states that during the low temperature oxidation phase, cool-flames accompanied by the formation of high concentrations of aldehydes and peroxides have been recorded in engine tests[121-127]. These observations are particularly important, since they confirm that the preliminary oxidation of diesel fuel under engine-operating conditions is a degenerately branched chain reaction involving aldehydic and peroxidic species. Further experimental evidence, confirming that the chemical processes occurring during the delay period are of the chain branching cool-flame type, is provided by Sokolik[128], Boyce[129] and Garner[127]. These workers have shown that the flame development can be greatly influenced by the addition to the reactants in the combustion chamber of fuel fractions exhibiting cool-flame characteristics. These experiments produce similar effects on the combustion mechanism of a spark-ignition engine[126].

Boyce[129] studied the combustion of diesel fuel in a flow reactor and compared the results obtained with those produced for the oxidation of heptane under similar conditions. Spectroscopic techniques confirmed the previously reported similarity[123,124] between the preignition reactions which occurs with these two fuels; the spectra recorded were very similar and exhibited a strong emission band corresponding to HCHO. With diesel fuel, the emission was accompanied by substantial quantities of white smoke which became more dense and acrid as the reaction progressed. The exhaust odour produced by the flow reactor was similar in most respects to that emitted by a diesel engine, a fact which Boyce[129] attributed to high concentrations of aldehydes. The formation of soot at low level temperature was found to decrease as the reaction temperature increased. Moreover the preignition glow was seen to increase in intensity with increasing cetane number or

paraffinic content of the fuel. From these observations, Boyce concluded that an increase in the paraffinic content of diesel fuel led to increased ease of ignition and smoother, more efficient engine operation. However, a fuel which is too reactive produced engine knock if the production of aldehydes, particularly formaldehyde and acetaldehyde, was superseded by by the formation of peroxides in the early stages of reaction. The subject of aldehyde and peroxide involvement will be discussed in more detail in Section 4.2.1.

4.1.2 Oxidation Kinetics

4.1.2.1 Diesel Fuel

Figures 3.11A and B show the pressure change and induction period data obtained during the oxidation of diesel fuel at 250°C and under increasing equivalence ratio. It is evident that, as the concentration of the fuel increases, ΔP_1 and ΔP_∞ increase and the induction period decreases. Similar trends were obtained at 280°C and 295°C (Figures 3.12 and 3.15 - 17). These observations are consistent with the basic kinetic principles outlined in Section 1.4.4.2. Assuming that the gases behave ideally, the magnitude of the pressure rise, ΔP_1, in a constant-volume reactor is given by the equation;

$$\Delta P_1 = Po\left(\frac{\bar{n}T}{noTo} - 1\right)$$

where Po, To and no are the pressure, temperature and molecular concentration of the unchanged mixture and $\bar{n}$ and T are the mean molecular concentration and temperature at the instant when the pressure rise is ΔP_1.

When the extent of the reaction is small, ΔP_1 is largely due to the exothermic nature of the reaction and consequently after the reaction has ceased, ΔP_∞ is not much greater than Po. As the concentration of fuel increases, at a constant initial pressure, the number of fragmentation products (n) increases leading to an increase in both ΔP_1 and ΔP_∞. If however,

Po is sufficiently high, the passage of a cool flame may be followed by a hot flame, giving a pressure time record similar to that shown in Figure 3.10(d). The rapid, non-isothermal increase in pressure during the ignition process is followed by an exponential decrease in pressure until the contents of the reaction vessel reach equilibrium with their surroundings. The final pressure change, ΔP_∞ , is considerable, showing that a substantial increase in molecular concentration has occurred. It can be seen from Figure 3.11A that when $\alpha = 0{\cdot}6$ a hot ignition occurred. The conditions prevailing were such as to preclude a time interval between ΔP_1 and the hot ignition; under these conditions ΔP_1 was just discernible as a shoulder on the hot ignition pressure curve.

The induction period leading to a two stage ignition is divisible into two parts, $\tau_{c.f.}$ and $\tau_{h.i.}$, where $\tau_{c.f.}$ is the time between injection and the first cool flame maximum and $\tau_{h.i.}$ is the time between the cool flame maximum and hot ignition. At constant temperature, $\tau_{c.f.}$ decreases with the initial pressure, Po, according to the equation:

$$\tau_{c.f.} = k^1 Po^{-n} + c^1$$

where n is positive and k^1 and c^1 are constants. This equation is found to be applicable at both high[21,130] and low pressures.[21,128,131]

The effects of Po and To on $\tau_{h.i.}$ are more complex since these quantities influence not only the second stage process itself but also the cool-flame intensity and thus the actual values of pressure and temperature at which the second stage ignition process occurs.[132] Recent studies[133] of the oxidation of isobutane have indicated that the occurrence of a hot ignition is dependent on the attainment of a critical concentration of hydrogen peroxide at a critical temperature. These studies indicate that hydrogen peroxide is the principal branching agent for this particular system, and that the subsequent decomposition of this compound results in an acceleration of the reaction to hot ignition. The rate equation governing this process therefore takes the form :-

$$\text{Rate} = Ae^{-E/RT}\left[H_2O_2\right]^a$$

The relationship between $\ln \tau_{cf}$ and $1/T_o$ has often provided a method of estimating the 'effective activation energy', E_A, for the cool-flame process. In the case of many fuels, this plot is linear over a considerable range of temperature and the values of E_A obtained correlate quite well with their octane numbers. In other cases, however, the plot of $\ln \tau_{cf}$ vs. $1/T_o$ is non linear and in view of the chemical complexity of the overall cool-flame process, the precise significance of E_A is not clear.

The effect which the addition of an inert diluent gas to the reactants has on the induction period is shown in the Figure 3·14. It can be seen that τ_{cf} was reduced slightly by the addition of nitrogen when the total pressure was below 300 torr; at higher pressures, however, the effect of the diluent on the induction period was virtually insignificant. Generally the addition of an inert gas, to the reactants in an uncoated vessel maintained within the low temperature region, does not affect the maximum reaction rate, although τ_{cf} is often reduced,[42] eg. as in propane[134] and isobutane[135] oxidation. The data trends shown in Figure 3·14 can be explained quite simply in terms of a degenerate chain-branching mechanism. At low pressure, ie: ca 300 torr, radical destruction occurs primarily by heterogeneous termination after diffusion of the radicals to the vessel walls. Addition of an inert gas will retard such diffusion and the radicals thus have a longer effective lifetime during which they can be involved in a chain-propagation step leading eventually to a cool-flame. Under these conditions, τ_{cf} is decreased. At higher pressures, homogeneous termination as a result of radical-radical combination is important. Under these conditions, the addition of inert gas has a smaller effect, unless the radicals have a restricted number of degrees of freedom in which case the inert gas will act as a third body for energy dissipation and hence increase the number of effective termination

reactions. Thus, for example, Figure 4·4 shows the results obtained[135] when four different inert gases were added to a mixture of isobutane and oxygen at 286°C. It is evident that helium has the smallest effect on the induction period, while carbon dioxide exerts the greatest influence. These observations are in accordance with the effectiveness with which the inert gas molecules act as third bodies in homogeneous termination reactions. It can be seen from Figure 3·14, that above 300 torr, the addition of diluent gas did not significantly affect the induction period, which suggests that the termination reactions were not greatly influenced by the presence of an inert gas.

The ineffectiveness of nitrogen in lengthening the induction period precluded this as a means by which the reaction could be retarded sufficiently to make possible the collection of kinetic data under equilibrium conditions.

Figure 3·20 shows the exponential decrease of T_{cf} with initial temperature at various equivalence ratios. At 310°C the reaction started almost before injection was complete, even with very lean mixtures, ie: σ = 0·33. Since complete premixing of the fuel with the oxidant prior to reaction could not have occurred, the continued collection of kinetic data was considered to be of little value.

4·1·2·2 Hexadecane Fuel

A comparison of Figure 3·19 with Figures 3·15 to 3·17 shows that the variation of ΔP_1 and ΔP_{∞} with σ obtained for hexadecane fuel were similar to those for diesel fuel. It was observed throughout the oxidation experiments, that under the same initial conditions of Po, To and σ, hexadecane was more reactive than diesel fuel as evidenced by the much shorter induction periods for the alkane fuel. However, the multiplicity of cool-flame propagation observed with diesel fuel, (see Figure 3·18) was not observed with hexadecane, a maximum of only three cool-flames

Figure 4·4

Effect of Four Different Inert Gases on the Induction Period[135]

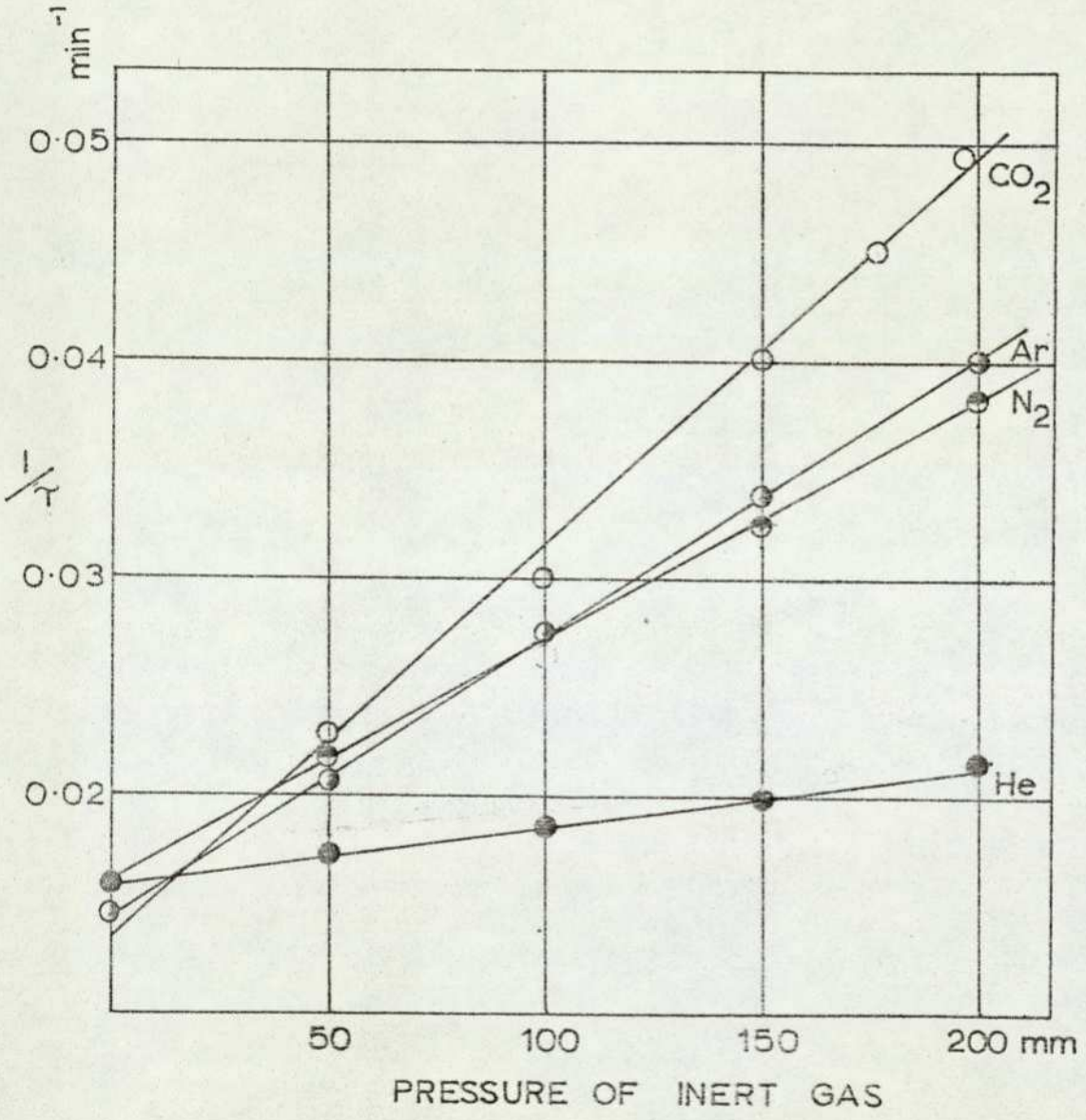

75mm Isobutane + 400mm Oxygen at 286°C

being recorded for the alkane fuel. This may be a reflection of the multiplicity of branching agents obtained from the many components in diesel fuel compared with the relatively few obtained from a single hydrocarbon.

4·1·2·3 n-Butylbenzene Fuel

The kinetic data obtained for n-butylbenzene confirmed the reported stability of this aromatic hydrocarbon, since the lowest temperature at which the measurable oxidation occurred was 310°C. A broad cool-flame was produced after a relatively long induction period (Figure 3·21), even with stoichiometric fuel to air ratios, and the value of dP/dt for all stoichiometries was smaller than those for other fuels. A comparison of the reactivities of butylbenzene, hexadecane and diesel fuel under the same initial conditions confirms that the ignition of diesel fuel is controlled primarily by the most easily oxidisable components, ie: the alkanes. However, under cool-flame conditions partial oxidation of the aromatic fraction will occur, since the exothermicity of the oxidation mechanism may give rise to transient temperatures in the range 360 to 460°C.

4·2 The Formation of Odorants During the Oxidation of Hydrocarbon Fuels

Before the results of the liquid chromatographic analysis of the oxidation products are discussed, it is important to consider whether the Arthur D. Little odour assessment technique is a reliable means of assessing the odour produced by widely different fuels. ADL [106,107] have investigated the effects of fuel composition on the correlation between the concentration of LCO and the exhaust odour intensity at 1000 : 1 dilution. The fuels used ranged from Kerosene (16% aromatic, s.g. 0·808, 90% B.Pt 235°C) to No2 diesel fuel 61339, (37% aromatic, s.g. 0·86, 90% B.Pt 311°C) and included a special low aromatic fuel, Soltrol 200 (1·3% aromatic, s.g. 0·78, 90% B.Pt 257°C). There was a good correlation between the predicted and the observed exhaust odour intensity for all the fuels tested, despite the widely different odour quality produced by Soltrol 200. It appears therefore, that the ADL odour assessment technique is applicable to a wide range of engines, fuels and operating conditions,- a conclusion which has been substantiated by more recent experiments.[136] The three main classes of hydrocarbons which constitute a standard blend of diesel fuel are the alkanes, alkenes and aromatics. Although the composition of diesel fuel varies considerably, depending on its origin and blending, the aliphatic fraction is always predominant, usually forming about 70% of the fuel volume. It is not surprising, therefore, that the aliphatic fraction exerts a profound influence on the kinetics of the fuel oxidation process. Several workers [123,124] have commented on the similarity between the combustion phenomena observed with a straight-chain hydrocarbon, often heptane, and diesel fuel. In order to compare the kinetic and analytical results obtained for diesel fuel with those of a pure alkane, hexadecane was selected in this study, since its molecular weight and carbon to hydrogen ratio were similar to the 'molecular weight' and C/H ratio of diesel fuel.

4.2.1 Hexadecane Fuel and Alkane Oxidation

Figures 3.25 and 3.29 show the analytical and kinetic data obtained during the oxidation of hexadecane at two temperatures, 280 and 295°C, but at the same initial pressure, 500 torr and equivalence ratio, 0·42.

The LCA and LCO analyses performed during the oxidation at these two temperatures indicated that the mechanism of odorant formation had changed with temperature. At 280°C, the LCA level increased steadily throughout the induction period, but unlike the LCO fraction, did not decay rapidly with the passage of the cool-flame. At 295°C, however, the LCA concentration fell during the passage of the cool-flame, while the LCO level rose to a maximum. These trends differed from those observed for the other fuels in which the LCA and LCO fractions displayed similar behaviour during the oxidation process. It is evident that before any firm conclusions can be drawn, further investigation of this fuel-oxidant system is necessary, including detailed chemical analysis of the products formed. However, certain aspects relating to the formation of LCA and LCO during the cool-flame processes in these studies are worthy of comment.

It is evident from the analytical data recorded that a close link exists between the cool-flame mechanism and the formation of LCA and LCO. The important ramifications emanating from this observation are those relating to the nature, origin and mechanism of formation of the odour components. These deductions evolve from a knowledge of alkane oxidation, the relevant aspects of which are described later.

After passage of the cool-flame, the levels of the two odour fractions remained fairly constant under the conditions of temperature and stoichiometry prevailing in the system. These conditions approximate to those which exist in the exhaust pipe of a diesel engine operating under mid-speed, mid-load modes. The stability of the LCA and LCO fractions suggests therefore, that, after formation, the two odour fractions are little affected by their passage through the exhaust system; i.e. the mass of LCA and LCO formed in the combustion chamber survives almost intact to be

emitted into the atmosphere. After emission, the odorants are cooled and diluted in the ambient atmosphere and are thus rendered even more stable. In order to prevent the emission of these partially oxidised compounds, two approaches to the problem are envisaged. The first involves afterburner treatment of the exhaust gases using catalysts to complete the oxidation process. The second involves improving the fuel-oxidant mixing process by various design modifications in order to increase the amount of fuel subjected to oxidation via the hot ignition mechanism. Evidence for the subsequent reduction in LCA and LCO under these conditions is shown in Figure 3·25. This Figure records the odour levels of samples collected during hot ignition which occurred under essentially cool-flame conditions due to a reduction in the evacuation time between fuel injections. Both the LCA and LCO fractions were extensively reduced during the hot ignition, an observation frequently recorded during the course of these studies with other fuels. It is evident that the increase in temperature accompanying hot ignition leads to destructive oxidation of the odorants formed during the first-stage reactions.

From their extensive analytical programme, ADL concluded that the LCA fraction consisted of aromatic molecules, the majority of which originated from unburnt fuel. Alkanes, including hexadecane, and alkenes do not absorb U.V. radiation at 254 nm and hence do not contribute to the LCA peak. It would appear, therefore,that in the present study the LCA fraction must consist of aromatic molecules formed during the oxidation process and not unburnt fuel. Aaronson and Matula,[137] in their study of the oxidation of hexadecane in a rapid compression machine, identified benzaldehyde, phenol, 2-5, dimethylpiperazine, cyclopentanol and γ-valerolactone in the products. Although some of these compounds contain oxygen and therefore cannot be LCA components their identification indicates that cyclisation reactions can lead to the formation of significant quantities of homocyclic, heterocyclic and aromatic molecules; moreover, some compounds like 2-5, dimethylpiperazine do not of course contain oxygen.

Tables 3·6 and 3·11 contain the TIA values corresponding to the LCO levels recorded, while Figure 4·5 shows the odour / analytical data collected by ADL,[107] which relates the TIA value to the concentration of LCO (μg/l) in diesel engine exhaust. It can be seen that the measured TIA values range from 0·8 to 2·2 on a scale which extends from)(, (threshold) to 3, (strong). Odours which have an intensity greater than 3 are not differentiated on this scale. However, most of the TIA values obtained in the oxidation experiments had values greater than 3. The very high LCO concentrations which correspond to these TIA values originate from the partial oxidation of fuel under conditions which preclude the occurence of a hot ignition. Although the LCO is formed by similar preignition reactions in the diesel engine, the hot ignition which occurs during each complete combustion cycle destroys some of the LCO formed, which results in lower TIA values than those recorded in these studies. Of course, as mentioned above, when a hot ignition occurred in the bomb the LCO fraction was considerably reduced and sometimes completely destroyed.

The rapid rate of formation of the LCA and LCO components during the first stage of the oxidation reactions is indicated by the initial gradients of the concentration vs. time plots for each odour fraction, Figures 3·25 and 3·29. A further indication of the rate of formation of each fraction is given by Figures 3·41 and 3·42, which show the chromatograms of vapour phase samples taken during the oxidation experiments.Thus, for example, the chromatogram in Figure 3·41 was obtained for a sample taken after only 1·00 seconds, while Figure 3·42 shows that for a sample taken 0·08 seconds later. The inset in Figure 3·41 shows the relative times at which the samples were taken in relation to the multiple cool-flame phenomena, which occurred 1·4 seconds after injection. Chromatograms taken at different times after the cool-flame indicated that no significant changes occurred in either the number of components or their relative concentrations. A number of factors, such as the limited resolution, the complexity of the chromatograms and the

Figure 4·5

Correlation Between Exhaust Odour Intensity and LCO[107]

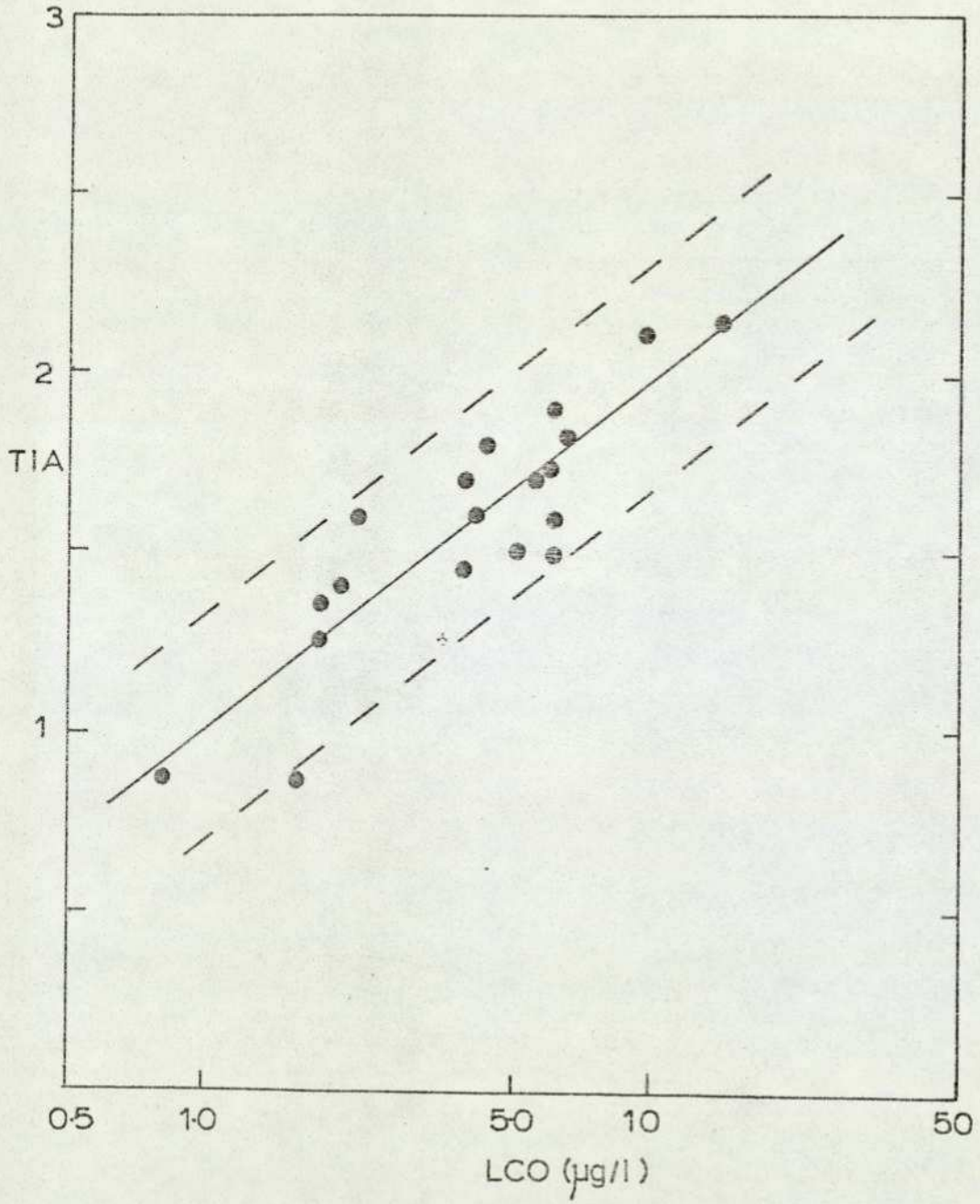

time involved prevented any attempt to identify each peak. The analytical studies of IIT,[108,109] revealed the complexity of peak identification, since they were only able to identify a few individual components even with the assistance of 200ft. capillary columns to improve resolution and a high resolution mass-spectrometer to assist assignment. The peak odour description experiments performed by IIT, however, indicate that diesel exhaust odour is mainly due to the presence of components which are eluted from a Carbowax 20M column after undecane (KI=1100). It can be seen from Figure 3·42 that this section of the chromatogram, from KI = 1100 to 1600, contains many partially resolved components. Previous studies have shown that components such as alkyl-benzaldehydes, aliphatic aldehydes and ketones and various O- and N-heterocycles have Kovats Indices on Carbowax 20M columns between 1100 and 1600. These compounds are common partial oxidation products from hydrocarbon fuels and many have low odour thresholds. The fundamentals of hydrocarbon oxidation, outlined in Section 1·3 will now be elaborated upon in order to describe the principal features of alkane oxidation and more specifically, the mechanism of formation of partial oxidation products such as these from hexadecane.

Investigations into hydrocarbon oxidation performed over the last fifteen years have indicated that many of the combustion phenomena observed, and the nature of the products formed, can be accounted for by the rearrangement of alkylperoxy radicals and the decomposition of the hydroperoxyalkyl radicals thus produced. These reactions are widely believed to constitute the principal chain-propagating step through the cool-flame region. Moreover, during the oxidation of 3-ethylpentane,[138] 3-methylpentane[139] and 2-methylpentane,[140,141] it remains the dominant reaction path at quite high temperatures, (ca 400°C). The distribution of products formed by the decomposition of the hydroperoxyalkyl radicals is continuous across the slow combustion/cool-flame boundary and is little affected by carbon deposits resulting from two-stage ignition or very large increases in the initial pressure,[21,141,142] thus confirming the

homogeneous nature of the reactions involved.

The isomerisation and subsequent decomposition of alkylperoxy radicals follows the scheme outlined below:-

$$CH_3CH(CH_2)_4CH_3 + O_2 \longrightarrow CH_3\underset{\underset{O\text{-}\dot{O}}{|}}{CH}(CH_2)_4CH_3 \qquad 1$$

$$CH_3CH(CH_2)_4CH_3 \xrightarrow[1:4\ H\ transfer]{\alpha} CH_3\underset{\underset{O\text{-}OH}{|}}{C\dot{H}}CH(CH_2)_3CH_3 \qquad 2\alpha$$

$$\xrightarrow[1:5\ H\ transfer]{\beta} CH_3\underset{\underset{O\text{-}OH}{|}}{CH}CH_2\dot{C}H(CH_2)_2CH_3 \qquad 2\beta$$

$$\xrightarrow[1:6\ H\ transfer]{\gamma} CH_3\underset{\underset{O\text{-}OH}{|}}{CH}(CH_2)_2\dot{C}HCH_2CH_3 \qquad 2\gamma$$

$$\alpha\text{-},\beta\text{-},\gamma\text{-}C_nH_{2n}OOH \longrightarrow \text{Products} + \dot{O}H \qquad 3$$

Reactions 1 to 3, together with the unselective attack of the hydroxyl radical on an original fuel molecule,

$$C_nH_{2n+2} + \dot{O}H \longrightarrow \dot{C}_nH_{2n+1} + H_2O \qquad 4$$

form the principal chain propagation cycle occurring just prior to and in the cool-flame. The α-, β- and γ-hydroperoxyalkyl radicals produced by the homogeneous intramolecular rearrangement, reaction 2, decompose to form a hydroxyl radical and stable products which include O-heterocycles, carbonyl compounds, alkenes and alcohols with rearranged carbon skeletons. Fish,[143,145] who has greatly extended the alkylperoxy radical isomerisation scheme, has accounted for the diversity of products formed on the basis of the following reactions:-

(i) <u>O-O bond fission, cyclisation and OH elimination</u>

$$CH_3\underset{\underset{O\text{-}OH}{|}}{CH}\text{-}\dot{C}H(CH_2)_3CH_3 \longrightarrow CH_3\underset{\underset{O}{\diagdown\ \diagup}}{CH\text{—}CH}(CH_2)_3CH_3 + \dot{O}H \qquad 5\alpha$$

oxiran

$$CH_3\underset{\underset{O\text{-}OH}{|}}{CH}\text{-}CH_2\text{-}\dot{C}H(CH_2)_3CH_3 \longrightarrow CH_3\underset{\underset{O}{\diagdown\ \diagup}}{CH}\overset{\overset{CH}{\diagup\ \diagdown}}{\ }CH(CH_2)_2CH_3 + \dot{O}H \qquad 5\beta$$

oxetan

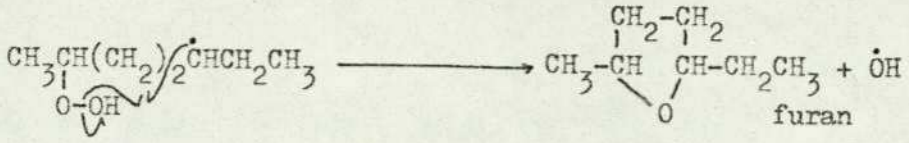

furan 5δ

(ii) C-O bond fission, α-radical only

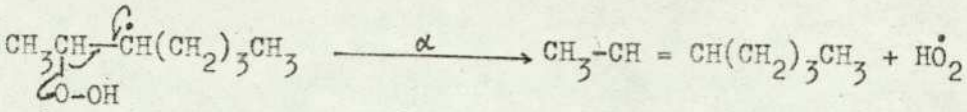

6

(iii) O-O and C-C bond fission, β-, and γ-radicals only

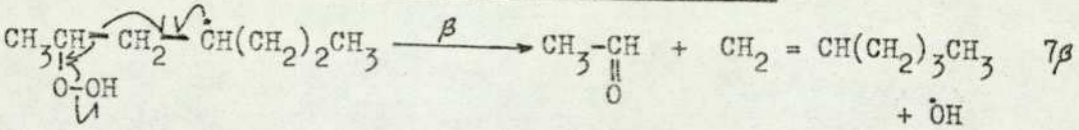

7β

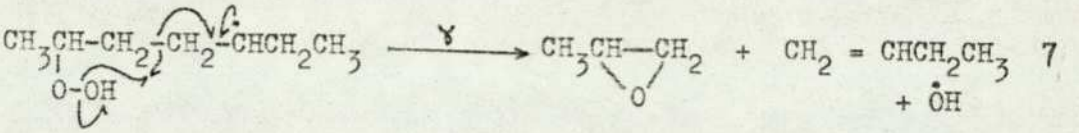

7

(iv) Alkyl group shift and O-O bond fission

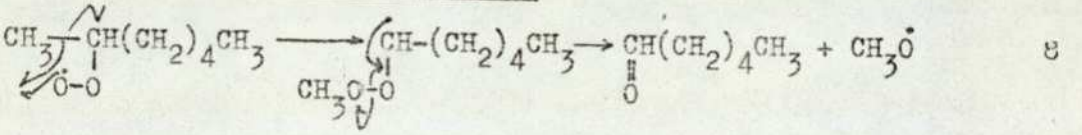

8

The molecular structure of the fuel molecule determines which hydrogen atom is abstracted in reaction 2 and therefore ultimately controls the structure of the products formed by decomposition of the hydroperoxy-alkyl radical. Parameters which are particularly important are the size of the transition-state ring and the strength of the C-H bond to be broken. The β- scission reaction available to β- and γ- radicals results in the formation of high yields of alkenes with fewer carbon atoms than the original fuel, while an increase in branching of the carbon skeleton of the fuel molecule increases the octane rating of the fuel and increases the relative propensity of the β- scission reaction. Thus fuels which have a high octane rating (or conversely a low cetane rating) tend to produce larger quantities of alkenes.[31] This fact has important implications with respect to the environment, since gasoline fuels will produce more alkenes which may react photochemically to produce fog. On the other hand, an increase in the length of the carbon chain increases the cetane number and is also conducive to the formation of O-heterocycles which may undergo further oxidation. At low temperatures, (230 to 300°C) oxetans are readily oxidised, tetrahydrofurans react somewhat

less rapidly, while oxirans are relatively stable. At higher temperatures, ($>400^{\circ}C$), tetrahydrofurans are less readily oxidised than either oxirans or oxetans.[146] The oxidation of O-heterocycles is accompanied by early ring fission and the formation of oxygenated products, eg: carbonyl compounds of lower carbon content than the original O-heterocycle. Summarising these observations it is apparent that the diesel engine requires for operation fuels which, by their nature, are conducive to the formation of O-heterocycles some of which are strong odorants.[103-107] Further oxidation of these compounds results in the formation of carbonyl compounds which are also strong odorants. The gasoline engine, however, operates with fuels containing a much higher proportion of branched-chain alkanes which results in the emission of alkenes which are essentially odour irrelevant.

In addition to the decomposition reactions outlined above, the hydroperoxyalkyl radicals may add on further oxygen to give hydroperoxy-alkylperoxy radicals, reaction 9 :

$$\dot{C}_nH_{2n}OOH + O_2 \longrightarrow \dot{O}OC_nH_{2n}OOH \qquad 9$$

This reaction competes successfully with decomposition, when the partial pressure of oxygen is high; intermolecular hydrogen abstraction then produces a dihydroperoxide, reaction 10 :

$$\dot{O}OC_nH_{2n}OOH + C_nH_{2n+2} \longrightarrow HOOC_nH_{2n}OOH + \dot{C}_nH_{2n+1} \qquad 10$$

Dihydroperoxides decompose by homolysis of both O-O bonds; in α-dihydro-peroxides this scission may be accompanied by the scission of a C-C bond leading to two carbonyl compounds and two hydroxyl radicals,

$$HOO(R^1R^2)C\text{-}C(R^3R^4)OOH \longrightarrow R^1R^2C{=}O + R^3R^4C{=}O + 2\dot{O}H \qquad 11$$

whereas β-, γ- or δ- hydroperoxides will decompose to dicarbonyl compounds

$$R^1R^2\underset{\underset{OOH}{|}}{C}\text{-}CH_2\text{-}\underset{\underset{OOH}{|}}{CR^3}R^4 \longrightarrow R^1\underset{\underset{O}{\|}}{C}\text{-}CH_2\text{-}\underset{\underset{O}{\|}}{CR^3} + R^2 + R^4 + 2\dot{O}H \qquad 12$$

Cartlidge and Tipper[147] have postulated the following reactions for the di-n-heptylperoxide to account for the dicarbonyl and furan derivatives found in the reaction products:

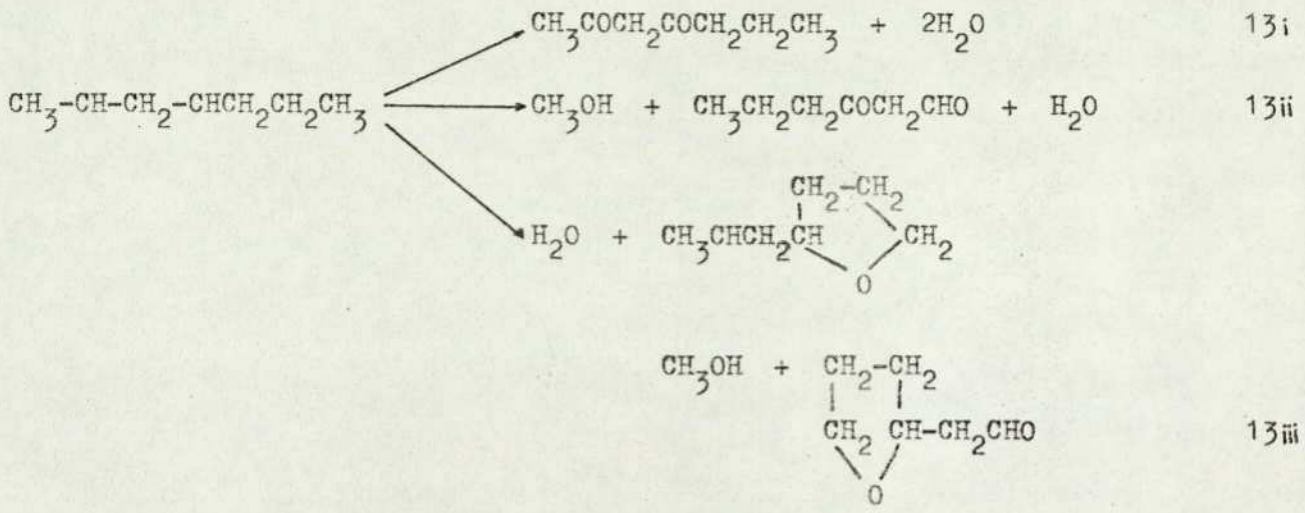

The nature of the combustion phenomena observed with diesel fuel indicates that the reaction mechanism involves a degenerate chain-branching agent, the decomposition of which results in increased reaction rates, which are manifested as cool-flame and hot ignition processes. The nature of the degenerate branching agent in hydrocarbon oxidation has been much discussed, and it is generally agreed that the most probable agents are peroxides, aldehydes and peracids.

In the low temperature region, i.e. below 300°C, where the oxidation is quite selective, Fish,[140,143] suggests that degenerate branching results from the alkyl monohydroperoxide produced by a linear chain involving intermolecular hydrogen abstraction by the alkylperoxy radical, reaction 14:

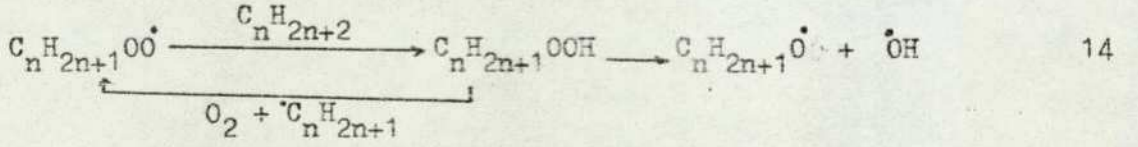

14

Some of the partial oxidation products formed during the propagation step may also act as degenerate branching agents, since the attack of molecular oxygen on moderately stable products with weak C-H bonds is considerably faster than the corresponding attack on alkanes, (i.e. faster than the initiation reaction). Aldehydes are by far the best example of such a class of products and reaction 15 has frequently been supposed to fill this role.[148-150] For formaldehyde[151] E_{15} = 32kcal mole^{-1}, whereas for acetaldehyde,[152] E_{15} may be as low as

14 kcal mole^{-1}.[152]

$$RCHO + O_2 \longrightarrow \dot{H}O_2 + R\dot{C}O \qquad 15$$

The facile H abstraction reaction for aldehydes is explained by the lower C-H bond strength (RCO - H = 88 ± 2 kcal mole^{-1}) found in these compounds compared with the C-H bonds in alkanes, (eg. C_2H_5 - H = 98±1kcal mole^{-1}; $(CH_3)_2CH$ - H = 94·5 kcal mole^{-1}; $(CH_3)_3C$ - H = 91±1kcal mole^{-1}).[153] However, higher aldehydes, including branched unsaturated aldehydes, are in general less reactive than acetaldehyde.[154]

The acyl radical formed in reaction15 may enter into the following sequence of reactions:-

$$R\dot{C}O + O_2 \longrightarrow R\dot{C}O_3 \qquad 16$$

$$R\dot{C}O_3 + RH \longrightarrow R\dot{C}O_3H + \dot{R} \qquad 17$$

$$R\dot{C}O_3H \longrightarrow R\dot{C}O_2 + \dot{O}H \qquad 18$$

in which the peracid formed leads to further degenerate chain branching.

The homolytic breakdown of peroxides and the oxidation of aldehydes are the most frequently cited modes of degenerate branching during the oxidation of alkanes. Branching reactions involving free radicals as reactants have received less attention, but it has been suggested that these may play a considerable part. In the oxidation of heptane for example, the hydroperoxyheptylperoxy radicals formed may decompose,[155] reaction 19, sufficiently rapidly to compete with hydrogen abstraction to give a dihydroperoxide, reaction 10. Furthermore, the reaction of free radicals with molecules, reactions 20 and 21, can lead to chain branching.

$$CH_3\text{-}\underset{\underset{OOH}{|}}{CH}CH_2\underset{\underset{O\dot{O}}{|}}{CH}C_3H_7 \longrightarrow 2\dot{O}H + (CH_3)_2C{=}O + \dot{C}_3H_7 + CO \qquad 19$$

$$R\dot{O}_2 + RCHO \longrightarrow R\dot{O} + \dot{O}H + R\dot{C}{=}O \qquad 20$$

$$R\dot{O}_2 + R'OOH \longrightarrow R\dot{O} + \dot{O}H + R'\dot{O}_2 \qquad 21$$

At higher temperatures, i.e. above 400°C, hydrogen peroxide may play a prominent role in the branching stage by decomposing homogeneously following the collision with a second molecule, reaction 22, the process

having an activation energy of 45 kcal mole^{-1}.[156]

$$HOOH + M \longrightarrow 2\dot{O}H + M \qquad 22$$

This high activation energy means that hydrogen peroxide involvement occurs only at temperatures higher than those at which organic peroxides decompose.

The concentration of peroxide needed to affect the course of the oxidation is very small. Moreover, even on the assumption that peroxides are stable enough, at ambient temperatures to be collected in the Chromosorb 102 traps, the alkylhydroperoxide molecule does not contain a strong chromophore and therefore would not contribute to the LCO trends observed in this study.

In Figure 4·6(a) and (b) the LCO concentrations measured are plotted as functions of time throughout the passage of two cool-flames. Figure 4·6 also includes similar data for the concentration of typical branching agents, such as aldehydes and peroxides, recorded during the oxidation of various fuels.[33, 157, 158] It can be seen that strong similarities exist between the LCO variations and those of the branching agents, which infers that the increase in reaction rate induced by the decomposition of the branching agent leads to the rapid formation of the LCO components, thus producing the similar trends observed. Aldehydes, other than formaldehyde, and their decomposition products will form part of the LCO fraction. It is presumed, however, that the decomposition products of the peroxides and not the peroxides themselves, will be detected.

Garner et al,[121] in studies of the preignition reactions, were able to measure the concentration of aldehydes and peroxides in a diesel engine. The data obtained are shown in Figure 4·7. It was found that for four different hydrocarbon fuels, the peak concentration of aldehydes and peroxides occurred just before the start of the pressure rise caused by combustion. Moreover, for high cetane fuels, the peak concentration of these intermediates occurred earlier than with lower cetane fuels. These observations, recorded in the diesel engine, are typical of the behaviour of branching agents previously observed in static and flow systems.

Figure 4·6

The Change in Concentration of Odorants and Branching Agents During the Oxidation of Various Fuels

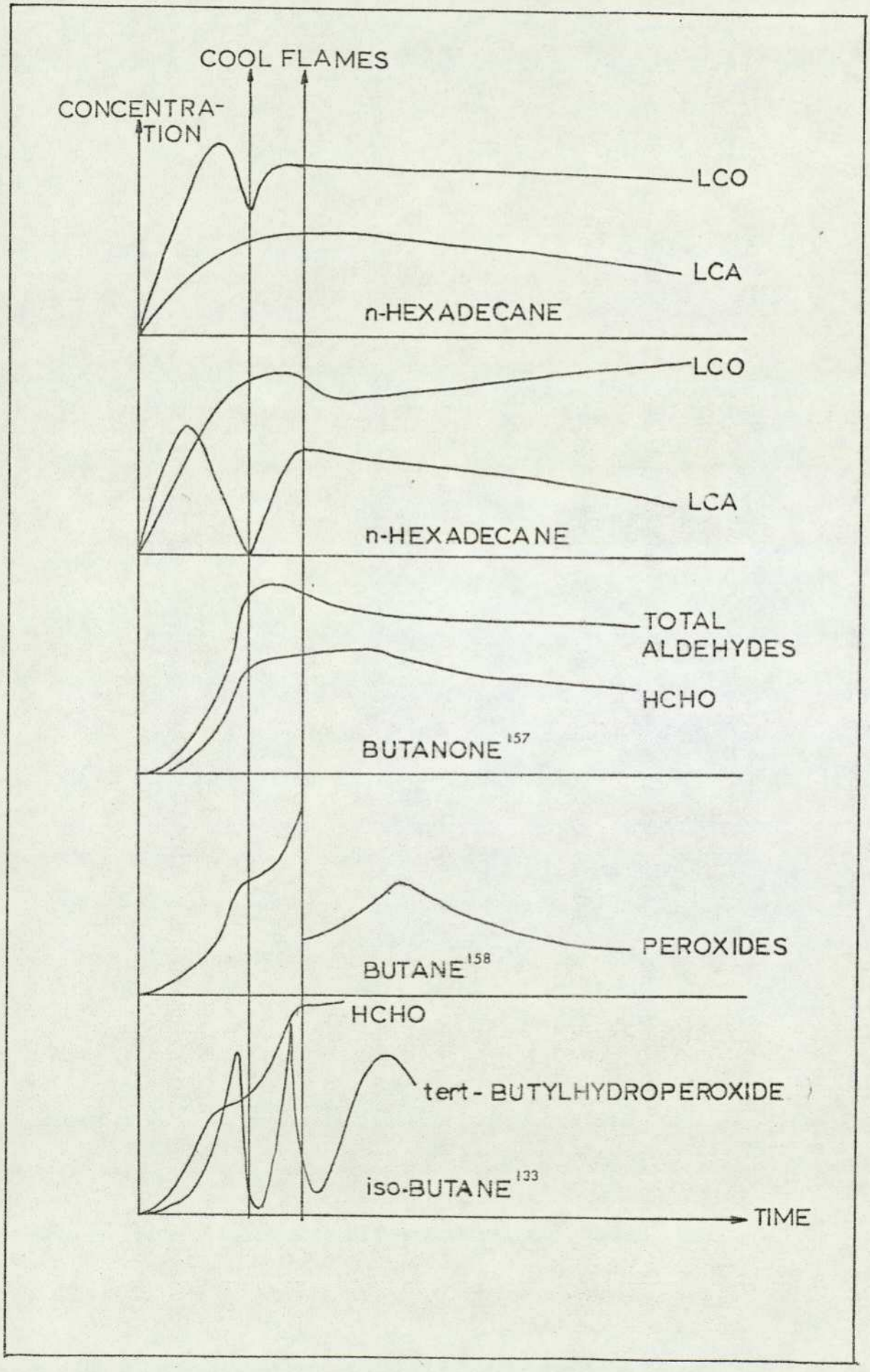

Figure 4.7

Concentration of Intermediates Recorded[121] During the Diesel Engine Combustion Process

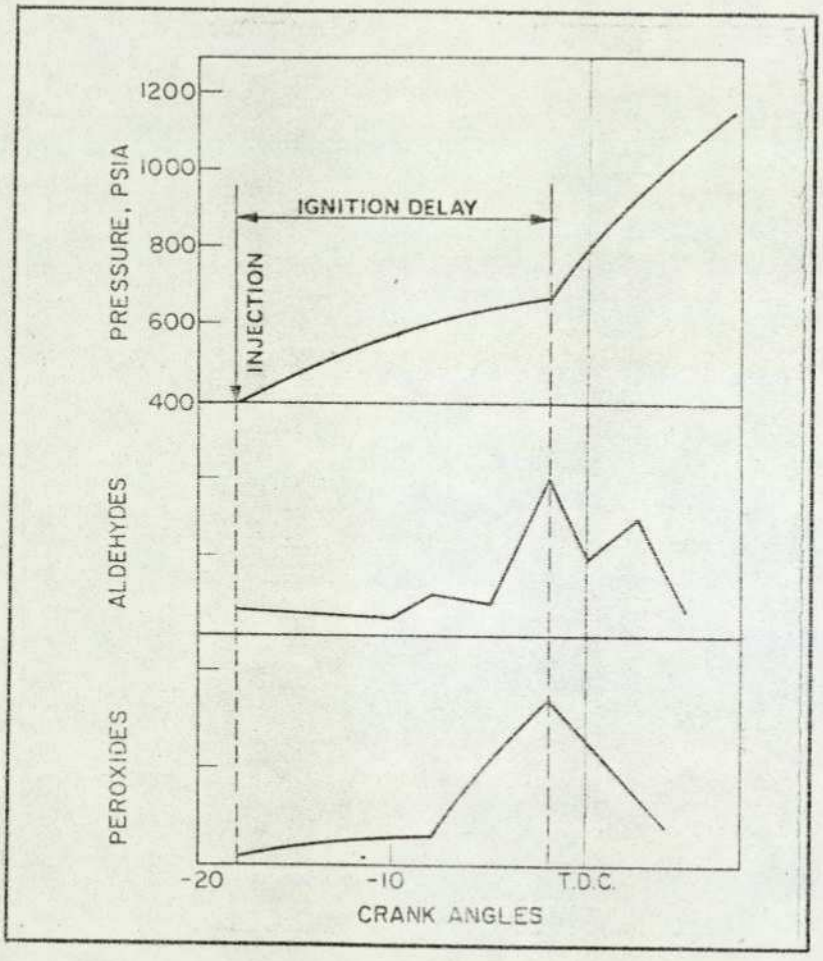

From this discussion of the nature of the products formed during alkane oxidation, it is anticipated that the LCO fraction consists mainly of O-heterocycles and carbonyl compounds. The low molecular weight unsaturated carbonyl compounds, which are notorious odorants, eg. acrolein and crotonaldehyde, possess a very strong chromophoric group, i.e. C=C-C=O, and their presence even in low concentrations will produce a significant LCO response. Similarly the oxygenated aromatic and heterocyclic compounds will absorb UV radiation at 254nm quite extensively. The aliphatic aldehydes and ketones do not possess chromophoric groups of the same intensity as the previously mentioned classes of chemical compounds, but their presence in the products will be detected by virtue of the C=O absorbance. It should be remembered, however, that the components producing the absorbance at 254 nm may not be the only important odorants but may also act as indicators of the concentration of components with low odour thresholds and relatively low values of ϵ_{max} at 254 nm. It may be concluded therefore, that the LCO trend observed is due to the fluctuating concentrations of the unsaturated aliphatic and aromatic carbonyl compounds and of the O-heterocycles such as the alkyl-substituted tetrahydrofurans.

The parallel rise in O-heterocycles with the cool-flame pressure pulse has been studied[146] in some depth and the results obtained are given in Figure 4·8, which shows the amount of n-hexane fuel remaining and of O-heterocycles formed as a function of time. It can be seen that the consumption of fuel almost ceases before the passage of the cool-flame, while concentrations of all the O-heterocycles continue to increase. After the cool-flame, the O-heterocycle concentration decreases which indicates that these intermediate compounds participate in further reactions. The maximum rate of O-heterocycle formation coincides with the cool-flame region of the ignition diagram, and only small quantities of these compounds are found at temperatures above the cool-flame limit. The transition from the cool-flame region to the hot ignition region was accompanied by a sharp decrease

Figure 4·8

The Variation with Time of Pressure Change and the Amounts of n-Hexane Remaining and O-heterocycles Formed During the Oxidation of n-hexane[146]

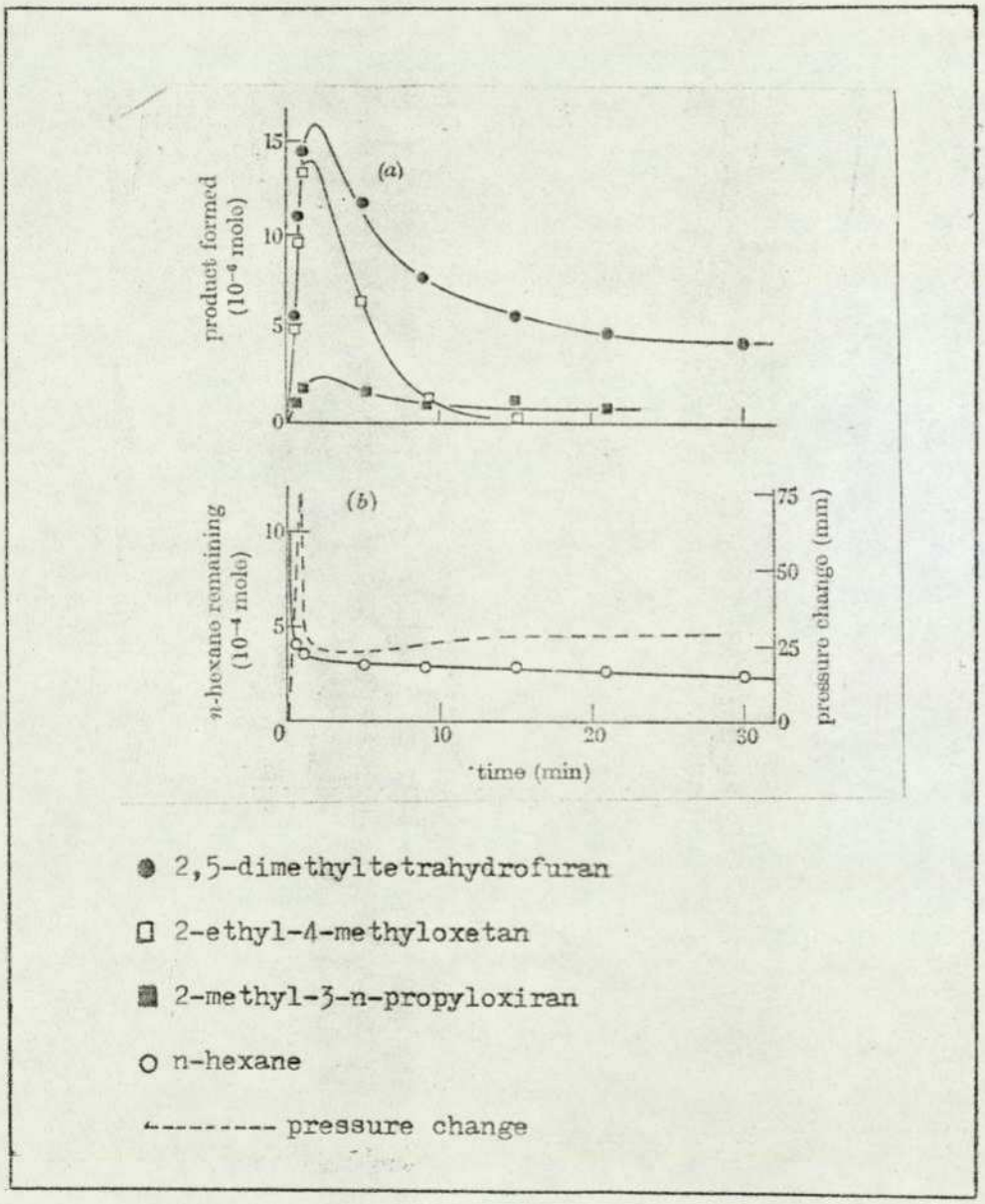

in the quantities of O-heterocycles detected. This observation is similar to that recorded for the LCO fraction under hot ignition conditions.

Another study which provides some very useful data was published by Cullis et al,[33] who traced the formation of pentene-1, 2,4-dimethyl oxetan, transpentene-2,propionaldehyde and acetone during the oxidation of n-pentane at 278°C as shown in Figure 4·9. It is apparent that some of the partial oxidation products eg. the alkenes and the O-heterocycles reflect the cool-flame pressure pulses more accurately than others, eg. the carbonyl compounds. Since in the present study the LCO absorbance is related to the combined concentrations of many oxygenates, it is evident that, unless one particular class of compound eg. the O-heterocycles, predominates in the products the LCO trend observed will not reflect the cool-flame pressure pulse with much accuracy.

Before concluding this section on alkane oxidation it is important that the high temperature, i.e. above 400°C, oxidation mechanism should be discussed. The alkene-theory of hydrocarbon oxidation was proposed by Knox[34] following studies of the oxidation of ethane,[159,160] propane and isobutane,[161,162] both alone and competitatively. It was found that the major primary product obtained during the oxidation of these alkanes was the conjugate alkene and that this accounted for up to 80% of the products formed. The reaction sequence proposed to account for this product distribution was as follows:-

$$\dot{C}_nH_{2n+1} + O_2 \longrightarrow C_nH_{2n} + H\dot{O}_2 \qquad 23$$

$$C_nH_{2n+2} + H\dot{O}_2 \longrightarrow \dot{C}_nH_{2n+1} + H_2O_2 \qquad 24$$

$$C_nH_{2n} + H\dot{O}_2 \longrightarrow \alpha\text{-}\dot{C}_nH_{2n}OOH \qquad 25$$

$$\alpha\text{-}\dot{C}_nH_{2n}OOH + O_2 \longrightarrow \dot{O}OC_nH_{2n}OOH \qquad 26$$

$$\dot{O}OC_nH_{2n}OOH + H\dot{O}_2 \longrightarrow HOOC_nH_{2n}OOH + O_2 \qquad 27$$

$$HOOC_nH_{2n}OOH \longrightarrow \text{Products} + 2\dot{O}H \qquad 28$$

$$C_nH_{2n+2} + \dot{O}H \longrightarrow \dot{C}_nH_{2n+1} + H_2O \qquad 4$$

Figure 4·9

The Variation with Time of the Pressure Change, the Amount of Fuel Remaining and the Amounts of Some Typical Oxidation Products Formed During the Oxidation of n-pentane[33]

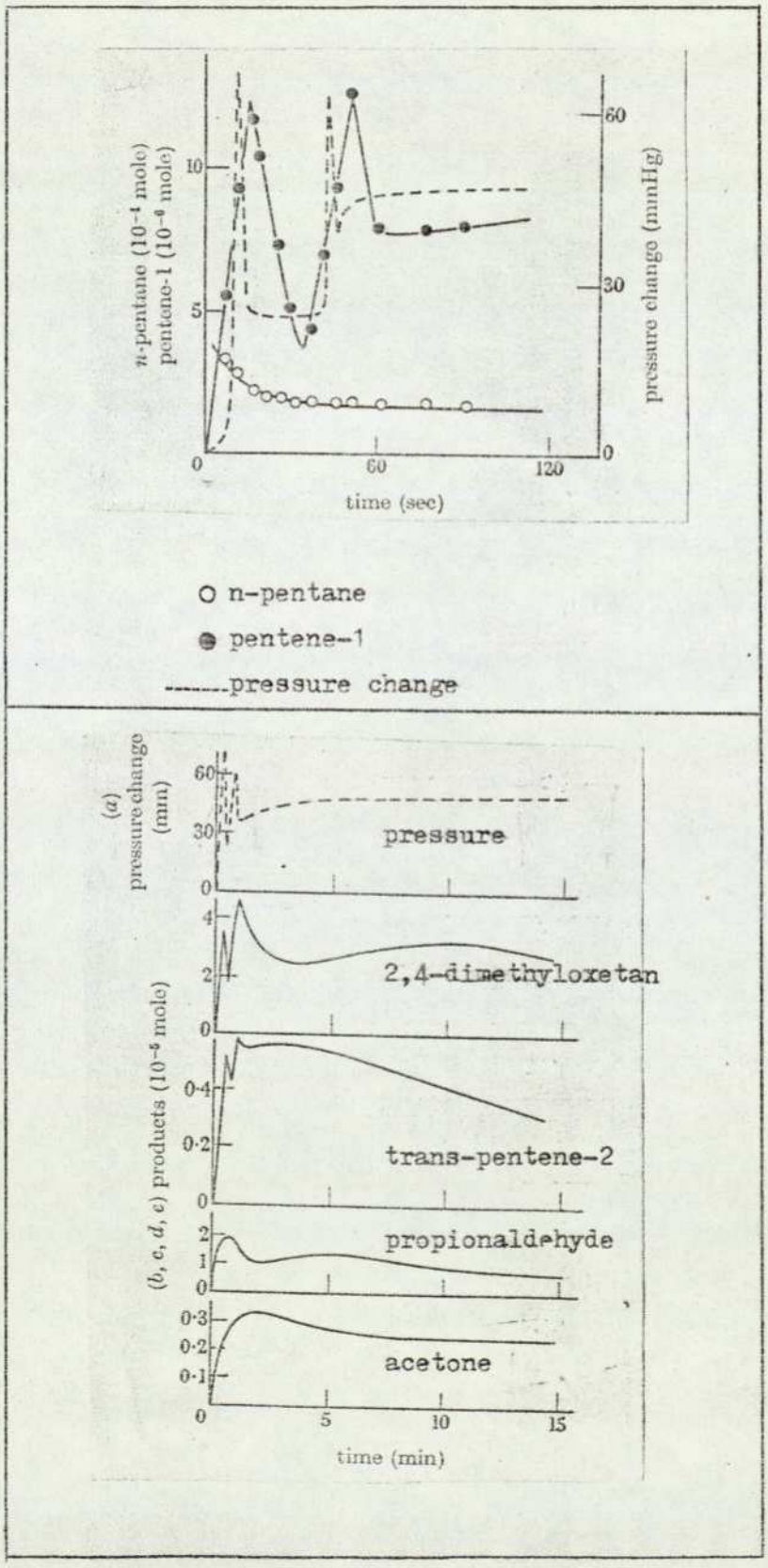

As a result of the change in mechanism with temperature, the principal products are alkenes and hydrogen peroxide and their secondary decomposition products, which of course include water.

It is obvious from an understanding of the diesel engine combustion process that clearly defined temperature zones do not exist in the combustion chamber. However, it may be said that as a first approximation, the alkyl-peroxy radical scheme will be the predominant reaction mechanism in the lower temperature regions i.e. near the chamber walls and in the exhaust system of the engine. The alkene mechanism and fuel pyrolysis predominate in the spray envelope where the gas temperatures are much higher. Rapid diffusion of reactants and of products of both mechanisms will occur and this process will be assisted by piston movements and by combustion-induced turbulent motion of the trapped gases. Thus conditions will be produced which are conducive to the interaction between intermediates and products from both oxidation mechanisms.

The alkenes formed by hydrogen abstraction, reaction 23, will undergo further oxidation, to produce a class of compounds which are extremely odour-relevant i.e. unsaturated carbonyl compounds. This aspect will be discussed further in the next section which deals with the oxidation of 1-decene.

4·2·2 1-Decene Fuel and Alkene Oxidation

Diesel fuel contains ca 2-3% by weight of alkenes. The preceding section of the Discussion has shown that the presence of relatively small concentrations of certain compounds, albeit reaction intermediates, can have a profound affect on the course and products of oxidation. Moreover, certain studies[164,165] have shown that alkenes may be the principal intermediates responsible for the ignition of fuel blends containing alkanes or aromatics at high temperatures i.e.; $T > 300^{o}C$.

Owing to the important role which may be attributed to alkenes under certain conditions, a brief discussion of the reactivity of this class of

compound, relative to the others found in diesel fuel, appears to be warranted.

The ease with which alkenes are oxidised increases with molecular weight in a manner similar to that observed for alkanes. Beginning with the low molecular weight alkenes, it is observed that ethylene does not exhibit a cool-flame but consideration of the explosion limits and the low cetane number indicates that this compound is more easily oxidised than ethane. Propylene exhibits well-defined cool-flame regimes, but the induction period preceding the first cool-flame and the ignition delay show that propylene is less easily oxidised than propane in the temperature range below 400°C. Above this temperature, the value of τ c.f. and τ h.i. increases for propane with temperature, while that of propylene decreases. Thus in this temperature range there is a reversal of the ease of oxidation for these conjugate species. From butylene upwards, the alkene is always less reactive than the corresponding alkane. Jost[166] has provided an explanation for this behaviour and suggests that higher alkenes react to form radicals which have relatively long lifetimes. For 1-decene the following sceme may be envisaged:-

$$C_7H_{15}\text{-}CH_2\text{-}CH{=}CH_2 + \dot{O}H \longrightarrow C_7H_{15}\text{-}\dot{C}H\text{-}CH{=}CH_2 + H_2O$$

$$C_7H_{15}\text{-}\dot{C}H\text{-}CH{=}CH_2 \rightleftharpoons C_7H_{15}\text{-}CH{=}CH\text{-}\dot{C}H_2$$

The radical shown is stabilised by resonance and is therefore less reactive, thus effectively reducing the probability of further reaction with oxygen.

Figure 3.26 shows the formation of LCA and LCO during the oxidation of 1-decene at 280°C and 500 torr with an equivalence ratio of 0·42. Injections of pure 1-decene on the HPLC column revealed that the LCO level of the fuel was zero and that the fuel contained an aromatic impurity, the concentration of which was comparable to the LCA levels recorded in samples taken prior to hot ignition. The formation of LCA and LCO differ from those obtained with hexadecane although the concentrations of LCO formed with both fuels were of the same order of magnitude i.e. ca 10 μg. After 2·3 seconds a hot ignition occurred, the effect of which was to reduce both the LCA and LCO levels to 10% of their previous values.

As previously stated, the alkene compounds present in diesel exhaust are considered to be insignificant with respect to the odour, and in fact their presence in diesel exhaust samples is undetected by the ADL scheme. However, the alkenes present in diesel fuel. and those formed during high temperature alkane oxidation, can participate extensively in the formation of odorants, since alkenes are precursors to carbonyl and heterocyclic compounds. The two main reaction paths leading to these compounds are:-

(1) Addition of atomic oxygen to the less substituted atom adjacent to the double bond in an alkene results in the formation of either an oxiran or a carbonyl compound:

$$(CH_3)_2C{=}CH_2 + O \longrightarrow (CH_3)_2\dot{C}HO \longrightarrow (CH_3)_2\underset{\diagdown\,\diagup\ O}{C}\text{-}CH_2$$

$$\text{or } (CH_3)_2CHCHO$$

(2) (i) The abstraction of a hydrogen atom followed by addition of molecular oxygen to produce unsaturated aldehydes, such as acrolein;

(ii) Alkyl radical addition to give saturated aldehydes such as acetaldehyde.

$$\text{(i) } CH_3CH{=}CH_2 \xrightarrow[+O_2]{-H} OOCH_2CH{=}CH_2 \longrightarrow CH_2{=}CHCHO + \dot{O}H$$

$$OOCH_2CH{=}CH_2 \longrightarrow CH_2O + \dot{C}H_2CHO \longrightarrow \dot{C}H_3 + \dot{C}O$$

$$\text{(ii) } CH_3CH{=}CH_2 + \dot{R} \longrightarrow CH_3\dot{C}H\text{-}CHR \xrightarrow[RH]{O_2} CH_3\underset{OOH}{CH}\text{-}CH_2R + \dot{R}$$

$$\longrightarrow CH_3CHO + RCH_2OH$$

These few examples indicate the important role which alkenes can play in the subsequent formation of odorants. The aldehydes formed are preserved from further oxidation by the presence of excess alkene[167] and hence are ultimately emitted in the exhaust.

4·2·3 n-Butylbenzene Fuel and Aromatic Hydrocarbon Oxidation

In carrying out experiments on the oxidation of benzene and its alkyl derivatives below 400°C, the field is limited by two considerations. First, the pressure limitation of the apparatus (less than 1 atmosphere) predetermines a very slow rate of reaction especially with benzene. Secondly, the lower aromatic homologues are so stable, that their respective ignition diagrams lack a cool-flame region. This situation is somewhat alleviated as the length of the side chain attached to the benzene nucleus is increased; the higher homologues being increasingly more readily oxidised as shown by the list of activation energies for the oxidation process[168] shown in Table 4·1 These considerations led to the choice of n-butylbenzene as the compound which could best be studied in the present apparatus as representative of the aromatic fraction of diesel fuel.

At 310°C, 600 torr and with an equivalence ratio of 0·42, a cool-flame was produced when n-butylbenzene was injected into the reaction vessel (Figure 3·30). The LCA and LCO levels followed the pressure trace accompanying the passage of the cool-flame; the maixima coinciding with $\Delta P_{c.f.}$ After the cool-flame had passed the LCO and LCA levels fell slightly before increasing again as ΔP_{∞} was approached.

The rise in LCA level above that originating from the unburnt fuel can be explained by the formation of products which possess intense chromophoric groups. Since the products are eluted from the HPLC column concurrently with the remaining fuel fraction, they must be aromatic in character and be of low polarity. These characteristics would be present in a molecule such as biphenyl, for example, which has an absorption band at 246 nm and a molar absorptivity, ϵ_{max}, of 20 000.[169] These spectroscopic data indicate that biphenyl, or a substituted derivative, absorb UV radiation in the region of 254 nm far more strongly than benzene ($\epsilon_{max}254$, $\epsilon_{max}230$)[170] or an alkyl benzene (such as n-butylbenzene) similarly, the polycyclic aromatic hydrocarbons would also exhibit much higher UV absorbance at 254 nm than n-butylbenzene. The

Table 4·1

Activation Energies for the Combustion of Some Aromatic Hydrocarbons in Air[168]

Hydrocarbon	Activation Energy kcal/mole
Benzene	68·0
Toluene	49·0
Ethylbenzene	41·5
n-propylbenzene	39·0
n-butylbenzene	34·0
o-xylene	38·0
m-xylene	39·0
p-xylene	40·0
Mesitylene	36·0

formation of polycyclic hydrocarbons in normal and reversed diffusion flames[171] and fuel-rich premixed flames has been studied[172-174] in some depth and is well documented. Although the temperature in such systems is higher by 100 to 200°C than in the present study in a static system, the formation of substituted biphenyls and polycyclic aromatic hydrocarbons under cool-flame conditions is highly probable. Prior to analysis of the trapped samples, it was noted that the C102 packing in the end of the trap nearest the reactor was discoloured with a sooty deposit. This observation would substantiate the formation of polycyclic aromatic hydrocarbons, since the formation of these compounds is considered to be precursory to soot formation.[175,176]

The relationship between the equivalence ratio and the levels of LCA and LCO produced is shown in Figure 3.31. At low ϕ ratios, the LCA level is high. Since the reaction under these conditions is slow and incomplete the conversion of fuel to oxygenated products is low and the LCO levels recorded are accordingly diminished. The high LCA level is therefore considered to be primarily unburnt butylbenzene. As the equivalence ratio is increased, proportionately more fuel is converted to LCO, while the LCA level falls. This process is self-limiting under cool-flame conditions and a situation is reached(ca.σ = 0·52) when the conversion of fuel is at a maximum; addition of more fuel under these conditions therefore effectively leads to a reduction in the LCO formed when this is expressed in terms of $\mu g/\mu l$ of fuel injected.

ADL concluded from their extensive investigations that the LCO fraction in diesel engine exhaust consists mainly of the partial oxidation products derived from the aromatic fuel fraction. It is therefore evident that the oxidation of aromatic compounds is fundamental to diesel exhaust odour and the mechanisms for these reactions will now be described.

In general the kinetics of alkylbenzene oxidation resembles that of the alkanes, especially if the side-chain contains more than two carbon atoms. The partial oxidation products from benzene and alkylbenzenes fall into three categories which depend on the severity of the oxidative attack.

Oxidation of the side-chain attached to the aromatic ring results in the formation of compounds such as acetophenone and benzaldehyde. ADL have identified these compounds in diesel engine exhaust[103,105] and conclude that species such as these are responsible for the 'burnt-odour' note associated with the exhaust. The mechanism whereby such compounds are produced from n-butylbenzene, the model aromatic fuel used in these studies, involves the formation and decomposition of the appropriate arylperoxy radical or the hydroperoxide. A suggested mechanism involving these intermediates for side-chain oxidation is shown in Figure 4·10.

At higher temperatures, oxidation of the ring without fission results in the formation of phenolic compounds, possibly via radical-radical reactions involving phenyl. Phenol and related compounds are strong odorants. In addition these compounds have been identified with the lachrymatory properties of diesel engine exhaust. A recent survey[80] gives the odour threshold concentration for phenol as 0·047ppm and that of p-cresol as 0·001ppm describing the odours as 'medicinal' and 'tar-like-pungent' respectively.

Oxidation accompanied by ring fission produces unsaturated acids and olefinic species. One route for the formation of these compounds from phenol has been suggested[177]. A decrease in pressure and an increase in temperature increases the probability of ring fission which may proceed by the following route:

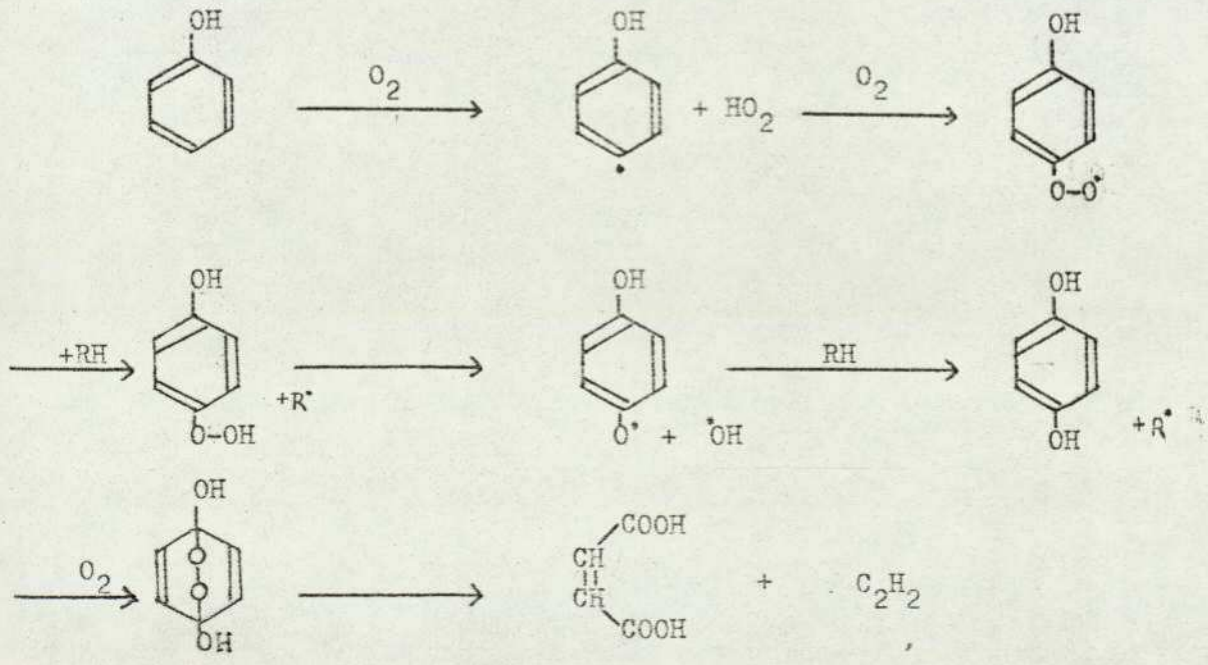

Figure 4·10

Possible Routes for Side-chain Oxidation of n-Butylbenzene

Leading to the Formation of Odorants

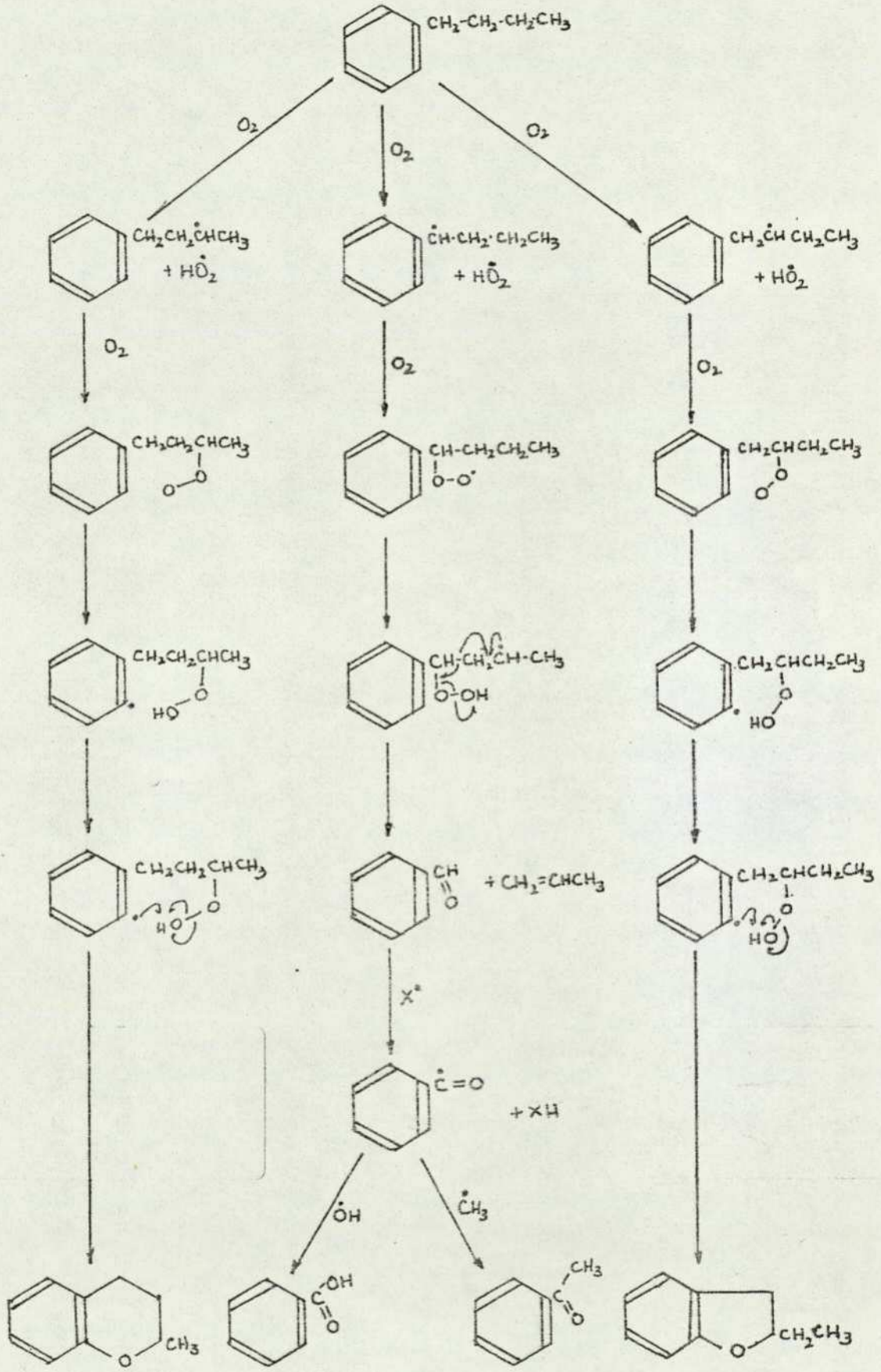

The unsaturated acids thus formed are strong odorants and also possess strong lachrymatory properties. It may be said, therefore, that side-chain oxidation of aromatic compounds leads to the formation of powerful odorants but more severe oxidation results in odorants with additional lachrymatory effects.

Burgoyne[178] studying the cool-flame oxidation of n-propylbenzene, traced the formation and decomposition of several important intermediates and products. Figure 4·11 shows the results of these analytical investigations in which the concentration of three different peroxides was recorded as a function of time. The behaviour observed suggests that the formation and propagation of the cool-flame is due to the involvement of hydrogen peroxide and the alkyl-peroxides. It is evident that, for a fuel with a complexity of diesel fuel, these intermediates will be formed first from the alkane fraction of the fuel. Once formed, these intermediates assist in the initiation of the oxidation of the aromatic fraction. This interaction is discussed in more detail in Section 4·2·4.

Figure 3·44 shows a chromatogram which is typical of those recorded for the products of n-butylbenzene oxidation collected in the C102 traps. It is clear that the majority of the compounds formed were eluted after the base fuel peak, indicating that they are either more polar or that they have higher molecular weights than n-butylbenzene. The absence of many low molecular weight components is another indication of the stability of the aromatic nucleus to gas phase oxidation under these conditions; for, if ring fission had occurred to any great extent, fragmentation molecules such as the lower alkenes and carbonyl compounds would have been recorded in the chromatograms between the cyclohexane solvent peak and the fuel peak.

4·2·4 Fuel Mixtures

One of the objects of the present work was to investigate the nature of the combustion phenomena which could be produced with diesel fuel under

Figure 4·11

The Formation of Peroxides and Other Compounds During the Cool-flame Oxidation of n-propylbenzene[178]

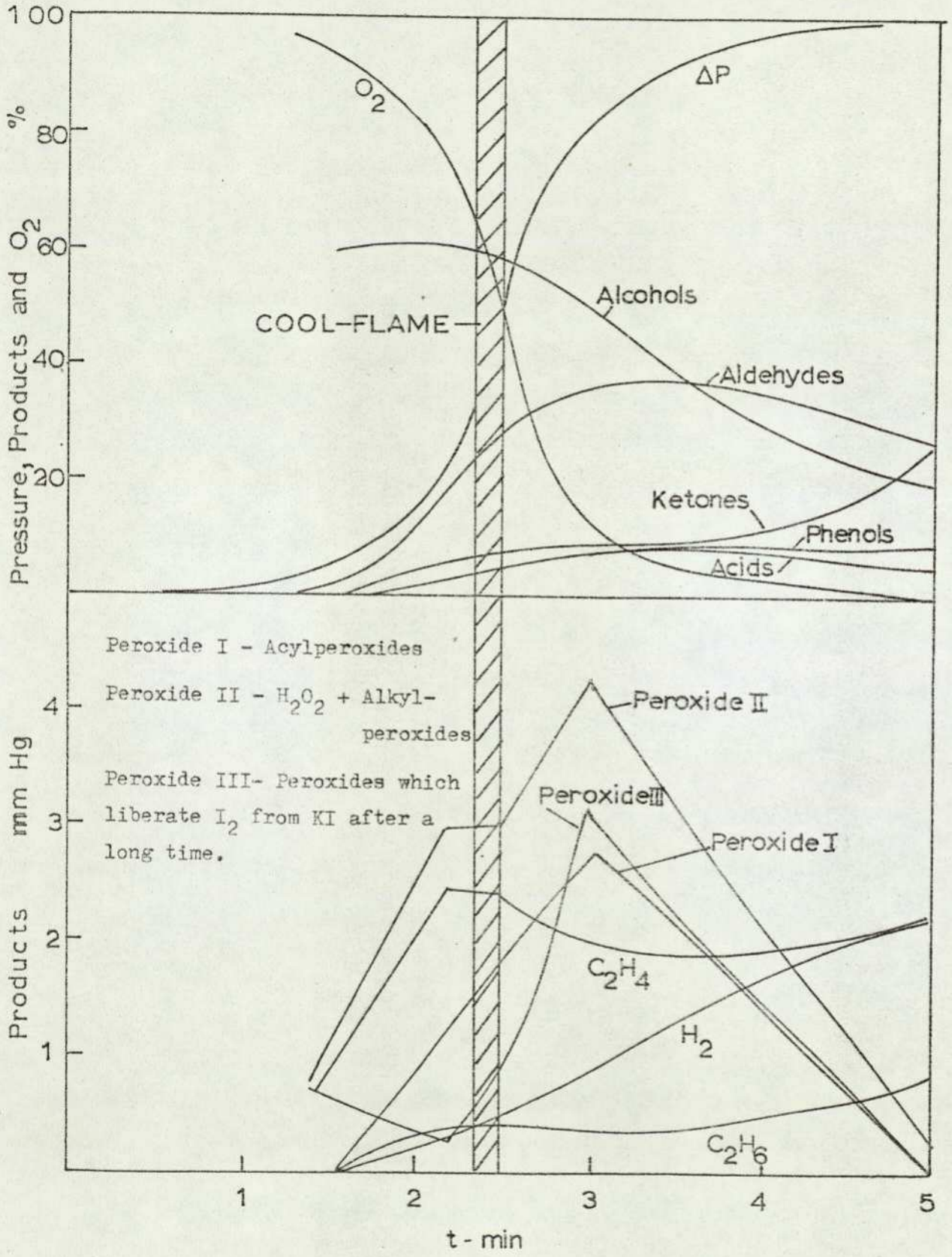

various conditions. A number of workers have investigated the oxidation of multi-component fuels in both static and flow systems, but no studies have previously been made of fuels as complex as diesel fuel. Nevertheless, the data obtained from relatively simple systems provide an insight to the interactions which may be anticipated for diesel fuel.

Salooja[165] observed that the ignition behaviour of binary fuel mixtures was influenced to a greater extent by the more readily ignitable component when the temperature was close to the lowest ignition temperature. Moreover, it was concluded that the type and extent of the preflame interaction were responsible for the ignition behaviour of the mixture. Thus, with mixtures of alkanes and alkenes, the ignition tendency increased even to the extent of exceeding that of the more readily ignitable component due to the enhanced preflame activity of the mixture. For example, in a mixture of hexane and 1-heptene, in which the alkene is slightly less reactive than the alkane, the ignition tendency above 300°C is increased by the presence of the alkene.[164] At lower temperatures the effect on ignition of adding 1-hexene is minimal. These observations suggest that alkenes may be the principal reation intermediates responsible for the high temperature ignition of alkanes and possibly aromatics.

The influence on ease if ignition of adding an aromatic compound to an aliphatic fuel has been investigated[165] using a number of hydrocarbons including benzene and hexane. At temperatures close to the ignition temperature of hexane, the ignition tendency of the fuel blend varied almost linearly with the concentration of the components.

The temperatures used in these studies are directly comparable with the temperatures of the diesel engine combustion chamber wall, i.e. 250-350°C. Here the influence of alkenes will be to promote ignition, but owing to their low concentration in the fuel (i.e. 2-3% by weight) the effect is expected to be small. On the other hand, the aromatic fraction constitutes up to 25% of the diesel fuel and therefore, the retarding influence of the aromatic fraction is appreciable and in fact necessary to prevent fuel detonation on

injection.

At high temperatures, i.e. 750°C, which may be reached by the gases at the centre of the combustion chamber, the ignition tendency of the fuel is influenced to an even greater extent by the more readily ignitable component. For example, a mixture of n-heptane and isopropylbenzene ignites more readily at 750°C than either component of the fuel on its own.[165]

In relation to the present studies, it was found from consideration of the induction periods leading to the first cool-flame that the reactivities of the four fuels tested decreased in the order: hexadecane > 1-decene > diesel fuel > n-butylbenzene. The multiplicity and intensity of, and the induction periods preceeding the the first cool-flame, indicated that diesel fuel behaved in a manner very similar to that of a pure aliphatic hydrocarbon fuel, with n-butylbenzene displaying unique behaviour as regards stabilty. It would appear reasonable, therefore, to consider diesel fuel as an essentially alkane-type fuel system with associated effects which vary in proportion with the concentration and relative reactivity of the alkene and aromatic components present.

4·2·5 Diesel Fuel

4·2·5·1 Constant-Volume Bomb Studies

At 280°C, a boundary condition between cool-flame oxidation and two-stage ignition occurs; the transition was found to be dependent on the equivalence ratio and the initial pressure. For an equivalence ratio of 0·42 and at an initial pressure of 500 torr, two cool-flames are observed. At an initial pressure of 600 torr, the second cool-flame develops into a hot ignition, but two cool-flames can be produced by reducing the equivalence ratio to 0·32. An investigation of the LCA and LCO concentrations near this boundary condition revealed that the two fractions behaved similarly rising and falling in concentration in phase with the pressure changes accompanying the combustion process (Figures 3·22 to 3·24).

Figure 3·22 shows the rapid rise in LCO from zero, prior to ignition, to ca 18 μg/μl less than 0·25 seconds after injection. As the cool-flame front approaches the rate of LCO formation decreases and then, as the first cool-flame passes the LCO concentration falls slightly. A rise in the LCO to a maximum concentration of ca 33 μg/μl occurred simultaneously with the passage of the second cool-flame and then the LCO level remained fairly constant over the remaining period of sampling.

The LCA fraction is seen to behave in much the same manner as the LCO throughout the passage of the cool-flame. However, unlike the LCO the initial LCA concentration is relatively high due to aromatic compounds in the fuel. Since the LCA concentration increases during the course of the reaction it is evident that this fraction does not consist entirely of unburnt fuel components. It will be remembered that a similar increase in LCA was observed for n-butylbenzene which prompted the conclusion that aromatic compounds with strong UV absorbance such as biphenyl and polycyclic aromatic hydrocarbons must be produced during the oxidation. Since these compounds do not possess strong odours their presence in the LCA fraction will weaken the correlation between TIA and LCA and in fact ADL report[106,107] that this correlation is less reliable than the corresponding TIA-LCO relationship.

Two differences in the behaviour of LCA and LCO are apparent from Figure 3·22. The first concerns the position of the maximum concentration of LCA relative to LCO and the second relates to the stabilities of the two fractions. The LCO maximum occurs during the second cool-flame while the LCA maximum occurs after the second cool-flame has passed through the reactants; the LCA concentration then decreases rapidly. The fairly constant LCO level may indicate either that the LCO components are relatively stable under these conditions or that the concurrent decrease in LCA is due to oxidation, the resulting oxygenates offsetting any decrease in LCO which may have occurred. A comparison of Figures 3·22 and 3·25 reveal that the post cool-flame concentration changes of LCA and LCO with time for hexadecane were similar to

those of diesel fuel. Therefore, the above explanation for this behaviour may also apply to the alkane fuel. It is also evident from Figures 3·22 and 3·25 that the LCO levels from diesel fuel are higher by a factor of ca 3·5 than for hexadecane. This is obviously due to the partial oxidation of the aromatic compounds present in diesel fuel.

An increase in the initial pressure to 600 torr, at 280°C produced a two-stage ignition for an equivalence ratio of 0·42, (Figure 3·23). The LCA and LCO levels rose much more sharply prior to the cool-flame than under any of the other conditions used. Both fractions were, however, completely destroyed by the ensuing hot ignition, after which the LCA level rose again fairly quickly although the LCO recovery rate was far more gradual. The final levels reached by the two fractions never equalled the post cool-flame levels recorded under any condition.

As explained previously, the conditions normally supporting two cool-flames would produce a hot ignition if the evacuation time between injections was less than ten minutes. Figure 3·24 contains the results of analysis of a sample collected during such a hot ignition, the extensive reduction in LCA, LCO and subsequently TIA being apparent. The observed destruction of the odorants during hot ignition suggests that a reduction of exhaust odour can be achieved by increasing the percentage of fuel that is subjected to hot ignition. This may be accomplished by improving the air-fuel mixing process thereby increasing the homogeneity of the air-fuel distribution in the combustion chamber.

Figure 3·27 shows the rapid formation of both LCA and LCO during the first few fractions of a second after injection. The oscillating concentrations of the two odour fractions then displayed the familiar trends in relation to the cool-flame pressure pulses. A comparison of these results obtained at 295°C with those produced at 280°C (Figure 3·22) indicates that the LCO fraction does not reflect so precisely the passage of the cool-flame at the higher temperature. It has been stated previously that O-heterocycles reflect with

greater accuracy cool-flame behaviour than do carbonyl compounds. The LCO trend in Figure 3·27 is, therefore, closer to that exhibited by carbonyl products than to that shown by O-heterocycles. This observation may indicate that further oxidation of the O-heterocycles to carbonyls with lower carbon content has occurred at the higher temperature. The TIA values corresponding to the LCO concentrations at 295°C and 280°C indicate that the products formed at the higher temperature are slightly more odorous. It is evident that further research is necessary to establish whether the product spectrum has indeed changed to include more carbonyl and other lower molecular weight oxygenated compounds.

The effect of increasing equivalence ratio on the LCA and LCO levels is shown in Figure 3·28. The results indicate that the two fractions were at maximum comcentrations when the equivalence ratios used were between 0·39 and 0·42. The conclusion to be drawn from these data is that as the equivalence ratio increases, proportionately more fuel is converted to LCO and therefore the odour of the products is much higher. This would appear acceptable on a kinetic basis, i.e. an increase in fuel concentration would increase the reaction rate and thus lead to the greater conversion of fuel to partial oxidation products prior to the sampling point. Above ϕ=0·42, the proportion of LCA and LCO per volume of fuel injected falls until hot ignition occurs and produces the dramatic decrease in both fractions and consequently the odour, as previously recorded.

Further information regarding the products of diesel fuel oxidation is contained in Figures 3·36 to 3·40, which show the pre- and post cool-flame gas chromatograms for samples collected by various methods. Despite the loss of low-molecular weight, low-polarity fuel fractions in the samples, comparison of the pre-cool-flame chromatogram (Figure 3·36) with the post cool-flame chromatogram (Figure 3·37) illustrates that a distinct change in the sample components has occurred. Table 4·2 lists the Kovats Indicies of 119 standard compounds which IIT[109] classified in their study of

Table 4·2

The Kovats Indices and Retention Time Data for Standard Compounds Used by IITRI to Identify the Odorants in Diesel Engine Exhaust

Compound	Kovats Index Carbowax 20M	Retention Time[a] Apiezon L (min)
Pentane	500	0.37
1-Pentene	536	0.30
3-Methylpentane	570	0.82
2-Pentene	571	0.43
Hexane	600	1.03
1-Hexene	642	0.85
2,2,4-Trimethylpentane	653	2.11
2-Hexene	670	1.07
Heptane	700	2.50
Cyclohexane	719	2.41
Dimethylhexane	723	3.15
1-Heptene	740	2.10
3-Heptene	743	2.33
2,3,4-Trimethylpentane	756	3.72
2,3,5-Trimethylhexane	764	4.04
Propanal	792	0.40
Octane	800	4.97
1,2-Epoxybutane	826	0.64
1-Octene	830	3.95
2-Methyltetrahydrofuran	858	1.22
2-Ethyl-1-hexene	860	4.09
Methanol	862	0.34
2-Octene	870	4.10
Butanal	871	0.60
2-Propanol	883	0.29
Diethylsulfide	889	1.35
2-Butanone	893	0.44
2,5-Dihydrofuran	897	0.69
Nonane	900	7.40
Tetrahydropyran	910	1.53
Ethanol	912	0.43
2-Methyltetrahydropyran	918	2.00
Benzene	920	1.12
Dihydropyran	925	1.21
1-Nonene	931	5.43
Ethyl-n-propanoate	946	0.76
2-Pentanone	966	0.70
Pentanal	970	0.79
Thiophene	984	0.96
Decane	1000	8.86
Ethyl-n-butanoate	1023	1.16
Toluene	1025	1.72
2-Butenal	1027	0.48
n-Propyl-n-propanoate	1033	1.30
2-Octyne	1034	2.50
1-Decene	1035	6.38
Di-n-propylsulfide	1060	2.74
Hexanal	1070	1.18
Furaldehyde	1075	0.91
Undecane	1100	9.40
n-Propyl-n-butanoate	1110	1.69
Ethylbenzene	1112	2.14
1-Butanol	1118	0.55
Ethyl-n-pentanoate	1123	1.53
p-Xylene	1124	2.32
Nitromethane	1130	0.09
m-Xylene	1130	2.27
2-Heptanone	1170	1.30
Heptanal	1175	1.41
Methyl-n-hexanoate	1175	1.46
Cyclopentanone	1176	0.75
o-Xylene	1176	2.20
Dodecane	1200	9.61
n-Propyl-n-pentanoate	1209	2.05
Ethyl-n-hexanoate	1223	1.88
1-Pentanol	1225	0.80
1,3,5-Trimethylbenzene[b]	1227	2.60
1-methyl-2-ethylbenzene[b]	1242	2.40
1-methyl-3-isopropylbenzene[b]	1248	2.77
1-methyl-4-isopropylbenzene[b]	1248	2.92
Di-n-butylsulfide	1257	3.72
1,2,4-trimethylbenzene[b]	1262	2.57
2-Octanone	1275	1.58
Methyl-n-heptanoate	1276	1.76
Octanal	1280	1.72
1,3-Diethylbenzene[b]	1281	2.85
1-Methyl-3-n-propylbenzene[b]	1284	2.87
Cyclohexanone	1288	1.02
1-Methyl-4-n-propylbenzene[b]	1289	2.92
1,4-Diethylbenzene[b]	1297	2.90
Tridecane	1300	9.83
1,3-Dimethyl-5-ethylbenzene[b]	1300	2.80
n-Propyl-n-hexanoate	1308	2.35
1,2,3-Trimethylbenzene	1320	2.39
Ethyl-n-heptanoate	1323	2.18
1-Hexanol	1331	1.03
4-Methylcyclohexanone	1338	1.22
1,1-dimethylindan[b]	1363	2.90
Cyclohexanol	1380	0.81
Methyl-n-octanoate	1380	2.02
Nonanal	1387	2.00
Tetradecane	1400	10.03
n-Propyl-n-heptanoate	1409	2.63
Ethyl-n-Octanoate	1425	2.49
1-Heptanol	1438	1.23
2-Furaldehyde	1467	0.63
Methyl-n-nonanoate	1483	2.29
Decanal	1494	2.27
Pentadecane	1500	10.28
n-Propyl-n-octanoate	1511	2.91
Furfurylacetate	1520	0.65
Benzaldehyde	1527	0.74
Ethyl-n-nonanoate	1527	2.75
1-Octanol	1547	1.44
Methyl-2-furoate	1573	0.55
Tetrahydrofurfurylacetate	1573	1.05
Methyl-n-decanoate	1587	2.53
1,1,4,6-Tetramethylindan[b]	1587	3.41
Undecanal	1600	2.57
Hexadecane	1600[c]	11.74
Tetrahydrofurfurylpropionate	1643	1.13
p-Tolualdehyde	1658	0.96
Acetophenone	1659	0.83
2,6-dimethyltetralin[b]	1669	3.61
Heptadecane	1700	15.8
Octadecane	1800	24.0
2,2,5,7-Tetramelhyltetralin[b]	1811	6.10
2,5,8-Trimethyltetralin[b]	1884	6.69
Nonadecane	1900	37.8

[a] Apiezon L retention time is corrected for column dead volume.

[b] Hydrocarbon standards supplied by Mobil Research and Development Corporation.

[c] After Kovats Index 1600 the temperature program has ended and the temperature is maintained at 180°C.

diesel engine exhaust. Figure 4·12 shows a C20M chromatograms obtained for a diesel engine exhaust sample. The odour descriptors have been assigned to each peak of interest. From a comparison of Figure 4·12 and Figure 3·37 it would appear that the chromatogram produced in this study contains all the odour-relevant components. This observation supports the conclusion that odour-relevant compounds, similar in molecular weight and polarity to those present in diesel engine exhaust, are produced during the cool-flame oxidation of diesel fuel in a static vacuum system.

The post cool-flame chromatogram contains components with KI > 900 which are missing from the pre-cool-flame sample analysis. Within this band, labelled (1) in Figure 3·37, the lower aliphatic aldehydes ranging from ethanal to butanal are eluted, and although IIT confirmed their presence by mass-spectroscopy, the contribution of these compounds to the odour of diesel exhaust was considered insignificant, - largely due to their low concentrations and realtively high odour thresholds. The alkyl substituted benzenes (LCA components) above ethylbenzene are eluted mainly in bands (2) and (3); the alkyl substituted indans(LCA) and the higher molecular weight carbonyl compounds above nonal (LCO) are eluted in bands (3) to (5); the alkyl substituted tetralins (LCA) and the aromatic aldehydes (LCO) have a much higher boiling point and polarity and are therefore eluted in and after band (5). Most of the ADL classified odour components are eluted before nonadecane (KI=1900) and as such, must be present, albeit unresolved, in Figure 3·37.

4·2·5·2 Engine Studies

One of the most enlightening studies of the formation of diesel exhaust odorants was carried out by Barnes[86], who used a threshold dilution technique to assess the odour of samples collected from a heptane-fuelled engine, operating with various intake atmospheres. The artificial atmospheres consisted of mixtures of an inert monatomic or polyatomic gas (He, Ar, N_2 and CO_2) and oxygen. The inert gas was either substituted for the proportion of

Figure 4·12

IITRI Carbowax 20M Chromatogram of Diesel Engine Exhaust

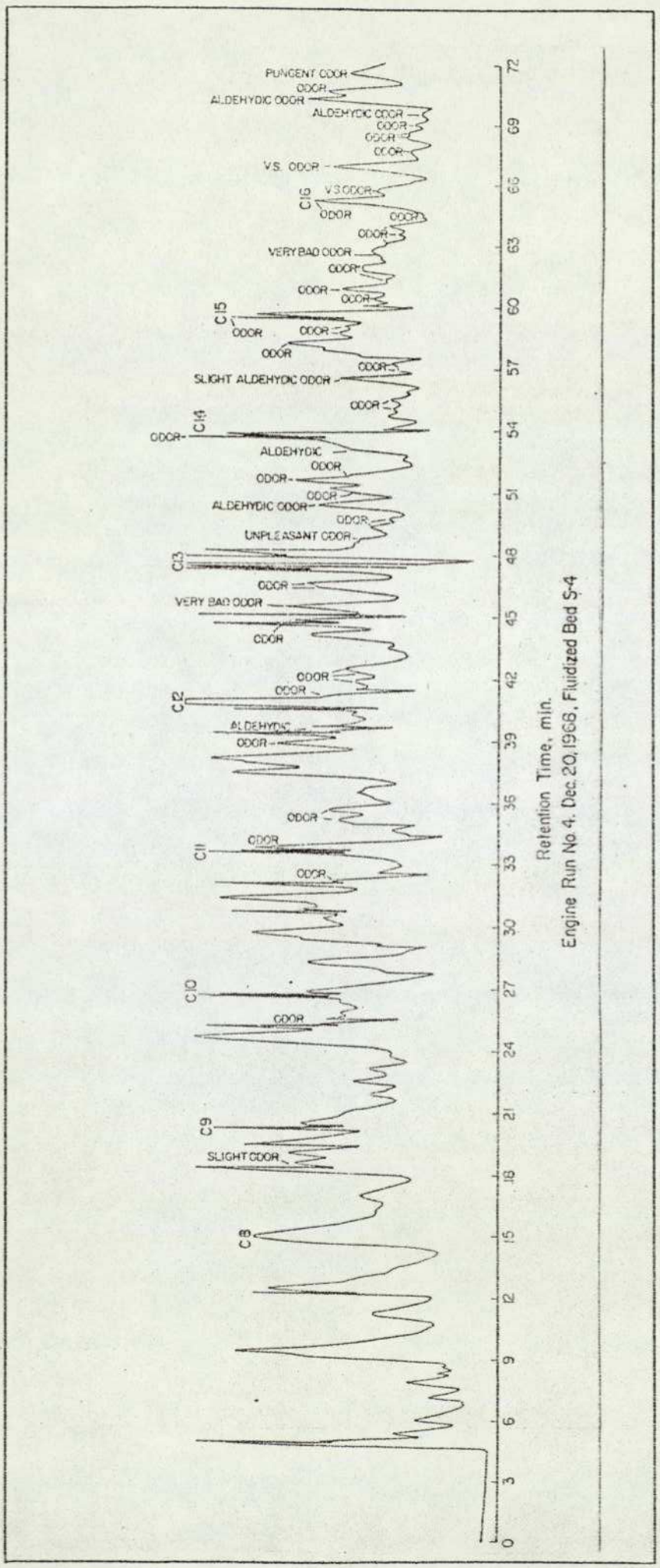

nitrogen in air or was added to air as a diluent. The three phases of combustion, defined in Section 4·1, are known to be affected by the nature of the intake atmosphere since the diffusional mixing processes, fuel spray patterns, droplet distributions, compression and combustion temperatures and combustion limits within the chamber, are altered. The odour results obtained could not be explained by changes in the diffusional processes, in the fuel spray patterns or the cycle temperatures; a good correlation was found, however, between the measured exhaust odour thresholds and the lean flammability limits of premixed heptane flames. The lean flammability data for heptane was obtained by extrapolating the results published by other workers who have studied the combustion of various fuels in the specified atmospheres. Since these results were published, Varghese et al[179] have produced data which have provided the necessary lower flammability limits of heptane in the artificial atmospheres used. The new data changed the correlation obtained by Barnes,[86] but it is still positive, thus supporting the conclusions originally drawn.

A normalised lean flammability limit (LFL), defined as the ratio of the LFL (% of fuel) in the intake atmosphere of interest to the LFL for the same fuel in air, was used to assess the effect of the inert gas on the flammability of the fuel-oxidant mixture. Values of this ratio greater than unity indicate that more fuel is required before the mixture is flammable as compared with the combustion of that fuel in air. Figure 4·13 shows the odour threshold dilution ratio vs. (LFL) / (LFL in air); a good correlation is evident. Table 4·3 contains other details of the LFL ratio - odour correlation reported[86] and the fuels used.

The correlation between the LFL's measured in homogeneous fuel oxidant mixtures and the odorous levels produced under heterogeneous diesel fuel combustion indicates that the reactions involved in the premixed burning phase of the combustion process are responsible for odorant formation. The odorants formed in the premixed burning phase of the process, suffer only partial oxidation due to the lean stoichiometry of the region; these partial

Figure 4·13

Effect of Combustion Limits on Exhaust Odour Levels[86]

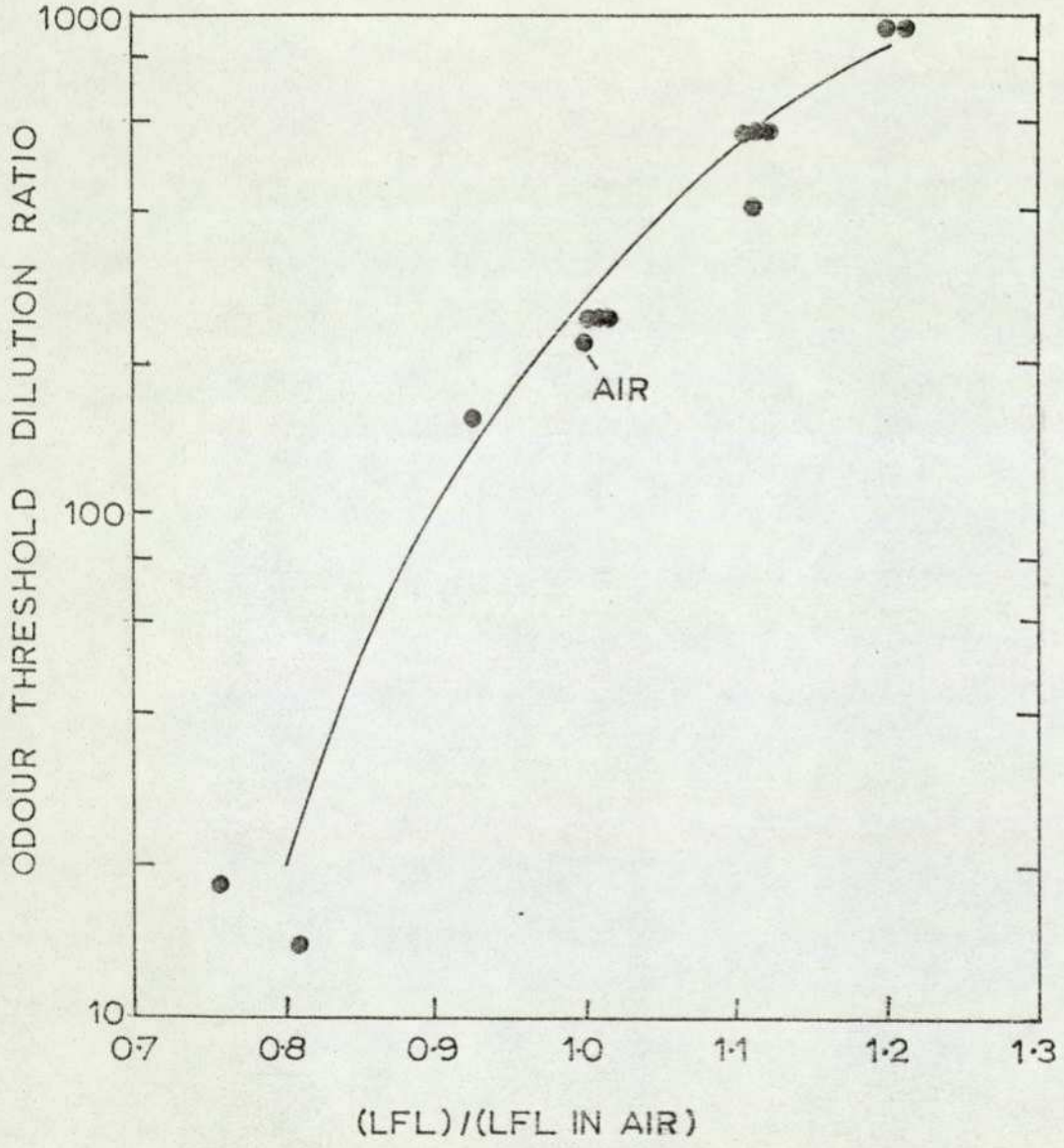

Table 4·3

Odour Levels vs. Lean Flammability Limits[86]

Intake Atmosphere % by Volume	Odour Level D_{50}	LFL/LFL in Air
21 O_2 + 79 N_2	228	1·000 (All Fuels)
21 O_2 + 79 Ar	17	0·752 (C_3H_8)
21 O_2 + 79 He	14	0·807 (C_3H_8)
		1·204 (CH_4)
71 O_2 + 29 CO_2	930	
		1·216 (C_3H_8)
17·5 O_2 + 65·8 N_2 + 16·7 Ar	160	0·930 (CH_4)
		1·013 (CH_4)
17·5 O_2 + 65·8 N_2 + 16·7 N_2	247	1·008 (C_3H_8)
		1·016 (n-C_6H_{14})
		1·112 (CH_4)
17·5 O_2 + 65·8 N_2 + 16·7 CO_2	545	1·168 (C_3H_8)
		1·183 (n-C_6H_{14})
12·2 O_2 + 45·8 N_2 + 42·0 N_2	392	1·168 (C_3H_8)

oxidation products then survive the subsequent diffusion combustion process and are emitted as odorants. This effect would be most pronounced at idle and light load, where the temperatures and the F/A ratios are lower.

The results obtained by Barnes[86] indicate that argon-oxygen and helium-oxygen mixtures permit the combustion of leaner mixtures than does air, and would therefore be expected to produce smaller amounts of partially oxidised fuel. Consequently the exhaust would be less odorous, a fact verified by the data in Table 4.3 . The converse situation occurs with carbon-dioxide, which will only support the combustion of mixtures richer than those which will just ignite in air.

Several contributory factors combine to influence the mechanism by which the addition of an inert gas alters the flammability limits of a fuel oxidant mixture. Additives such as oxygen, nitrogen, helium and argon are chemically inert but they do influence the physical properties of the mixture, such as the thermal conductivity, specific heat etc. Carbon dioxide and nitrogen have been found in many other studies[180] to reduce the speed with which a flame propagates through the reactant mixture, to narrow the flammability range and to shift the maximum flame speed towards smaller percentage fuel content. The addition of the inert gas seems mainly to affect the flame speed by altering the ratio of the thermal conductivity to the specific heat. Addition of helium or argon increases this ratio and therefore the flame speed. The observations reported by Barnes[86] can be rationalised on this basis.

It will be appreciated from Section 1.4.5. that the LFL conditions exist in the lean flame out region (LFOR) specified by Henein[68] in his combustion model. Henein proposed that this region would be a rich source of partially oxidised hydrocarbons and pollutants. Further support for this hypothesis is provided by Trumpy[181] et al who studied the effect of inlet temperature and equivalence ratio on the odour produced by a premixed n-heptane-air fuelled, motored CFR engine. The results are shown in Figure 4.14 (a) and (b). Pressure recordings showed that below the lower line in (a), no energy was released

Figure 4·14

(a) Summary of Smoke, Odour and Eye Irritation Results from an n-heptane Fuelled Engine[181]

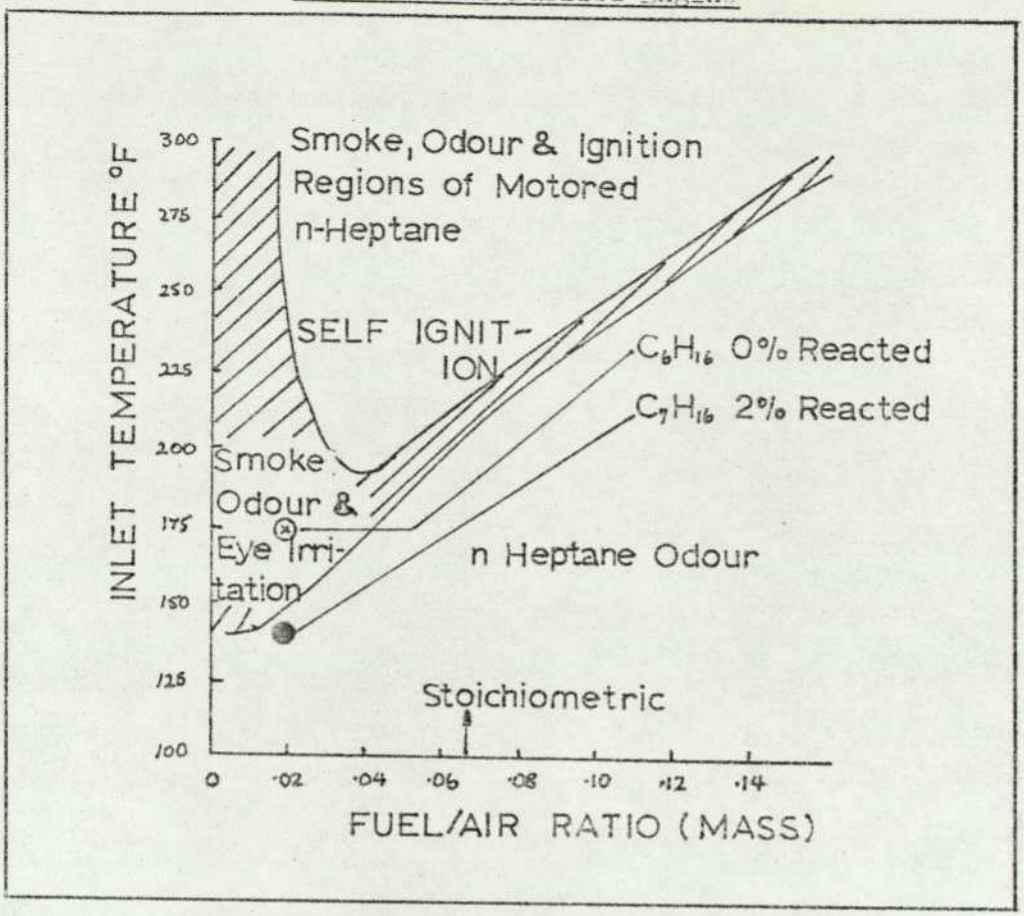

(b) Pressure History Showing Self Ignition of an 80:1 A/F Mixture

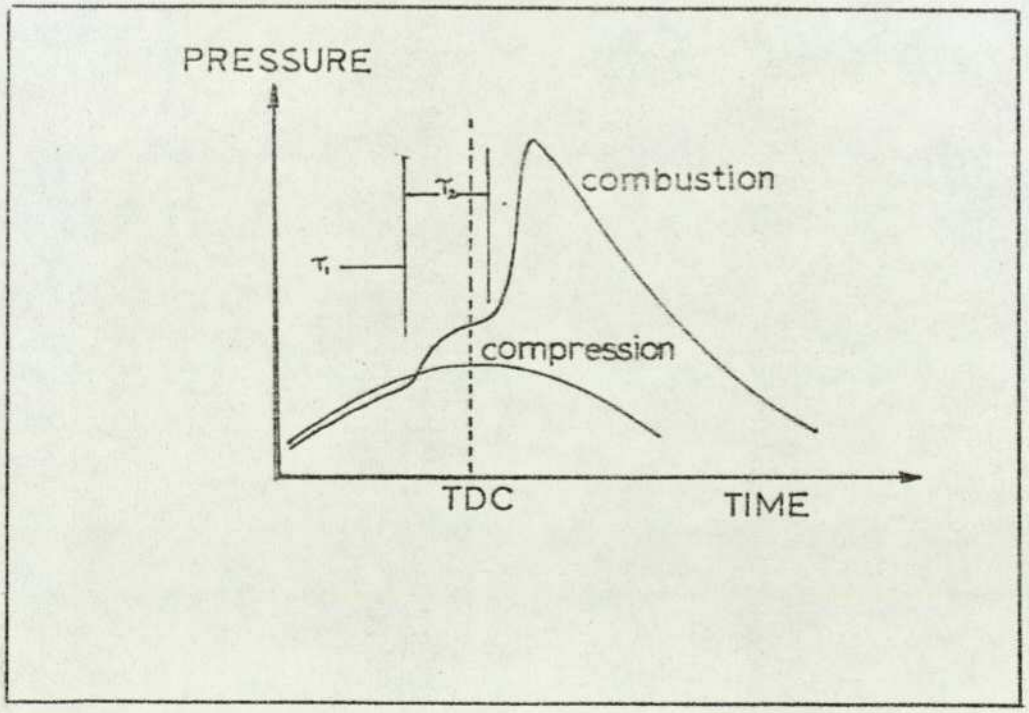

during the compression stroke and the observed odour was that of n-heptane only. In the area between the two unshaded regions, smoke, odour and eye-irritation were observed in the exhaust. Under these conditions, the pressure traces showed energy release, indicating the occurrence of oxidation reactions. In the upper region, ignition occurred in two stages, as shown in Figure 4·14 (b) which reduced the concentration of the partially oxidised products. Trumpy[181] concluded that the smoke, odour and eye-irritaion were a result of exposure to the exhaust components when the second stage of combustion was quenched.

It is evident that the results recorded during these engine studies are very similar to those obtained during the present work. Experimental evidence from the bomb and the engines confirms that the odorous components in diesel engine exhaust are formed mainly during the premixed phase of combustion. Oxidation of various fuels in the bomb under premixed conditions shows that the principal mechanism for odorant formation is the classical degenerately branched chain reaction. This mechanism, which is manifested in the propagation of cool-flames, occurs with fuel-lean mixtures at temperatures and pressures which are too lean for hot ignition. These studies have also shown that as the fuel concentration decreases towards the LFL under conditions of fixed temperature and pressure, the oxidation mechanism changes from single or multi-stage ignition to cool-flame oxidation. This change in mechanism is accompanied by a large increase in odorant concentration - an observation which correlates well with the LFL hypothesis established on the basis of engine studies. Conversely, the change from cool-flame to hot ignition results in a sharp decrease in odour, both in the engines and in the bomb.

4·2·5·3 Odour-Relevant Chemical Classes

Information obtained from conventional gas phase oxidation studies involving a variety of fuels shows that odorants are formed via decomposition of organic intermediates and by fuel pyrolysis which occurs in the high temperature, fuel-rich zones of the combustion chamber. The reaction mechanism

involves the production of aldehydes and peroxides as a first stage reaction, which occurs slowly. Then in the second stage, there is rapid decomposition of these same compounds leading to autoignition. If the critical conditions for hot ignition are not attained uniformly throughout the combustion volume then partial oxidation products, such as aldehydes, will remain after hot ignition has occurred in other regions of the chamber. Since the odour-producing species in diesel exhaust are known to be present in very low concentrations, i.e. ppm or less, the amounts of aldehyde surviving the hot ignition process would not have to be very large to produce a significant odour.

Many investigators have sought a correlation between the concentration of aldehydes in the exhaust and the odour intensity; some have claimed that the correlation is positive,[76,182-186] while others[187,188] have dismissed any relationship. Often the correlation is weakened or even destroyed through inefficient collection or inappropriate analysis techniques. The two most frequently used methods for measuring aldehyde concentrations employ MBTH (3-methyl-2-benzothiazolone hydrazone hydrochloride) or 2:4 DNPH (2:4-dinitrophenylhydrazine) reagents. The first reagent, used in a method devised by Sawicki et al,[189] is sensitive to formaldehyde and other water-soluble aliphatic aldehydes. The second reagent will form a hydrazone with many aldehydic and ketonic compounds but is less sensitive to large sterically hidered aromatic carbonyl compounds. Since the aromatic aldehydes may constitute more than 25% of the total aldehydes[185] in diesel exhaust it is evident that neither of these methods is entirely satisfactory for estimation of the total carbonyl content of diesel exhaust. Skala et al,[186] with the assistance of mass spectrometric data suggest that the main odorants are the aromatic carbonyl compounds, benzaldehyde, indanone, indenone, cinnamaldehyde, naphthaldehyde, acenaphthenone, fluorenone and higher homologues. Moreover, it is stated that the exhaust gases were free of 'diesel odour' when the engine was operated with a fuel containing only n-alkanes. The results pertaining to the predominance of the aromatic carbonyls supports the results of the ADL programme since the LCO fraction is said to consist

primarily of these compounds. Besides the aromatic carbonyls, Skala[186] identified aldehydes and ketones formed from alkanes, cycloalkanes and alkenes. The levels of the aldehydes are said[185,190] to be related to those of the unburned hydrocarbons, the levels of the latter being a very good measure of the odour[191] provided that the hydrocarbon levels are in excess of 100ppm. These observations are in agreement with the combustion model in which the regions of the combustion mixture which are excessively lean or rich permit the survival of fuel molecules and are also conducive to the formation of partial oxidation products.

Analogous to the concept of co-carcinogens is the idea that some of the other components in diesel exhaust exert a synergistic effect in conjunction with the true odorants. Examples of compounds falling into this category are the oxides of nitrogen, the oxides of sulphur, particulates and acids. A brief review of the current theories relating to these species is given below.

Vogh[187] has suggested that NO_x is of some importance in the overall odour stimulus of diesel exhaust, but this view is not widely accepted.[185,192] With regard to SO_x, O'Donnell and Dravnieks[109] found from mass spectrometric data that in addition to the partial oxidation products of hydrocarbons, sulphur species were among the important odour contributors, while more recent work,[193] in aggreement with Vogh[187] suggests that this is not so. It is evident that these opposing views must await further investigation before the role of the individual species can be assessed.

Finally, particulates and especially organic acids are often quoted as contributing to the perception of odour, acting via an irritation effect which increases the olfactory sensitivity to the real odorants. Once again further investigation is needed to resolve the contribution of these components but the consensus of opinion indicates that they are important in determining the overall character of diesel odour, providing a background on which the more characteristic odour notes are superimposed.

4.3 Summary and Conclusions

Combustion studies performed, both 'in cylinder' and in a laboratory combustion apparatus indicate that the initial stages of diesel engine combustion is a degenerately branched chain reaction, the mechanism being fundamentally dependent on the formation and decomposition of aldehydes and peroxides. Results obtained from laboratory combustion studies which are applicable to the diesel engine have shown that the variety and diversity of the chemical compounds formed can be explained on the basis of the further reactions of alkylperoxy radicals initially formed. The trends exhibited by the LCA and LCO fractions in the present study indicate that the odorants are being formed,at low temperatures, by the alkylperoxyradical route and that odorant formation is highest under cool-flame conditions.

With regard to the engine system, it is evident that the partial oxidation products which constitute the odorants, are formed primarily, although not exclusively, in the regions of lean combustion, ie: the extreme edges of the fuel spray. It is at these positions that the cool-flame preignition reactions are quenched prior to the onset of hot ignition, possibly by diffusion of radicals to the walls; thus high concentrations of partial oxidation products which make up the LCO fraction remain.

Since the alkane components in diesel fuel are the most readily ignitable, it is to be expected that these compounds will initiate the combustion process. At low temperatures, the combustion mechanism involves the formation of alkylhydroperoxides and hydroperoxyalkyl radicals. The decomposition of the former leads to chain-branching, while decomposition of the latter results in the formation of a wide variety of oxidation products, many of which such as the O-heterocycles, eg: alkyl substituted furans and furanones have very low odour thresholds. At higher temperatures, large quantities of alkenes are probable reaction intermediates; further

oxidation of these compounds produces unsaturated carbonyls e.g. acrolein and crotonaldehyde, which have been identified in diesel engine exhaust and have extremely strong odours.

The aromatic and branched chain alkane fuel components are less easily oxidised and are therefore expected to produce large quantities of only partially oxidised compounds at low temperatures. It is the oxygenated aromatic fraction which has been identified as being the most odorous in diesel exhaust. However, the concentrations of these compounds, together with those of any other components, are greatly decreased as a result of hot ignition. Thus, if the whole of the diesel engine combustion volume were to undergo hot ignition, the exhaust would not present a serious odour problem.

Throughout this study, the ADL correlation between the concentration of LCO in the exhaust and the odour intensity was assumed to be correct, since the extensive facilities required to test the correlation were not available. The consensus of opinion regarding the possibility of legislation being based on the measurement technique is, that, even if further investigation reveals that the present correlation, or a derivative thereof, is applicable to a wide range of engine designs and fuel types, the method must be simplified before it is accepted as a standard technique. One method of reducing the sample analysis time would be to eliminate the liquid chromatography separation step. A very brief investigation into the possibility of relating the odour intensity, as measured by the LCO concentration, to the total U.V. absorbance of the combined LCA and LCO fractions, was made in this work. Figures 3·33 and 3·35 contain the data collected during the analysis of the products formed from diesel fuel and from hexadecane respectively. The plots of LCO and LCA against total absorbance of the cyclohexane eluent indicates that a high degree of correlation does indeed exist between both odour fractions and the total absorbance. These results suggest therefore, that for high concentrations of LCA and LCO, the odour may be estimated from the total U.V. absorbance at 254 nm of the products eluted from the traps, thus removing

the necessity for LC separation of the LCA and LCO fractions. However, further investigation involving the analysis of diesel exhaust samples is necessary before liquid chromatographic separation of the odour fractions can be assumed to be redundant.

Diesel exhaust odour is indicative of incomplete fuel combustion, two fundamental consequences of which are energy wastage and pollution. In view of the very favouable brake specific fuel consumption figures of the diesel engine, (in comparison with the gasoline and other engines) energy wastage is perhaps less important than pollution. Indeed, it is the latter aspect which will affect the prospects of the diesel engine and the plans for 'dieselisation' of the lighter transport vehicles e.g. passenger cars.

This study, in the broader sense, shows that the ADL technique produces results which are not only reproducible, but are meaningful in the context of current combustion theory. It is suggested, therefore, that the technique should be used for assessing diesel engine combustion chamber and fuel injection equipment designs in an attempt to optimise efficient combustion characteristics. A significant and noticeable reduction of diesel exhaust odour would remove one of the main obstacles to the widespread use of one of the most efficient and reliable forms of power plant available today.

REFERENCES

1. Springer, K.J and Stahman, R.C.SAE Paper 750332, Feb 24-28th (1975)

2. Product Notes, Chemistry and Industry, No.9,p v, 7 May (1977)

3. Larsen, R.I.J.Air Polln. Control Assoc. 20, 4, (1970)

4. 'Managing the Environment', pp 6 and 17, A report of the Subcommittee on Science, Research and Development, U.S. House of Representatives, Washington, D.C. (1968)

5. Reading, A.R.'The Carcinogenic Potential of Diesel and Gasoline Engine Emissions' June (1975)

6. Levins, P.L., Kendall, D.A., Caragay,A.B., Leonardos, G and Oberholtzer, J.E. SAE Paper 740216 Feb 25- March 1 (1974)

7. Reckner, L.R., Scott, W.E and Biller, W.E Proc. Am. Petrol. Inst. 45, 111 (1965)

8. 'Particulate Polycyclic Organic Matter'. Committee on Biologic Effects of Atmospheric Pollutants. Natl. Acad. Sciences, Washington, D.C. (1972)

9. Kotin, P., Falk, H.L., Mader, P and Thomas,M. A.M.A. Arch Ind. Hyg. 9, 153 (1954)

10 Begeman, C.R and Colucci, J.M. SAE Paper 700469 (1970)

11 Kotin, P.,Falk, H.L and Thomas, M. A.M.A. Arch. Ind. Health 9, 146 (1954)

12 Kotin, P., Falk, H.L and Thomas, M. A.M.A. Arch. Ind Health 11, 113 (1955)

13 Donnovan, B.J., Mason, W.A., Orman, P.L and Daniels, P.H. Proc. of Conf. 'The Mechanical Engineers' Contribution to Clean Air'. Inst. Mech. Eng. 19-21 Feb (1957)

14 Johnston, H and Lyons, M.J. Brit. J. Cancer 11, 60 (1957)

15 Kotin, P., Falk, H.L and Thomas, M. Cancer 9, 905 (1956)

16 Concawe Ad Hoc Group Report No. 6/74 'Effect of Gasoline Aromatic Content on Polynuclear Aromatic Exhaust Emissions.

17 Doll, R. Brit. Med. J. 2, 521 (1953)

18 Commins, B.J., Waller, R.E and Lawther, P.J. Brit. J. Ind. Med. 14, 232 (1957)

19 Raffle, P.A.B. Brit. J. Ind. Med. 14, 73 (1957)

20 Moore,G.E and Katz, M. Int. Journal Air Polln. 2, 221 (1960)

21 Affleck, W.S and Fish, A. Eleventh Symp. (Int.) on Comb., p. 1003 The Comb. Institute (1967)

22 Semenov,N.N.'Some Problems of Chemical Kinetics and Reactivity' Pergamon Press London (1958)

23 Cullis, C.F and Hinshelwood, C.N. Disc. Faraday Soc. 2, 117 (1947)

24 Semenov,N.N.'Some Problems of Chemical Kinetics and Reactivity' Pergamon Press London 2, 128 (1958)

25 Szabo, Z.G. Thirteenth Symp. (Int.) on Comb., p. 216, The Comb. Institute (1971)

26 Benson, S.W. 'The Mechanisms of Pyrolysis, Oxidation and Burning of Organic Compounds' NBS Publication 357, p. 121. U.S. Dept. of Commerce, (1972)

27 Markevich, A.M. Zh. Fiz. Khim. 22, 94 (1948)

28 Baker, R.R and Yorke, D.A. J.Chem. Ed. 49, 351 (1972)

29 Zeelenberg, A.P and Bickel, A.F. J. Chem. Soc. 4014, (1961)

30 Fish,A. Proc. Roy. Soc. A298, 204 (1967)

31 Barat, P., Cullis, C.F and Pollard, R.T. Thirteenth Symp. (Int.) on Comb., p. 179, The Comb. Institute.(1971)

32 Cullis,C.F., Fish, A and Trimm, D.L. Proc. Roy. Soc. A273, 427 (1963)

33 Cullis, C.F., Saeed, M and Trimm, D.L. Proc. Roy. Soc. A300, 455 (1967)

34 Knox, J.H. Comb. and Flame, 9, 297 (1965)

35 Ray, D.J.M and Waddington, D.J. Symp. on Mechanism of Hydrocarbon Oxidation,Hungary (1973)

36 Cullis, C.F., Saeed, M and Trimm, D.L. Proc. Roy. Soc. A289, 402 (1966)

37 Berry, T., Cullis, C.F and Trimm D.L. Proc. Roy. Soc. A316, 373 (1970)

38 Bawn, C.H and Skirrow, G. Fifth Symp.(Int.) on Comb., p. 521 (1955)

39 Walsh, A.D. Trans. Faraday Soc. 42, 269 (1946)

40 Schmidt, C and Sehon, A.H. Canad. J. Chem. 41, 1819 (1963)

41 Fish, A. Quart. Rev. (London) 18, 243 (1964)

42 Minkoff, J.G and Tipper, C.F.H.'The Chemistry of Combustion Reactions' Butterworths (1962)

43 Poroikova, A.I and Nalbandyan, A.B., Kinetika i Kataliz, 12, 849 (1971)

44 Cullis, C.F., Fish, A and Gibson, J.F. Proc. Roy. Soc. A284, 108 (1965)

45 Lewis, B and von Elbe, G. 'Combustion, Flames and Explosions of Gases' Second Ed. Acad. Press. Inc. p. 668 (1961)

46 Boerlage, G.D and Broeze, J.J. Ind. Engng. Chem. 28, 10 (1936)

47 Henein, N.A. Prog. Energy Combustion Sci. 1, 165 (1976)

48 Austen, A.E.W and Lyn, W.T. Comb. and Flame 2, 438 (1958)

49 Lyn, W.T. J. Inst. Petrol. 43, 25 (1957)

50 Schlichting, H.'Boundary Layer Theory' McGraw-Hill N.Y. (1955)

51 El Wakil, M.M., Myers, P.S and Uyehara, O.A. SAE Trans. 64, 712 (1956)

52 Chow, W., Uyehara, O.A and Myers, P.S. SAE Natl. Diesel Engine Meeting St. Louis Oct. 31 (1952)

53 Yu, T.C., Collins, R.N., Mahadevan, K., Uyehara, O.A and Myers, P.S. SAE Trans. 64, 690 (1956)

54 Hinze, J.O. Appl. Sci. Res. A1 (1949)

55 Sass, R.'Compressorless Diesel Engines' Springer, Berlin (1929)

56 Lee, D.W.'The Effect of Nozzle Design and Operating Conditions on the Atomisation and Distribution of Fuel Sprays' NACA Report 425, (1932)

57 Lichty, L.C.'Combustion Engine Processes' McGraw-Hill. N.Y. (1967)

58 Hurn, R.W.'Combustion Characteristics-Ignition Delay Bomb' CRC Diesel Bomb Advisory Group Progress Report Feb (1951)

59 Miller, C.D. SAE Transactions 53, 719 (1945)

60 Rothrock, A.M and Waldron, C.D.'Fuel Vaporisation and its Effect on Combustion in High Speed Compression Ignition Engines' NACA TRR 435 (1932)

61 Wentzel, W. 'Ignition Process in Diesel Engines' NACA TM 797 (1936)

62 Schmidt, F.A.F. 'Theoretical and Experimental Study of Ignition Lag and Engine Knock' NACA TM 891 (1939)

63 Small, J. Engineer 164, 668 (1937)

64 Stringer, F.W., Clarke, A.E and Clarke, J.S. Lucas Engng. Rev. 5, 30 (1971)

65 Henein, N.A and Bolt, J.A. SAE Paper 670007 (1967)

66 Ranz, W.E and Marshall, W.R. Chem. Eng. Prog. 48, 141 (1952)

67 Borman, G.L and Johnson, J.H. Paper 598C Presented at SAE Natl. Powerplant Meeting Philadelphia Oct (1962)

68 Henein, N.A. SAE Paper 710220 (1971)

69 Scott, W.M. SAE Paper 690002 (1969)

70 Rife, J and Heywood, J.B. SAE Paper 740948 (1974)

71 Watts, R and Scott, W.M. Diesel Engine Combustion Symposium pp 167-177 Inst. Mech. Eng. London April (1970)

72 Henein, N.A and Bolt, J.A. Transactions CIMAC 9th Int. Congress on Combustion Engines, Stockholm, Sweden Paper A-7 pp1-36 (1971)

73 Fristrom, R.M and Westenberg, A.A. 'Flame Structure' McGraw-Hill N.Y. (1965)

74 Landen, E.W. SAE Journal 54, 270 (1946)

75 McCreath, C.G and Chigier, N.A. Fourteenth Symp.(Int.) on Comb., The Comb. Institute (1972)

76 Rounds, F.G and Pearsall, H.W. SAE Quart. Trans. 65, 608 (1957)

77 Dravnieks, A. Tech. Ass. Pulp and Paper Ind. 55, 737 (1972)

78 Woskow, M.H. In 'Theories of Odour and Odour Measurement', Robert College Bebek, Istanbul, Turkey (1968) p. 147

79 Engen, T. and McBurney, D.H. J. Exp. Psychol. 68, 435 (1964)

80 Leonardos, G., Kendall, D and Barnard, N. J. Air Polln. Control Assoc. 19, 51 (1959)

81 Foster, D. 'Limitations of Subjective Measurement of Odours' ASTM Special Technical Publication No. 440, p17, (1968)

82 Turk, A. 'Selection and Training of Judges for Sensory Evaluation of Diesel Odours' Cincinnati, Ohio, U.S. Dept. Health, Educ. Welf. NCAPC (1967)

83 Green, D.M and Swets, J.A. 'Signal Detection Theory and Psychophysics' New York, John Wiley and Sons (1966)

84 Egan, J.P. and Clarke, F.R. In 'Experimental Methods and Instrumentation in Psychology'(Sidowski. Ed.) New York, McGraw-Hill (1966)

85 Engan, T. In'Advances in Chemosensing' Vol. 1 (Moulton, Johnston and Turk Ed.) New York, Appleton Century Crofts (1970)

86 Barnes, G.J. SAE Paper 680445 (1968)

87 Colucci, J.M and Barnes, G.J. SAE Paper 700105 (1970)

88 Urlaub, A.'Investigations into the Question of Exhaust Gas Odour from Direct Injection Diesel Engines' MAN-Nuremberg Works (1974)

89 Katz, S.H and Talbert, E.J. U.S. Dept. Commerce. Bureau of Mines Tech. Paper 1930 p.480

90 Stevens, S.S.'Handbook of Experimental Psychology' John Wiley and Sons New York (1951)

91 Stevens, S.S.Psychol. Rev. 64, 153 (1957)

92 Stevens, S.S. 'Sensory Communications' (Rosenblith Ed.) Cambridge Mass. MIT Press (1961)

93 Beck, L.H., Kruger, L and Calabresi.P. Am. N.Y. Acad. Sci. 58, 225 (1954)

94 Kruger, L. , Feldzamen, A.N and Miles, W.R. Am.J.Psychol. 68, 386 (1958)

95 Jones, F.N. Am. J. Psychol. 71, 305 (1958)

96 Cairncross, S.E and Sjostrom, L.B. 'Flavour Profiles-A New Approach to Flavour Problem' Arthur D. Little Inc., (1949)

97 Kendall, D.A Levins, P.L. and Leonardos, G. SAE Paper 740215 (1974)

98 Dravnieks, A. Odour Measurement Environmental Letters 3, 81 (1972)

99 Hare, C.T., Springer,K.L., Somers, J.H and Huls, T.A. SAE Paper 740214 (1974)

100 Dravnieks, A. 'Chemistry and Psychology of Flavours' Schultz et al Ed. AVI Publ. Co. Westport Conn. (1967) p. 94

101 Dravnieks, A.'Theories of Odour and Odour Measurement' Tanyolac Ed. Robert College, Bebek, Istanbul Turkey, (1968) p.373

102 Powers, J.J and Keith, E. J.Food Sci. 33, 207 (1968)

103 Arthur D.Little Inc. 'Chemical Identification of the Odour Components in Diesel Engine Exhaust' Final Report, CRC Project CAPE-7-68 HEW Contract PH 22-68-20 (1969)

104 Arthur D.Little Inc. 'Chemical Identification of the Odour Components in Diesel Engine Exhaust' Final Report, CRC Project CAPE-7-68 HEW Contract 22-69-63 (1970)

105 Arthur D.Little Inc. 'Chemical Identification of the Odour Components in Diesel Engine Exhaust' Final Report, CRC Project CAPE-7-68 EPA Contract EHSD 71-18 (1971)

106 Arthur D.Little Inc. 'Analysis of the Odorous Compounds in Diesel Engine Exhaust' Final Report CRC Project CAPE-7-68, EPA Contract 68-02-0087 (1972)

107 Arthur D.Little Inc. 'Analysis of the Odorous Compounds in Diesel Engine Exhaust' Final Report, CRC Project CAPE-7-68, EPA Contract 68-02-0561 (1973)

108 'Chemical Species in Engine Exhaust and their Contribution to Exhaust Odour' IITRI Report No. C8150-5 to the CRC and NAPCA. U.S. Pub. Health Service Dept. of Health, Ed. and Welfare (CRC Project CAPE-7-68)

109 'Chemical Species in Engine Exhaust and their Contribution to Exhaust Odour' IITRI Report No. C6183-5 to the CRC and NAPCA. U.S. Pub. Health Service Dept. of Health, Ed. and Welfare (CRC Project CAPE-7-68)

110 Spindt, R.S, Barnes, G.J and Somers, J.H. SAE Paper 710605 (1971)

111 Springer, K.J and Stahman, R.C. SAE Paper 750332 (1975)

112 Moncrieff, R.W. J.Appl. Phys. 16, 742 (1960)

113 Wilkens, W.F Hartman, J.D. Annals N.Y. Acad. Sci. 116, 608 (1964)

114 Meinhard, J.H. U.S. Pat. 3,428,892 (1969)

115 'Fieldnotes' Ed. No. 8, Pub. by Field Instruments Co. Ltd. England Winter (1970)

116 'Boiling Range Distribution of Petroleum Fractions by Gas Chromatography' ASTM Pub. D 2887-70T (1970)

117 'Diesel Engines-Principles and Practice' Ed. Pounder, C.C., George Newnes Ltd.(London) Second Edn. (1962)

118 Barnard, J.A and Harwood, B.A. Comb. and Flame 22, 35 (1974)

119 Haskell, W.W and Read, I.A. Appl. Spectroscopy 23, 532 (1969)

120 Hoelzer, J.C. SAE Paper 751002 (1975)

121 Garner, F.H., Morton, M and Saunby, J.B. J. Inst. Petrol. 47, 450 (1961)

122 Brioda, H.P., Levedahl, W.T and Harvard, F.L. J.Chem. and Phys. 19. 797 (1951)

123 Downs, D., Street, J.C and Wheeler, R.W. Fuel 32, 279 (1953)

124 Malmberg, E.W., Smith, M.L., Bigler, J.E and Bobbit, J.A. Fifth Symp. (Int.) on Comb., p. 383 (1955)

125 Pahnke, A.J., Cohen, P.N and Sturgis, B.M. Ind. and Eng. Chem. 46, 1024 (1954)

126 Downes, D., Walsh, A.D and Wheeler, R.W. Phil. Trans. Roy. Soc. London A243, 463 (1951)

127 Garner, F.H., Morton, F., Nissan, A.H and Wright, E.P. J. Inst. Petrol. 38, 301 (1952)

128 Sokolik, A.S. Israel Programme for Sci. Transl., Jerusalem (1963)

129 Boyce, T.R. 'The Pre-Ignition Processes in Compression-Ignition Engines' PhD Thesis, London University, (1969)

130 Yantovskii, S.A. Kinetika i Kataliz 5, 399 (1967); 7, 21 (1966)

131 Fish, A. Proc. Roy. Soc. (London) A293, 378 (1966)

132 Jost, W and Martinengo, A. SAE Paper 660347 (1966)

133 Brown, A.J., Burt, N.H., Luckett, C.A and Pollard, R.T. Symp. on the Mechanisms of Hydrocarbon Reactions p. 751, Hungary (1973)

134 Pease, R.N. Chem.Rev. 21,279 (1937)

135 Ridge, M.J. Trans. Faraday Soc. 52, 858 (1956)

136 Personal Communication from Dr.P Levins, ADL, April (1977)

137 Aaronson, A.E and Matula, R.A. Thirteenth Symp. (Int.) on Comb., p.471 The Comb. Institute (1971)

138 Barat,P., Cullis, C.F and Pollard, R.T. Proc. Roy. Soc. (London),A325 , 469 (1971)

139 Barat, P., Cullis, C.F and Pollard, R.T. Proc. Roy. Soc. (London), A329, 433 (1972)

140 Fish, A. Proc. Roy. Soc. (London), A298, 204 (1967)

141 Fish, A., Haskell, W.W and Read, I.A. Proc. Roy. Soc. (London) A313, 261 (1969)

142 Burgess, A.R., Luck, C.J., Desty, D.H., Whitehead, D.M and Pratley, G. Fourteenth Symp. (Int.) on Comb., p.501 The Comb. Institute (1973)

143 Fish, A. Quart. Rev. (London) 18, 243 (1964)

144 Fish, A. 'Advances in Chemistry No. 76' (Ed. Gould, R.F) Am. Chem. Soc., 2, 69 (1968)

145 Fish, A. Angew Chem. 7, 45 (1968)

146 Cullis, C.F., Fish, A., Saeed, M and Trimm, D.L. Proc. Roy. Soc. A289, 402 (1966)

147 Cartlidge, J and Tipper, C.F.H. Proc. Roy. Soc. A261, 388, (1961)

148 Szabo, Z.G and Gal, D. Acta Chem.,Hungary 16, 29 (1958)

149 Norrish, R.G.W. Disc. Faraday Soc. 10, 269 (1951)

150 Knox, J.H and Norrish, R.G.W. Proc. Roy. Soc. (London) A221, 151 (1954)

151 Karmilova, L.V., Enikolopyan, N.S., Nalbandyan, A.B and Semenov, N.N Z. fiz. Chim. 34, 562 (1960)

152 McDowall,C.A and Thomas, J.H. J. Chem. Soc. 1462, (1950)

153 Baldwin, R.R and Walker, R.W. Fourteenth Symp.(Int.) on Comb., p.241. The Comb. Institute (1973)

154 Salooja, K.C. Comb. and Flame 9, 373 (1965)

155 Bonner, B.H and Tipper, C.F.H. Comb. and Flame 9, 387 (1965)

156 Hoare,D.E., Protheroe, J.B and Walsh, A.D. Trans. Faraday Soc. 55, 548 (1959)

157 Bardwell, J and Hinshelwood, C. Proc. Roy. Soc. A205, 375 (1951)

158 Bardwell, J. Fifth Symp. (Int.) on Comb., p. 529 (1955)

159 Knox, J.H and Wells, C.H.J. Trans. Faraday Soc. 59, 2786 (1963)

160 Knox, J.H and Wells, C.H.J. Trans. Faraday Soc. 59, 2801 (1963)

161 Knox, J.H. Trans. Faraday Soc. 56, 1225 (1960)

162 Knox, J.H. Trans. Faraday Soc. 55, 1362 (1959)

163 Hay, J., Knox, J.H and Turner, J.M.C. Tenth Symp. (Int.) on Comb., p.331 The Comb. Institute (1965)

164 Cullis, C.F., Fish, A and Gibson, J.F. Proc. Roy. Soc. A311, 253 (1969)

165 Salooja, K. C. Comb. and Flame 12, 597 (1968)

166 Jost, W. 'Explosions-und Verbrennungsvorgange in Gasen' p. 488, Springer, Berlin (1939)

167 Minkof, J.G and Tipper, C.F.H. 'The Chemistry of Combustion Reactions' Butterworths (1962) p. 172

168 Burgoyne, J.H. Proc. Roy. Soc. A161, 48 (1937)

169 'Basic Liquid Chromatography' Varian Aerograph (1971) p. 6-11

170 Finar, I.L. 'Organic Chemistry' Vol. 1 p. 830 Longmans (1967)

171 Lindsey, A.J. Comb. and Flame 4, 261 (1960)

172 Crittenden, B.D and Long, R. Comb. and Flame 20, 359 (1973)

173 Homann, K.H., Mochizuki, M and Wagner, H.Gg. Z. Phys. Chem. N.F. 37, 299 (1963)

174 Chakraborty, B.B and Long, R. Comb. and Flame 12, 226, 237, 469, (1968)

175 Palmer, H.B and Cullis, C.F. 'Chemistry and Physics of Carbon' Vol. 1 (P. L. Walker, Jr., Ed.) Arnold, London and Dekker, New York (1965) Chap. 5. p. 265

176 Porter,G. Combustion Researches and Reviews A.G. ARD., Butterworths London (1955) p. 108

177 Ioffe,I.I. J. Phys. Chem., Moscou 28, 772 (1954)

178 Burgoyne, J.H. Proc. Roy. Soc. A175, 539 (1940)

179 Varghese, T., Matula, R.A and Savery, C.W. Comb. and Flame 21, 131 (1973)

180 Kanury, A.M. 'Introduction to Combustion Phenomena'. Gordon and Breach Science Publishers, New York (1975) p.293

181 Trumpy, D.K., Sorenson,S.C and Myers, P.S. Discussion Following Paper by Barnes, G.J. SAE 680445 (1968)

182 Merrion, D.F. SAE Paper 680422 (1968)

183 Mathur, H.B. I.E(I) Journal-ME 55, 169 (1975)

184 Schumann, C.E and Gruber, C.W. J.Air Polln. Control Assoc. 142, 53 (1964)

185 Marshall, W.F and Fleming, R.D. Diesel Emissions Reinventoried. U.S. Dept. of Interior, Bur. of Mines Report 7530

186 Skala, H., Padrta, F.F and Sampson, P.S. Proc. 1st. Natl. Symp. on Het. Cat. for Control of Air Polln. Phil. Pa. Nov (1968)

187 Vogh, J.W. Bureau of Mines Report 7632 (1972)

188 Linnell, R.H and Scott, W.E. J. Air Polln. Control Assoc. 12, 10 (1962)

189 Sawicki, E., Hauser, T.R., Stanley, T.W and Elbert, W.C. Anal. Chem. 33, 93 (1961)

190 Springer, K.J and Stahman, R.C. SAE Paper 750332 (1975)

191 Dietzmann, H.E., Springer K.J and Stahman, R.C. SAE Paper 720757 (1972)

192 Padrta, F.G and Samson, P.C. 'Diesel Odour-Part 1 : Identification, Presented at CRC Meeting, Chicago, Illinois Oct. (1969)

193 Spindt, R.S., Barnes, G.J and Somers, J.H. SAE Paper 710605 (1971)